UNIVERSITÄT FÜR BODENKULTUR WIEN
University of Natural Resources
and Life Sciences, Vienna

Masterarbeit

The influence of NH_4^+ fertilisation and clay mineral amendments on Cs^+ in soil solution.

verfasst von

Mike Robert ROHLING, B.Sc.

im Rahmen des Masterstudiums

Umwelt- und Bioressourcenmanagement

zur Erlangung des akademischen Grades

Diplom-Ingenieur

Wien, September 2022

Betreut von:
Univ. Prof. Dipl.-Ing. Dr. Dr.h.c.mult. Martin Gerzabek
Institut für Bodenforschung
Department für Wald- und Bodenwissenschaften

Contact e-mail: mike.rohling1995@gmail.com

The present research has been financially supported by the Coordinated Research Project D1.50.19 approved by the Joint FAO/IAEA Programme, with a contribution from the Institute of Soil Research from the University of Natural Resources and Life Sciences, Vienna (Austria).

I hereby declare that I am the sole author of this work; no further assistance other than the permitted mentorship and the feedback provided by the supervisors of this thesis has been used. All quotes and concepts taken from every source, unpublished and published literature, have been given verbatim or textual citation.

Ich erkläre eidesstattlich, dass ich die Arbeit selbständig angefertigt habe. Es wurden keine anderen als die angegebenen Hilfsmittel benutzt. Die aus fremden Quellen direkt oder indirekt übernommenen Formulierungen und Gedanken sind als solche kenntlich gemacht. Diese schriftliche Arbeit wurde noch an keiner Stelle vorgelegt.

Disclaimer

This publication has been prepared from the original material as submitted by the contributors and has not been edited by the editorial staff of the IAEA. The views expressed remain the responsibility of the contributors and do not necessarily represent the views of the IAEA or its Member States.

Neither the IAEA nor its Member States assume any responsibility for consequences which may arise from the use of this publication. This publication does not address questions of responsibility, legal or otherwise, for acts or omissions on the part of any person.

The use of particular designations of countries or territories does not imply any judgement by the publisher, the IAEA, as to the legal status of such countries or territories, of their authorities and institutions or of the delimitation of their boundaries.

The mention of names of specific companies or products (whether or not indicated as registered) does not imply any intention to infringe proprietary rights, nor should it be construed as an endorsement or recommendation on the part of the IAEA.

The authors are responsible for having obtained the necessary permission for the IAEA to reproduce, translate or use material from sources already protected by copyrights.
The IAEA has no responsibility for the persistence or accuracy of URLs for external or third party Internet websites referred to in this publication.

Abstracts

[English] : Large amounts of the nuclear fission product radiocaesium (RC) were deposited onto soils after the Chernobyl nuclear power plant (CNPP) and Fukushima Daiichi Nuclear Power Plant (FDNPP) accidents. The dynamic of RC in soils is majorly determined by soil mineralogy. In particular, 2:1 clay minerals (weathered mica, vermiculite, smectite) and zeolite, are able to selectively retain RC and hence prevent its absorption by plant roots. Ammonium (NH_4^+) is a strong competitor for those sites and might induce the release of RC into the soil solution. Therefore, this study attempted to elucidate the effect of a NH_4^+ - N fertilisation (300 kg ha^{-1}) on the solution ^{133}Caesium (Cs) (as a proxy for RC) dynamics of five soil types (Chernozem, Podzol, Cambisol, Gleysol and Andosol) from Austria, Belarus and Japan, that clearly differed in their clay mineralogical composition. One soil (Japanese Andosol) with low radiocaesium interception potential (RIP) was additionally treated with smectite, vermiculite and zeolite at 10 and 40 t ha^{-1} application rates, respectively. Over five weeks of incubation, a large share of the applied NH_4^+ was lost from the investigated soil fractions, which were 2 M KCl extractable NH_4^+, nitrite (NO_2^-) and nitrate (NO_3^-) as well as soil solution NH_4^+ (mNH_4^+). It was assumed that NH_4^+ fixation in the interlayers of 2:1 clay minerals accounted for the largest share of those losses. With exception of a vermiculitic Cambisol, mNH_4^+ exhibited a strong positive correlation with mCs^+. The presence of vermiculite and weathered mica tended to cause a reduced Cs^+ desorption during the incubation, which was most likely related to highly Cs^+ selective sites on those minerals. Analogously, the clay mineral amendments decreased mCs^+ after NH_4^+ - fertilisation following the order: vermiculite > zeolite > smectite and 40t ha^{-1} > 10t ha^{-1} for each mineral. Moreover, the NH_4^+ fertilisation caused potassium (K^+) desorption which implied a decrease of the calculated RC concentration factor (CF) for ryegrass. This effect exceeded the effect of increased mCs^+ in most cases, implying that the fertilisation treatment unexpectedly caused the calculated Cs^+ uptake (of ryegrass) to decrease. Due to the previous K^+ depletion of the clay minerals, their use caused an mK^+ reduction that resulted in an increased calculated Cs^+ uptake of the zeolite and smectite enriched soils compared to the control. This effect tended to be due to the strong K^+ retention by zeolite and the comparatively weak Cs^+ retention by smectite. Only the vermiculite treatments decreased the relative Cs^+ uptake, which was attributable to a strong Cs^+ selectivity combined with a moderate mK^+ reduction. As K^+ depletion of vermiculite is economically not feasible in large scale, this insight was, however, of pure scientific interest.

Keywords: 2:1 phyllosilicate, agricultural remediation, ammonium fertilisation, radiocaesium, smectite, vermiculite, zeolite

[Deutsch]: Große Mengen des nuklearen Spaltproduktes Radiocäsium (RC) sind nach nuklearen Unfällen aus den Atomkraftwerken in Tschernobyl und Fukushima freigesetzt und auf Böden abgelagert worden. Die Dynamik von RC in Böden ist maßgeblich durch Bodenmineralogie beeinflusst. Insbesondere 2:1 Tonminerale (verwitterter Glimmer, Vermikulit, Smektit) und Zeolith besitzen die Eigenschaft RC selektiv zu adsorbieren und damit die RC Absorption von Pflanzenwurzeln zu verhindern. Ammonium (NH_4^+) ist ein starker Konkurrent an diesen Austauschpositionen und kann die Freisetzung von RC in die Bodenlösung bewirken. Daher wurde in dieser Studie versucht, die Auswirkungen einer NH_4^+ - N-Düngung (300 kg ha^{-1}) auf die Dynamik von ^{133}Cäsium (Cs) in Lösung (als Proxy für RC) auf fünf unterschiedlichen Böden (Tschernosem, Podsol, Cambisol, Gleysol und Andosol) aus Österreich, Weißrussland und Japan, die sich deutlich in ihrer tonmineralogischen Zusammensetzung unterschieden, zu untersuchen. Ein Boden mit geringem Cs^+ Austauschvermögen wurde zusätzlich mit Smektit, Vermikulit und Zeolith mit Applikationen von jeweils 10 und 40 t ha^{-1} verändert. Während der fünfwöchigen Inkubation verschwand ein großer Teil des applizierten NH_4^+ aus den untersuchten Bodenfraktionen, welche 2 M KCl extrahierbares NH_4^+, Nitrit (NO_2^-) und Nitrat (NO_3^-) sowie $NH4^+$ in Bodenlösung (mNH_4^+) umfassten. Es wurde angenommen, dass NH_4^+ - Fixierung in den Zwischenschichten von 2:1 Tonmineralen den größten Teil dieser Verluste verursachte. Mit Ausnahme eines vermikulitischen Cambisols zeigte mNH_4^+ eine starke positive Korrelation mit mCs^+. Die Anwesenheit von Vermikulit und verwittertem Glimmer verursachte tendenziell geringere Cs^+ - Desorption während der Inkubation, was wahrscheinlich in Zusammenhang mit stark selektiven Cs^+ Austauschpositionen dieser Minerale steht. Analog dazu reduzierten die Tonmineralapplikationen mCs^+ nach NH_4^+ - Düngung in der Reihenfolge: Vermikulit > Zeolith > Smektit und 40 t ha^{-1} > 10 t ha^{-1} für das jeweilige Mineral. Weiterhin verursachte die NH_4^+ - Düngung Kalium (K^+) - Desorption, was eine Reduzierung des berechneten Konzentrationsfaktors (KF) für Weidelgras implizierte. Dieser Effekt überstieg den Effekt von erhöhtem mCs^+ in den meisten Fällen, was wider Erwarten eine Dünger - verursachte Reduzierung der berechneten Cs^+ Aufnahme (von Weidelgras) zur Folge hatte. Aufgrund des K^+ - Entzugs der Tonminerale vor Ausbringung bewirkte ihre Anwendung eine mK^+ Reduktion, die zu einer erhöhten berechneten Cs^+ - Aufnahme der mit Zeolith und Smektit behandelten Böden im Vergleich zur Kontrolle führte. Dieser Effekt war tendenziell auf die starke K^+ - Adsorption durch Zeolith und die vergleichsweise schwache Cs^+ - Adsorption durch Smektit zurückzuführen. Lediglich die Vermikulit Applikationen verursachten einen relativen Rückgang der berechnten Cs^+ - Aufnahme, was der starken Cs^+ Selektivität in Verbindung mit einer moderaten mK^+ Reduktion zuzurechnen war. Da der K^+ Entzug von Vermikulit im großen Maßstab ökonomisch nicht umsetzbar ist, ist diese Erkenntnis jedoch von rein wissenschaftlichem Interesse.

Schlüsselworte: 2:1 Phyllosilikat, landwirtschaftliche Remediation, Ammonium Düngung, Radiocäsium, Smektit, Vermikulit, Zeolith

[日本語]：チェルノブイリ原子力発電所 (CNPP) および福島第一原子力発電所における事故により、核分裂生成物である放射性セシウム (RC) が多量に土壌へと沈着した。RC の土壌中での挙動は 2:1 型粘土鉱物（風化雲母、バーミキュライト、スメクタイト）やゼオライトに強く規定される。これらの鉱物は RC を強く保持し、植物根による吸収を阻害することが良く知られている。しかし、これらの鉱物に保持された RC はアンモニウムイオンとの競合により土壌溶液に放出されることが危惧される。そのため、本研究では、300 kg ha^{-1} - N 相当の窒素施肥が土壌溶液中の RC の挙動に与える影響を、セシウム-133 を RC に代替とし、粘土鉱物組成の異なる 5 土壌を用いた培養試験により明らかとすることを目的とした。供試した土壌のうち、放射性セシウム補足容量（Radiocesium Interception Potential, RIP）が低い火山灰土壌については、鉱物資材（スメクタイト、バーミキュライトまたはゼオライト）1 t $10a^{-1}$ または４ t $10a^{-1}$ 相当を添加した処理を設けた。5 週間にわたる培養試験中の土壌溶液アンモニウム濃度 (mNH_4) および交換性アンモニウム含量の変化から、2：1 型粘土鉱物によるアンモニウムイオンの固定が示唆された。バーミキュライト質土壌を除き、mNH_4 と土壌溶液の Cs 濃度 (mCs^+) の間に強い正の相関がみられた。バーミキュライトや風化雲母を多く含む土壌でアンモニウム施用による mCs^+ の上昇程度が低い傾向にあった。同様に、粘土鉱物資材施用によってもアンモニウム施用による mCs^+上昇程度は低下し、その効果はバーミキュライト > ゼオライト > スメクタイトであった。しかしながら、鉱物資材、特にゼオライトは、土壌溶液 K 濃度も同時に低減させ、施用量によっては RC 移行係数（Transfer Factor, TF）をかえって高めることが懸念された。本研究により、アンモニウムの多量施用が作物による RC 吸収リスクを高めることが明らかとなった。

Keywords: アンモニア施肥, 吸収抑制, スメクタイト, ゼオライト, 放射性セシウム 2:1

Acknowledgements

I would like to thank my supervisors Prof. Martin Gerzabek, Dr. Gerd Dercon and Dr. Tetsuya Eguchi for guiding me through the process of this master - thesis without restricting my creativity and freedom. In particular, I would like to thank Dr. Tetsuya Eguchi, who did not just support me with his great mineralogical expertise but also taught me the importance of patience, precision, coherence and honesty in the creative process of a scientific work. In times in which the term “science” is used to describe a wide range of phenomena, I am now glad to have learned this lesson. Furthermore, I would like to thank all the other people that supported me in the last one and a half years, be it by just listening when the work seemed unmanageable or by fruitful content - related contributions. Now that my studies are also coming to an end, I would like to mention that my scientific interest was clearly sparked by the many inspiring people I met along the way and the countless open discussions I was privileged to have with them.

List of symbols

Symbol	Description	Unit
,	Thousand separator	
.	Decimal separator	
ex. – X	Exchangeable cation (X)	mmol kg^{-1} oven - dried soil
mX	Cation (X) in soil solution	mmol L^{-1}
K_D	Solid - liquid partitioning coefficient	kg L^{-1}
zX	Cation (X) in solid state	mmol kg^{-1} oven - dried soil
wt	Dry - weight basis	%
$t_{1/2}$	Half - life	a

Table of contents

Abstracts 4

Acknowledgements 8

List of symbols 9

1. Introduction

1.1 Global soil threats and soil contamination 12

1.2 Health effects of radionuclides 13

1.3 Artificial radionuclide pollution 15

1.4 Chemical and biological properties of Caesium - isotopes 20

1.5 Caesium - clay mineral interactions 24

1.6 Caesium soil - to - plant transfer 31

1.7 Geology, pedogenesis and climate of Europe and Japan 36

2. Objectives and hypotheses 41

3. Material and Methods

3.1 Soil collection 43

3.2 Sample preparation 44

3.3 General physicochemical properties 47

3.4. Solid - liquid distribution determination 52

3.5 Statistical analysis 57

3.6 Prediction of the concertation factor 58

4. Results and Discussion

4.1 Mineralogical and physicochemical soil properties 59

4.2 Ammonium dynamics of the unamended soils 64

4.3 Caesium dynamics of the unamended soils 74

4.4 Ammonium dynamics of the clay - amended soil 83

4.5 Caesium dynamics of the clay - amended soil 90

4.6 Implications for the Caesium plant uptake 98

5. Conclusions 105

6. Bibliography 107

7. Appendices

Appendix A I

Appendix B XI

Appendix C XVI

Appendix D XVII

Appendix E XXII

1. Introduction

1.1 Global soil threats and soil contamination

Soils are defined as „*transition points between atmosphere, geosphere, biosphere and hydrosphere*…“ (Herrmann, 2018). They fulfil manifold services to humans as among others biomass production for agricultural and forestry purposes, harbouring of biodiversity (gene reservoir), provision of raw materials, filtering and storage of water and nutrients as well as providing space for infrastructure (Robinson et al., 2017). Simultaneously, soils are globally exposed to diverse threats, among them erosion, compaction, salinization, acidification, sealing, waterlogging, nutrient imbalance, and contamination, of which most are human - induced (Montanarella et al., 2016; Vargas, 2017). Moreover, there are interacting and amplifying effects between certain soil threats, resulting in a higher degree of complexity and difficulties in finding appropriate countermeasures (Hemati Matin & Jalali, 2017, 2017; Schroth et al., 2003). It is assumed that the current global soil crisis exceeds known ones from the past. Approximately 27% (35 million km^2) of earth´s soils were defined as degraded in 2007 (Karlen & Rice, 2015). This consequently led to decreasing agricultural yields, declining water quality, loss of biodiversity and acceleration of climate change (Koch et al., 2013; Montanarella et al., 2016).

Different primary drivers of soil threats can be identified. The first driver is represented by the coupled pair of population growth and agricultural production. Crop- and grassland covered 26% of earth´s surface in 2008, meaning a six-fold increase since 1700. Agricultural practices not solely but dominantly contribute to global soil degradation (Karlen & Rice, 2015). Moreover, population growth is assumed to happen in countries suffering from unfertile soils and limited agricultural productivity. Societal issues such as lack of education, dysfunctional markets, civil conflicts and inequal distribution of wealth can further exacerbate soil degradation. The second driver is economic growth, even if a successive decoupling of resource consumption and economic growth may happen. The third primary driver is climate change (Montanarella et al., 2016). Climate change and certain soil threats display feedback loops, as climate change is driver of and is driven by certain soil threats. This driver is often underestimated and comes with a high degree of uncertainty, whereby changes in soil temperature and moisture as well as carbon dioxide (CO_2) concentration in the atmosphere are assumed to have the biggest impact on soils (Pareek, 2017).

Soil threats differ in their severity globally. The greatest global soil threats are soil erosion, soil sealing and acidification. These are followed by salinization and sodification, organic carbon change and nutrient imbalance. Soil contamination is the third greatest soil threat in Europe and Eurasia and fourth greatest in northern Africa and the middle East (Montanarella et al., 2016). Furthermore, soil contamination interacts with other soil threats as acidification and nutrient imbalance, influences them and *vice versa* (Robinson et al., 2017). Soil contamination is defined as the "*presence of a chemical or substance out of place and/or present at a higher than normal concentration that has adverse effects on any non-targeted organism*" (Rodríguez-Eugenio et al., 2018). Additionally, it does not only induce soil degradation, but also affects quality of other environmental media as air and water (Sethi & Gupta, 2020). In 2017, the United Nations Environmental Assembly (UNEA-3) concluded with a political declaration on combating soil pollution globally and linked it with the sustainable development goals (SDG´s). More than 170 countries agreed upon the declaration, revealing soil contamination as a global concern. As soil contamination is difficult to assess, it is often denoted as a "hidden danger" (Rodríguez-Eugenio et al., 2018; Sethi & Gupta, 2020). In the 1990´s, the International Soil Reference and Information Centre (ISRIC) and the United Nations Environment Prorgramme (UNEP) estimated soil contamination to affect approximately 22 million hectares (Oldeman et al., 1991). However, it is assumed that this value underestimates actual global soil contamination, due to incomplete data especially from low- and middle-income countries (Rodríguez-Eugenio et al., 2018).

Soil contamination can affect human health via i) ingestion, ii) inhalation, or iii) dermal absorption (Brevik & Burgess, 2012). Ingestion mainly occurs indirectly via consumption of crops and livestock, that accumulated soil pollutants before. Direct ingestion particularly matters to children, as their mouthing behaviour is assumed to differ to adults (Davis and Mirick, 2006). Inhalation happens if polluted soil - borne particulate matter is breathed in. Resuspension of soil material into the atmosphere is thereby primarily induced anthropogenically by field cultivation techniques or naturally by soil eruptions (Manisalidis et al., 2020). Finally, dermal absorption can occur after direct skin contact to polluted soils or their deriving particulate matter in air or water. Again, exposure through direct contact is higher for children due to play habits in public spaces and poor hygiene (Egendorf et al., 2020). However, dermal absorption seems to mainly derive from volatile organic compounds (Brevik & Burgess, 2012).

1.2 Health effects of radionuclides

The importance of radionuclides in this context arises from the complexity concerning their dynamics in the environment while considering their relevant timescales (Deblonde et al., 2020). Radionuclides possess unstable nuclei that produce ionizing radiation while they decay to a stable configuration (Mirsal, 2004). The decay time is described by the half - life ($T_{1/2}$), indicating the elapsed time until the amount of a radionuclide declined by its half. It is reflected in the formula:

$$N\left(T_{\frac{1}{2}}\right)=N_0\cdot e^{-\lambda\cdot T_{\frac{1}{2}}} \qquad (1)$$

where N denotes the activity (e.g., in Bq), N_0 the activity at $t = 0$, λ the decay constant and $T_{1/2}$ the half - life. The ionizing radiation includes five different types, namely α-, β- and neutron - particle as well as ɣ - Ray and X - Ray radiation (Table 1). All radiation types differ in their properties, particularly in their ionization capability and their penetration level. This finds reflection in specific radiation weighting factors, which are incorporated in the SI - unit Sievert (Sv) (Choi et al., 2015; Valentin, 2003). In contrast, the SI - unit Becquerel (Bq) describes the number of disintegrated atoms per second without taking radiation quality into consideration (Brevik & Burgess, 2012).

The impingement of ionizing radiation on cells can cause direct damage to chemical bonds in DNA - molecules as well as cell membranes. Long - time effects of those events are cell death, DNA mutation and carcinogenesis (Pöschl & Nollet, 2006). These processes are mainly caused by radiation with high linear energy transfer (LET) (> 10 keV μm^{-1}). Indirect damage is predominantly induced by low LET radiation through breakdown of H_2O molecules forming hydrogen ($H\cdot$) and hydroxide ($HO\cdot$) radicals as well as hydrogen peroxide (H_2O_2) causing a subsequent oxidation of DNA molecules (Choi et al., 2015). However, different cells exhibit different radiosensitivity and mechanisms to repair radiation caused damage (Choi et al., 2015; Pöschl & Nollet, 2006). To more precisely estimate human exposure towards radiation, the SI - unit gray (Gy) reflects the ionization radiation induced energy in Joule (J) that is absorbed per mass unit (kg):

$$\mathrm{Gy} = \frac{\mathrm{J}}{\mathrm{kg}} \qquad (2)$$

The SI-unit Sievert finally reflects both weighting factor and specific organ sensitivity in the following formulas:

$$\text{Effective dose in Sievert (Sv)} = \sum H_T \cdot w_T \qquad (3)$$

$$\text{Equivalent dose to tissue T} = H_T = \sum w_R \cdot D_{T,R} \qquad (4)$$

with $D_{T,R}$ indicating the absorbed dose in tissue or organ T due to incident radiation R (in Gy), w_R the radiation weighting factor and w_T the tissue weighting factor.

Radiation exposure is differentiated according acute and chronic effects. The acute radiation syndrome (ARS) is a complex of syndromes occurring after whole - body short - term radiation exposure exceeding 0.7 – 1 Gy (Gus´kova et al., 1987). Generally, acute high radiation doses mainly affect precursor or stem cells of hematopoietic cells, skin, epithelium, intestine and vascular epithelium (Mettler et al., 2007). The ARS is divided into four development stages and three syndromes, namely the i) bone marrow (0.7 Gy), ii) gastrointestinal (10 Gy), and iii) cardiovascular/central nervous system (50 Gy) syndrome. Each syndrome exhibits its own symptoms at each stage and shows distinct chances to reach a recovery. Generally, higher radiation comes along with smaller chance of recovery (Clements & Casani, 2016). Moreover, acute radiation impacts several organs as kidneys, liver, lungs, respiratory and cardiovascular directly or indirectly as a consequence of an interplay with other organs and can cause (multi)organ disease or even failure (Fliedner et al., 2005). Some sensible tissues as the cataracts in the eye lens, or the ovaries and testis may already develop clinically relevant dysfunctions from doses < 1 Gy, necessitating a life - long follow - up (Brown & Rzucidlo, 2011; Dörr & Schmidt, 2014).

Table 1: *Characteristics of nuclear radiations (Keith et al., 2012).*

Radiation	**Notation**	**Charge**	**Mass** (amu)	**Typical energy range**
Alpha Particles	α, ${}_2^4He$	+2	4.00	4 - 10 MeV
Beta Particles	β, ${}_{-1}^0e$, ${}_{+1}^0e$	-1/+1	5.5×10^{-4}	0 - 4 MeV
ɣ - Rays	ɣ, ${}_0^0$ɣ	0	-	10 keV - 3 MeV
Neutron	n, ${}_1^0n$	0	1	0 - 15 MeV
X - rays	X-ray	0	-	5 keV - 100 MeV

In contrast, chronic exposure to low doses radiation does not exhibit immediate symptoms. The same radiation doses seem to cause less harm if affecting over a longer period (Keith et al. 2012). To date, there are debates about assessments of chronic radiation health effects (Choi et al., 2015). Some studies suggest an increased risk for leukemia, thyroid and breast cancer, while clear coherences for exposure below certain thresholds (< 100 mGy) can hardly be inferred (Linet et al., 2005; National Research Council (US) Board on Radiation Effects Research, 1998; Zielinski et al., 2008). Often, studies conducted with the exposed population of the Hiroshima and Nagasaki bombing in 1945 are taken as a central reference for chronic radiation health effects, clearly indicating an increased risk for cancer (Preston et al., 2007). However, this reference is questioned as the exposure was brief and intense, doses had to be estimated retrospectively, and the affected population shows lack of representativeness (Wakeford, 2009).

1.3 Artificial radionuclide pollution

Radionuclides are generally distinguished by their origin. In contrast to natural radionuclides, artificial radionuclides are of anthropogenic origin (Michel et al., 2008). Among them are ^{3}H, ^{14}C, ^{90}Sr, ^{99}Tc, ^{129}I, ^{137}Cs, ^{237}Np, and ^{241}Am, which gain importance by their toxicity, mobility, and abundance in the environment (Hu et al., 2010). These radionuclides are themselves often fission products of anthropogenically manufactured radioactive substances (Wild, 1993). Sources are nuclear weapon production and testing, commercial fuel reprocessing, geological repositories of highly radioactive waste and nuclear accidents (Jagetiya et al., 2014). It is assumed, that on average 21% of human exposure to radioactive radiation is caused by artificial radionuclides, whereby medical application accounts for 19% and fallout from nuclear weapon tests and nuclear power industry for 2%. However, public concern is mostly focusing on the last two (Wild, 1993). Both sources contributed to global spreading of radionuclides in the atmosphere, water, and soil.

Above ground atomic weapon tests were mainly conducted by the USA, the UK, and the USSR from 1945 on, but officially ended with the Partial Test Ban Treaty (PTBT) in 1963. Although further testing was conducted since then, testing scope was reduced drastically (Wild, 1993). It is assumed that nuclear weapon testing released approximately 2×10^8 TBq into the stratosphere and upper atmosphere (Choppin, 2003). After their release, these nuclides were attached to particulate matter and subsequently deposited globally as "radioactive fallout". Most of the released radionuclides show a short half - life and are therefore only of minor importance. However, there are radionuclides like ^{3}H, ^{90}Sr, ^{137}Cs, ^{241}Am and Pu which exhibit half - lifes of several years (Table 2). Not just half - life, but also type of radiation and specific behavior in organisms play an important role considering health impacts of radionuclides, as elaborated in *1.2* (Echols et al., 2009).

The second source of artificial radionuclide pollution raising public awareness are nuclear accidents. In 1990, the International Nuclear and Radiological Event Scale (INES) was introduced by the International Atomic Energy Agency (IAEA) and the OECD Nuclear Energy Agency (OECD/NEA). The INES is logarithmically structured, to ensure nuclear events are strictly distinguished by their severity. Events without safety significance are thereby labelled as level 0, levels 1 - 3 are termed "incidents" and levels 4 - 7 "accidents". Events that show no safety relevance are not labelled on the scale. Level seven is defined as a "major accident", containing the description: "*major release of radioactive material with widespread health and environmental effects requiring implementation of planned and extrended countermeasures*". Historically, only two events were ever defined as such (International Atomic Energy Agency, 2013).

The first level seven nuclear accident took place on the 26th of April 1986 at the Chernobyl nuclear power plant (CNPP) in the former USSR, present day Ukraine. During a low - energy test of flawed reactor 4, successive steam explosions occurred and finally destroyed the reactor. Two workers died immediately, another 28 plant and safety staff members died from the consequences of an acute radiation syndrome (ARS) with a whole - body exposure exceeding > 6.5 Gy in most cases (Mettler et al., 2007; United Nations Scientific Committee on the Effects of Atomic Radiation, 2011). More than 500,000 recovery operation workers are currently documented in special health registers. Additionally, fallout contamination and omitted countermeasures led to loss of livelihood for several million people, resulting in psychological, social, and economic disruptions, which were amplified by the subsequent collapse of the USSR (United Nations Scientific Committee on the Effects of Atomic Radiation, 2011). Due to the exposure to ^{131}I, there were 6,848 identified cases suffering from thyroid cancer between 1991 and 2005, most of them having been exposed in childhood and adolescents. A fatal course could be observed in 15 cases (Wakeford, 2018). However, it is assumed that public provision of stable I right after the accident was insufficient and most likely too late in many cases (Shakhtarin et al., 2003; Steinhauser et al., 2014).

Overall, approximately 1.2 × 10^7 TBq radioactivity was released in a period of 10 days, meaning the highest uncontrolled release in history. Radionuclide dispersion occurred in every cardinal direction yet with a north - western tendency. Subsequent deposition strongly depended on intensity of precipitation, topography and on radionuclide characteristics (United Nations Scientific Committee on the Effects of Atomic Radiation, 2011). An area of approximately 29,400 km^2 exceeded a threshold of 185 kBq $(m^2)^{-1}$ (Steinhauser et al., 2014). For instance, ^{137}Cs contaminations ranging between 37 - 200 kBq $(m^2)^{-1}$ could be detected over an area of 45,000 km^2 (Figure 1). Trace concentrations of released radionuclides were even found all over the northern hemisphere. However, most of the radionuclides had short half - lives and already decayed to negligible present - day levels. Current concerns about radionuclide activity are represented by long - lived radionuclides. Among these, ^{137}Cs generated the biggest share of accrued total radiation and is assumed to only be superseded by ^{241}Am and ^{239}Pu/^{240}Pu in > 300 a from the accident happening, whilst radiation is expected to be declined to trace levels (< 0.1 PBq) by then (United Nations Scientific Committee on the Effects of Atomic Radiation, 2011).

The second major accident took place on the 11th of March 2011 at the Fukushima Daiichi Nuclear Power Plant (FDNPP) in the prefecture Fukushima, region Tōhoku, Japan. The power plant is located at the Pacific Ocean coast and was exposed to a Tsunami released by a 9.0 earthquake along the Japanese trench. Initially, the earthquake destroyed essential power supply lines to which the plant was linked. Subsequently, the tsunami caused damage to operational and safety infrastructure of the plant. Four destroyed reactor cores induced venting processes and explosions which eventually caused radionuclide discharge into the environment (Aliyu et al., 2015; Baba, 2013; International Atomic Energy Agency, 2015; National Research Council., 2014; Synolakis & Kânoğlu, 2015).

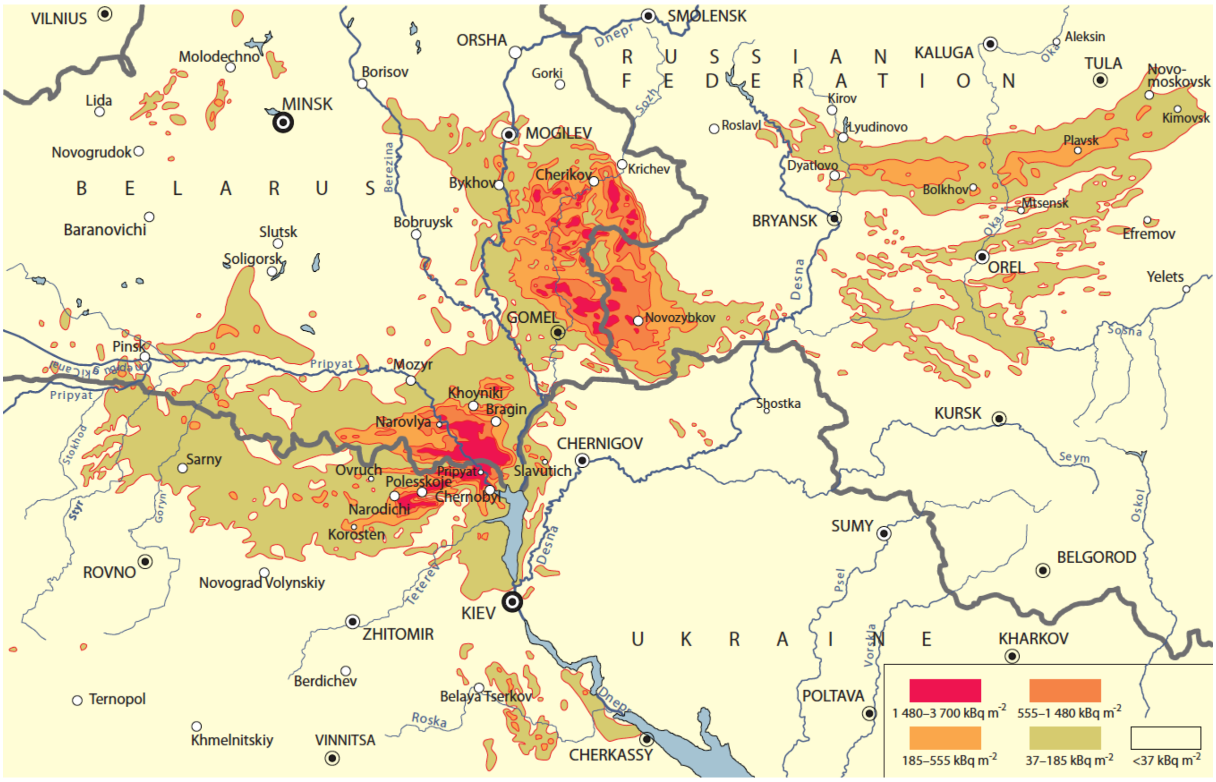

Figure 1: *Deposition density map of ^{137}Cs activity around the CNPP in 1989 (United Nations Scientific Committee on the Effects of Atomic Radiation, 2011).*

Table 2: *Released radionuclide activity after the CNPP and the FDNPP accident (Steinhauser et al., 2014).*

Radionuclide	**Half-life** ($T_{1/2}$)	**FDNPP release** (PBq)	**CNPP release** (PBq)
Noble gases			
^{133}Xe	5.2 d	14000	6500
^{3}H	12.3 a	0.1 - 0.5	1.4
^{131}I	8 d	65 - 380	~ 1760
^{134}Cs	2.3 a	18	~ 47
^{137}Cs	30.2 a	6.1 - 15	74 – 85
Semi-volatile fission products			
^{90}Sr	29.1 a	~ 0.02	~ 10
Refractory elements			
^{238}Pu	87.7 a	$2 \times 10^{-6} - 5 \times 10^{-6}$	0.015
^{239}Pu	24.1 a	-	0.013
^{240}Pu	6552.2 a	-	0.018
$^{239+240}$Pu		$1 \times 10^{-6} - 2.4 \times 10^{-6}$	0.031

In contrast to the CNPP accident, released radiation induced neither immediate deaths nor acute diseases. However, estimations for human health impacts range up to 10,000 deaths, taking into consideration long - term effects. Cancer mortality and morbidity are projected to be up to 1,500 and 1,800, respectively (Aliyu et al., 2015). As children (0 - 18a) are approximately 30% more vulnerable towards radiation exposure, these risks may mainly affect them (International Comission on Radiological Protection, 2007). However, stable I pills and powder were distributed to affected people in the Fukushima prefecture in order to prevent ^{131}I assimilation and hence the risk of thyroid cancer (Hamada et al., 2012). Other than that, mental health and social well - being of affected people has suffered severely and was intensified by the additional damage caused by the earthquake and following tsunami (United Nations Scientific Committee on the Effects of Atomic Radiation, 2014).

It is estimated that the FDNPP total radioactive release was in the order of 10% of the CNPP release (Steinhauser et al., 2014). In contrast to the CNPP accident, hardly any semi - volatile or refractory radionuclides were released (Table 2) (Gaschak et al., 2011). The released nuclides were volatile fission products and dispersed directly or indirectly via atmospheric transport in the North Pacific, hampering precise determination of amount and isotopic ratio. Atmospheric dispersion towards Europe and Northern America occurred but was only detected on negligible levels (International Atomic Energy Agency, 2015). Onshore deposition accounted for approximately 20% of all released radionuclides. Notable amounts of ^{137}Cs, ^{134}Cs and ^{131}I were deposited over the Japanese mainland, mainly northwestern from the FDNPP (Mathieu et al., 2018; Steinhauser et al., 2014). As after the CNPP accident, deposition depended on intensity of precipitation, topography, and radionuclide characteristics. Estimations indicate that ^{137}Cs contamination with levels exceeding 185 kBq $(m^2)^{-1}$ spans over 1,700 km^2 of the Japanese main island Honshu. This area consists of > 75% forests, > 10% rice paddy fields, > 10% other agricultural areas and > 5% urban areas (Figure 2) (Steinhauser et al., 2014).

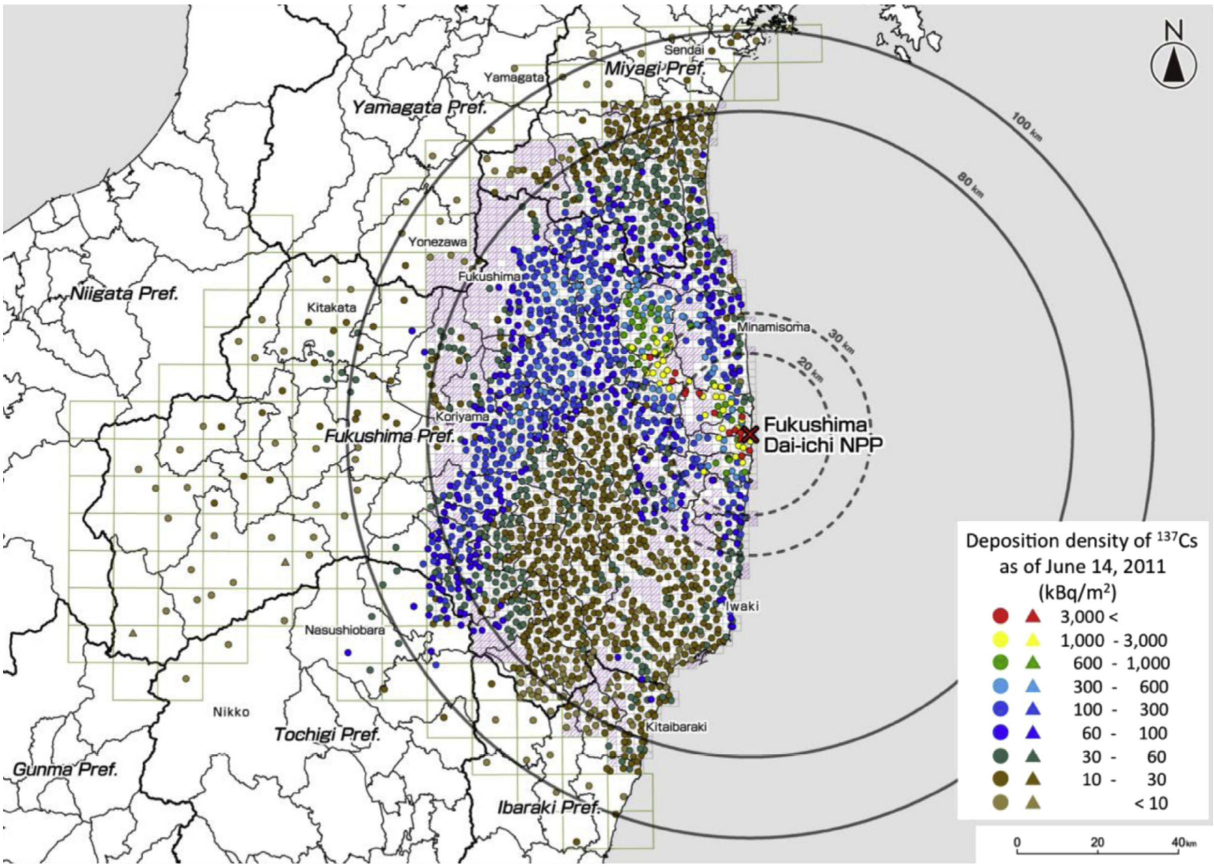

Figure 2: *Deposition densitiy map of ^{137}Cs activity around the FDNPP in 2011 (Saito et al., 2015).*

1.4 Chemical and biological properties of Caesium - isotopes

Long half - lifes and widespread deposition after nuclear accidents make ^{134}Cs and ^{137}Cs radionuclides of particular concern (Ishikawa et al., 2014; Rai & Kawabata, 2020). As merely nuclear masses of stable Cs and RC differ, they reveal wide overlaps regarding their properties and interactions in environmental media and organisms (Agency for Toxic Substances and Disease Registry, 2004; Ishikawa et al., 2014; Tsukada et al., 2002; Yoshida et al., 2004). Caesium is an alkali metal with the atomic number 55 and a mass of 132.9 g mol^{-1} in stable condition ^{133}Cs (Laeter et al., 2003). It exclusively occurs in the valence state (I) and exhibits the highest electropositivity among all elements when excluding unstable Francium (Fr) (Allred, 1961). Inorganic Cs compounds are highly soluble and form mobile Cs^{+} cations in water (Cornell, 1993). As Cs exhibits a low radius/charge ratio and a low tendency of being liganded, it predominantly stays as monovalent cation in solution (Avery, 1995; White & Broadley, 2000). Average Cs concentrations range around 0.3 mg L^{-1} in the oceans and around 2.15 mg kg^{-1} in the earth´s crust, with highest concentrations occurring in the Cs_2O-rich mineral pollucite ($(Cs)_2Al_2Si_4O_{12} \cdot H_2O$) (Kennedy, 1938; McDonough et al., 1992).

Caesium is detected at trace concentrations in most living organisms, although to date no vital function was demonstrated (Ghosh et al., 1993). Due to similar chemical properties with the potassium cation (K^+), Cs^+ and other ionic alkali metals exhibit high mobility in biological systems. However, Cs^+ and K^+ reveal ionic radii of 165 pm and 133 pm, respectively, distinguishing them from the significantly smaller Lithium (Li^+) and sodium (Na^+) ions (Avery, 1995). Potassium is an essential macro - nutrient for all forms of life, playing a key role in regulation of osmotic pressure, enzyme activation, regulation of membrane potential, overall electrolyte balance and several more (Deshpande et al., 2013). Intracellular concentrations are on average around 150 mmol for mammal cells, 100 mmol for plant cells, and range from several hundred millimole up to one mole in microorganisms (Deshpande et al., 2013; Jarrell et al., 1984; Stautz et al., 2021). There are different operating K^+ transporters and channels in cell membranes with different response to Cs^+ cations as well as different K^+ and Cs^+ selectivity (Adams et al., 2019; Bossemeyer et al., 1989). However, recent studies suggest that Cs^+ in contrast to K^+ can pass the cell membrane spontaneously and independently of transporters and channels. This phenomenon was explained by the hydrophobic properties of the Cs^+ cation (Kimura et al., 2016; Shirai et al., 2013).

In the human body, Cs^+ seems to predominantly accumulate in liver, lungs, blood, skeletal muscle, and red blood cells. Excretion in turn occurs with a share of 85% via kidneys (Leggett et al. 2003). As for K^+, stomach uptake of Cs^+ is negligible. If in compound with chloride (Cl^-), and most likely other halides such as I^- and Br^-, Cs^+ absorption in the human body is nearly 100% (Melnikov & Zanoni, 2010; Rosoff et al., 1963). Studies concerning the biological half - life of Cs^+ differ but show maximum means of 100 d for men and 75 d for women (Melnikov & Zanoni, 2010; Rääf et al., 2006). Furthermore, it is assumed that approximately 10% of the ingested dose is excreted with a half - life of only 2 d, indicating merely plasma transport (Rääf et al., 2006). Generally, ^{133}Cs toxicity is doses - depended and can cause decreased appetite, nausea, diarrhea and cardiac arrhythmias, yet no exact reliable data for humans is available (Agency for Toxic Substances and Disease Registry, 2004; Melnikov & Zanoni, 2010). LD_{50} rates for mice and rats after oral uptake range from 800 - 2000 mg kg^{-1} revealing low toxicity of Cs, yet CsOH indicated higher toxicity than other Cs salts (Agency for Toxic Substances and Disease Registry, 2004).

Severe health effects are rather deriving from radioactive Cs isotopes. Overall, there are 40 known Cs isotopes, ranging from ^{112}Cs to ^{151}Cs (Andersen et al., 2004). For afore mentioned reasons, ^{134}Cs and ^{137}Cs have received ample scientific attention. ^{134}Caesium decays most likely to ^{134}Ba via β^- - decay, which is in every case accompanied with subsequent γ - decay (Sonzogni, 2004). In contrast, ^{137}Cs merely decays via β^- - decay, with little chance (5.3%) of direct decay to ^{137}Ba (Table 3). In every other case, ^{137}Cs decay is accompanied by γ - decay

***Table 3:** Decay properties of ^{134}Cs and ^{137}Cs* (Sonzogni, 2004).

Cs-isotope	**Decay**	**Intensity**	**Endpoint energy** (keV)	**Stable daughter nucleus**
^{134}Cs	β^- (99,9997%)	β_1^- (27,27%) β_2^- (2,399%) β_3^- (70,17%)	88.6 415.4 658	^{134}Ba
^{137}Cs	β^- (100%)	β_1^- (94,7%) β_2^- (5,3%)	513,97 1175,63	^{137}Ba

(Browne & Tuli, 2007). Stable and radioactive Cs$^+$ dynamics in organisms are not distinguishable. Adverse health effects deriving from Cs radioisotopes below ^{133}Cs toxicity levels are solely attributable to β^-- and ɣ - radiation and affect human health as described in section *1.3*. Consequently, distinctions to other β^-- and ɣ - emitters are predominantly determined by characteristics of the element itself and its biodynamics in organisms (Agency for Toxic Substances and Disease Registry, 2004).

Caesium radioisotopes can be incorporated into the human food chain via plant root uptake of crops (Rai & Kawabata, 2020). In addition, livestock can ingest contaminated plants which causes a subsequent contamination of animal foodstuff. The uptake rate of RC contaminated foodstuff ranges from 65 - 90% and is considered as comparatively high (Henrichs et al., 1989). After the CNPP accident, ^{137}Cs contaminated foodstuff displayed the major radiation exposure to the public (Fesenko et al., 2007). Due to the ionic similarities, it is assumed that Cs$^+$ and K$^+$ share plant uptake mechanisms (White & Broadley, 2000). There are high - affinity HAK, low - affinity inward - rectifying K$^+$ (KIR), outward - rectifying K$^+$ (KOR) and voltage - insensitive (VIC) channels which have proved Cs$^+$ permeability. KIR mediated uptake reveals different Cs$^+$/K$^+$ ratios, depending on the respective culture and ranging between 0.39 – 0.43 for barley, and 0.07 for *Arabidopsis thaliana* (Maathuis & Sanders, 1995; Wegner & Raschke, 1994). However, extracellular Cs$^+$ concentrations under normal ionic conditions in soils can block KIR transporters. In contrast, VICs are insensible towards extracellular Cs$^+$ and exhibit Cs$^+$/K$^+$ ratios of 0.85 for barley (White & Tester, 1992). VICs mediated Cs$^+$ uptake is predominantly found in environments with sufficient K$^+$ levels. It is assumed, that 30 - 90% of Cs$^+$ root uptake in stereotypical conditions is mediated by VICs (White & Broadley, 2000). Contrastingly, HAK transporters are expressed at low extracellular K$^+$ conditions. For instance, OsHAK1 in rice and AtHAK5 in *Arabidopsis Thaliana* proved to play a central role for Cs$^+$ uptake (Qi et al., 2008; Rai et al., 2017). However, Rai et al. (2017) found that HAK mediated transport was the major pathway for Cs$^+$ uptake even under normal extracellular K$^+$ conditions for rice plants. As plants merely take up nutrients that are dissolved in soil solution, it is crucial to consider ion´s soil solution concentrations (Jungk & Claassen, 1997). Naturally, $^{133}Cs^+$ concentrations in soils range from 0.3 to 2.5 µg g^{-1} and exhibit soil solution concentrations of approx. 10 µg L^{-1} (75 nmol). ^{133}Caesium concentrations are at least six orders of magnitude higher than those of $^{134/137}Cs$ (Rai & Kawabata, 2020). In contrast, K^+ is the fourth most abundant element in the earth´s crust and predominantly found in the upper most soil layers fixed in mica, illites and feldspars. Its concentrations in the earth's crust range around 20 g kg^{-1}, of which approximately 1 - 2% are considered as exchangeable and 0.1 - 0.2% as dissolved in soil solution, respectively (Britzke et al., 2012; Tsukada et al., 2002). Hence, the resulting K^+/Cs^+ ratio in soil solution is about 10^3 - 10^5. Overall, Cs^+ accumulation of plants grown in Cs^+ enriched solutions of different concentrations decreased by addition of extracellular monovalent cations. The order in which equimolar monovalent cations decreased Cs^+ uptake in an external 100 µmol Cs^+ solution was $Li^+ \leq Na^+ < NH_4^+ < Rb^+ \leq K^+$ (Figure 3). Divalent cations followed the order $Ca^{2+} \leq Mg^{2+} < Ba^{2+}$ at the same Cs^+ concentration (Bange & Overstreet, 1960; Handley & Overstreet, 1961). Studies of Shaw et al. (1992) indicated that the effect of competitor cations (NH_4^+ and K^+) is increased with raising external Cs^+ concentration. Higher K^+ and NH_4^+ concentrations decreased Cs^+ uptake compared to the control, while K^+ proved to more efficiently reduce Cs^+ uptake in *triticum aestivum* roots (Figure 3). This effect was confirmed by several other studies (Belli et al., 1995; Shaw et al., 1992; Smolders et al., 1997) and partly explained by higher Cs^+ efflux rates in presence of higher external K^+ concentrations that may induce the opening of KOR - channels and a subsequent Cs^+ leakage (Maathuis & Sanders, 1997; Zhu et al., 1999). External K^+ concentrations are a key element for RC uptake and find reflection in Cs^+ plant uptake modelling further explained in *1.6*.

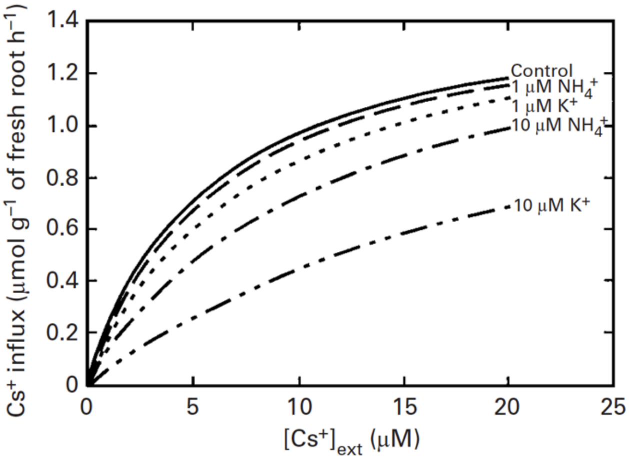

Figure 3: *Effect of different NH_4^+ and K^+ concentrations on the Cs^+ root uptake of wheat (triticum aestivum) in presence of 2mM Ca^{2+} (White & Broadley, 2000).*

1.5 Caesium - clay mineral interactions

Despite the high solubility of Cs^+ salts, Cs^+ is highly immobile in soils and mostly accumulated in the upper soil profile after atmospherical deposition (Almgren & Isaksson, 2006; Beckmann & Faas, 1992; Park et al., 2019a). Due to their cation adsorption capacities, organic matter and clay minerals influence Cs^+ dynamics in soils. Organic matter is subjected to frequent structural changes and hence exhibits different interactions with Cs^+. However, adsorption by functional groups of humic substances is negligible and organic matter can even hinder Cs^+ adsorption by clay minerals (Fan et al., 2014a; Loft et al., 2002; Sadhu et al., 2015; Uematsu et al., 2015). To better understand Cs^+ interactions with clay minerals, it is crucial to elucidate their central properties. According to the two major particle size fraction systems of the International Union of Soil Sciences (IUSS), and the Food and Agriculture (FAO)/United States Department of Agriculture (USDA), clay particles are defined by diameters ≤ 2µm (Takahashi et al. 2020). Much attention is paid to phyllosilicates which are characterized by continuous crystalline structures consisting of tetrahedral (T) and octahedral (O) layers. Recurring T-O layers are defined as 1:1, recurring sandwiched O-layers (T-O-T) as 2:1 and recurring T-O-T-O layers as 2:1:1 phyllosilicates (Figure 4). Isomorphic substitution of central cations in the tetrahedrons and/or octahedrons with cations of lower valency induces a net negative charge of those minerals, which is compensated by cations in the interlayers of T-O-T structures (Brigatti et al., 2013; Velde & Barré, 2009). In 2:1 clay minerals, interlayer cations exhibit different ionic radii and occur hydrated or dehydrated in dependence of the present phyllosilicate. The half unit cell ($O_{10}(OH)_2$) charges follow the order mica > vermiculite > smectite. For vermiculites and smectites, interlayer cations are exchangeable and hydrated under normal soil conditions. Additionally, lower charges allow intercalation of free H_2O molecules in interlayer spaces that induce expansions between layers, i.e., shrink and swell capacity (Kumari & Mohan, 2021). In contrast, micas exhibit charges which induce detachment of hydration shells and finally reduce the distance between T-O-T layers and inhibit H_2O intercalation. Their interlayers are mainly occupied by K^+ (Velde & Barré, 2009). Due to these properties, smectites and vermiculites are known to have higher cation exchange capacity (CEC) than micas. However, cation exchange also takes place on the planar external surfaces (“planar”) and broken bond sites (“edge”) of clay minerals (Figure 5 (a)). Planar and edge CEC is thereby mainly depended on the equivalent diameter and thickness of a clay particle (Carrier et al., 2016). Overall, these exchange sites are considered as regular exchange sites (RES) (Saha et al., 2001).

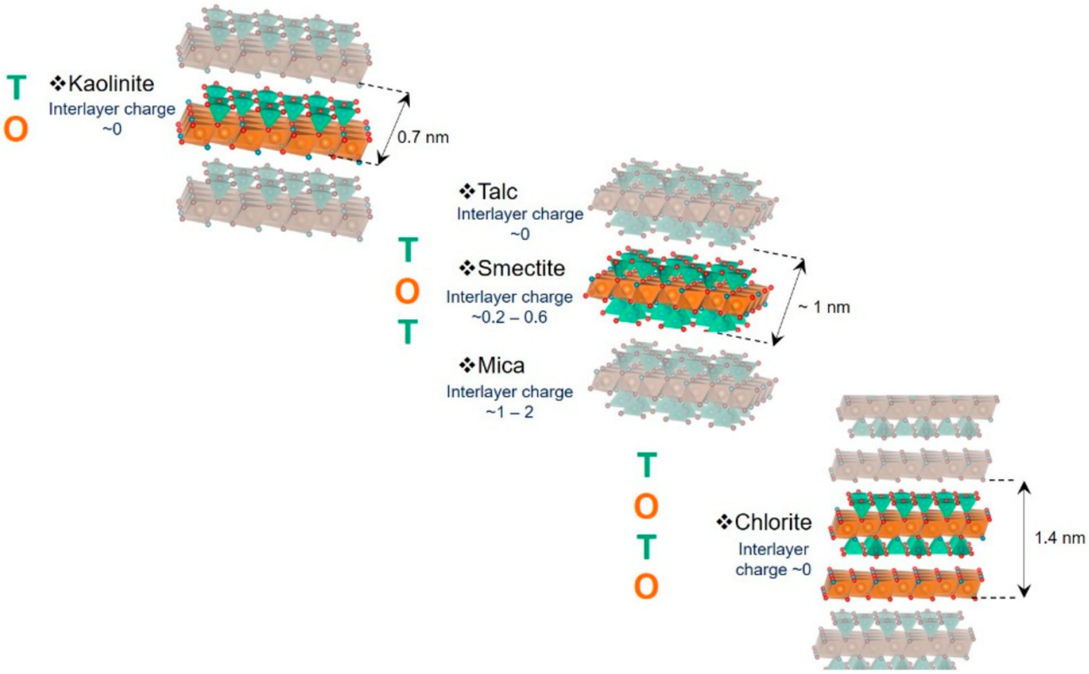

Figure 4: *Layer structures of phyllosilicates (Claverie et al., 2019).*

In equivalent cation exchange on RES, smaller hydrated radii are generally preferred (e.g.: $Cs^+ < Rb^+ < K^+$). In heterovalent exchange reactions, the higher charged cation is preferred (e.g.: $Al^{3+} > Ca^{2+} > Cs^+$) (Sparks, 2003). Caesium adsorption on planar or hydrated interlayer sites builds outer - sphere (OS) complexes, which are defined by relatively weak electrostatic bonding and short Cs-O interatomic distance. In contrast, inner - sphere (IS) complexes are characterized by relatively strong bonding and larger Cs-O interatomic distance (Park et al., 2019a). They occur on dissociated OH^- - groups of edge sites, dehydrated interlayers or frayed - edge sites (FES) of clay minerals (Fan et al., 2014a). Caesium selectivity on planar or edge exchange sites of clay minerals is low, while FES and interlayer sites exhibit high Cs^+ selectivity (Park et al., 2019a).

Frayed edge sites are weathering induced wedge - shaped zones between non - expansible (1 nm) and hydrated (1.4 nm) layers in mica (Figure 5 (b)). They account for approx. 0.1 - 2% of a soil´s CEC. To date, the exact mechanisms of cation adsorption on FES are not fully understood, although it is believed that the relative charge density, hydration radius, and hydration energy of the cation have a crucial influence (Park et al., 2019a). Adsorption onto FES follows the order $Cs^+ > NH_4^+ > Ba^{2+} > Ca^{2+} > Mg^{2+}$, which is equivalent to the hydration energy order. Moreover, the hydrated radii of Mg^{2+} and Ca^{2+} are significantly bigger than those of K^+, NH_4^+, and Cs^+, thus their adsorption on FES in hindered, although Ca^{2+} was found to facilitate Cs^+ intercalation due to edge expansion of illites (Benedicto et al., 2014). Further, hydrated Cs^+ has a slightly higher charge density than hydrated K^+ and NH_4^+, causing superior attraction force between FES and hydrated Cs^+. In addition, the hydration energy of Cs^+ is lower than that of K^+ and NH_4^+, facilitating water shell shedding and subsequent water transfer to dehydrated NH_4^+ or K^+ (Lee et al., 2017). Caesium fixation after FES adsorption can either be driven electrostatically and happen as an exchange reaction with dehydrated K^+ (or other cations) located on the edge of the not - expanded interlayer (Figure 6 (b)) or as an interlayer collapse (Figure 6(a)), after which new (pseudo) FES may develop (Absalom et al., 1995).

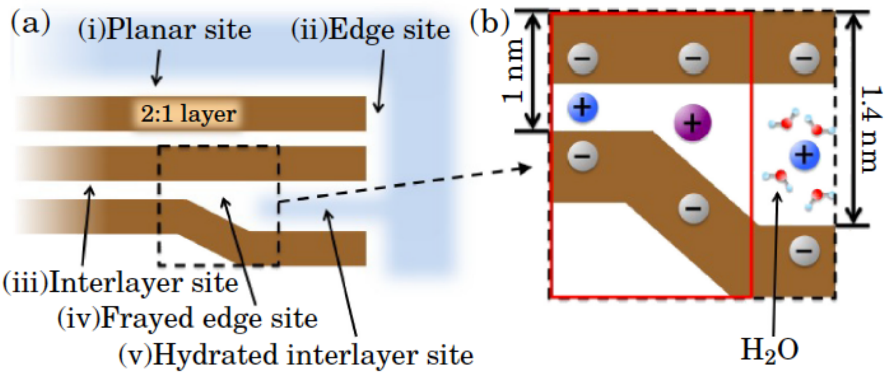

Figure 5: *(a) Structure and different exchange sites on a 2:1 clay mineral, (b) Structure of a FES (Okumura et al., 2013).*

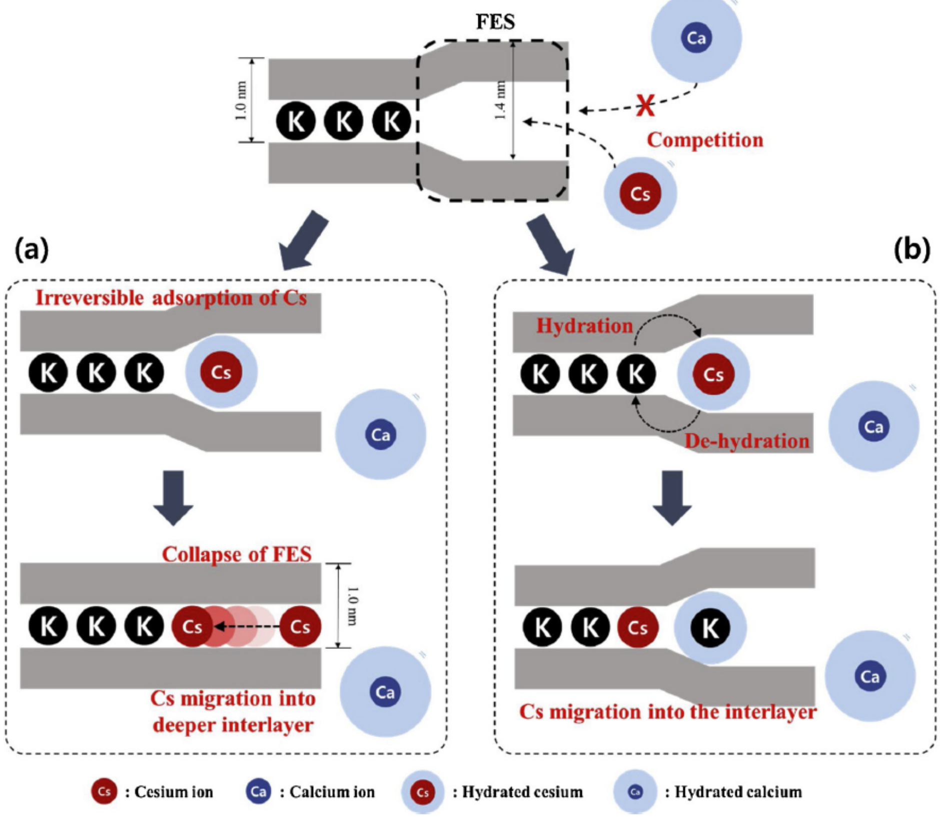

Figure 6: *Cs^+ Adsorption and fixation processes on FES, with (a) 2:1 interlayer collapse and (b) cation exchange reaction with K^+ (Park et al., 2019a).*

Once Cs^+ migrated into mica interlayers, it can hardly be desorbed (Figure 6). Moreover, basal spacing of Cs^+ (1.07 nm) occupied mica is slightly larger than that of K^+ (1 nm) and assumed to be more stable (Benedicto et al., 2014; Bergaoui et al., 2005; Fuller et al., 2015; Lee et al., 2017; Park et al., 2019a). It has been shown that Cs^+ fixation induced by an interlayer collapse at FES of micaceous clay is particularly caused by high external NH_4^+ (> 10^{-4} M), Cs^+ (> 8 x 10^{-7}) and K^+ concentrations (Absalom et al., 1995; de Koning & Comans, 2004). Due to irreversible adsorption of cations with low hydration energy and inaccessibility for cations with large hydration shells, FES cannot be determined by standard adsorption-desorption methods (Nakao et al., 2008a). However, Cremers et al. (1988) developed a method to determine the radiocaesium interception potential (RIP). The method makes use of the soild - to liquid distribution (K_D^i):

$$K_D^i = \frac{[FES]_i}{m_i} \tag{5}$$

where [FES] depicts the retained concentration on frayed edge sites and *m* the concentration in soil solution of the ion *i*, respectively. The RIP is described by:

$$RIP = K_D^{Cs} \cdot mK^+ = K_c^{FES}{}_{(Cs\text{-}K)} \cdot [FES] \tag{6}$$

where $K_c^{FES}{}_{(Cs\text{-}K)}$ is the trace selectivity coefficient of Cs^+ over K^+ on FES, and FES is the amount of frayed edge sites in mol kg^{-1}. $K_c^{FES}{}_{(Cs\text{-}K)}$ can be described by:

$$K_c^{FES}{}_{(Cs\text{-}K)} = \frac{K_D^{Cs}}{K_D^{K}} = \frac{(zCs^+ \cdot mK^+)}{(zK^+ \cdot mCs^+)} \tag{7}$$

where z_i stands for a FES - adsorbed cation. When the radiocasesium concentration vanishes, z_K converges to the total amount of FES:

$$K_c^{FES}{}_{(Cs\text{-}K)}\,(Cs \rightarrow 0) = \frac{(K_D^{Cs} \cdot mK^+)}{[FES]} \tag{8}$$

As $K_c^{FES}{}_{(Cs\text{-}K)}$ is a constant with a value of approximately 10^3 at extremely low Cs^+ concentrations (Wauters et al., 1996a), the amount of FES is proportional to $K_D^{Cs} \cdot mK^+$ and hence the RIP. If K_D^{Cs} and mK^+ are known, rearranging the formula to:

$$[FES] = \frac{RIP}{10^3} \tag{9}$$

yields the FES amount in mol kg^{-1} soil (Nakao et al., 2015).

Formation of FES and weathering of micaceous minerals may happen simultaneously and is therefore associated with each other. However, there are manifold assumptions on the exact mechanisms that may have an impact, among them vermiculization, vermiculitc layer charge and vermiculite interlayering of hydroxy - Al (Nakao et al., 2009). Thereby, hydroxy - Al interlayering in acidic soils and sediments near nuclear power plants proved to decrease vermiculitic layer charge and block FES (Elprince et al., 1977; Nakao et al., 2009). Moreover, investigations of Nakao et al. (2008b) suggested that vermiculization is closely related to the RIP (and hence FES) and can even be used as a predictor for it. In recent studies, artificially induced biotite weathering revealed that K^+ loss caused increased vermiculitic layer charge (Cs^+ - fixation) that was accompanied with FES formation in stages where biotite interlayers were only slightly enlarged (Ogasawara et al., 2017). However, this correlation vanished after advanced vermiculization although vermiculitic charge (Cs - fixation) still increased with increasing K^+ release. Thus, advanced vermiculization was not found to necessarily form FES and hence contradicted earlier assumptions. Further results revealed that far advanced vermiculization through K^+ depletion finally deleted all FES (Kitayama et al., 2020). Due to the high Cs^+ selectivity of interlayer sites, those might be responsible for Cs^+ fixation in the absence of FES (Fan et al., 2014b). Considering total Cs^+ sorption, partially vermiculized biotite exceeded fresh biotite, illite, smectite, kaolinite, halloysite, allophane and imogolite (Mukai et al., 2016a). Overall, the weathering state of micaceous clays can vary greatly and is strongly dependent on soil pedogenetic factors that have to be taken into consideration (Nakao et al., 2008b; Waegeneers et al., 1999).

Further relevant minerals in the context of Cs^+ adsorption/desorption processes in soils are zeolites. Zeolites consist of linked SiO_4^{4-} tetrahedrons which jointly exhibit microporous structures with inlet ports of different diameters enabling entrance for cations and H_2O (Figure 7) (Calvo et al., 2009; Ming & Mumpton, 1989). Isomorphic substitution of a lower valency cation (mostly Al^{3+}) in the SiO_4^{4-} tetrahedrons causes a net negative charge which must be balanced elsewhere in the structure (Colella & Wise, 2014). A general formula for zeolites can be depicted as:

$$(M_x^+, M_y^{2+})\left(Al_{(x+2y)}Si_{n-(x+2y)}O_{2n}\right)\cdot m\ H_2O \qquad (10)$$

where M^+ represents a monovalent and M^{2+} a divalent cation, respectively (Passaglia & Sheppard, 2001). The overall Si and Al/O ratio is 1:2 with an Si/Al ratio of ≥ 1:1 (Ming & Mumpton, 1989). Zeolite´s CEC ranges between 0.6 and 2.3 meq g^{-1} and is depended on isomorphic substitution. The cation selectivity of zeolites depends on the sizes of the micropores in which the exchange takes place. As certain cations are excluded, zeolites are often considered as “molecular sieves” (Schulze, 2005). Generally, high - field - strength cations (z/r > 2) often cannot reach zeolite´s exchange sites due to their large, hydrated radii. Moreover, higher charge density causes higher selectivity towards divalent cations, whereas lower charge density is associated with preference for monovalent cations (Ming & Mumpton, 1989; Salters, 1998). As an example, the naturally most abundant and globally used zeolite clinoptilolite exhibits a Si/Al ratio of 4.3 - 5.3 and a CEC of 225 cmol kg^{-1}. The selectivity order follows $Cs^+ > Rb^+ > K^+ > NH_4^+$ (Ames, 1960; Zhao et al., 1998).

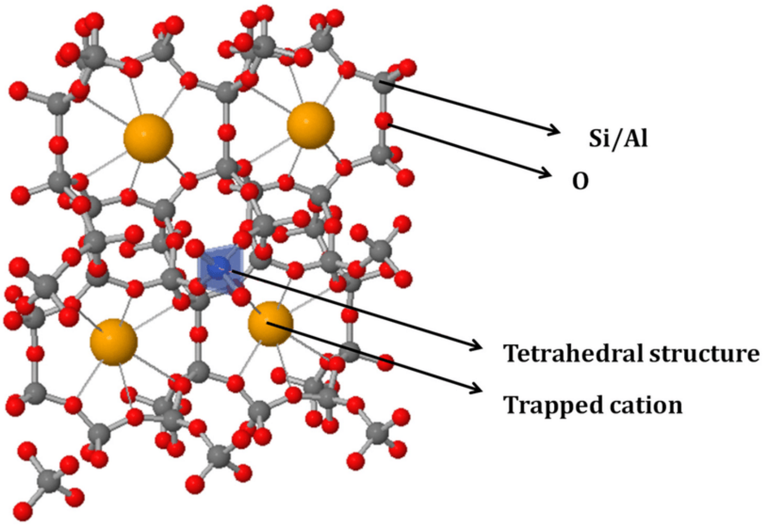

Figure 7: Ball - and stick model of the Zeolite Clinoptilolite (Mondal et al., 2021).

However, there are differences in zeolite´s Cs^+ selectivity. For instance, synthetically produced zeolite A with an Al/Si ratio of 1 exhibits least selectivity for Cs^+ among all alkali metals (Breck, 1973). For mordenite (Al/Si = 4 - 5), it was found that a uniformly distributed $Si^{4+} \rightarrow Al^{3+}$ substitution in the Cs^+ surrounding ring favours its binding capacity. As $Si^{4+} \rightarrow Al^{3+}$ substitution increases, the Cs^+ selectivity decreases, which is explained by an energetically more favourable state between smaller cations and the negatively charged tetrahedrons, so that a moderate substitution is most favourable for Cs^+ adsorption. Overall, micropore diameters should at least be 0.3 nm to allow entrance to Cs^+ (Okumura et al., 2013). Investigations regarding the Cs^+/K^+ selectivity coefficient ($K_c{}^i{}_{(Cs/K)}$) on clinoptilolite and natural as well as synthetic mordenite distinguished between three different sites with different abundances on the respective mineral. Highest $K_c{}^i{}_{(Cs/K)}$ values were obtained for least abundant exchange sites, although $K_c{}^i{}_{(Cs/K)}$ was ≥ 3.9 for all minerals and all sites. Overall, commercial mordenite (Zeolon) showed higher Cs^+ adsorption capacity than a reference clinoptilolite and a natural mordenite. Additional NH_4^+ hardly decreased $K_D{}^{Cs}$ at trace Cs^+ concentrations, which was in sharp contrast to observations on FES of micaceous minerals suggesting zeolite to work as an appropriate soil amendment in NH_4^+ rich environments such as peats (Valcke et al., 1997a). The effectiveness of a zeolite amendment on a soil´s K_D^{Cs} can be calculated by:

$$\text{Effect} = 1 + \frac{[RIP]_z \cdot f_z \cdot [mK^+ + k_4 \cdot mNH_4^+]}{[RIP]_s \cdot f_s \cdot [mK^+ + mNH_4^+]} \qquad (11)$$

where f depicts the mass of soil (s) and applied zeolite (z), respectively. Further, k_4 represents a selectivity coefficient for NH_4^+ over K^+ on FES which ranges between 4 - 7, depending on soil type and clay mineralogy (Bruneel et al., 2021; de Preter, 1990; Valcke et al., 1997b; Wauters et al., 1994). As $K_c^i{}_{(NH4\text{-}K)}$ for zeolites is approximately one, the factor was merely used for the soil fraction. However, these terms can be precluded in NH_4^+ poor environments (Valcke et al., 1997b).

Valcke et al., (1997b) checked this approach with experiments on twelve different soils using the same zeolites and found that the predicted effects would differ from experimental data within a factor of two while the amendments showed considerable effects in increasing K_D^{Cs}. As is indicated by Equation (11), a linear relation between the amendment effect and the applied wt% was confirmed. Overall, zeolite amendment effects seemed to be larger in soils with small RIP, which was confirmed not just for zeolite but also vermiculite amendments (Yamaguchi et al., 2019). Later, pot experiments conducted with spinach on a sandy podzol with low K_D^{Cs} revealed that the soil to plant transfer (discussed in *1.6*) was significantly reduced by 1 wt% zeolite amendment (Valcke et al., 1997c). However, mRC decreased stronger than the transfer factor (TF), which was explained by a simultaneous strong mK^+ decrease that is associated with RC plant root uptake mechanisms (discussed in *1.4*). Furthermore, the RC TF of sunflowers grown on a brown earth and an Andosol collected nearby the FDNPP was significantly decreased by clinoptilolite amendments, (Parajuli et al., 2016). This was explained by K^+ release from the minerals, particularly at higher application rates and has been reported in other studies but is contradicting the results of Valcke et al. (1997c) (Paasikallio, 1999; Parajuli et al., 2016; Shenber & Johanson, 1992; Yamaguchi et al., 2019). Another pot experiment performed on a peaty soil proved the effectiveness of zeolite amendments in NH_4^+ - rich environments (Shenber & Johanson, 1992). Differences to other clay mineral amendments were also investigated on a peaty soil and indicated that the RC TF was decreased until the first crop cut following the order clinoptilolite > heavy clay (illitic type clay) > bentonite > biotite > apatite; however, further cuts proved biotite to be more effective (Paasikallio, 1999). Experiments conducted on paddy fields affected by the FDNPP accident found zeolite to be limited and additionally less effective than vermiculite amendments in reducing the RC TF in rice plants (Kato et al., 2015). This was confirmed in a field experiment on a grey lowland soil likewise affected by the FDNPP accident, although insufficient quantity (1 t ha^{-1}) was considered as an explanation for the result (Kubo et al., 2015).

Moreover, Cs^+ adsorption/desorption experiments under laboratory conditions revealed that mordenite adsorption rates exceeded that of illite, montmorillonite, kaolinite, manganese oxide (MnO_2), halloysite and sericite at three different Cs^+ concentrations (Ohnuki & Kozai, 2013). The same study showed that $^{137}Cs^+$ desorption from mordenite was increased up to 80% following the exchange cation order $Li^+ < Na^+ < K^+ < Rb^+ < Cs^+$, while merely halloysite yielded higher desorption rates. Furthermore, the Cs^+ residual share of mordenite was independent of the Cs^+ adsorbate solution concentration, while that of illite strongly decreased with rising Cs^+ concentrations, which has been reported by Fan et al. (2014a) before (Ohnuki & Kozai, 2013). Consequently, the high Cs^+ selectivity of zeolites does not provide information about the Cs^+ retention strength (Fan et al., 2014b; Seaman et al., 2001; Yamaguchi et al., 2019). Zeolite amendments may increase the overall Cs^+ selectivity of soils, while the desorption risk may be increased due to reduced Cs^+ adsorption onto FES and interlayer sites (Yamaguchi et al., 2019).

1.6 Caesium soil - to - plant transfer

The transfer factor (TF) combines Cs^+ dynamics in soils with Cs^+ uptake mechanisms on plant roots. Generally, it describes the ratio of RC activity in the soil to that in the plant (Bq kg^{-1} plant/Bq kg^{-1} *whole* soil). Further, the concentration factor (CF) is defined as the ratio between Cs^+ concentration in the plant and its activity in soil *solution* (Bq kg^{-1} plant/Bq kg^{-1} soil solution) (Dahlgren, Saigusa, and Ugolini 2004). Finally, K_D^{Cs} describes the Cs^+ solid to liquid distribution. Thus, Cs^+ soil - plant interaction systems can generally be described by:

$$Cs_{soil} \underset{K_D^{Cs}}{\longleftrightarrow} Cs_{solution} \underset{CF}{\rightarrow} Cs_{plant} \tag{12}$$

The CF and the TF can then be deduced as:

$$CF = \frac{Cs_{plant}}{Cs_{solution}} \tag{13}$$

$$TF = \frac{CF}{K_D^{Cs}} \tag{14}$$

Studies of Smolders et al. (1997) investigated the RC TF for ryegrass on 30 different mineral soils. Regression analyses with soil properties as CEC, organic C, *p*H or exchangeable K^+ (ex. - K^+), as regressors for TF indicated insignificant effects, although later studies on organic soils contradicted that (Absalom et al., 2001; Sanchez et al., 1999). The major effects seemed to have mK^+ and K_D^{Cs}. Additionally, it was found that K_D^{Cs} and the TF correlated negatively in dependence of mK^+. Clay content as single regressor showed only little effect, as it increased K_D^{Cs}, but decreased mK^+ so that it was cancelled out. Hence, both regressors were considered simultaneously.

Similar investigations were conducted with 23 organic soils. The TF was positively correlated with organic matter content and was highest for soils with low K_D^{Cs}. In contrast to mineral soils, K_D^{Cs} was decreased by considerable mNH_4^+. In alignment with observations for mineral soils, mK^+ and CF correlated negatively, whereas this effect was not observable for mNH_4^+, as plant root uptake and NH_4^+ seems not to hinder Cs^+ uptake as drastically as K^+ (Figure 3) (Sanchez et al., 1999; Shaw et al., 1992). Overall, 94% of the TF variability could be explained by mK^+ and K_D^{Cs}. As K^+ levels in organic soils are generally lower, the CF median was one order of magnitude above that of mineral soils. The combined effects of increased mNH_4^+ and decreased mK^+ made organic soils significantly more prone for RC uptake (Sanchez et al., 1999).

Absalom et al. (1999) then presented a semi - mechanistic model in which ex. - K^+, clay content, inorganic CEC and initial RC activity in the soil were used as empirical base data. Exchangeable – K^+ and inorganic CEC should predict mK^+, which itself was used to calculate the CF. The clay content and mK^+ should determine K_D^{Cs}, which was again matched with mK^+ for determining the RIP. The total RC activity was matched with K_D^{Cs} considering time effects by distinguishing between slow and rapid RC adsorption to obtain mRC. Finally, this was merged with the CF to yield actual Cs_{plant}. The CF equation contained two empirical constants k_1, k_2 and k_{lim}, which describes the K^+ limit above which CF merges to a minimum value. The values for k_1, k_2 and k_{lim} were first taken from ryegrass models and subsequently tested for a better fit. For all crop species a highly significant ($p < 0.001$) better fit could be obtained, particularly in crops with little taxonomical and morphological similarities to ryegrass (potato and cabbage), indicating the importance of differentiating between species for modulations (Gerzabek et al., 1998; Nisbet & Woodman, 2000).

Later on, Absalom et al. (2001) developed a model for organic soils. The required input data for this model extended the previous one by mNH_4^+, organic matter (in %) and p*H* and caused a significantly ($p < 0.001$) better fit. A central addition was the further distinction between organic and inorganic CEC revealing differentiated K_D^{Cs} for humus and clay, respectively. Moreover, k_{lim} did not affect the model fit. As Sanchez et al. (1999) found mNH_4^+ to play an important role in organic soils, this was reflected in the following formula:

$$K_{D(clay)}^{Cs} = \frac{RIP \cdot clay}{(mK^+ + k_4 \cdot mNH_4^+)} \qquad (15)$$

where k_4 is a fitted parameter displaying higher selectivity of NH_4^+ over K^+ on FES as was already shown in Equation (11). A later check of the model using a wider range of soils, crops and times yielded better predictive power after omitting four model variables and one input variable (*p*H), additionally making the model less complex and more practical (Tarsitano et al., 2011).

After the FDNPP accident however, the application of the Absalom et al. (1999) model on Japanese soils revealed merely limited predictive power, although RIP and ex. - K^+ seemed to be the central predictors that control the RC TF on the affected soils. It was assumed that this was due to low RC selectivity of common clay minerals occurring in Japanese soils. Analyses of different globally sampled soil types showed the lowest RIP values for Andosols (< 2000 mmol kg^{-1}), a typical Japanese upland soil formed by volcanic ash containing considerable amounts of amorphous minerals and hardly micaceous clays (discussed in *1.8*) (Kögel-Knabner & Amelung, 2014; Matus et al., 2014; Uematsu et al., 2015; Vandebroek et al., 2012). Investigations of 51 soils sampled from areas affected by the FDNPP accident revealed that the slope of the RIP and clay content correlation was significantly lower ($p < 0.001$) than in Belgian soils, for which the clay mineral content was found to be the most significant parameter determining the RIP (Uematsu et al., 2015; Waegeneers et al., 1999). Furthermore, the slope for Andosols was even flatter than for other sampled soil types (Gleysol, Cambisol, Acrisol and Histosol), suggesting an RIP overestimation particularly for this soil type when applying the model of Absalom et al. (1999). This was also confirmed by Dengra I Grau et al. (2021) by means of empirical mCs^+ and mK^+ on an allophanic Andosol at low K^+ application rates, while at high rates ex. - K^+ underestimated mK^+ which compensated for the underestimated RIP and consequently overestimated the CF and TF. An adjusted model introduced by Uematsu et al. (2015) included the variables “loss of ignition” and CEC, whereby loss of ignition negatively and CEC positively influenced the predicted RIP, again emphasizing the low RIP of Andosols, which are rich in organic matter as previously confirmed by Takeda et al. (2014). However, organic matter did neither exhibit this effect in global nor in European investigations (Takeda et al., 2014; Vandebroek et al., 2012; Waegeneers et al., 1999). Finally, adjusted RIP predictions were on average one third and one tenth of Absalmom´s predictions for mineral and organic soils, respectively (Absalom et al., 1999, 2001; Uematsu et al., 2015, 2016).

Extensions of this study revealed that the model of Absalom et al. (2001) for organic soils also underestimated the TF with a factor of 10 in comparison to the TF deriving from measured mK^+ and RIP. This overestimation was assumed to be caused by an overestimation of mK^+, i.e., an underestimation of the CF, and an overestimation of K_D^{Cs}, even though the latter would have been compensated by overestimated mK^+, as indicated by Equation (15) (Uematsu et al., 2016). The model of Absalom et al. (2001) inferred mCa^{2+} and mMg^{2+} from the measured *p*H to finally predict mK^+. However, this approach resulted in mCa^{2+} and mMg^{2+} that were on average four-fold higher than empirical data. Using measured mCa^{2+} and mMg^{2+} was able to improve the mK^{+} prediction. Overall, different soil types (Andosol, Gleysol, Cambisol, Acrisol and Histosol) exhibited no significant effect on the TF, although Andosols indicated a tendency towards higher TF and a significantly lower K_D^{Cs} prediction, which was in alignment with earlier findings of significantly lower RIP values for Andosols (Dengra I Grau et al., 2021; Nakamaru et al., 2006; Uematsu et al., 2015).

1.7 Ammonium – Caesium interactions

The interactions between NH_4^+ and RC in soil - plant systems are characterized by several phenomena, of which most were already introduced in earlier sections. As NH_4^+ strongly influences RC dynamics in soils, it is crucial to elucidate some basic properties and applications of the latter. Almost 80 wt% of the NH_4^+ compound consists of N, which is quantitively the most abundant mineral in plants. Therefore, it is the central yield limiting factor in agricultural systems all over the world and hence the most frequently fertilised element. In soils, there are several organic as well as inorganic N - compounds that are transformed into one another along the N - cycle (Miller & Cramer, 2005). Basically, there are five different N - transformation flows in the N - cycle: Ammonification, nitrification, denitrification, annamox and organic matter assimilation and mineralization. Thereby, ammonification is considered as the reduction of atmospherical N_2 as well as dissimilatory and assimilatory reduction of NO_2^- to NH_4^+ or ammonia (NH_3). Nitrification comprises NH_4^+ oxidation via NO_2^- to NO_3^- and denitrification NO_2^- reduction to N_2. Furthermore, anammox can be described as a coupled reaction of denitrification and nitrification, as N_2 is formed from the NH_4^+ and NO_2^- pool simultaneously. Finally, organic matter assimilation and mineralization of NH_4^+ and NH_3 complete the N - cycle (Stein & Klotz, 2016). This cycle is fully controlled by microbial activity, which in turn is dependent on several soil conditions such as *p*H, moisture, aeration, temperature and redox potential (Dancer et al., 1973; Dorland & Beauchamp, 1991; Kralova et al., 1992).

Generally, plant roots absorb NH_4^+ and NO_3^- from the soil solution, even though NO_3^- uptake dominates on most agricultural soils (Miller & Cramer, 2005). However, low *p*H, low temperature as well as hydric and anaerobic conditions lower nitrification rates and result in NH_4^+ accumulation in soils (Subba Rao et al., 2017). In addition, dissimilatory nitrate reduction to ammonium (DNRA) contributes to NH_4^+ accumulation under anaerobic conditions, although its effect seems to be negligible and rather present in neutral and alkaline environments (Inselsbacher et al., 2010; Schmidt et al., 2011). In soils, NH_4^+ is mostly retained by cation exchange reactions on negatively charged particles, whereas NO_3^- is prone to groundwater leaching, particularly under humid conditions. This is not only of economical, but also of public health concern as elevated NO_3^- concentrations are cancerogenic and toxic to infants (Bohn et al., 1980). Moreover, the application of different types and forms of organic as well as inorganic N - fertilisers increases N - levels in soils artificially. While the use of NO_3^- and NH_4^+ successively declined since the 1960´s, the usage of urea (CH_4N_2O) has become more prominent and had a share of 50% among the globally applied N - fertilisers in 2000, even though NH_4^+ - fertilisers still had a share of at least 35% in Japan in 2016 (Association of Agriculture and Forestry Statistics Japan, 2021). Urea is not directly available for plant uptake but undergoes enzymatic hydrolysis in soils to form NH_4^+. Generally, there are advantages and disadvantages coming with NH_4^+ and urea fertilisers. On the one hand, (urea deriving) NH_4^+ is relatively immobile in soils, possesses higher specific N - content and avoids energy intensive plant intern NO_3^- to NH_4^+ reduction (Miller & Cramer, 2005). On the other hand, NH_4^+ application induces rapid soil acidification by root H^+ extrusion and nitrification that produces two H^+ per NH_4^+ to NO_3^- transformation, although this is counteracted by urea hydrolysis caused H^+ consumption (Gould et al., 1986; Marschner et al., 1991). In addition, NH_4^+ is prone to retention and fixation on FES and collapsed interlayers of micaceous clays (see *1.5*) (de Koning & Comans, 2004; Ross et al., 1985).

As NH_4^+ and Cs^+ exhibit the same charge and similar hydration radii, NH_4^+ application might generally induce Cs^+ desorption in cation exchange reactions on negatively charged particles in soils (Chiang et al., 2008). Given this, NH_4^+ was used for phytoremediation of RC polluted soils. Phytoremediation is an alternative to cost - intensive and environmentally harmful soil cleaning methods in case of moderate large area pollution (Baker et al., 1994; Salt et al., 1995). It is based on the principal of pollutant bioaccumulation in eligible plants such as cabbage and amaranth for RC (Dushenkov et al., 1999; Ioannides et al., 2003; Lasat et al., 1997). Consequently, knowledge about RC phytoremediation can help to elucidate the effect of NH_4^+ fertilisation under usual agricultural conditions. Several studies revealed that NH_4^+ salts are most successful for Cs^+ desorption in soils. However, NH_4^+ effects on RC bioaccumulation are limited and ambiguous to date.

Studies of Sun et al. (2019) revealed that the TF for brown rice grown on soils affected by the FDNPP accident was significantly increased by $(NH_4)_2SO_4$ application. Furthermore, pot experiments performed with RC contaminated soils from the CNPP region showed that $(NH_4)_2SO_4$ caused highest RC desorption and subsequent bioaccumulation among 20 tested amendments. However, later field experiments could not confirm these findings, although $(NH_4)_2SO_4$ showed slightly better effects than NH_4NO_3 (Dushenkov et al., 1999). Lasat et al. (1997) found significant RC phytoextraction after NH_4NO_3 application in a pot experiment with four different plant species, while doubling the application rate did only show further significant effects in one culture (cabbage). Ioannides et al. (2003) found NH_4^+ to increase and K^+ to decrease the RC TF, which was explained by higher Cs^+ desorption capacities of NH_4^+ and stronger Cs^+ uptake depression induced by K^+. Similarly, Paasikallio & Sormunen-

Cristian (2002) reported that NH_4^+ fertilisation significantly increased the RC TF of ryegrass on a peat soil but biotite applications would mitigate the effect due to the release of K^+. However, further studies found no clear evidence that NH_4^+ application affects bioaccumulation, TF and percentage of RC removal (Fuhrmann et al., 2003; Lasat et al., 1998; Sugiura et al., 2016). Overall, these ambiguous findings may partly be explained by different NH_4^+ application amounts, NH_4^+ percolation, NH_4^+ plant toxicity, and discrimination of RC root absorption in presence of excessive NH_4^+ concentrations (Dushenkov, 2003; Lasat et al., 1998, 1997; Shaw et al., 1992; Sugiura et al., 2016).

1.7 Geology, pedogenesis and climate of Europe and Japan

Due to the CNPP accident in 1986, mainly European soils were investigated in the context of RC dynamics. Deepened investigations on Japanese soils began only from 2011 on, hence after the FDNPP accident. As stated afore, prediction models for RC crop uptake have been proven sufficiently successful for European soils but lacked precision for Japanese soils. To better understand the differences between European and Japanese soils and consequently their influence on RC dynamics, it is crucial to elucidate their fundamental geological, pedogenetic and climatic properties. Present day Europe is part of the Eurasian plate and surrounded by 12 large and many further small plates. Europe´s growth began approximately 3.5 ga ago with the formation of extensive greenstone and granite - gneiss terraces, which are to date merely exposed but mostly covered by sedimentary rocks. Sedimentary rocks are thereby either still flat - lying as for instance in the Russian platform or deformed and metamorphized in orogenic belts such as the Alps or Pyrenees (Berthelsen, 1992). Further, Europe is roughly divided into an older and stable Precambrian craton ("Baltic shield") and a younger and more mobile Phanerozoic belt, consisting of crustal fragments successively attaching to the ancient European nucleus. The first is extending over north - eastern and the latter over southern and western Europe (Plant et al., 2005). While northern European landscapes are often shaped by Pleistocenic glaciation, southern Europe is typically stronger affected by seismic activity and hence orogenesis (Cvetkovic et al., 2015; Mather, 2009; Plant et al., 2005).

The world reference base published by the food and agriculture organization (FAO) reveals 32 reference soil types, of which 23 occur in Europe (Tóth et al., 2008; World Refernce Book, 2014). Luvisols (14.74%), Podzols (13.67%), Cambisols (26.71%) and Leptosols (10.51%) represent two thirds of the European soils. Thereby, Luvisols and Cambisols can be found all over the European land mass, while Podzols are mainly concentrated in northern and Leptosols in southern Europe (Figure 8). Mineral soils amount for nearly 95%, while their formation is in most cases conditioned by their limited age, the topography/physiography of the terrain or the climate in (sub-) humid temperate regions (Tóth et al., 2008). Sandy soils are prevalently found in northern Europe and indicate glacial transport of coarser particle fractions (Ballabio et al., 2016). The extent of the last glacial maximum is clearly designated by an abrupt transition into soils dominated by finer particles, which are deriving from fluvial outwash of sedimentary rocks and loess depositions (Haase et al., 2007). Elevated clay contents are mostly found on soils that developed on sedimentary rocks, particularly limestone and claystone, as in the Mediterranean regions (Ballabio et al., 2016; Durn et al., 1999). Generally, the clay fraction of western Europe is dominated by dioctahedral mica such as muscovite or its weathered derivative illite (Ito & Wagai, 2017; Mengel et al., 2001).

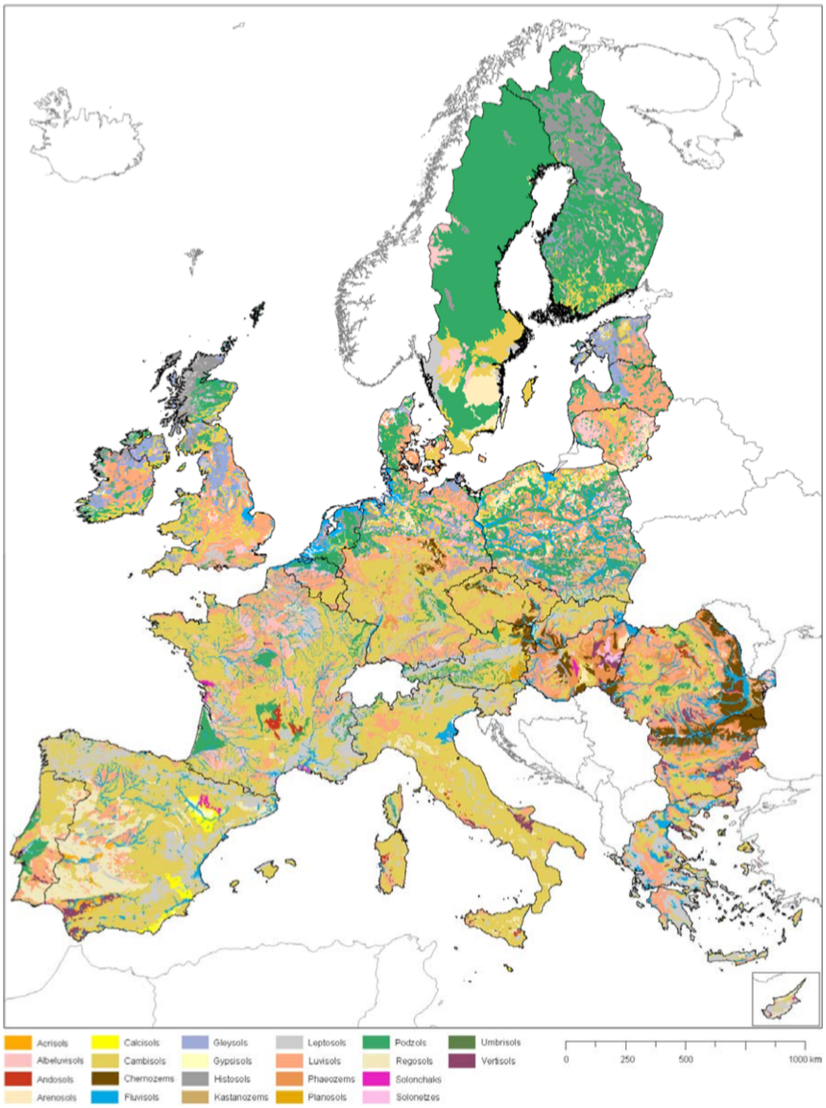

Figure 8: *Soil map of the European Union according to the soil types defined by the World Reference Base for Soil Resources 1998 (Spaargaren & Deckers, 1998).*

Due to stronger repulsive forces between interlayer K^+ and H^+ in the octahedral layer and the high solubility of Fe^{2+}, trioctahedral mica such as biotite exhibits higher tendency towards weathering than dioctahedral mica and is hence seldomly found in old European soils

(Bisdom et al., 1982; Bonneville et al., 2016; Mengel et al., 2001; Nanzyo & Kanno, 2018; Sugimori et al., 2008). Moreover, there are small patches spread all over Europe in which smectites or kaolinites are dominant. The east European plain is in turn dominated by kaolinite (Ito & Wagai, 2017).

Another aspect majorly contributing to pedogenesis is climate, which is basically distinguished by temperature and precipitation. Those factors are interacting and generally determine occurrence and speed of chemical reactions, biological activity, translocation of soil material and eventually soil weathering (Anderson et al., 2004; Jenny, 1994). According to the Köppen - Geiger system, four climate types are present in Europe. They comprise continental (D), arid (B), temperate (C) and to a minimal extent polar (E). Generally, phenomena as the jet stream, the Gulf stream and the positive phase of the north - Atlantic oscillation (NAO) are assumed to cause milder climate in Europe compared to north - west America and north - east Asia on similar latitudes (Peel et al., 2007). Moreover, Europe exhibits a climate shift from maritime to continental in east - western and from arctic to Mediterranean in north - southern span. Temperate climate is hence predominantly found in Mediterranean and mid - western Europe while cold climate characterizes north- and mid-eastern Europe (Maracchi et al., 2005). In particular, the CNPP lays in mid - eastern Europe and is thereby distinguished by continental climate with warm summers but missing dry season, regarding the Köppen - Geiger system (Peel et al., 2007). Adversely, it is assumed that climate change will significantly alter the pedogenesis of central European soils in the future, mainly due to temperature and hydric regime changes favouring salt accumulation and erosion accompanied by agricultural productivity loss (Trnka et al., 2013).

In contrast, Japan is an archipelago comprising 6,852 islands situated off the east Asian mainland. Thereby, the five main islands Honshu, Shikoku, Kyushu, and Hokkaido have a share of over 95%. Japan´s geological history began with the formation of a passive margin on the south China block and its subsequent uplift by subduction of the Paleo - Pacific plate (Wakita, 2013). Since then, Japan is located on a convergent margin causing high seismicity to the present (Tsuru et al., 2000). The islands exhibit unconsolidated sediments, sedimentary, igneous, and metamorphic rocks that mainly date from the Cambrian to the Quaternary period, although a Precambrian basement is assumed (Shibata & Adachi, 1974; Tagiri et al., 2011; Wakita, 2013). While paleozoic rocks are rarely found, Cenozoic and Mesozoic rocks are widely distributed over the island. Neogene sedimentary and volcanic rocks are distinctive for Japan´s east, while youngest Quaternary sediment occurs in alluvial plains near the coasts and volcanic rocks from active volcanoes (Wakita, 2013). To date, there are more than 111 active volcanoes, shaping Japan´s landscapes and majorly contributing to its pedogenesis (Tamura et al., 2021).

Japan exhibits immature soils that formed within the last 10,000 a from volcanic tephra or ejecta and mountain eroded material sedimented in alluvial plains (Hatano et al., 2021). According to the WRB classification system, Cambisols (38%), Andosols (31%) and Fluvisols (13%) are the dominating present day soil - types (Figure 9). Thereby, Cambisols are usually found in mountainous areas far from active volcanoes all over the Japanese archipelago. Fluvisols are predominantly present in flood plains and river deltas on the main island Honshu. Andosols are distributed over the east of Hokkaido, Kyushu´s south and the north and the east of the main island Honshu, where the FDNPP is located (Kanda et al., 2018). As Andosols are hardly represented in Europe, their occurrence denotes a central distinction between European and Japanese soils, particularly when considering their importance regarding upland farming in Japan. Andosols are built upon volcanoclastic, vitric material and exhibit distinctive characteristics as low bulk density, high water retention and phosphate fixation, variable charge as well as high organic matter content (Shoji et al., 1993). About 70% of the Japanese Andosols are considered as allophanic, meaning that allophane and imogolite are the dominating clays, while 2:1 and 2:1:1 layer silicates are dominating the remaining 30% non - allophanic Andosols (Saisuga & Matsuyama, 1998). The absence of allophane and imogolite is assumed to be caused by acidic soil conditions inducing the dissolution of $Al(OH)_3$ with subsequent Al^{3+} intercalation in 2:1 clay minerals and the formation of Al - humus complexes, hindering Al^{3+} hydrolysis and polymerization which is necessary for allophane and imogolite formation (Dahlgren et al., 2004). Non - allophanic Andosols are additionally characterized by older tephra deposits that are generally more acidified and assumed to have been exposed to mainland Asian loess depositions rich in 2:1 clay minerals (Eguchi et al., 2012; Mizota et al., 1990; Mizota & Matsuhisa, 1985; Saisuga & Matsuyama, 1998). In the context of RC soil pollution, it is noteworthy that soils in the eastern Fukushima prefecture are predominantly built upon granitic parent material that contains considerable amounts of biotite (Ogasawara et al., 2019, 2020). As indicated earlier, biotite shows quicker K^+ depletion and hence formation of FES than dioctahedral muscovite, which might strongly contribute to a reduced RC TF in those areas.

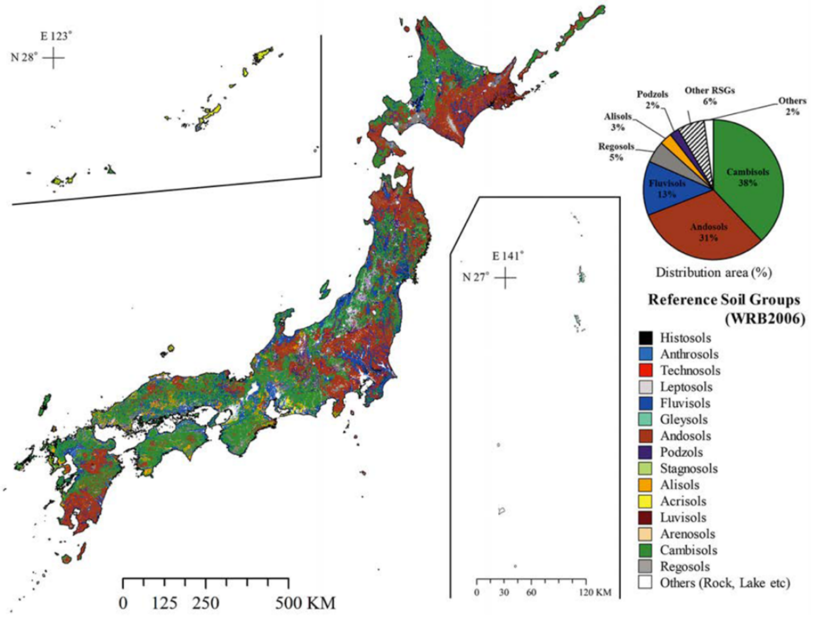

Figure 9: *Soil map of Japan according to the soil types defined by the World Reference Base for Soil Resources 2006 (Kanda et al., 2018; World Refernce Book, 2006).*

Japan´s heterogenous and complex climate derives from its wide vertical north - south span, topographical characteristics, the monsoons, the ocean currents, and the proximity to the Asian mainland (Hatano et al., 2021; Kamoshita, 1959). According to the Köppen - Geiger system, Japan exhibits diverse climate classifications, extending from subarctic to subtropical (Peel et al., 2007; Tamura et al., 2021). As Japan lays in the northern hemisphere, annual mean temperatures are generally increasing with decreasing latitude, although altitude differences must be considered. In turn, precipitation patterns are season depended. The side of the Sea of Japan experiences winter monsoons in the form of heavy snowfalls caused by prevailing northwesterlies carrying cold Siberian air. Instead, the Pacific Ocean side is strongly affected by the summer monsoon raised by southeasterlies advecting moist and warm air from the subtropical high of the Pacific Ocean (Issar, 2003; Kamoshita, 1959). The humid climate is also reflected in pedogenesis by widespread soil nutrient elution and soil acidification. As climate change is assumed to affect higher latitudes more severely, the predicted average temperature rise in Japan (4.5°C) lays above the global average (3.7°C) by the end of the 21st century. This could cause a shift of climate zones and significant alterations in pedogenetic processes (Tamura et al., 2021).

2. Objectives and hypotheses

On April 1st in 2019, the International Atomic Energy Agency (IAEA) approved upon a new Coordinated Research Project (CRP) D.1.50.19 with the title “Remediation of Radioactive Contaminated Agricultural Land” in order to “*enhance readiness and capabilities of societies for optimizing remediation of agricultural areas affected by large-scale nuclear accidents through innovative monitoring, decision-making and prediction techniques*” (International Atomic Energy Agency, 2019). A specific objective of this CRP is the field monitoring and modelling of RC transfer into the human food chain and its dynamics in underexplored agro - ecological environments, such as under monsoonal, arid, and tropical climate, in order to optimize remediation of radioactively contaminated agricultural land and hence preserve food security (International Atomic Energy Agency, 2019).

Knowledge about RC dynamics in soil - plant systems is strongly required to remediate the impact of nuclear accidents on food and agriculture. Remediation can be carried out through a wide range of measures. Hence, research focused on possible influencing soil parameters to develop eligible soil amendments and models that were supposed to control its dynamics and uptake by crops. Specifically, clay mineral amendments and K^+ fertilisation were investigated, as these measures increase the RC retention in soils and discriminate RC from plant root absorption, respectively. Some studies addressed the favoured effect of NH_4^+ induced RC desorption in the context of phytoextraction. However, little attention has yet been paid to unintended RC mobilization resulting from NH_4^+ fertilisation, which is globally practiced on agricultural soils. In addition, ambiguity regarding the predictive power of RC TF models and the effectiveness of clay mineral amendments proved to be crucially caused by differences in climate conditions, pedogenesis and land use. The risk of unsuitable clay amendments and NH_4^+ fertilisation urge for up - to - date data from distinct soils to ensure better preparedness and response in case of a nuclear event and subsequent RC soil contamination.

With respect to the CRP - D1.50.19, an attempt was made to elucidate the effect of an NH_4^+ fertilisation on mCs^+ in dependence of a soil´s clay mineralogy, clay mineral amendments and elapsed time. The influence of heterogenous land use, pedogenesis, and climate characteristics was considered by choosing five different soil types (three Japanese, one Austrian, one Belarussian) for the experiment. Solely an allophanic Andosol with low RC selectivity was additionally treated with smectite, vermiculite and zeolite (clinoptilolite) applications at rates of 10 t ha^{-1} and 40 t ha^{-1}, respectively. It is hypothesized, that NH_4^+ induced RC desorption is weaker on soils possessing considerable amounts of micaceous and vermiculitic clays. In case of the allophanic Andosol, clay amendments are assumed to have the capacity to buffer this effect. Moreover, it is foreseen that mNH_4^+ will vanish over time as it is prone to fixation and nitrification and hence loses its competitive character towards RC. Calculating the RC CF and consequently the RC uptake of ryegrass with empirical mK^+ and mCs^+ as suggested by Smolders et al. (1997) should give an idea of the actual risk of NH_4^+ - fertilisation and the relative benefit of a clay amendment on a soil with low RIP. Critically reflecting and discussing these findings with existing European and Japanese literature aims to contribute to more appropriate and locally adapted fertilisation techniques and countermeasure recommendations in the context of RC soil remediation. An insight of this study might be the underestimation of NH_4^+ - induced RC desorption that occurs globally on fertilised soils and promotes RC crop absorption. However, NH_4^+ induced K^+ desorption might compensate this effect, as it discriminates Cs^+ from plant root absorption. Eventually, the newly generated data is admittedly spatially limited to Europe and Japan but may still provide useful information for regions that have not suffered from a nuclear aftermath yet.

3. Material and Methods

3.1 Soil collection

In total, two European and three Japanese soils were used for this experiment. An attempt was made to choose soils that are relevant in the context of either the FDNPP or the CNPP accident but differ in major clay mineralogy, pedogenesis, particle size fractionation and type. The first European soil was sampled form a fertilisation and crop rotation long - term trial plot in Groß - Enzersdorf (48° 14’ N, 16° 33’ E; altitude: 153 m a.s.l.), located in an agriculturally important region in eastern Austria. The sample was taken from a plot that has been subjected to a fallow – winter rye – spring barley crop rotation without fertilisation since 1906. Overall, the soil is considered as a (micaceous) silty loam and classified as a Chernozem with high content of calcareous sediment (Neugschwandtner et al., 2020). Chernozems are highly productive soils built upon aeolian or glacial till sediments (Jordanova, 2017). As they typically occur in the central and eastern European steppe, approximately 30% of the CNPP accident affected soils were classified as such (Dutov et al., 2021; Kögel-Knabner & Amelung, 2014; Komissarova & Paramonova, 2019). The second European soil was sampled in Deshchenka, central Belarus, approximately 450 km north - west off the CNPP compound. The region is characterized by the gentle - wavy Stolbtsovskaya plain composed of loess - like rocks and poorly productive sod - podzolic (boggy) soils. More precisely, the sampled soil is classified as a Sod - Podzolic sandy loam build upon Pleistocenic glacial till and underlain from 1 m depth on by a glacial moraine. Podzols represent approximately 66% of the CNPP accident contaminated soils. In contrast to Chernozems, podzols are relatively infertile soils with less RC selective clay minerals, bearing the risk of RC uptake (Alexakhin et al., 2006; Singh et al., 2014). The first Japanese soil was sampled in the Miyakonojo municipality (Miyazaki prefecture) and follows the definition of an Andosol with lack of 2:1 phyllosilicates. It developed from repeated volcanic ash depositions between 23,000 and 88 YBP, which is reflected in a multi - stories soil profile. The dark colour of the profile derives from highly humified humic acids and soil organic matter shares up to 21%. Typically, non - crystalline clay minerals distinguish the Miyakonojo soil, with allophane and imogolite dominating in the upper soil layers and silica enrichment inducing halloysite formation in deeper layers (Shoji & Takahashi, 2002). A kaolinitic Cambisol with significant amounts of vermiculite was sampled in Yoshiki, prefecture Fukuoka, located in northern Kyushu. Although the soil profile has not been well described yet, ex. - K^+ seems to be below average values for that region, suggesting considerable K^+ fixation in vermiculite interlayers (Mori et al., 2012). The last soil was sampled close to the former Hachirogata lake in the Akita prefecture, located on the north - western coast of the Japanese main island Honshu. It is classified as a strong Gleysol with heavy clay texture. Dominance of smectitic clays, high organic matter content and the presence of large quantities of silt - sized (10 µm) cylindrically formed diatoms contribute to a plasticity index exceeding the value 100 (Nishida & Sato, 2016). The porous structure of the diatom frustules additionally induces increased water - holding capacity while their chemical composition (SiO_2) increases the soil´s Si/Al ratio (Kiuchi et al., 1961; Tanaka, 2007).

3.2 Sample preparation

3.2.1 Soil incubation

Before sampling, all soils were air - dried, sieved to 2 mm particle size, and stored in trunks at room temperature. Sampling was conducted for four sampling dates, namely 1, 8, 22 and 36 days after the incubation start. This was performed due to expected nitrification processes over time. Additionally, every variant was fertilised in an equivalent of 300 kg NH_4^+- N ha^{-1} (in the form of $(NH_4)_2SO_4$) or not, as NH_4^+ is a worldwide commonly applied N - fertiliser and 300 kg ha^{-1} an average given dose. Each sample was triplicated, which finally resulted in 4 (sampling dates) x 2 (fertilisation) x 3 (replicates) = 24 samples per soil. As Miyakonojo furthermore received three clay mineral treatments (smectite, vermiculite, zeolite) at two different application rates (10 and 40 t ha^{-1}) by independent addition per sample, six artificial soils were produced. In total, 11 distinct soils with 24 samples each gave 264 samples (Figure 10). Prior to the incubation, individual amounts of soil were weighed into 185 mL circular - cylinder shaped plastic containers (Art Nr. 10336210; FloraCura, Garmisch-Partenkirchen, Germany), pre - incubated for 14 days and irrigated with deionized water to 50% water - holding - capacity (WHC) (Table 4). Furthermore, the samples were covered with a piece of aluminum foil which was perforated with a needle to ensure little gas exchange while preventing desiccation of the sample. By the end of the pre - incubation time, the samples were emptied on aluminum foil, watered with either deionized water or with $(NH_4)_2SO_4$ dissolved in deionized water to 60% WHC and turbated (Table 4). Note, that the fertiliser application amount was calculated assuming a topsoil depth of 15 cm. Afterwards, the samples were transferred back into the containers and again covered with perforated aluminum foil. On each sampling date, samples were partly prepared for immediate soil solution sampling and partly air - dried for later analysis of *p*H, CEC, ex. - K^+ and ex. - NH_4^+, NO_2^- and NO_3^-. To prevent nitrification as effectively as possible, the soils were thinly spread for the air - drying procedure.

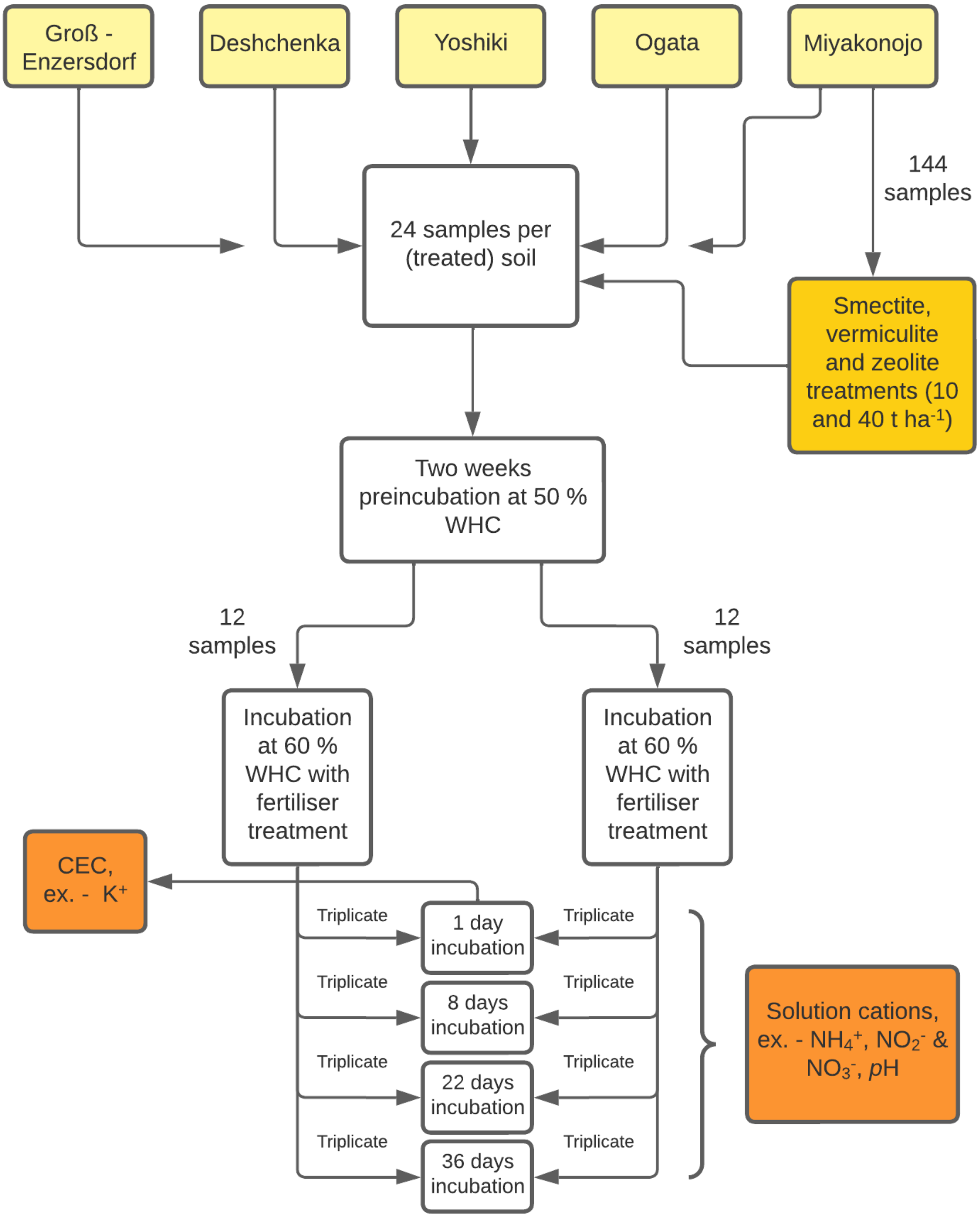

Figure 10: *Flow-chart of the experimental design. Bulk soil analyses are not depicted.*

***Table 4:** Preliminary measured, calculated and specified data for the experimental procedure.*

Soil	**Soil weight in container** (g)	**Topsoil bulk density** (kg $(dm^3)^{-1}$)	**Water addition at 60% WHC*** (L kg^{-1} OD soil)	**Fertiliser addition** (mmol NH_4^+ - N kg^{-1} OD soil)
Groß - Enzersdorf	155	1.27	0.23	11.26
Deshchenka	160	1.38	0.2	10.39
Yoshiki	140	1.25	0.27	11.43
Ogata	140	1.03	0.43	13.91
Miyakonojo	120	0.88	0.54	16.23

** Dividing the values by 0.6 and subsequently multiplying by 0.5 gives the water amount added at 50% WHC.*

3.2.2 Clay mineral pre - treatment

All investigated clay minerals were subjected to K^+ depletion and subsequent *p*H adjustment prior to their application onto Miyakonojo. The K^+ depletion of smectite followed the method of Noble et al. (2001). Therefore, 25 g of purified bentonite (Kunipia F; Kunimine Industries, Tokyo, Japan) were filled into 250 mL centrifuge bottles in duplicate and either filled up with 100 mL of 0.5 M $CaCl_2$ or $MgCl_2$, vigorously shaken by hand and again filled up with another 100 mL of the respective solutions. Thereafter, the bottles were centrifuged at 2,000 rpm for 5 min and the supernatants discarded. This process was once repeated and subsequently three times repeated with deionized water instead of the salt solutions. Then, the process was performed a fourth time without a subsequent centrifugation, allowing the clay particles to disperse. Ultimately, the $MgCl_2$ and the $CaCl_2$ treated minerals were mixed in a 3:1 ratio and dried at 50°C. The vermiculite K^+ depletion was adopted by Eguchi et al. (2015) and performed with phlogopite powder (Matale, Sri Lanka; distributed by Japan Mica Industries, Tokyo, Japan). First, the powder was dispersed into water, vigorously shaken and the 20 µm fractions separated by sedimentation. An aliquot of 50 mg was weighed into a plastic bottle and 1 L of 0.2 M Na - Tetraphenylboron (TPB), 1.7 M NaCl and 0.01 M Na - ethylenediaminetetraacetic acid (EDTA) was added. The bottle was left for two weeks, occasionally shaken, and subsequently transferred into four 250 mL plastic bottles. After the clay particles sedimented, the supernatant was discarded and 150 mL of a 60:40 (v/v) acetone (C_3H_6O) to water solution containing 1.7 M NaCl was added to each respective bottle, which were then rigorously shaken by hand. Thereafter, the bottles were centrifuged at 2,000 rpm for 5 min. and the supernatants discarded. This process was repeated thrice. Then, one bottle was filled up with 100 mL of 0.5 M $MgCl_2$ and the remaining ones with 0.5 M $CaCl_2$. All bottles were vigorously hand - shaken, the solutions transferred into 1 L glass beakers and the $MgCl_2$ and $CaCl_2$ solutions filled up with 900 mL of 0.5 M $MgCl_2$ and 0.5 M $CaCl_2$ solutions, respectively. The beakers were left until the clear supernatant could be discarded. In total, this process was repeated twice with the respective salt solutions and subsequently twice with deionized water. In a last step, deionized water was added to the clay particles, the $MgCl_2$ and $CaCl_2$ treatments mixed in a 3:1 ratio and subsequently dried at 50° C. The zeolite pre - treatment followed the procedure suggested by Dengra I Grau et al. (2021). Therefore, 100 g of 1 - 2 mm zeolite (Iwamilite, MINDECO) was weighed into 2 L plastic bottles in duplicate. The bottles were filled up with 2 L of 1 M NaCl solution and dried at 100°C for 20 h with lids loosely screwed on. Afterwards, the supernatants were discarded and the process once more iterated. Then, the bottles were made up with 1 L of 0.5 M $MgCl_2$ and 0.5 M $CaCl_2$, respectively, and left again for 20 h at 100°C. The supernatant was discarded, and the process repeated twice. The same process was subsequently conducted with 2 L deionized water instead of 1 L salt solution. After the last supernatant decantation, the bottles were dried at 50°C and $MgCl_2$ and $CaCl_2$ treated clays were mixed in a 3:1 ratio. The *p*H adjustment followed the same procedure for each respective clay mineral and aimed for the natural *p*H of Miyakonojo to avoid clay induced *p*H change that may affect nitrification rates. First, 50 mg of the respective mineral was weighed into a 2 L glass beaker to which 2 L of deionized was added. The *p*H was adjusted with 1 M HCl until a value of 5 - 5.1 was reached, whereupon the suspension was left for 1 h. If the *p*H did not exceed a value of 5.2 afterwards, the supernatant was investigated for its electrical conductivity (EC). Otherwise, deionized water addition and *p*H adjustment had to be iterated. If the *p*H was below 5.2 but the EC was above 0.4 mS cm^{-1}, the process had to be iterated again from the addition of 2 L deionized water on until the EC fell below the desired threshold.

3.3 General physicochemical properties

3.3.1 pH

The *p*H measurements were conducted for all samples and adapted from Wolt (1994). Therefore, 5 g of soil were weighed in and transferred into 50 mL centrifuge tubes, filled up with deionized water and shaken for 1 h on a linear shaker. Immediately afterwards, the samples were again shortly and roughly shaken by hand and a *p*H-electrode (WTW SenTix 41) that was connected to a portable meter (WTW ProfiLine pH 3100) was immersed and gently stirred until a stable value was reached.

3.3.2 Cation Exchange Capacity

Cation exchange capacity (CEC) was determined by means of the 1st day samples. Therefore, the fertilised and unfertilised air - dried samples were separately mixed, containing 10 g of each replicate, respectively. This was conducted twice, so that two replicates were obtained for both the fertilised and the unfertilised variant. The analysis followed the protocol 11260:2018 of the international organization of standards (ISO) and was earlier suggested by Kubo et al. (2018) for Japanese soils to avoid an overestimation on soils with significant *p*H dependent charge and an underestimation on soils with vermiculitic clay composition that fixes NH_4^+ when using conventional NH_4OAc. First, 2.5 g of air - dried soils were weighed in, transferred into a 50 mL centrifuge tube, and filled up with 30 mL 0.1 M $BaCl_2$. Afterwards, the tubes were shaken for 1 h and subsequently centrifuged for 10 min. at 3,000 rpm. The supernatant was discarded, and the process repeated twice more. Then, the soil cake was made up with 30 mL 0.025 M $BaCl_2$ and shaken over - night to equilibrate exchange positions in the soils to approximately 0.01 M $BaCl_2$. Again, the tubes were centrifuged as the first time. In a further step, the tubes were filled up with 30 mL 0.02 M $MgSO_4$, shaken over - night, and centrifuged. This time, the supernatant was filtered through 0.2 µm pore - size syringe filters. The filtrates as well as the $MgSO_4$ stock solution were analysed for their Mg^{2+} concentrations with IEC (section *3.4.3*). As a Mg^{2+} reduction in the filtrate indicated occupation of negatively charged particles, the CEC could be deduced by:

$$\text{CEC (cmol kg}^{-1}\text{)} = \frac{(c_b - c_s) \cdot 2 \cdot V}{w \cdot 10} \qquad (16)$$

where c_b and c_s depict the respective Mg^{2+} blank and sample concentration in mmol L^{-1}, V the added volume of $MgSO_4$ solution (30 mL), V the valency of Mg^{2+} (i.e., 2) and w the oven - dry corrected soil weight. The denominator is multiplied by 10 to yield a value in cmol kg^{-1} OD soil.

3.3.3 Particle Size Distribution

Determination of the particle size distribution followed the method applied in (Kubo et al., 2018). Sand (≥ 63 µm), silt (< 63 µm, ≥ 2 µm) and clay (< 2 µm) were distinguished by ISO 11277 (ISO 11277:2009). The first method aimed to remove gypsum ($CaSO_4 \cdot 2H_2O$) if the presence could not be excluded beforehand. As the Japanese and the Belarussian soil exhibit *p*H conditions that are unfavourable for the presence of those compartments, this method was only applied for the Austrian soil. Therefore, approximately 5 g of soil was weighed - in in duplicates and transferred to 50 mL centrifuge tubes, which were filled up with

30 mL of deionized water and vortexed. Subsequently, the tubes were centrifuged at 1,500 repetitions per minute (rpm) for 5 min. with minimal deceleration. If the supernatant was still turbid, a few drops of 1 M NaCl solution were added. The clear supernatant was transferred to another 50 mL tube and filled up with 5 mL acetone (C_3H_6O). As no gypsum precipitated, decomposition of calcium carbonates ($CaCO_3$) followed.

Therefore, 1 M sodium acetate ($NaCH_3COO$) solution was adjusted to *p*H 5 with pure acetic acid (CH_3COOH). Then, 100 mL of this solution was transferred to 250 mL polypropylene bottles, which contained 10 g of air - dried soil. The bottle was placed in a water bath at 80°C and loosely closed with a lit allowing CO_2 gas to escape. Once the bubbling mitigated, the bottle was centrifuged at 1,500 rpm for 5 min. with minimum deceleration. The supernatant was discarded, and the process iterated until the bubbling significantly reduced. In a second step, the bottle was filled up with 100 mL of deionized water, hand - shaken, and centrifuged as described before. If the supernatant was turbid after centrifugation, a few drops of 1 M NaCl were added, and the process was repeated. Overall, washing with deionized was conducted twice.

Thereafter, organic matter was decomposed. As this was conducted for all soils, 10 g of the respective remaining soils had to be weighed - in into 250 mL plastic bottles. Then, 30 mL of a *p*H adjusted (~ 8) Na - hypochlorite (NaClO) solution was filled into the bottles, which were subsequently vortexed and placed in a hot water bath at 80°C for at least 1 h. Subsequently, they were centrifuged at 1,500 rpm for 15 min. with minimum deceleration. The supernatants were transferred into 50 mL glass beakers to assess their colour intensity. Once a pale supernatant was achieved, the soils were washed twice by deionized water, as explained for the $CaCO_3$ removal.

Subsequently, the soil cakes were transferred to 500 mL glass beakers by spraying deionized water. The suspensions were then passed through a 160 µm mesh sieve, collected in 500 mL glass beakers, and sonicated (2200 Ultrasonc Cleaner, Branson) for 1 h. As the clay fraction of Miyakonojo still flocked and sedimented after sonification, the suspension was mixed with a Na^+ saturated ion - exchange resin (wet - sieved to > 250 µm), transferred into a 500 mL plastic bottle, and shaken on a linear shaker at 120 rpm over - night. Thereafter, the resin was filtered out again by wet sieving the suspension through a 160 µm mesh sieve. This procedure was iterated until flocculation was reduced to a minimum.

The silt and clay fractions could then be determined by a quantitative recovery method at 23°C. First, all suspensions were filled into glass beakers with at least 1 L volume. Then, the suspensions were thoroughly stirred with a glass rod to swirl up all particles homogenously. After approximately 7 ½ h, the clay fraction was gently syphoned to a depth of 10 cm from the surface. This process was iterated until the suspension in that range was almost clear.

The silt and remaining sand fraction (< 160, ≥ 63 µm) were separated by wet - sieving through a 63 µm mesh - sieve. The sand fraction was added to the afore separated sand fraction (> 160 µm). Both, sand and silt fraction were transferred into preliminary weighed - in 50 mL glass beakers. In turn, the syphoned clay fraction was collected in different glass beakers and brought to flocculate and sediment by addition of 0.1 M NaCl. The clear supernatant was decanted, and the clay suspension transferred into a preliminary weighed - in 500 mL plastic bottle. To keep the clay suspension for later XRD analysis, only 10 mL were pipetted out after the bottle was vigorously hand - shaken and the new weight of the bottle recorded. The 10 mL suspension was then transferred into a 15 mL centrifuge tube, that was vortexed and centrifuged for 10 min. at 2,000 rpm. The clear supernatant was decanted, and 2 mL of deionized water were added and the tube vortexed until the clay was suspended again. Then, it was filled up with 8 mL ethanol (C_2H_5OH), thoroughly hand - shaken, and centrifuged again as in the last run. Ethanol rinsing was repeated twice before the clay suspension was transferred into a preliminary weighed - in 50 mL glass beaker by pure water spraying. The preliminary weighed - in beakers of each respective fraction were incubated in the oven at 105°C overnight and allowed to cool down in a desiccator. Afterwards, the respective weights were recorded. For the clay fraction, the content had to be counted back to the clay suspension mass that was previously recorded.

3.3.4 Clay mineralogy

Bulk soil minerals and clay minerals were studied by means of X-ray diffraction (XRD) using a Panalytical XPert Pro MPD diffractometer. Along the analyses, several sample preparation and modification steps were required. Thus, bulk soils were milled to 10 µm particle size with a vibratory disc mill and equally distributed on a sample holder for later analysis. The clay mineral analysis (see *3.3.3*) was conducted separately. Therefore, 10 mL of 4 M $MgCl_2$ and KCl solutions were respectively mixed with 40 mL of previously prepared clay suspensions, shaken overnight and subsequently sonicated. Afterwards, samples were sucked through a porous ceramic plate to obtain the preferential orientation of the clay minerals. To avoid orientation disturbance, the samples were equilibrated above saturated NH_4NO_3 solution for seven days in a desiccator at room temperature. Clay expansion tests were performed by ethylenglycol ($C_2H_6O_2$) and dimethyl sulfoxide (C_2H_6OS) vapor treatments in a desiccator for 24 h at room temperature. Moreover, clay contraction was tested by sample incubation at 550°C. After each treatment, the samples were analysed from 2 - 40 ° 2 θ with an X-Ray diffractometer.

Principally, this makes use of constructive reflections of monochromatic X-rays impinging crystalline samples to allow the determination of basal spacings in crystal lattices. XRD diffractometers consist of an X-ray tube, a sample holder, and an X-Ray detector. In the X-ray tube, a tungsten filament cathode is heated up to produce electrons that are bombarded towards a target by voltage application. The target is ionized by dislodging an electron of the inner shell (K-shell) that is replaced by an electron from outer-shells (e.g., L-shell or M-shell). The electron energy gap is emitted in the form of target element specific X-ray photons (Bunaciu et al., 2015; Suryanarayana & Norton, 1998). To obtain the high intensity radiation of the electron jump from the K to the L shell (K_α), the spectrum is filtered by either a foil or a monochromator. Then, K_α is directed on the sample, which is rotating at an angle of θ. The detector is rotating at 2 θ and converts the incoming signal to a count rate (Bunaciu et al., 2015). When parallel in phase X-rays impinge on matter of periodic nature (i.e., crystalline), destructive or constructive scattered radiation is produced in dependence of the incident angle. Thereby, the lower beams must travel an integer number of wavelengths (n.) more than the upper beam, so that the scattered rays are still in phase. This can be expressed by the following equations referring to Figure 11:

$$FG + GH = n.\ \lambda \tag{17}$$

$$FG = GH \tag{18}$$

$$FG = d \cdot \sin(\theta) \tag{19}$$

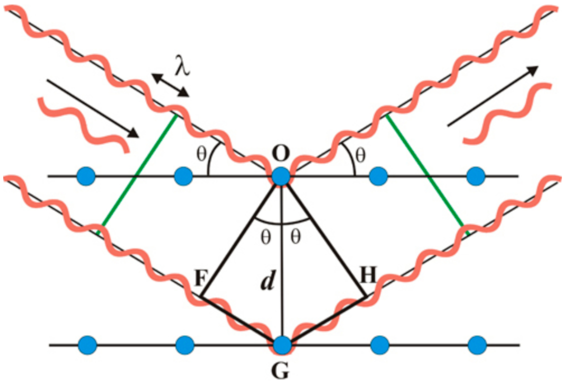

Figure 11: *Two impinging X-ray beams on two crystal planes with the wavelength λ, the incident and diffraction angle θ and basal plane spacing d. The figure is taken from: xtal.iqfr.csic.es/Cristalografia/parte_05_5-en.htm.l.*

Finally, Bragg´s law can be formulated as:

$$n \cdot \lambda = 2 \cdot d \cdot \sin(\theta) \tag{20}$$

where n depicts the order of diffraction, λ the wavelength of the incoming beam in nm (0.15418 nm for copper), d the lattice spacing in nm and θ the incident angle in degrees (Suryanarayana and Norton 1998). As the *n*th order of reflection can always be described as a first order, n is practically cancelled out (Le Pevelen, 2010). Finally, constructive interference is detected in form of a count peak at a certain angle (2θ) on a diffraction pattern. Transposing Equation (20) to d yields the d - spacing of the investigated mineral.

3.3.6 Water holding capacity and soil moisture

The determination of the water holding capacity was adapted from Amacher & Brown (2000) and conducted once with each bulk soil. First, a filter paper was attached to a core sampler with a rubber - band and air - dried soil was filled in. For later calculations, the combined weight of core sampler, rubber band, filter paper and soil as well as the weight of a dry and a moistened filter paper were recorded. Then, the filled core sampler was incubated at 105°C for 72 h, allowed to cool in a desiccator and weighed - in again. Then, the core sampler was placed in a petri - dish that was filled with water to achieve soil water saturation. Thereafter, the core sampler was taken out of the petri - dish, the filter paper at the bottom gently tabbed and the combined weight recorded. The gravimetric water content (θ) can be formulated as:

$$\theta = \frac{w_s - (f_w - f_d)}{w_o} \qquad (21)$$

where w_s represents the water saturated core sampler weight, w_o the oven-dry core sampler weight, f_w the weight of the moistened and f_d of the dry filter paper.

3.4. Solid - liquid distribution determination

3.4.1 Soil solution extraction

For soil solution extractions, 30 mL syringes were prepared by stitching narrow wholes through the bottom of the barrel and removing tip and plunger. Subsequently, a filter paper was introduced into the barrel and placed at its bottom to cover the wholes. The syringes were then filled up with soils at 60% WHC, covered with aluminum foil at the top and inserted into 50 mL polypropylene centrifuge tubes. Thereafter, the tubes were centrifuged at 4,000 rpm twice for 15 and 30 min., respectively. After each run, the obtained solution was transferred to a 15 mL centrifuge tube. Finally, the collected solution was filtered through a 0.2 µm polypropylene pore - size syringe filter and stored at 5°C.

3.4.2 Soil solution ammonium

Dissolved NH_4^+ concentrations were determined with an ammonia gas sensing electrode (Orion High performance ammonia electrode, Thermo ScientificA) that was connected to a portable *p*H meter (Orion Star A221, Thermo Scientific). For measurements, the electrode was immersed into a glass beaker containing 20 mL diluted sample that was homogenized by a magnet - stirrer and alkalized by 20 µL of 10 M Na(OH) until a stable current was displayed on the portable meter. To prevent contamination, the electrode was rinsed by deionized water and gently dabbed before each measurement. The principle of this method is based upon the detection of *p*H changes that correspond to NH_3 concentrations in the inner solution of the instrument. Thus, its central components are a *p*H electrode that is immersed in a NH_4Cl solution and an NH_3 passable membrane at its tip. Generally, the analysed sample needs to be alkalized to yield the chemical reaction from NH_4^+ to NH_3. Thereafter, NH_3 diffuses through the membrane at the electrode´s tip until the partial pressure on both sides of the membrane is equilibrated (Wen et al., 2019). In the inner body, NH_3 reacts with H_2O to a small extent to NH_4^+ and OH^-. The reaction can be depicted as:

$$\frac{[NH_4^+] \cdot [OH^-]}{[NH_3] \cdot [H_2O]} = \text{constant} \tag{22}$$

As the inner solution contains sufficient H_2O and NH_4^+, they can be deleted from the equation. Transposing the equation after $[OH^-]$ yields:

$$[OH^-] = [NH_3] \cdot \text{constant} \tag{23}$$

Additionally, $[OH^-]$ and $[H^+]$ are interrelated due to the ionic product of H_2O, that is described by:

$$-\log [OH^-] + \{-\log [H^+]\} = pH + pOH = 14 \tag{24}$$

Finally, it can be inferred, that *p*H and $[NH_3]$ are proportionally related. As the NH_3 concentration in the inner solution is proportional to both its partial pressure and the *p*H change, the sample concentration can be inferred from the signal detected by the *p*H electrode. According to Henry´s law, the partial pressure of NH_3 is strongly dependent on temperature and other dissolved species, so that all samples were measured at room temperature and measurements in 2 M KCl extracts were conducted after matrix matched calibration (Dasgupta & Dong, 1986).

3.4.3 Soil solution major cations

The extracted soil solutions were investigated for Mg^{2+}, Ca^{2+}, Na^{+}, and K^{+} with an ion exchange chromatography (IEC) (863 Compact IC Autosampler, Metrohm). IEC is based on the principal of adsorption of diversely charged ions in liquid phase on a solid - state column with a fixed charge. In dependence of the analytes charge, the column is negatively or positively charged. For cation analysis, negative charge is often produced by conjugated bases of strong acids, such as sulfonates (SO_4^{2-}) and phosphates (PO_4^{3-}). Resins as silica and polystyrene, agarose, dextran or cellulose are derivatized with these charged groups (Gottschalk, 2011). In a first step, the resin needs to be equilibrated with an eluent of opposite charge and low ionic strength. Subsequently, the analyte is replacing the eluent as is indicated in:

$$S\text{-}X^-C^+ + M^+ \leftrightarrow S\text{-}X^-M^+ + C^+ \qquad (25)$$

where S represents the resin, X^- the negatively charged functional group, C^+ the eluent and M^+ the analyte (Bhattacharyya & Rohrer, 2012). After the sample is adsorbed onto the column, the eluent is again injected and successively exchanging with the analytes. The eluted analyte is detected through electric conductivity, after an eluent specific suppressor reduced its conductivity to gain precision. Finally, the analytes retention time and peak area is used to infer its concentration (Fritz & Gjerde, 2009).

3.4.4 Soil solution Caesium

Caesium concentrations in soil solution were detected with an Agilent 7700 Series inductively coupled plasma mass spectrometer (ICP-MS), which is suitable for trace- and ultra - trace concentrations (Cubadda, 2007; Epov et al., 2004). In a first step, the sample is sucked in and nebulized along with inflowing Argon (Ar) gas. In a subsequent atomizing chamber, finer nebulized particles are selected, so that a fine Ar - sample aerosol is forwarded to a plasma-torch. The plasma is produced by a coil which is wound around the plasma torch and fed by a high - frequency generator (Hölzer, 2018). Further Ar gas is inflowing into the plasma torch and ionized by a high voltage spark, leading to motion of electrons and ions that collide with Ar atoms causing additional ionization and ohmic heating of the plasma up to 10,000 K. The inflowed sample sparklets are penetrating the plasma causing their solvation, vaporization, atomization, and ionization. Afterwards, the sample ions are forwarded through an interface into a high - vacuum (10^{-4} - 10^{-5} torr) system (Cubadda, 2007). There, the ions are accelerated and shaped by electrostatic lenses possessing negative voltage to extract positively charged particles from the beam. Negatively charged and neutral particles are repelled. After transition of this sequence, ions are introduced into the quadrupole, consisting of four metallic rods to which alternating (AC) and direct current (DC) is applied. In dependence of the analytes mass to charge ratio (m/z), the voltages must be adjusted, so that a stable ion beam is created. Finally, the analytes concentration is determined through an electron - multiplier principle, in which amplification cascades of electrons on several dynodes produce a sufficiently large analysis signal which is counted (Wilschefski & Baxter, 2019).

3.4.5 Solid-phase, exchangeable potassium

Exchangeable K^+ was determined with the samples also used for CEC (see *3.3.2*). First, 2 g of sample was weighed in and transferred to a 50 mL centrifuge tube. This was filled up with 40 mL of 1 M ammonium acetate (CH_3COONH_4) and shaken for 1 h to induce an ion exchange reaction between K^+ and NH_4^+. Thereafter, the samples were centrifuged at 3,000 rpm for 1 min. to obtain a lucid solution. Last, the supernatant was filtered through 0.2 µm pore - size syringe filters and analysed with flame atomic absorption spectrometry (FAAS) to determine the K^+ concentration. Final values were obtained by:

$$\text{ex. - K}^+ \ (\text{mmol kg}^{-1}) = \frac{(c_S \cdot V)}{w} \tag{26}$$

with c_s indicating K^+ concentration in the filtrate in mmol L^{-1}, V the extracted volume in L and w the oven - dried soil weight in kg.

Flame atomic absorption spectrometry is an eligible method to determine metal and metalloid concentrations as low as mg L^{-1} in aqueous solutions relatively interference free and with negligible requirements for sample preparation (Hill & Fisher, 2017; Worden, 2005). Principally, the desired element is atomized in a gas that absorbs electromagnetic radiation (light) at its element specific wavelength directly proportional to its concentration. Therefore, the sample is first sucked up and nebulized into coarse droplets before entering a spray chamber. There, the aerosol is further shattered into smaller droplets by a flame feeding gas, consisting of acetylene (C_2H_2) and air. Those gases further carry the aerosol mist towards the flame, where it is finally volatilized and atomized (Hill & Fisher, 2017; Ott, 2013). The electromagnetic radiation in turn is produced by a hollow - cathode lamp. The cathode is coated with the element of interest and bombarded by an ionized noble gas (Ar or Neon) at 1 - 5 torr pressure, so that the coating element is excited and consequently emits electromagnetic radiation at the wavelength of the analyte. The emitted light then excites free ground state atoms in the flame. In addition, a beam chopper is correcting for light emission of excited analyte atoms that have not been excited by the hollow - cathode lamp. Behind the flame, a monochromator is installed to extract the narrow wavelength band of the analyte (Hussain & Keçili, 2020). The extracted beam then impinges on a photocathode that transfers photons into electrons which are further accelerated along a sequence of dynodes. Finally, the absorption intensity is counted back from the electric signal and the sample concentration can be inferred from the Lambert - Beer law which states the direct proportional relation between absorption intensity and sample concentration (Hill & Fisher, 2017; Worden, 2005).

3.4.6 Solid-phase, exchangeable NH_4^+ and NO_3^-

Exchangeable NH_4^+, NO_2^- and NO_3^- fractions of air - dried soil samples were extracted by a 2 M KCl solution. Therefore, 12.5 g of air - dried soils were weighed in and transferred into 150 mL polypropylene bottles. The bottles were filled up with 125 mL of a 2 M KCl solution, giving a soil/solution ratio of ten. Subsequently, the samples were shaken for 1 h on a linear shaker to cause the desired ion exchange reaction between NH_4^+ and K^+. After centrifugation at 3,000 rpm for 15 min., the clear supernatants were decanted into 150 mL glass beakers, filtered through 0.2 µm pore - size syringe filters and stored at 5ºC in 150 mL polyproplylene bottles. Ammonium concentrations were determined with an ammonia electrode (see *3.4.2*) and NO_2^- and NO_3^- with a microplate absorbance reader. To avoid matrix - effects, standards for both methods were prepared in extractant solution. Additionally, NH_4^+ - N and NO_3^- - N were calculated by the relative N - share of the respective molecule, hence the factors 0.78 and 0.23 for NH_4^+ and NO_3^-, respectively. It should be noted that the NO_2^- and NO_3^- fractions were not distinguishable but were both corrected for total N with the molecular mass of NO_3^-, as NO_2^- concentration levels in soils are clearly below that of NO_3^- (Kurt et al., 2012). Final calculations followed Equation (26). Moreover, it was assumed that the obtained solution NH_4^+ as described in *3.4.1* was included in the 2 M KCl extractable NH_4^+ and a simple subtraction of the solution NH_4^+ would give the pure exchangeable fraction.

Nitrite and NO_3^- concentrations were determined in 2 M KCl extracts colourimetrically after the Griess/VCl_3 colour reaction. This method is applicable in a range between 0.2 and 5 mg N L^{-1} and proved to be rapid, simple, and low - cost (Hood-Nowotny et al., 2010; Miranda et al., 2001; Schnetger & Lehners, 2014). The VCl_3/Griess reaction induces a reduction of NO_3^- to NO_2^- and a subsequent formation of a diazonium that functions as a chromophore for colourimetrical analysis. Therefore, a 60 mmol L^{-1} VCl_3 solution was prepared by the dissolution of 400 mg VCl_3 in 50 mL 1 M HCl and a subsequent filtration through filter paper. For Griess reagent 1, 50 mg of *N*-napthylethylenediamine dihydrochloride were dissolved in 250 mL of deionized water. For Griess reagent 2, 5 g of sulfanilamide were dissolved in 500 mL of 3 M HCl. Then, 100 µL of sample, standard or blank, 100 µL of VCl_3 and 50 µL of Griess reagent 1 and 2, respectively, were pipetted into the microtiter plates and incubated for 60 min. at 37°C (Hood-Nowotny et al., 2010). The measurement was conducted with an absorbance microplate reader at 540 nm wavelength (BMG Labtech – Platereader SPECTROstar Nano). Thereby, the desired wavelength is created by a monochromator that isolates the light emitted from a xenon flash lamp that is targeted towards the microplate titer. A photodiode is placed underneath the plate carrier to detect the transmitted light. According to the Lambert - Beer law, the illuminated sample is absorbing the emitted light relative to its concentration, which can hence be inferred from the known light intensity before (I_0) and after (I) passing the sample (Jones et al., 2004).

3.5 Statistical analysis

Inferential statistical analyses were either conducted as two - factorial analysis of variance (ANOVA) or t-tests with the statistics software *R* (R Core Team, 2021). The output variables NH_4^+, Cs^+ and K^+ concentrations in soil solution were therefore analysed as two - factorial analyses of variance (ANOVA) or t-tests with the analysed per day, respectively. While t-tests were performed on fertilisation treatments, two - way ANOVAs comprised both fertilisation and clay mineral treatments. In case of an ANOVA, classically three aspects must be fulfilled: residual normality, residual homoscedasticity, and sample independence (Yanyan, 2008). As the experiment was assumed to be sufficiently invulnerable towards nuisance factors, blocking was neglected, and a complete randomized design (CRD) chosen (Casella, 2008). Additionally, three biological replications (from the respective soil stock) per factor combination were generated to avoid autocorrelation and ultimately assure sample independence (Taberlet et al., 2018). The normality assumption was checked visually by histograms and quantile-quantile (QQ) plots of the model residuals.

As usual for data in which standard deviations and means are proportionally related, every ANOVA model required a logarithmic transformation of the respective dependent variable to obtain residual normality (Fernandez, 1992). Residual homoscedasticity was assumed by passing a Levene´s test above a significance level of $\alpha = 0.05$ (Gastwirth et al., 2010). If ANOVA results were significant ($\alpha = 0.05$) for at least one factor or factor interaction, post-hoc testing was conducted following the method of Tukey´s honest significance difference (HSD) test, likewise on a significance level of $\alpha = 0.05$ (Haynes, 2013). Furthermore, t-tests were conducted as unpaired because of sample independence. As Welsh´s t-test exhibits better control over type - 1 error rates in case of unequal variances while proving robustness towards equal variances, it was preferred over student´s t-test (Delacre et al., 2017). Normal distribution was assessed by Shapiro-Wilk´s test performed on a significance level of $\alpha = 0.05$ (Mohd Razali & Yap, 2011). According to de Winter (2013), statistical power (i.e., 1 –

Type II error rate) of a t-test with small sample sizes (n = 3, respectively) and non - normal distributions is dependent on the effect size (Cohen´s D), which was calculated for comparisons in which data of at least one group was significantly ($\alpha < 0.05$) non - normal distributed. As effect size exceeded the “huge” (> 2) threshold and statistical power would range around $1 - \beta = 0.95$ in those cases, t-tests were conducted despite non - normality of data (Sawilowsky, 2009; de Winter, 2013).

3.6 Prediction of the concertation factor

The empirical determination of Cs^+ and K^+ in soil solution enabled to predict the Cs^+ uptake when applying the concentration factor (CF) equation given in Smolders et al. (1997) and Absalom et al. (1999). Therefore, Equation (13) needed to be rearranged to Cs_{plant}:

$$Cs_{plant} = CF \cdot Cs_{solution} \tag{27}$$

while the CF can be calculated with mK^+:

$$CF = 10^{-(k_1 \cdot \log \cdot (mK^+;\, k_{lim}) + k_2))} \tag{28}$$

where k_1, k_2 and k_{lim} are empirical constants representing the values 2.24, 5.23 and 0.0024, respectively. These values are plant - depended and refer to ryegrass (*Lollium perenne*) in this study (Absalom et al., 1999; Smolders et al., 1997). As ^{133}Cs was used as a proxy for RC, $Cs_{solution}$ was given in nmol L^{-1} instead of Bq L^{-1}, resulting in nmol kg^{-1} for Cs_{plant}.

4. Results and Discussion

4.1 Mineralogical and physicochemical soil properties

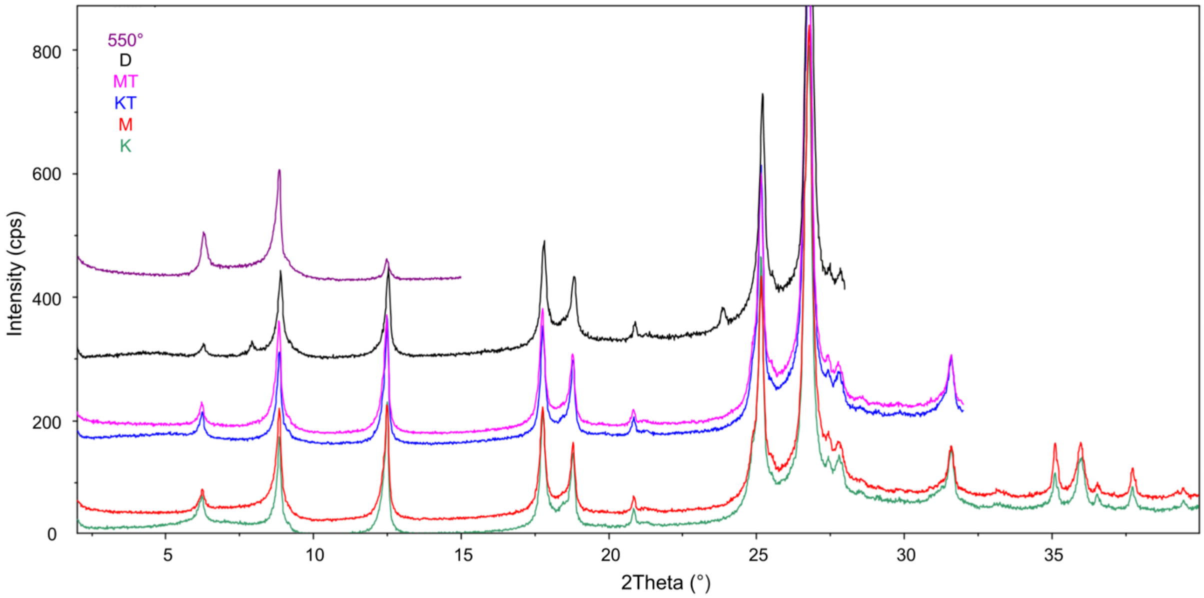

Figure 12: *X-ray diffraction pattern for Groß - Enzersdorf. The legend abbreviations are defined as: K = K^+ saturation, M = Mg^{2+} saturation, KE and ME = ethylenglycol treatment after K^+ or Mg^{2+} treatment, D = dimethyl sulfoxide treatment after K^+ saturation and MT5 = 550°C tempering of Mg^{2+} treated samples.*

The ≤ 2 µm particle fraction of Groß - Enzersdorf contains considerable amounts of micaceous/illitic compounds which are identified by clear peaks at 8 2θ° (001) and 18 2θ° (002) and correspond to a basal spacing of 1 nm (Figure 12). The presence of the 2:1:1 clay mineral chlorite was confirmed by the 1.4 nm peak at 6.3 2θ° that persisted the 550°C heat treatment. Neither K^+/Mg^{2+} nor ethylene glycol (EG) treatments affected the diffraction pattern at 6 2θ° significantly, revealing the absence of vermiculitic and smectitic compounds (Harris & Norman White, 2008). A peak reduction at 12.3 2θ° and the formation of a small peak at 7.5 2θ° angle after the dimethyl sulfoxide (DMSO) treatment refers to interlayer widening of kaolinite, enabling the distinction between chlorite and kaolinite (Abdel-Kader et al., 1978). Overall, the predominant occurrence of chlorite and mica in the clay fraction is typical for Chernozems developed upon a loamy loess sediment (Sokolova et al., 2010).

Likewise, chlorite is present in the ≤ 2 µm particle fraction of Deshchenka. However, the 1.4 nm (6.3 2θ°) peak diminishes and widens until the 1 nm (8.8 2θ°) peak after the 550°C heat treatment, pointing towards significant occurrence of Al-hydroxyl interlayered smectite/vermiculite, which is a typical phenomenon on podzols (Figure 13) (Bain et al., 1990; Rich, 1968; Skiba, 2007). The identified 1 nm peak after Mg^{2+} saturation allows inferences about the presence of illite/mica. Besides chlorite and mica, considerable amounts of kaolinite were distinguished by the DMSO treatment. The presence of kaolinitic compounds is characteristic for podzols of the temperate climates and assumed to be caused by strong chemical weathering and subsequent neoformation from Al^{3+} and Si^{4+} in the soil solution (Skiba, 2007).

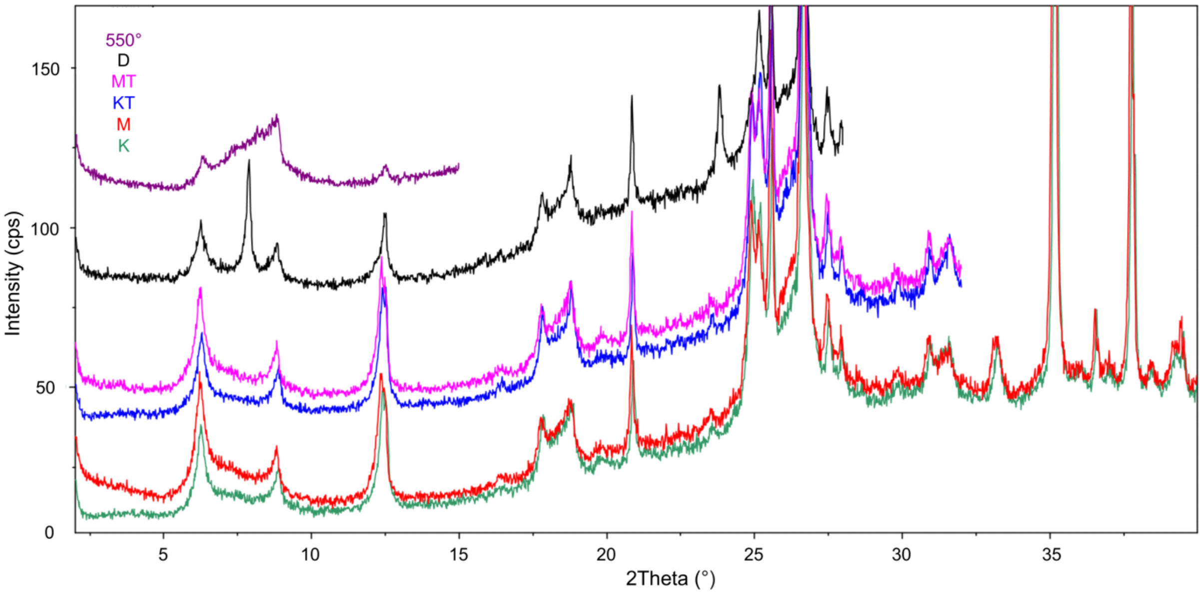

Figure 13: *X-ray diffraction pattern for Deshchenka. The legend abbreviations are defined as: K = K^+ saturation, M = Mg^{2+} saturation, KE and ME = ethylenglycol treatment after K^+ or Mg^{2+} treatment, D = dimethyl sulfoxide treatment after K^+ saturation and MT5 = 550°C tempering of Mg^{2+} treated samples.*

The clay mineral composition of Yoshiki is clearly dominated by kaoline minerals. This is supported by a 12.3 2θ° peak resistant towards K^+, Mg^{2+} and EG treatments, its disappearance after the 550°C heat treatment and a peak shift to 7.5 2θ° after the DMSO treatment (Figure 14) (Abdel-Kader et al., 1978; Schaetzl & Anderson, 2005). As the 1.4 nm peak was not shifted towards sharper angles after EG solvation and disappeared after the 550°C heat treatment, the detectable presence of smectite and chlorite could be excluded, respectively. In contrast, considerable amounts of vermiculite were detected, as indicated by a 1.4 nm peak after Mg^{2+} saturation and an increase of the 1 nm peak after K^+ saturation (Harris & Norman White, 2008; Kowalska et al., 2022). However, the vermiculitic compounds seemed to be partly Al-hydroxy interlayered, as the 1.4 nm peak not fully vanishes after K^+ saturation (Egli et al., 2001). The relatively wide 1 nm peak after 550°C heat treatment substantiates this assumption. Furthermore, trace amounts of mica can be inferred from 1 nm peaks after Mg^{2+} saturation (Yin et al., 2014). As the parent material in the Yoshiki area is biotite - granite, it can be assumed that this reflex corresponds to biotite.

In contrast, Ogata´s clay fraction exhibits a distinct peak at 1.4 nm after Mg^{2+} saturation that shifts to 1.7 nm with additional EG salvation and indicates predominant presence of smectitic compounds, which coincides with the site´s description by Nishida & Sato (2016), Tanaka (2007) and Ohtsubo et al. (2002) (Figure 15). Furthermore, K^+ saturation induced an interlayer collapse to approximately 1.2 nm, which allows conclusions about humidity induced K^+ hydration and H_2O layer intercalation (Ferrage et al., 2005). A minor 1 nm peak reveals traces of mica. Vermiculitic and kaoline compounds are identified by an increase of the 1 nm peak after K^+ saturation and a 1.12 nm peak after DMSO treatment, respectively. Even though the smectitic and vermiculitic compounds collapsed to 1 nm d - spacing after the 550°C heat treatment, traces of chlorite were detectable in form of a minor 1.4 nm peak. The presence of chlorite, vermiculite, mica and kaoline minerals at the Ogata site is underpinned by findings of Ohtsubo et al. (2002).

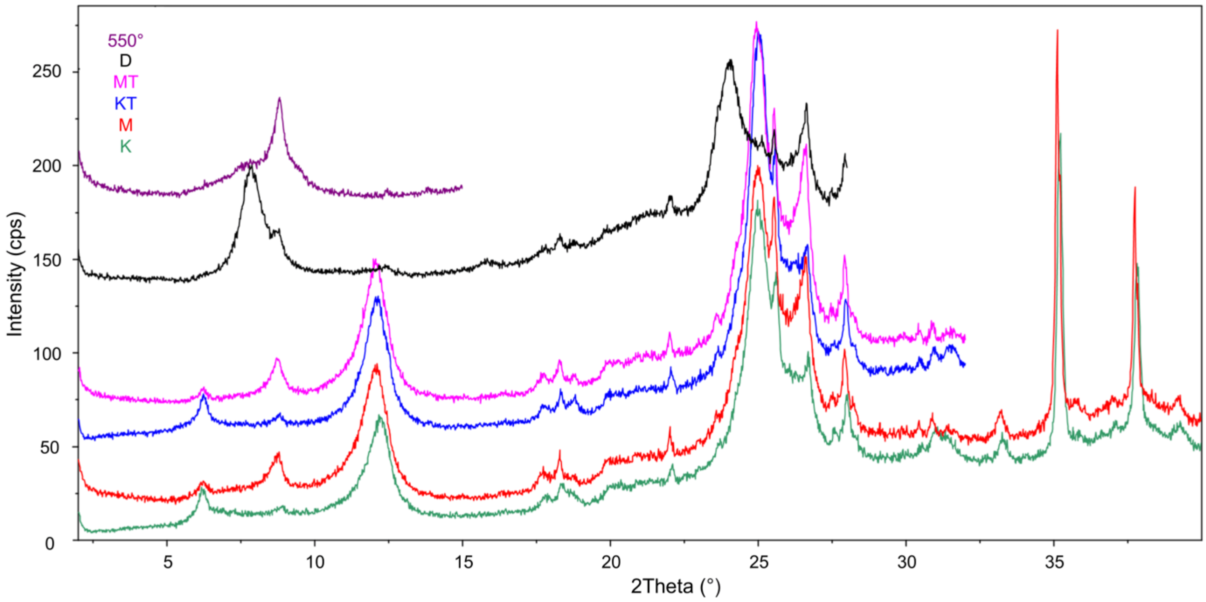

Figure 14: *X-ray diffraction pattern for Yoshiki. The legend abbreviations are defined as: K = K^+ saturation, M = Mg^{2+} saturation, KE and ME = ethylenglycol treatment after K^+ or Mg^{2+} treatment, D = dimethyl sulfoxide treatment after K^+ saturation and MT5 = 550°C tempering of Mg^{2+} treated samples.*

Reflections of Miyakonojo´s clay fraction reveal a low degree of crystallization. An increasing peak from 15° 2θ on indicates the presence of amorphous silica (Figure 16) (Zhang et al., 2012). Distinct peaks around 2θ ~ 26° show predominant presence of allophane (Arai et al., 2005; Ohashi et al., 2002; Rouff et al., 2012). The minor peaks at 6° and 12° 2θ that diminish after the 550°C heat treatment most likely prove the occurrence of halloysite. The nanotube - shaped clay mineral exhibits a similar d - spacing as kaolinite in its dehydrated state and is characteristically for weathered Andosols (Joussein et al., 2006; Ndayiragije & Delvaux, 2004). Previous findings regarding the clay mineralogy of Andosols sampled in Miyakonojo support both the presence of allophane and halloysite (Hara & Tamai, 1968; Yoshida, 1992).
Several XRD-analyses results coincide with some basic physicochemical properties of the investigated soils. Groß - Enzersdorf exhibits a *p*H of 8.3 and is hence the only soil that can be classified as alkaline (Table 5) (Eckert & Sims, 1995). XRD analysis of the ≥ 10 μm fraction revealed that approximately 25% of the minerals present in Groß-Enzersdorf are

represented by calcite and dolomite, minerals that show alkaline properties and are typically occurring in east - Austrian Chernozems (Appendix E) (Bruckman & Wriessnig, 2013; Wu et al., 2021). Further typical Chernozem characteristics can be inferred from the high content of loess deriving silt and comparatively high CEC (Jordanova, 2017; Kögel-Knabner & Amelung, 2014).

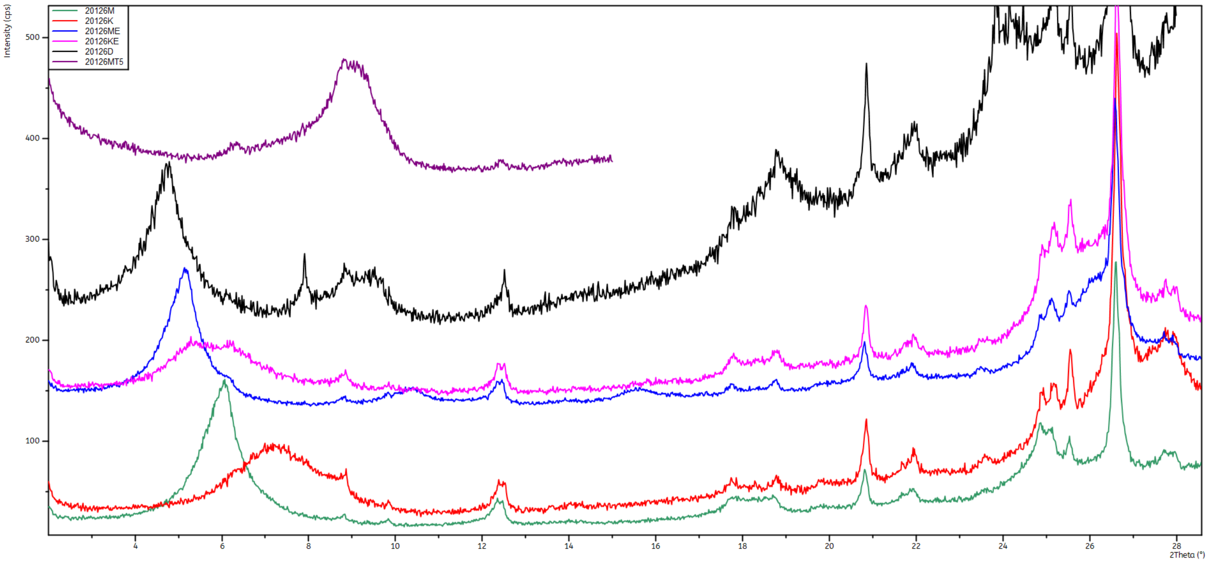

Figure 15: *X-ray diffraction pattern for Ogata. The legend abbreviations are defined as: K = K^+ saturation, M = Mg^{2+} saturation, KE and ME = ethylenglycol treatment after K^+ or Mg^{2+} treatment, D = dimethyl sulfoxide treatment after K^+ saturation and MT5 = 550°C tempering of Mg^{2+} treated samples.*

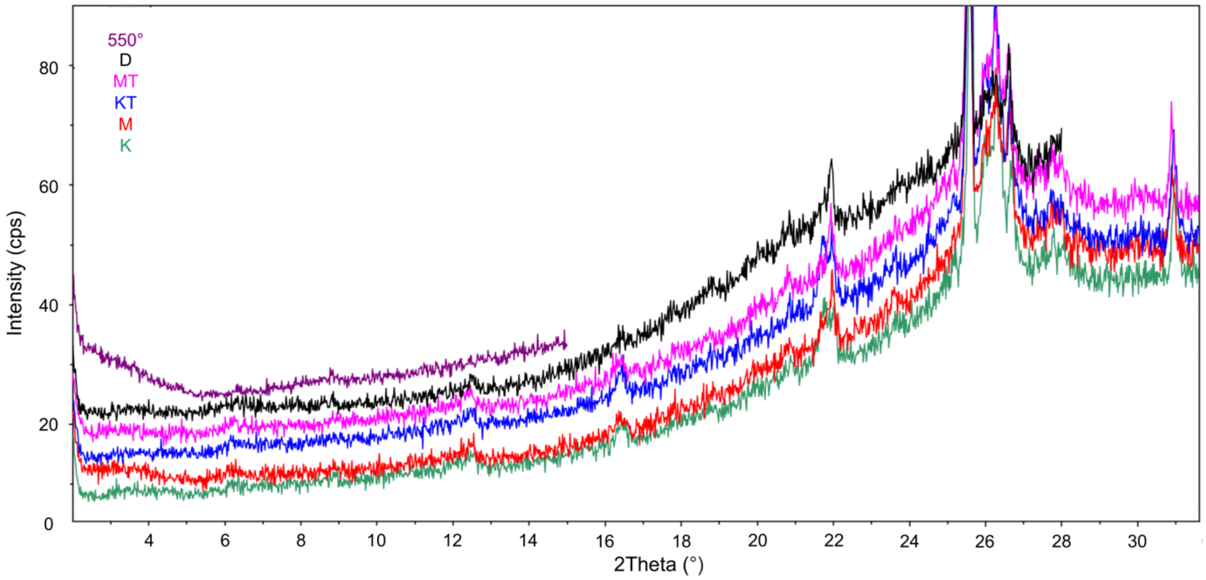

Figure 16: *X-ray diffraction pattern for Miyakonojo. The legend abbreviations are defined as: K = K^+ saturation, M = Mg^{2+} saturation, KE and ME = ethylenglycol treatment after K^+ or Mg^{2+} treatment, D = dimethyl sulfoxide treatment after K^+ saturation and MT5 = 550°C tempering of Mg^{2+} treated samples.*

In contrast, the podzolic properties of Deshchenka are comprehensible by its high sand content that majorly contributes to its extremely low CEC (Kimpe, 1970). However, the relatively high *p*H indicates an early stage of podzolization, which coincides with the significant presence of hydroxy interlayered clay minerals, mica and chlorite (Georgiadis et al., 2020; Kitagawa, 2005; Krettek & Rennert, 2021). Like Deshechnka, Yoshiki can be considered as a sandy soil. The slightly increased CEC as opposed to Deshchenka is most likely attributable to considerable amounts of vermiculite (Malla, 1978). In contrast, Ogata shows a clay content of more than one third, which is straightforwardly reflected in both high WHC and CEC. The predominance of smectite in Ogata´s clay fraction reinforces these characteristics additionally (Kumari & Mohan, 2021; Mile & Mitkova, 2012). The largest WHC among the investigated soils was determined for Miyakonojo. In Andosols, amorphous minerals and organic matter (e.g. metal - humus complexes, allophane - humus and humus) tend to build highly stable aggregates with several macro-, meso- and micropores which can retain both water and air, causing two distinct andic properties: large WHC and low bulk density (Dahlgren et al., 2008; Nanzyo, 2010). Moreover, it is well documented that organic matter and amorphous minerals exhibit high affinity to retain H^+ ions and consequently contribute to the characteristic *p*H-dependent charge variability in Andosols (Kawai, 1969; Nanzyo, 2010; Poudel & West, 1999; Wada, 1985). It might hence be inferred, that Miyakonojo´s low *p*H and CEC are closely linked, which will be further discussed in *4.2.5*.

Table 5: *Physicochemical soil properties of the different soils without fertiliser treatment and clay amendments.*

Soil	***p*H**[a]	**CEC**[a] (cmol $_{(+)}$ kg^{-1} OD soil)	**Particle Size (%)**			**WHC** (L H_2O kg^{-1} OD soil)
			Clay (< 2 µm)	**Silt** (> 2, < 63 µm)	**Sand** (> 63 µm)	
Groß - Enzersdorf	8.3 ± 0.1	17.1 ± 1.9	24	42	34	0.39
Deshchenka	6.3 ± 0.1	4.9 ± 0.7	28	9	63	0.33
Yoshiki	6.4 ± 0.3	7.7 ± 0.5	7	23	69	0.44
Ogata	5.8 ± 0.2	27.9 ± 2	36	32	32	0.71
Miyakonojo	5.4 ± 0.1	9.5 ± 0.7	23	31	45	0.9

[a] *Values in those columns show the arithmetic means of triplicates and ± the standard deviation.*

4.2 Ammonium dynamics of the unamended soils

Based on these different central properties, every soil exhibited its own response to the 300 kg ha^{-1} NH_4^+ - N fertilisation treatment along the 36 - day period. The treatment caused significantly ($p < 0.05$) higher mNH_4^+ for all soils on every sampling day, with exception of Ogata on the 36th day and all comparisons which were not feasible due to concentrations below the detection level (Figure 17). Generally, the mNH_4^+ range clearly varied among the soils, particularly in the fertilised variants. For instance, maximum mNH_4^+ after the fertilisation treatment reached from 1.16 (1st day Yoshiki) up to 15.07 mmol L^{-1} (1st day Deshchenka), while Miyakonojo´s control resembled fertilised Yoshiki on the first day and Groß - Enzersdorf´s control did not exhibit any detectable mNH_4^+. For agricultural soils, Wolt (1994) stated solution NH_4^+ concentration to range from 2 - 20 mmol L^{-1}, while Britto et al. (2001) described concentrations of 0.1 - 1 mmol L^{-1} as “moderate” and 10 mmol L^{-1} as maximum concentrations. It has furthermore been reported that NH_4^+ toxicity can already occur from concentrations between 0.01 - 0.5 mmol L^{-1} on, although sensitivity varies greatly among plant species (Britto et al., 2001). Considering this, particularly Miyakonojo´s and Deshchenka´s mNH_4^+ on the 1st and 8th after the fertilisation treatment were alarmingly high, suggesting a different fertiliser management for those soils when agriculturally used. Zeolite amendments counteract this phenomenon and their effectiveness was tested for Miyakonojo, which will be discussed in *4.4.3*. In contrast, soils as Yoshiki and Ogata could most probably prevent the risk of severe NH_4^+ toxification, while a large share of the applied NH_4^+ must have undergone translocation from the soil solution pool. It is therefore crucial to reflect potential N - pools and losses, including compounds in the N - cycle, most prominently NO_3^-. In this experiment, 2 M KCl extractable NH_4^+, NO_2^- and NO_3^- were determined. In a simplified approach, the fertiliser N - recovery rate was calculated under the assumption that 2 M extractable NH_4^+, NO_2^- and NO_3^- was merely attributable to the applied fertiliser, as the N - dynamics of the unfertilised variants seemed to be majorly influenced by N - mineralization at the incubation start, while 300 kg N ha^{-1} would certainly exceed microbial N - demand and therefore suppress N - mineralization (Appendix B) (Mahal et al., 2019; Zhang et al., 2011).
According to Beauchamp & Drury (1991), the non - 2 M KCl extractable NH_4^+ fractions include fixation, volatilization, denitrification, and immobilization. The fixed fraction was determined following the method of Silva & Bremner (1966) and immobilization defined as the difference between the total N extraction as suggested by Bremner & Mulvaney (1983) and the sum of 2 M KCl extractable NH_4^+ and NO_3^- and the fixed fraction. Consequently, the authors stated that a simple subtraction of the 2 M KCl extracted NH_4^+ from the fertilised NH_4^+ would equal the fixed NH_4^+ did not hold true for neither a soil with low nor with high NH_4^+ fixing capacity in a soil incubation experiment with similar $(NH_4)_2SO_4$ application rates. As volatilization and denitrification seemed negligible, the authors inferred the immobilized

fraction to play the second significant role when tracing fertilised NH_4^+. Furthermore, Nömmik (1957) suggested the existence of an equilibrium - like state between the solution, exchangeable and non - exchangeable NH_4^+ pools in soils, as long as the respective K^+ pools are considered simultaneously. As later studies showed, NH_4^+ dynamics are strongly influenced by plant root uptake, contributing in particular to diffusion - induced enhanced release of the non - exchangeable NH_4^+ fraction (Scherer, 1984, 1987). Even though further investigation would have been needed to holistically comprehend these dynamics and apply them to the field, some central findings of this experiment can be summarized.

In almost all cases, the ex. - NH_4^+ - N fraction was larger than the soluble phase after the fertilisation treatment (Table 6, Figure 18). This is alignment with the literature, generally suggesting the order: fixed NH_4^+ > ex. NH_4^+ > soluble NH_4^+, reflecting diffusion from higher to lower concentrations when solution NH_4^+ is exhausted (Beauchamp & Drury, 1991; Kowalenko & Yu, 1996; Ranjbar & Jalali, 2014). In contrast to the fixed fraction, the soluble and exchangeable fractions are highly dynamical and easily accessible for microbial oxidation and assimilation (Allison et al., 1953b, 1953a; Beauchamp & Drury, 1991; Bower, 1951; Scherer, 1993). These assumptions are comprehensible by the time - depended fraction shifts for every soil. Moreover, every soil suffered a drastic loss of extractable N, which coincides with earlier findings, but might have been artificially increased by air - drying the soils prior to the 2 M KCl extraction (Kowalenko & Yu, 1996; Tong et al., 2004).

4.2.1 NH_4^+ - dynamics Groß - Enzersdorf

Groß - Enzersdorf´s NO_2^- and NO_3^- - N gains from the first to the 22nd day neither approached mNH_4^+ nor ex. - NH_4^+ losses, suggesting significant fixation and release from the beginning on, which finds support in the literature (Table 6, Figure 19) (Steffens & Sparks, 1997, 1999). This is also reflected in the comparatively low fertiliser recovery rate and most likely attributable to the predominance of illite (Allison et al., 1953a). However, it was found that particularly weathered illite sequences are responsible for NH_4^+ fixation, while unweathered illite hardly exhibits NH_4^+ fixation capacities (Allison, 1973; Allison & Roller, 1955; Nommik & Vahtras, 1982). Typically for Chernozems, the > 10 µm fraction of Groß - Enzersdorf is dominated by the Ca^{2+} bearing minerals calcite and dolomite, which was reflected in comparatively high mCa^{2+} (from the 8th day on) (Appendix D & E). The presence of Ca^{2+} in soil solution might induce a widening of mica interlayers from 1 to 1.4 nm which is accompanied by a CEC increase and contributes to the presence of FES, which will be further discussed in *4.3.2* (Fuller et al., 2015). However, increased mNH_4^+ might oppositely induce an interlayer collapse and hence the fixation of NH_4^+ (de Koning & Comans, 2004). The time increasing NO_2^- and NO_3^- - N pool between the 22nd and 36th day nevertheless indicated successive release of the previously fixed NH_4^+ (Figure 18). Another factor that might have contributed to NH_4^+ - losses is NH_3 volatilization due to the alkaline *p*H of Groß - Enzersdorf, which might possibly explain the non - detectable mNH_4^+ in the control (Rao & Batra, 1983).

4.2.2 NH_4^+ - dynamics Deshchenka

In case of Deshchenka, the first three week´s mNH_4^+ - N shrinkage approached the simultaneous NO_2^- and NO_3^- - N gain (Table 6). This may imply nitrification of the soluble NH_4^+ - N with little replenishment from the ex. or fixed NH_4^+ - N pool, assuming that biological assimilation was not significant. In parallel, significant amounts of ex. - NH_4^+ would have further diffused into the illitic interlayers and therefore became unextractable. Additionally, Deshchenka´s ex. - K^+ fraction on the first day (after NH_4^+ - fertilisation) ranged around 3.1 mmol kg^{-1} OD soil of which approximately 1.1 mmol kg^{-1} OD soil were detected as solution K^+, giving a relatively low K_D^K that reflects the soil´s low K^+ selectivity (Table 7, Figure 19). As stated earlier, NH_4^+ and K^+ compete on exchange and ultimately fixation sites of clay minerals. Ajazi et al. (2013) found that K^+ fertilisation prior to NH_4^+ - fertilisation led to decreased NH_4^+ fixation rates, which is in alignment with results of Beauchamp (1982), who confirmed reduced NH_4^+ adsorption and fixation when K^+ was fertilised the day before and *vice versa*. Analogously, Scherer (1982) found that the release of fixed NH_4^+ was increased on soils with low K^+ application rates. Thus, it is hypothesized that the K^+ occupation of exchange sites contributed to the high share of mNH_4^+ - N on day one and eight. However, it has severally been reported that this effect might be temporarily limited to the initial phase after NH_4^+ application (Beauchamp & Drury, 1991; Osborne, 1976). Furthermore, extractable N recovery rate was lowest on the 22nd day and increased from there again as NO_2^- and NO_3^- - N was raising. As has been stated afore, NH_4^+ fixation is a rapid process initiated by a solution NH_4^+ pool increase, while the fixed fraction operates as a slow - release reservoir in the opposite case. The first part of this dynamic is apparent by an unproportioned decrease of the ex. - and solution NH_4^+ - N fractions in comparison to the NO_2^- and NO_3^- - N increase. However, there was no detectable ex. - and solution NH_4^+ - N on the 22nd day while the NO_2^- and NO_3^- - N fraction increased considerably form the 22nd to 36th day, demasking the process of slow and successive NH_4^+ release from the fixed fraction. If only considering soil solution NH_4^+, a light increase was detectable on the 36th day, which was not detected by the in the 2 M KCl extract, most likely due to air - drying induced fixation processes (Table 6, Figure 17).

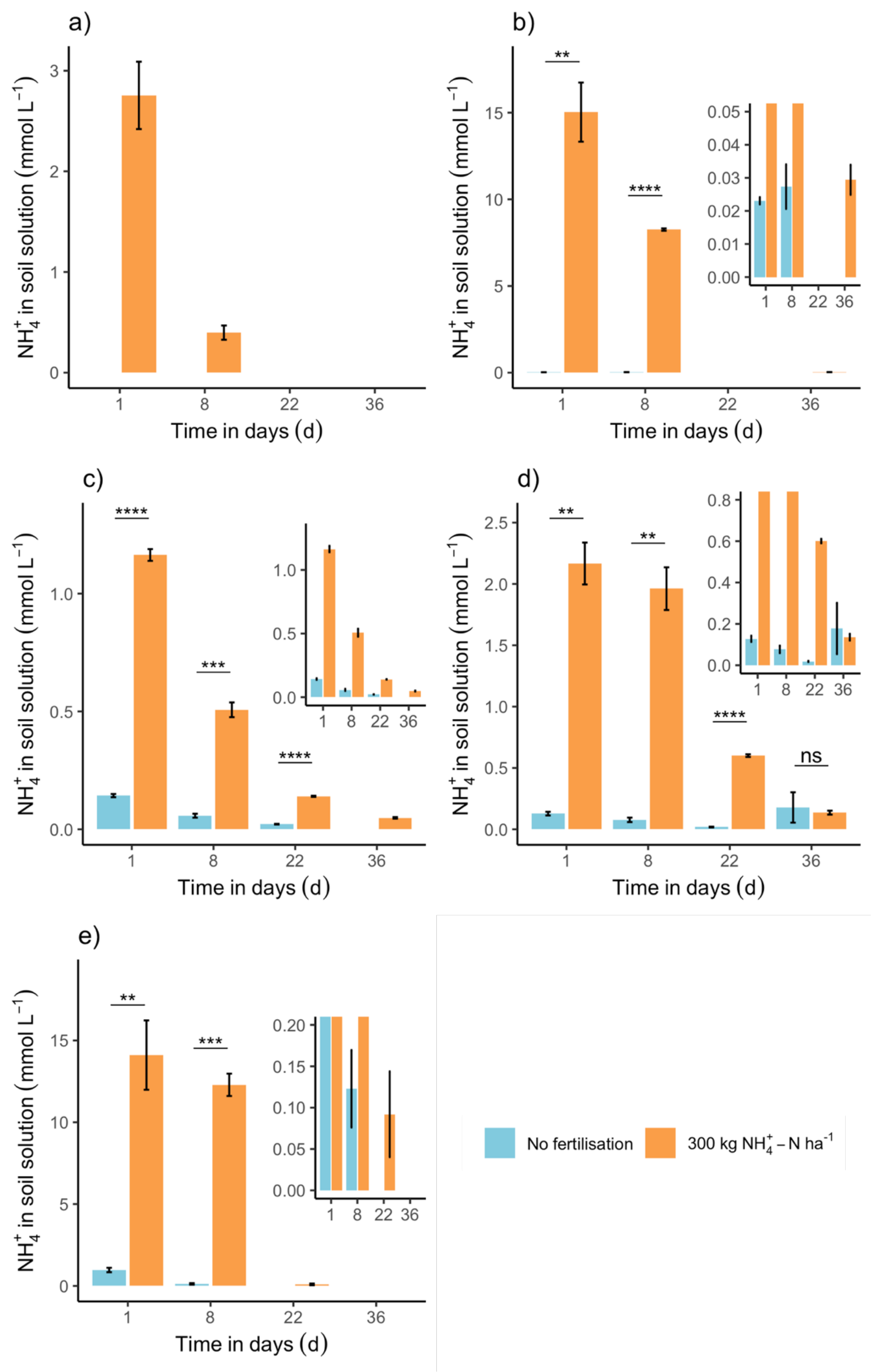

Figure 17: *Soil solution NH_4^+ concentration (mNH_4^+) with and without fertilisation treatment on all sampling dates. Asterisks indicate significant differences between the treatments on the respective day after performance of Welsh´s t-test (* : $p \leq 0.05$, **: $p \leq 0.01$, ***: $p \leq 0.001$, ****: $p \leq 10^{-4}$). The plot titles correspond to a) = Groß – Enzersdorf, b) = Deshchenka, c) = Yoshiki, d) = Ogata and e) = Miyakonojo. Error bars indicate the standard - deviation and the bar height the arithmetic mean. Embedded graphs display zoomed in variants of the original graphs. If bars are not shown, NH_4^+ concentration was below detection level (< 0.01 mmol).*

4.2.3 NH_4^+ - dynamics Yoshiki

The N - dynamics of Yoshiki are apparently unique. First, N - recovery rates of Yoshiki were lowest among all investigated soils on every day and exhibited the smallest difference to the control variants (Table 6, Figure 18, Appendix B). On the 1st day, merely 10% of the applied fertiliser were recoverable, which is in alignment with drastic K^+ losses as observed by Dengra I Grau et al. (2021) and Mori et al. (2012) on the same soil. As suggested by the authors, these phenomena are most likely based on Yoshiki´s vermiculitic clay mineralogy. Several investigations have shown that vermiculite has strong NH_4^+ fixing capacities, mainly due to an interlayer collapse that induces its entrapment (Allison et al., 1953a; Doram & Evans, 1983; Liang & MacKenzie, 1994; Mamo et al., 1993; Nommik & Vahtras, 1982). Furthermore, the ex. - K^+ level ranged around 0.5 and 0.3 mmol kg^{-1} OD soil for the control and the fertilisation treatment, respectively, and coincide with earlier findings of Mori et al. (2012) (Table 7). The slight ex. - K^+ decrease after the fertilisation might have been caused by previous NH_4^+ induced K^+ entrapment. The low extraction levels of K^+ and NH_4^+ introduce the question, if these cations are suitable for mutual extraction in vermicultiic soils. For instance, Hanway et al. (1957) found that up to 98% of the fixed NH_4^+ from a saturated vermiculite were released by boiling in NaCl solution, while already low K^+ additions induced a blocking effect towards NH_4^+ and sufficiently high concentrations entirely blocked the release. These results find further support in the work of Leggett & Moodie (1963). *Vice versa*, it has been reported that NH_4^+ addition to diluted NaCl and even HCl solutions caused decreasing K^+ concentrations in a leachate from a vermiculitic soil, while this effect was enhanced with increasing NH_4^+ concentrations (Nömmik, 1957). Scott et al. (1960) reported that the NH_4^+ release from saturated illite and vermiculite after 1 M KCl extraction was 22.1 and 8.1 mmol g^{-1}, while using 1 M NaCl yielded 22.4 and 66.5 mmol g^{-1}, respectively. These findings elucidate the risk of over- and underestimating ex. - NH_4^+ (or K^+), when using Na^+ and K^+ (or NH_4^+) as exchange cation, respectively (Scott & Smith, 1966). Reflecting this is essential, particularly if attempting to directly compare the investigated soils. Furthermore, merely Yoshiki exhibited a net N - recovery gain throughout the time period after the fertilisation treatment (Table 6, Figure 18). In light of the afore elaborated, this finding deserves at least two considerations. First: The KCl extraction might have drastically underestimated the ex. - NH_4^+ fraction, while the ex. - NO_2^- and NO_3^- fraction would however have been unaffected by the presence of K^+. Consequently, a structural increase in the NH_4^+ - N fraction might have resulted in an N - loss over time, as observed on the other soils. However, as mNH_4^+ could not have been affected by K^+ induced entrapment and remained on a low level, this hypothesis might be questionable. Moreover, Steffens & Sparks (1999) have shown that vermiculite in comparison to illite released a significantly higher share (84%

for vermiculite and 12% for illite, respectively) of non - exchangeable NH_4^+ after 1 day residence time and extraction with a H^+ - resin, which supported their supposition of previous soil experiments (Steffens & Sparks, 1997). Accelerated NH_4^+ kinetics in the presence of vermiculitic clays have also been reported of a fertilisation trial on a paddy rice soil and furthermore been proven for K^+ under laboratory conditions (Keerthisinghe et al., 1985; Scott & Smith, 1966). This may explain the strong relative increase of the NO_2^- and NO_3^- - N pool over the experiment period, even though absolute values were lowest among all soils even on the 36th day.

4.2.4 NH_4^+ - dynamics Ogata

In contrast, Ogata´s N recovery rate was 48% on the 1st day (Table 6). Slightly different, Dengra I Grau et al. (2021) reported a K^+ recovery of 35 % at a fertiliser application rate of 10.6 mmol kg^{-1} OD soil. This seems surprising, as it has been reported that NH_4^+ selectivity of smectites exceeds that of K^+ (Bajwa, 1987). On the other hand, Barshad (1954) showed that K^+ fixation in intermediately charged (150 - 160 me 100 g^{-1}) 2:1 clay minerals was clearly preferred over NH_4^+ fixation, which the author explained with the slightly smaller ionic radius of K^+ favouring a stronger crystal lattice contraction. Nonetheless, this selectivity diminished with both increasing and decreasing charge, consequently causing equal fixation at high charges and no fixation at low charges for both ions. As fixation still took place on smectite, the author suspected its occurrence in higher charged sequences of the mineral. Investigations of Chen et al. (1989) confirmed NH_4^+ fixation capacities of high charged smectite and highlighted the significant contribution of the tetrahedral layer charge. As layer charge and charge location were not part of these investigations, an interpretation of the underlying fact might be that the occurring smectite contained impurities that were able to fix NH_4^+, while some intermediately charged sequences were able to fix K^+ while NH_4^+ fixation did not occur. It is furthermore likely, that some fixation was caused by the illitic compounds, that were also detected by XRD analysis (see *4.1*). However, considering Ogata´s clay content, its N recovery rates are comparatively high, which is most likely attributable to the fact that smectite subordinately fixes NH_4^+ in comparison to illite and vermiculite (Allison et al., 1953a; Mamo et al., 1993; Steffens & Sparks, 1999). Simultaneously, Ogata exhibited the smallest solution to solid NH_4^+ - N ratio on the first day among all investigated soils, indicating that NH_4^+ was predominantly adsorbed onto exchangeable sites of the smectitic compounds (Table 6). Strong adsorption capacities of smectites have severally been confirmed in the literature (Alshameri et al., 2018; Griffin et al., 1976; Huang et al., 2021; Mazloomi & Jalali, 2017). However, NH_4^+ adsorbed onto smectite is well desorbed by salt solutions as for instance 1 M or 2 M KCl, even though Mg^{2+} salts are assumed to yield

Table 6: *Different N - pools of the unamended soils after the fertilisation treatment.*

Soil	**Day**	**2 M KCl - extracted NH_4^+ - N**[a] (mmol kg^{-1} OD soil)	**Solution NH_4^+ - N at 60% WHC**[a,b] (mmol kg^{-1} OD soil)	**Solution NH_4^+ - N/ 2 M KCl extracted NH_4^+ - N** (in %)	**2 M KCl extracted NO_2^- - & NO_3^- - N**[a] (mmol kg^{-1} OD soil)	**2 M KCl extracted NH_4^+ -, NO_2^- - & NO_3^- - N** (mmol kg^{-1} OD soil)	**N - recovery rate**[c] (in %)
Groß - Enzersdorf	1	3.37 ± 0.42	0.49 ± 0.06	14	0.3 ± 0.05	3.85	33
	8	1.38 ± 0.17	0.07 ± 0.01	5	1.26 ± 0.03	2.64	23
	22	0.04 ± 0.06	-	-	1.76 ± 0.52	1.76	17
	36	-*	-	-	2.32 ± 0.08	2.32	21
Deshchenka	1	5.86 ± 0.49	2.34 ± 0.27	41	0.62 ± 0.06	6.46	62
	8	3.17 ± 0.58	1.28 ± 0.01	40	1.5 ± 0.24	4.68	45
	22	-	-	-	2.59 ± 0.35	2.59	25
	36	-	0.005 ± 0.001	n.c.**	3.5 ± 0.2	3.5	34
Ogata	1	6.53 ± 0.74	0.72 ± 0.06	11	0.17 ± 0.02	6.7	48
	8	4.21 ± 0.28	0.66 ± 0.06	16	0.87 ± 0.38	5.08	37
	22	2.51 ± 0.22	0.2 ± 0.004	8	1.9 ± 0.05	4.41	32
	36	1.13 ± 0.17	0.05 ± 0.01	4	3.32 ± 0.06	4.45	32
Yoshiki	1	1.06 ± 0.07	0.24 ± 0.0052	23	0.12 ± 0.01	1.18	10
	8	0.73 ± 0.04	0.11 ± 0.0065	15	0.43 ± 0.02	1.16	10
	22	0.53 ± 0.09	0.03 ± 0.0005	6	1.13 ± 0.01	1.66	15
	36	0.37 ± 0.05	0.01 ± 0.0007	3	1.5 ± 0.3	1.87	16
Miyakonojo	1	12.2 ± 0.71	5.92 ± 0.89	48	1.02 ± 0.06	13.24	82
	8	7.5 ± 0.7	5.16 ± 0.29	69	2.1 ± 0.07	9.6	59
	22	0.17 ± 0.01	0.04 ± 0.02	24	4.76 ± 0.18	4.93	30
	36	-	-	-	5 ± 0.35	5	31

[a] *Values in those columns show the arithmetic means of triplicates and ± indicates the standard - deviation.*

[b] *Solution NH_4^+ - N kg^{-1} OD soil was obtained by multiplication of the solution concentration with the added water per kg OD soil.*

[c] *N - recovery was calculated by dividing the extracted NH_4^+ -, NO_2^- - and NO_3^- - N by the applied fertiliser amount.*

** The hyphen (-) denotes NH_4^+ concentrations that were below the detection level of 0.01 mM L^{-1}.*

*** n.c. denotes not calculable.*

highest NH_4^+ exchange (Huang et al., 2021; Mamo et al., 1993; Mazloomi & Jalali, 2017). Positive linear relations between $K_DNH_4^+$ and CEC have therefore been reported before (Griffin et al., 1976; Thornton et al., 2001). Indeed, Ogata exhibited highest CEC and $K_DNH_4^+$ on the first day among all soils, while a Mg^{2+} salt extraction might have further reinforced this phenomenon (Table 5 & 6).

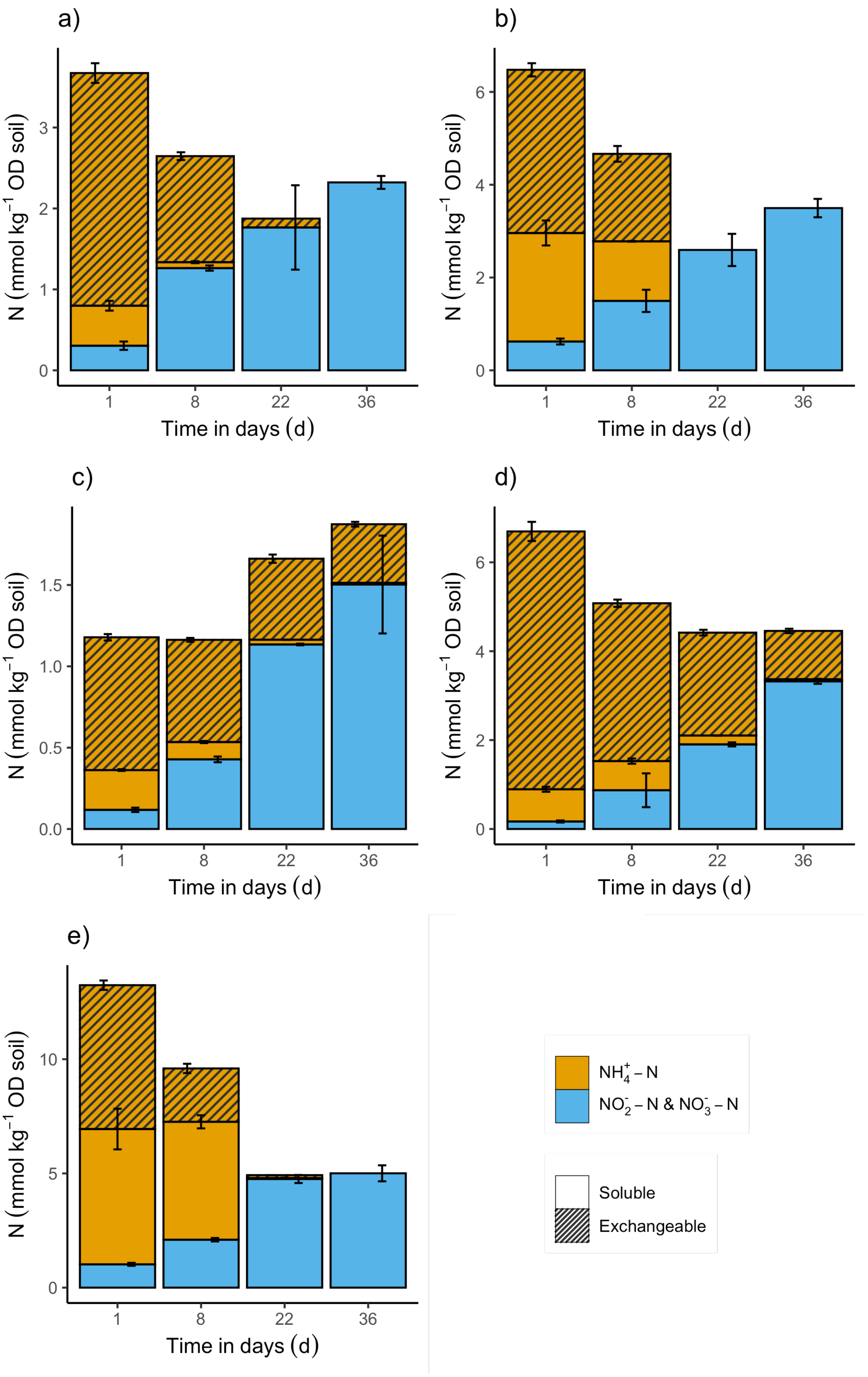

Figure 18: *N - fractions of unamended soils after the fertilisation treatment. The graph´s captions correspond to: a) = Groß - Enzersdorf, b) = Deshchenka, c) = Yoshiki, d) = Ogata and e) = Miyakonojo. Error bars indicate the standard - deviation and the bar height the arithmetic mean. Note, that NO_2^- and NO_3^- were determined in the 2 M KCl extract but are assumed to be equivalent to the respective solution concentrations.*

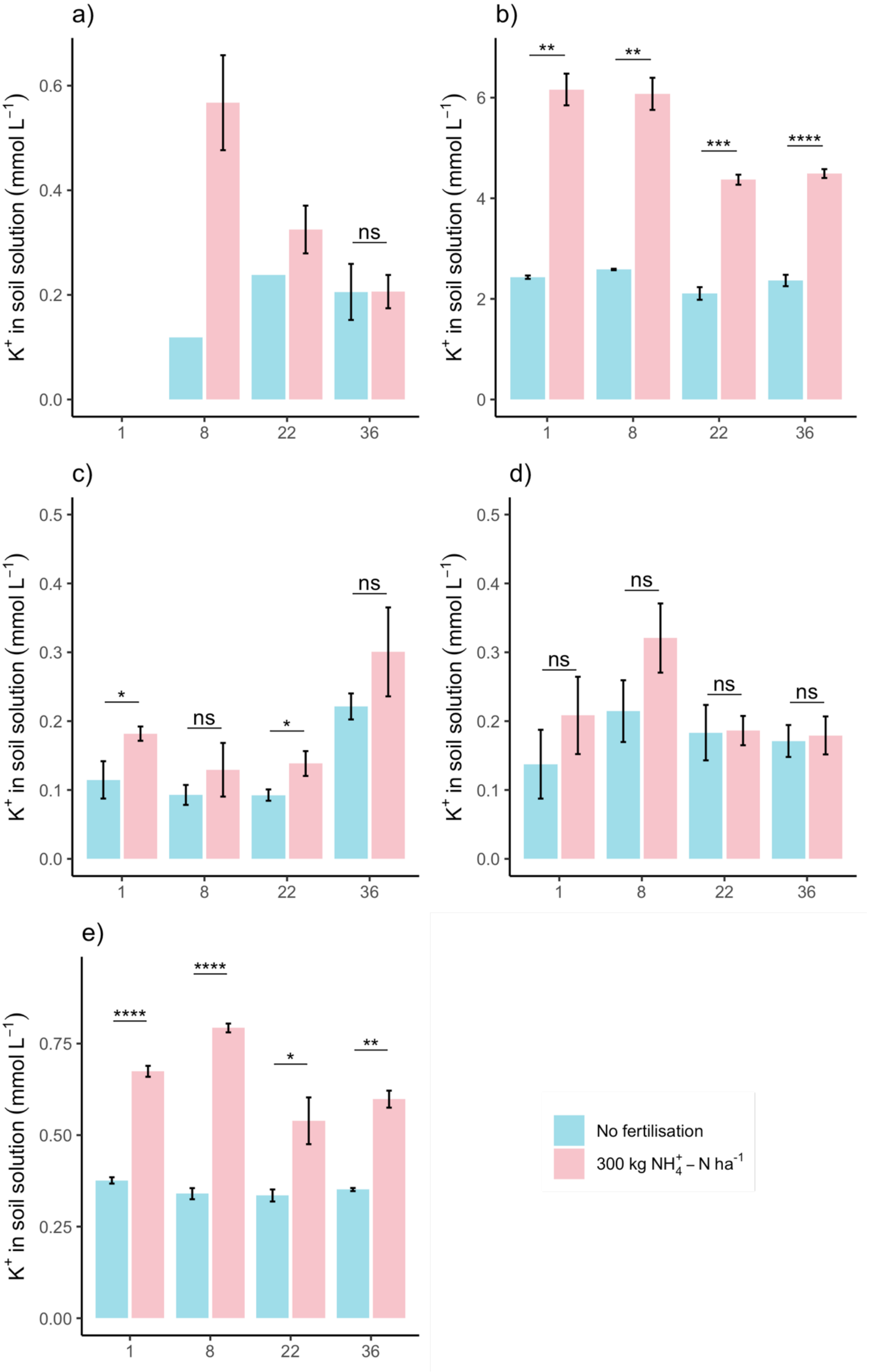

Figure 19: *Solution K^+ concentration (mK^+) with and without fertilisation treatment on all sampling dates. Asterisks indicate significant differences between the treatments on the respective day after performance of Welsh´s t-test (* : $p \le 0.05$, **: $p \le 0.01$, ***: $p \le 0.001$, ****: $p \le 10^{-4}$). The plot titles correspond to a) = Groß – Enzersdorf, b) = Deshchenka, c) = Yoshiki, d) = Ogata and e) = Miyakonojo. Error bars indicate the standard - deviation and the bar height the arithmetic mean. In cases where bars or error bars are not shown, soil solution sampling was hindered.*

Table 7: *1 M NH_4OAc extractable K^+ of the unamended soils.*

Soil	**Fertilisation** (kg NH_4^+ - N ha^{-1})	**1 M NH_4OAc Ex. - $K^{+\,a}$** (mM kg^{-1} OD soil)
Groß - Enzersdorf	0	2.83 ± 0.004
	300	3.04 ± 0.29
Deshchenka	0	3.15 ± 0.16
	300	3.38 ± 0.002
Yoshiki	0	0.5 ± 0.22
	300	0.3 ± 0.02
Ogata	0	2.19 ± 0.17
	300	2.16 ± 0.25
Miyakonojo	0	1.42 ± 0.26
	300	1.4 ± 0.28

[a] Values in those columns show the arithmetic means of triplicates and ± indicates the standard deviation.

4.2.5 NH_4^+ - dynamics Miyakonojo

Miyakonojo´s control exhibited the highest mNH_4^+ among all soils on the 1st day, pointing towards significant N mineralization processes, most likely induced by aeration and WHC adjustment to 60% at the incubation start (Figure 17). Elevated net N transformations have been reported for Japanese Andosols before and were linked to their high organic matter content (Urakawa et al., 2016). Furthermore, Miyakonojo showed the highest fertiliser recovery rate on the 1st day, which is in alignment with findings of K^+ recovery rates performed on the same soil (Table 6) (Dengra I Grau et al., 2021). On the 8th day, however, total N recovery was reduced by 22%, which was mainly attributable to a decrease of the ex. - NH_4^+ - N fraction (Figure 18). In contrast, the sum of mNH_4^+ - N and the NO_2^- and NO_3^- - N pool increased, suggesting replenishment from the exchangeable NH_4^+ - N pool (Roberge, 1972). It is striking that the mNH_4^+ - N share of the 2 M KCl extractable NH_4^+ - N increased by approximately 20% from the 1st to the 8th day, which is exceeding observations of the other soils by far. An effect that might have played a role in this context is a notable *p*H decrease, that will be further discussed in *4.5.1 - 4.5.3* (Figure 24). Time - depended *p*H decrease after $(NH_4)_2SO_4$ fertilisation has previously been confirmed by Hayashi et al. (2009) and is most likely induced by nitrification, which produces 2 H^+ per NH_4^+ to NO_3^- conversion (He et al., 1999) (Figure 24 & 25). Furthermore, it is well documented, that allophane´s CEC is strongly *p*H dependent and its point of zero net charge (PZNC) ranges around 5 - 6. The variable charge is caused by functional groups (Al - OH) on the mineral´s surface that are highly selective towards H^+ and develop positive charges once H^+ is adsorbed from the soil solution (Harsh et al., 2002; Wada & Ataka, 1958). As the *p*H decreased from 5.6 to 5.3, the variable charged sites of allophane probably contributed to a decreasing CEC of Miyakonojo. A possible dynamic could have been a simultaneous mNH_4^+ and *p*H decrease that was interlinked with a decrease in the capacity to hold NH_4^+ on the exchange sites which was ultimately released into the soil solution, again refilling the solution NH_4^+ pool (Wada & Okamura, 1980). Aside from the N - pool distribution, the 22% total N loss (corresponding to 3.7 mmol N) need to find consideration. Gaseous N - losses in form of NH_3 or N_2O might have occurred but unlikely by a significant share, as has been proven before on Japanese Andosols (Hayashi et al., 2009; McTaggart & Tsuruta, 2003). Another possibility for NH_4^+ losses from the investigated pool might have been caused by intercalation in halloysite interlayers. Indeed, several authors confirmed a high selectivity of halloysite towards poorly hydrated ions such as NH_4^+, Cs^+, Rb^+ and K^+ and large light weighted anions that neutralize the excess positive charge of the respective cation. More precisely, it was found that salts of neither too small alkali metals such as Na^+ and Li^+, nor divalent cations as Mg^{2+}, Ca^{2+} or Ba^{2+} would intercalate in halloysite. Halloysite that was suspended in NH_4Cl and CsCl solutions exhibited an increase in d - spacing after subsequent drying, which was only partly observed for KCl and not observable with LiCl and NaCl (Wada, 1958, 1959). Interestingly, mCs^+ and mNH_4^+ were particularly high on the first two sample days but drastically decreased on the 22nd and 36th day, while a similar but less clear pattern was observable for K^+ (Figure 17, 19 & 20). These observations would fit the descriptions of halloysite intercalation processes well, although conclusions might not as easy be drawn. For instance, Wada (1958) suggested that significant intercalation would occur with salt concentrations of 200 - 400 mmol 100 g^{-1} clay, which is far from the concentrations used in this experiment. Apart from this, microbial immobilization might pose a further possible NH_4^+ sink, which is favoured by the high organic matter content of Miyakonojo (Barrett & Burke, 2000). However, the N - loss scope is clearly above values that have been reported in the literature (Beauchamp & Drury, 1991). It might eventually be questioned if the absence of 2:1 clay minerals can certainly be assumed. Ogasawara et al. (2013) reported that XRD analysis may inappropriately detect traces of 2:1 clay minerals when other bulk minerals are present. The presence of 2:1 clay mineral traces originating in aeolian dust from the Chinese mainland is likely even in Japanese allophanic Andosols and might be the most appropriate elucidation of the strong NH_4^+ - N losses towards the end of the experiment (Eguchi et al., 2012).

4.3 Caesium dynamics of the unamended soils

The mCs^+ ranges were clearly distinct among the investigated soils. Generally, mCs^+ was up to six orders of magnitude smaller than mNH_4^+. It has been reported that solution ^{133}Cs concentrations in soils are usually below 100 nmol L^{-1}, which coincides with concentrations of all investigated soils in the control variant (Rai & Kawabata, 2020). However, straight comparisons among the soils are hindered as each soil exhibits individual naturally occurring Cs^+ concentrations which accordingly determine the respective response levels. Furthermore, Dengra I Grau et al. (2021) attempted to determine ex. - Cs^+ by 1 M NH_4OAc

extraction in previous studies on the Japanese soils used in this study but obtained unsatisfactory results when soils contained considerable amounts of 2:1 clay minerals. These insights were previously confirmed on European soils by weak correlation between RIP and 1 M NH_4Cl extracted Cs^+ (Roig et al., 2007). For Japanese soils, Yamaguchi et al. (2019) found 1 M NH_4OAc to be suitable for Cs^+ extraction on soils with low RIP but obtained large variation in soils with high RIP in the control as well as with zeolite and vermiculite amendments, respectively. The reason for this might be a NH_4^+ - induced collapse of the interlayers in 2:1 clay minerals when applying this method (de Koning & Comans, 2004). Therefore, merely mCs^+ was determined in this study. With exception of Yoshiki, mCs^+ was significantly ($p < 0.05$) higher after the fertilisation treatment on the 1st and 8th day, basically revealing that NH_4^+ was capable of desorbing Cs^+ from exchange sites, as has severally been stated in the literature (Ioannides et al., 2003; Sun et al., 2019). As was observed for mNH_4^+, mCs^+ generally decreased with time and hence with decreasing mNH_4^+ (Figure 20). This phenomenon is well described by a linear regression in which mCs^+ is predicted by mNH_4^+ (Figure 21). Every soil exhibited a positive slope β and mNH_4^+ proves to be an appropriate predictor for mCs^+ ($R^2 \geq 0.86$) in case of Ogata, Deshchenka and Miyakonojo, which confirms earlier findings of Wakabayashi et al. (2017).

4.3.1 Cs^+ - dynamics Groß - Enzersdorf

Groß - Enzersdorf´s mCs^+ ranged on a trace level (< 0.6 nmol L^{-1}), which might partly explain the large variances among the triplicates. The treatment concentrations on the 1st and 8th day were significantly higher than those of the respective control variant, while no statistical significance was obtained for the other sampling dates. In parallel, mNH_4^+ was below the detection level for both the control and the treatment on those dates. A successive mCs^+ decrease furthermore consolidates its correspondence to NH_4^+ concentrations (Figure 21). However, the absolute differences between treatment and control were at most approximately 0.3 nmol, indicating that quantitively hardly any Cs^+ desorption occurred. This fact might be interpreted by both possibly low natural Cs^+ concentrations and the soil´s clay mineralogy. Groß - Enzersdorf is strongly dominated by illite, that exhibits high Cs^+ selectivity due to the abundance of FES (Brouwer et al., 1983; Cremers et al., 1988; Sawhney, 1964). However, increased mNH_4^+ might induce an interlayer collapse on these sites and hence entrap Cs^+ that was previously located on FES and potentially exchangeable. It was shown that Cs^+ desorption on pure illite follows a reversible ion exchange reaction if the NH_4^+ concentration does not exceed 0.1 mmol L^{-1} and enough time was granted (de Koning & Comans, 2004). In this study, mNH_4^+ exceeded that concentration on both the 1st and the 8th day, consolidating the assumption of Cs^+ fixation processes. It is still most likely that the increased mCs^+ derived from FES desorption, as the concentrations ranged on a level ($< 10^{-9}$ mol L^{-1}) on which other exchange sites are subordinated, particularly RES if higher valency ions are abundant in soil solution (Bradbury & Baeyens, 2000; Brouwer et al., 1983; Comans et al., 1991). Besides illite, chlorite was abundantly represented in Groß - Enzersdorf´s clay fraction. As chlorite is known to have extremely low K_D^{Cs} values, it is highly unlikely that significant Cs^+ desorption at these concentration ranges occurred on the mineral (Ohnuki & Kozai, 2013). As the same is assumed to hold true for organic matter, referring to literature of adsorption/desorption experiments on pure illite might be a good approximation of Cs^+ dynamics in case of Groß - Enzersdorf (Mukai et al., 2016b).

4.3.2 Cs^+ - dynamics Deshchenka

Deshchenka exhibited significantly ($p < 0.05$) increased mCs^+ after the fertiliser treatment on the 1st, 8th and 22nd day. Like Groß - Enzersdorf, the concentrations decreased successively and corresponded to decreasing NH_4^+ concentrations (Figure 20 & 21). The factor between the control and the treatment concentration levels on the 1st and 8th day is nonetheless clearly higher than in case of Groß - Enzersdorf. As indicated by XRD analysis, chlorite, kaolinite and illite represented the biggest share of Deshchenka´s clay fraction. Further, mCs^+ ranges on a level which would still cause Cs^+ to predominantly bind on FES. The stronger response towards NH_4^+ fertilisation in comparison to Groß - Enzersdorf is diversly interpretable. First, Groß - Enzersdorf´s illite content is clearly higher as Deshchenka´s, basically implying the presence of more highly Cs^+ selective sites and consequently higher probability for Cs^+ adsorption on those (Figure 12 & 13). Moreover, kaolinite exhibits higher K_D^{Cs} values than chlorite, while Cs^+ is desorbed well (~ 60%) even at low concentrated (10^{-9} mol L^{-1}) Cs^+ adsorbate solutions (Ohnuki & Kozai, 2013). Moreover, the weathering degree of illite might play a central role in this context, as was already discussed for NH_4^+ in *4.2.1* and *4.2.2*. Studies of Fuller et al. (2015) showed that suspending unweathered illite in $CaCl_2$ solution caused an interlayer widening (1.4 nm) on the edges of the mineral while no changes were detected after suspension in deionized water. This process is described as the initial weathering step from mica to vermiculite and induces the formation of FES (Fuller et al., 2015; Jackson et al., 1952; Lee et al., 2017; Ogasawara et al., 2017). Resuspension in CsCl solutions caused the FES to collapse and entrap Cs^+. Due to the high mK^+ levels observed for Deshchenka, it is likely that the edge zones of illite were collapsed through the intercalation of K^+ which consequently induced the reduction of FES and finally Cs^+ exchange on RES (Murota et al., 2020). This hypothesis is supported by studies of Ogasawara et al. (2017), which showed that K^+ release from biotite correlated positively with the formation of FES in the initial weathering stages. In contrast, Groß - Enzersdorf´s ≥ 10

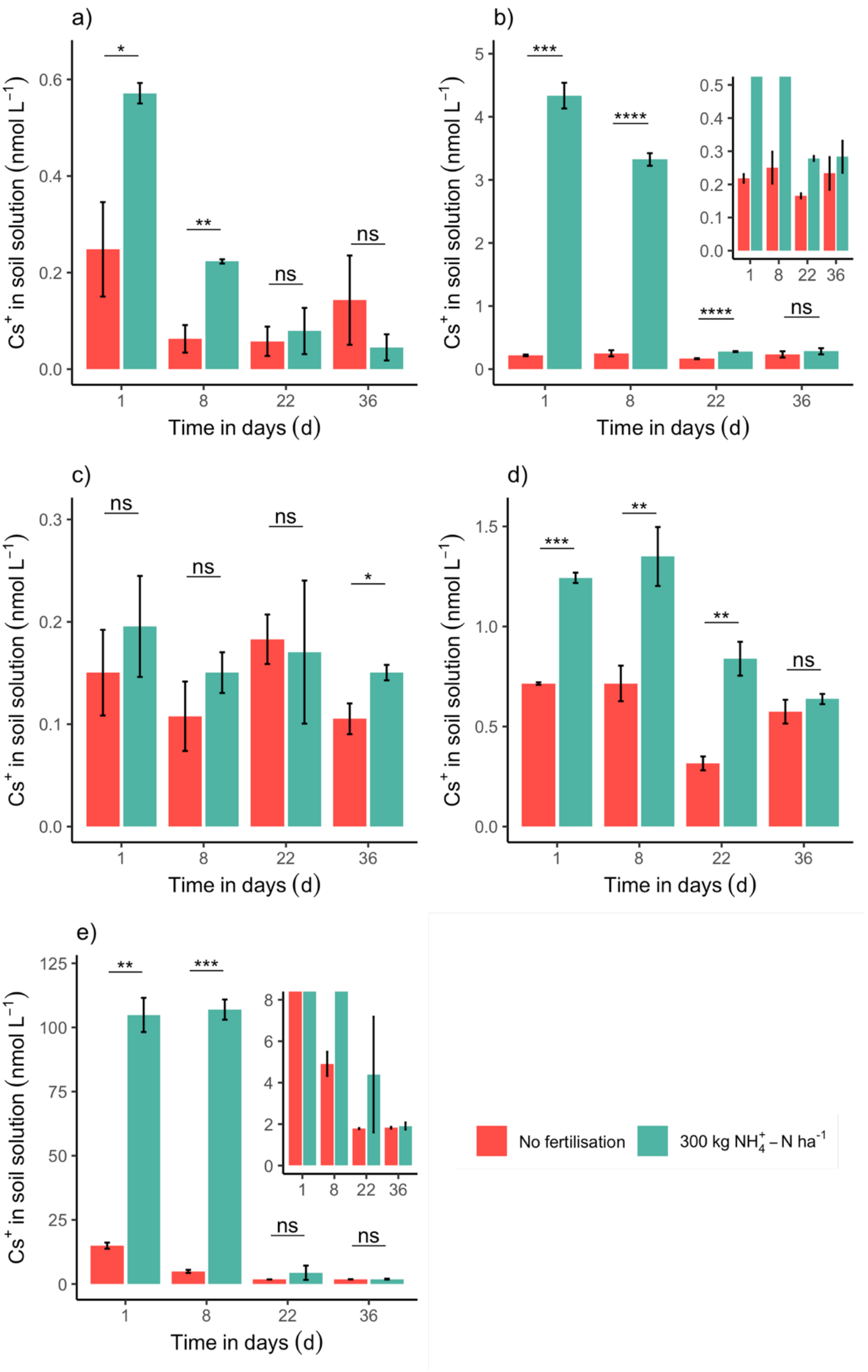

Figure 20: *Solution Cs$^+$ concentration (mCs$^+$) with and without fertilisation treatment on all sampling dates. Asterisks indicate significant differences between the treatments on the respective day after performance of Welsh´s t-test (* : $p \leq 0.05$, **: $p \leq 0.01$, ***: $p \leq 0.001$, ****: $p \leq 10^{-4}$). The plot titles correspond to a) = Groß – Enzersdorf, b) = Deshchenka, c) = Yoshiki, d) = Ogata and e) = Miyakonojo. Error bars indicate the standard - deviation and the bar height the arithmetic mean. Embedded graphs display zoomed in variants of the original graphs.*

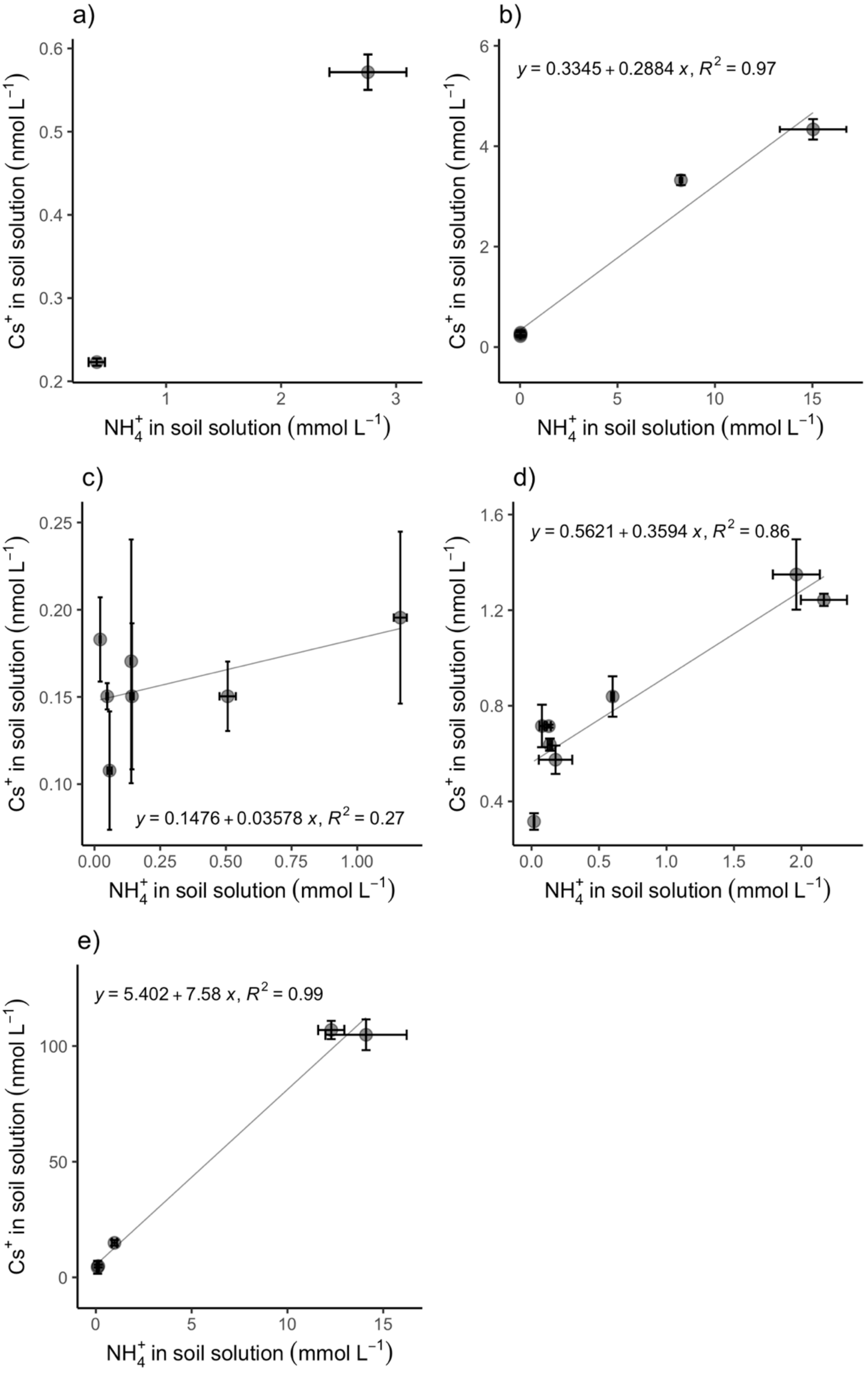

Figure 21: *Relationship between solution NH_4^+ concentration (mNH_4^+) and solution Cs^+ concentration (mCs^+). The graph´s captions correspond to a) = Groß – Enzersdorf, b) = Deshchenka, c) = Yoshiki, d) = Ogata and e) = Miyakonojo. Data - points include both fertilised and unfertilised variants, respectively. Error bars indicate the standard - deviation. Note, that Groß - Enzersdorf did not obtain a linear fit as merely two data - points were available.*

µm mineralogy is dominated by the Ca^{2+} bearing minerals calcite and dolomite, which was reflected in relatively high mCa^{2+}, while mK^+ was clearly below that of Deshchenka (Figure 19, Appendix E) (Henderson et al., 1976). This might also explain the comparatively high CEC of Groß - Enzersdorf, obtained by divalent exchange cations (Ba^{2+}, Mg^{2+}). Indeed, Dolcater et al. (1972) found that the CEC of muscovite and biotite decreased after K^+ saturation, while the presence of Ca^{2+} in the equilibration solution mitigated this effect. Similarly, Murota et al. (2020) found that the CEC of Ca^{2+} saturated illite was increased towards K^+ saturated illite, although silver thiourea (AgTU) was used as cation exchanger. Simultaneously, the study revealed that Ca^{2+} as background electrolyte caused 90% Cs^+ adsorption onto illite, while only 50 - 70% were adsorbed in the presence of K^+. Nevertheless, XRD patterns of the minerals were undistinguishable. As assumed in this study, the authors suggested that these special properties would be attributable to the peripherical zones of the clay and the concept of FES.

4.3.3 Cs^+ - dynamics Yoshiki

The mCs^+ dynamic pattern of Yoshiki does not follow a comprehensible logic. The concentrations were on the lowest level among all soils (< 0.2 nmol L^{-1}) and did not differ significantly between control and treatment with exception of the 36th day, which is however rather a statistical effect due to small variances observed for those replicates (Figure 20). All other variants exhibited high coefficients of variation (CV), ultimately causing non - significant results while reflecting the low mCs^+ levels (Reed et al., 2002). Consequently, Yoshiki exhibited the lowest mCs^+ and mNH_4^+ as well as the smallest fertiliser recovery rate, as elaborated in *4.2.3*. Again, this is most likely attributable to significant shares of vermiculite in Yoshiki´s clay fraction. It has been reported by several authors that vermiculite possesses strong Cs^+ fixation capacities. For instance, ^{137}Cs desorption from illite with 0.1 M (stable) CsCl was approximately three times higher (19% vs. 6%) than from vermiculite with adsorbate to adsorbent ratios of 1.38×10^{-10} M ^{137}Cs g^{-1} clay (Koshikawa et al., 2019). When 1 M NH_4NO_3 (equivalent to 0.3 M NH_4^+ g^{-1} clay) instead of 0.1 M CsCl (equivalent to 30 mmol Cs^+ g^{-1} clay) was used as extractant solution, desorption from illite was even five times higher (9% vs. 55%). Furthermore, Fan et al. (2014) reported that at a 5.42×10^{-4} M Cs^+ g^{-1} adsorbate to adsorbent ratio on vermiculite Cs^+ was hardly desorbed by 0.12 M NH_4^+ g^{-1}, while the same reagent desorbed approximately one third of Cs^+ adsorbed onto illite at even slightly lower initial Cs^+ levels. Results of batch experiments conducted with isolated minerals and known adsorbate concentrations are apparently difficult to apply onto soils. However, if vermiculite is assumed to represent approximately 1% of Yohiki´s soil mass, while 1.14×10^{-5} M NH_4^+ g^{-1} soil was fertilised and other NH_4^+ sinks are not considered, the adsorbate to adsorbent ratio would increase by two orders of magnitude, which is still far from the concentrations used in the afore discussed experiments. In light of that, Yoshiki´s results seem not surprising. Fan et al. (2014) elaborated that vermiculite in comparison to illite possesses additional highly selective sites for Cs^+, while FES, Type II sites and planar sites are shared by both minerals. These sites still showed comparatively high selectivity coefficient towards alkali metals with low hydration energy ($\log K_{c\,(Cs-K)} = 1.5$) and contributed to 40% of vermiculite´s CEC, which in turn was already clearly above that of illite. This is in alignment with findings Nakao et al. (2008b), who reported RIP values of 11.8 and 25.9 mmol kg^{-1} for illite and vermiculite, respectively. Caesium over K^+ selectivity on interlayer sites of 2:1 clay minerals has already been reported by Sawhney (1972) and was attributed to the lower hydration energy of Cs^+ in comparison to K^+. Consequently, Cs^+ might also be preferred over NH_4^+ on those sites. Furthermore, it was found that vermiculite almost entirely adsorbed Cs^+ even when the ratio of Cs^+ to other cations in solution was extremely small (10^{-8}) and highly competitive cations as K^+ and NH_4^+ were present (Sikalidis et al., 1988). The authors reported the Cs^+ selectivity coefficients towards NH_4^+ and K^+ at those concentrations to be 400 and 320, respectively, although clear decreases with shrinking ion ratios were observed. Consequently, the high selectivity of vermiculite towards Cs^+ at low concentrations even in the presence of strong competitors as NH_4^+ might qualitatively elucidate the observed phenomena. Moreover, Dengra I Grau et al. (2021) reported a significant RIP increase with increasing K^+ loadings (0 - 500 K_2O kg^{-1}) for Yoshiki. Similar to this study, their mCs^+ ranged on an extreme low level but slightly decreased with increasing K^+ applications. It is likely that K^+ application caused an interlayer collapse in hydrated vermiculite sequences and hence the formation of new FES. As stated in *4.2.3*, NH_4^+ fixation in vermiculitic interlayers was made responsible for the low fertiliser recovery rate. However, the lack of a pattern compared to the results of Dengra I Grau et al. (2021) could be due to the higher selectivity of NH_4^+ over K^+ at FES, Type II and interlayer sites, which eventually compensated for Cs^+ fixation (Bradbury & Baeyens, 2000; Fan et al., 2014a).

4.3.4 Cs^+ - dynamics Ogata

In case of Ogata, mCs^+ and mNH_4^+ are well correlated (Figure 21). The fertiliser treatment exhibited significantly ($p < 0.01$) higher mCs^+ on the 1st, 8th and 22nd day, while no significant effect was observed on the 36th day. However, absolute differences between the treatment and the control were comparatively small. Ogata´s clay fraction was clearly dominated by smectite that was accompanied by small amounts of illite, chlorite and kaoline minerals. Caesium adsorption onto smectite over a Cs^+ adsorbate solution range can be described linearly, reflecting the homogeneity of exchange sites on the mineral (Durrant et al., 2018).

However, higher charged interstratifications in smectite have been reported to cause non - linear Cs^+ adsorption and the presence of two distinct exchange sites (Missana et al., 2004). Thereby, higher charged sequences possess specific Cs^+ adsorption sites with high selectivity at trace solution concentrations, while sites associated with smectite (less charged part of complex) gain in significance when the former are saturated. Similar results were obtained when Cs^+ adsorption was investigated in the presence of both pure illite and smectite (Missana et al., 2014). As elaborated in *4.2.4*, K^+ and NH_4^+ fixation in Ogata was assumed to be caused by both intermediately charged interstratifications in smectite and the illitic compounds (Dengra I Grau et al., 2021). Furthermore, Dengra I Grau et al., (2021) found increased K^+ applications to induce a reduction of both mCs^+ and ex. - Cs^+. More precisely, the highest K^+ application (10.62 mmol K^+ kg^{-1}) more than halved mCs^+ in comparison to the control. This is in straight contrast to the results presented in this study, where the treatment (13.91 mmol NH_4^+ kg^{-1}) nearly doubled mCs^+ on the 1st day. On the one hand, mNH_4^+ in this experiment exceeded mK^+ of the results of Dengra I Grau et al. (2021) approximately seven - to eight - fold. Increased Cs^+ desorption might hence basically be inferred by the law of mass order. On the other hand, mNH_4^+ ranged around 2×10^{-3} M L^{-1} and thereby exceeded the critical value of 10^{-4} M L^{-1} that might induce a partial interlayer collapse and subsequent Cs^+ fixation, at least on illite (de Koning & Comans, 2004). Moreover, it is likely that Cs^+ at those low concentration ranges ($< 1.5 \times 10^{-9}$ M L^{-1}), was adsorbed onto FES, which exhibit an approximately fivefold higher selectivity for NH_4^+ compared to K^+ (Wauters et al., 1996a). It might hence be hypothesized, that the higher concentration gradient of NH_4^+ and its stronger competitivity on FES caused Cs^+ desorption that exceeded Cs^+ fixation. That this effect was subjected to a strong dynamic is seen from the mCs^+ decrease after 22 and 36 days, that was accompanied by further NH_4^+ fixation and nitrification processes which signified a successive loss of power to desorb Cs^+ from FES and could allow Cs^+ to subsequently re - adsorb onto those sites. However, the distinct influence of K^+ and NH_4^+ on Cs^+ in both Ogata and Yoshiki remains speculative and should find consideration in future mineralogical investigations.

4.3.5 Cs^+ - dynamics Miyakonojo

The mCs^+ dynamic pattern of Miyakonojo was characterized by a treatment induced plateau on the 1st and 8th day, that showed significantly ($p < 0.01$) higher concentrations than the control, respectively (Figure 20). This plateau, however, decreased to the control´s level on the 22nd and 36th day, which was indicated by non - significant treatment effects on those days. Moreover, Miyakonojo exhibited a clear decreasing mCs^+ pattern in the control, reflecting the increased mNH_4^+ through N mineralization processes at the incubation start as discussed in *4.2.5*. Generally, the mCs^+ of both the control and the treatment exceeded that of the other investigated soils on the 1st and 8th day, which could be related to elevated total natural Cs^+ contents. However, results of Dengra I Grau et al. (2021) might contradict this assumption, reporting that 1 M NH_4OAc extracted 727.17 and 744.46 nmol Cs^+ kg^{-1} in case of Miyakonojo and Ogata, respectively. Due to the NH_4^+ induced interlayer collapse of 2:1 clay minerals, the authors stated that this extraction method would even underestimate the actual ex. - Cs^+ fraction of Ogata. It is hence assumed, that the high mCs^+ levels in contrast to the other investigated soils might rather be related to the specific clay mineralogy of Miyakonojo. The XRD analyses revealed the presence of allophane and halloysite, while 2:1 phyllosilicates were not detected. Long-time investigations of Cs^+ spiked soils showed that 1 M NH_4OAc extractions rates of allophanic Andosols were significantly higher than those of a smectitic Gleysol, a sandy regosol and a nonallophanic Andosol (Takeda et al., 2013). Furthermore, the allophanic Andosols exhibited low RIP, which is proportionally related to the amount of FES (Equation 9), consequently indicating that Cs^+ exchange predominantly took place on RES. The $K_{c(Cs\text{-}NH4)}$ of these sites is approximately two orders of magnitude smaller than that of FES, facilitating Cs^+ desorption by NH_4^+ (Wauters et al., 1996a, 1996b). Dengra I Grau et al. (2021) reported Miyakonojo´s control RIP to be approximately 12 and 5% of the control of Yoshiki and Ogata, respectively. As elaborated in the literature review, low RIP has severally been reported on Andosols (Nakao et al., 2015; Takeda et al., 2014; Uematsu et al., 2015; Vandebroek et al., 2012; Yamaguchi et al., 2019). Moreover, Miyakonojo´s clay content was significantly higher than Yoshiki´s, supporting the inappropriateness of clay content as an RIP predictor when volcanic ash soils are considered (Uematsu et al., 2015). On the other hand, the results of Takeda et al. (2013) also showed that only 4 h after Cs^+ spiking an allophanic Andosol, merely a share of 72% was extractable with 1M NH_4OAc, while after 1212 days it further reduced to 22%, although this value already stabilized after approximately 100 days. Earlier investigations on nine Andosols and two Fluvisols from Japan showed that on average 70% of ^{137}Cs was considered as fixed, while 20 and 10% were found to be organically bound and NH_4OAc extractable, respectively (Tsukada et al., 2008). Furthermore, the specific activity of ^{137}Cs decreased in the order exchangeable > organically bound > fixed, indicating that an equilibrium between ^{133}Cs and ^{137}Cs had not been reached, even though ^{137}Cs must have derived from atomic weapon test fallouts happened decades before the experiment was conducted. These findings elucidate two central aspects: Cs^+ migration from the exchangeable and organically bound fractions to the fixed fraction might at least span over decades in which the risk of NH_4^+ induced desorption is increased. However, allophanic Andosols exhibit the ability to quickly adsorb significant amounts of Cs^+ into fractions that are not exchangeable by NH_4^+, although other soil - types are clearly better protected against Cs^+ desorption. Takeda et al. (2013) found 30% of the spiked Cs^+ to be NH_4^+ extractable after 100 days, which resembles the extracted NH_4^+, NO_2^- and NO_3^- - N from the 22nd day on in this study. As discussed in *4.2.5*, the presence of 2:1 clay mineral traces is likely on Japanese allophanic Andosols and might be missed out in XRD analyses. Similarly, Takeda et al. (2013) assumed the presence of crystalline clay minerals in allophanic Andosols to be responsible for the non-extractable Cs^+ share.

4.4 Ammonium dynamics of the clay - amended soil

In addition to the fertiliser treatment, Miyakonojo received two distinct amounts (10 and 40 t ha^{-1}) of three different clay amendments, respectively. The aim was to comprehend their effects on ex. - NH_4^+, mNH_4^+ as well as mCs^+ dynamics and ultimately evaluate their appropriateness as a countermeasure for RC polluted soils while simultaneously considering potential adverse effects in the context of agricultural N management. In the following discussion, the abbreviations S, V, and Z correspond to Smectite, Vermiculite and Zeolite while the digits 1 and 4 indicate the application rates with 10 and 40 t ha^{-1}, respectively. As shown by Figure 22, mNH_4^+ decreased from the 1st day until the 22nd day for all variants. The 36th day is not depicted, as with exception of Z4 all concentrations were below the detection level. On the 1st and the 8th day, the fertiliser treatment induced significantly higher mNH_4^+ for the control and all amendments. More precisely, mNH_4^+ of V4 was significantly below V1 and the control, while Z4 was significantly below all other fertilised variants on the 1st day. The pattern on the 8th day resembled that of the 1st day, although this time the control and S1 concentrations were significantly above that of V4, while Z4 was still significantly below all other treatments and the control. It is evident that the amendment effect on mNH_4^+ is becoming rather apparent when 40 t ha^{-1} clay amendments were applied, respectively. Thereby, mNH_4^+ increases in the order zeolite > vermiculite > smectite, which is in good agreement with the literature (Alshameri et al., 2018; Mazloomi & Jalali, 2019). As stated in *4.2.5*, mNH_4^+ of Miyakonojo was on a level that would expose sensitive cultures to severe risks of NH_4^+ toxicity (Britto et al., 2001). However, V4 and Z4 operated as solution NH_4^+ sinks on the 1st and 8th day. Significantly higher mNH_4^+ concentrations of the Z4 treatment on the 22nd and 36th day suggest this amendment to operate as a slow - release fertiliser reservoir, which will be further elaborated in the following discussion (Kavoosi, 2007; Li et al., 2013). To better understand the NH_4^+ dynamics in the clay amended soils, attention will be paid to the ex. NH_4^+, NO_2^- and NO_3^- fraction. As the unfertilised variants did not exhibit exceptional patterns, they are marginally considered in the following discussion.

4.4.1 NH_4^+ - dynamics Smectite amendments

In comparison to the control, the S1 variant reduced the NH_4^+ - N solution share on the 1st and 8th day by approximately 10%, respectively. This effect was intensified with higher application amounts in the S4 variant and indicates that NH_4^+ was retained on the exchange sites of the applied mineral (Table 8, Figure 23). Furthermore, N - recovery and ex. NH_4^+ - N were both increased by S4, while this effect was not observable for the S1 treatment.

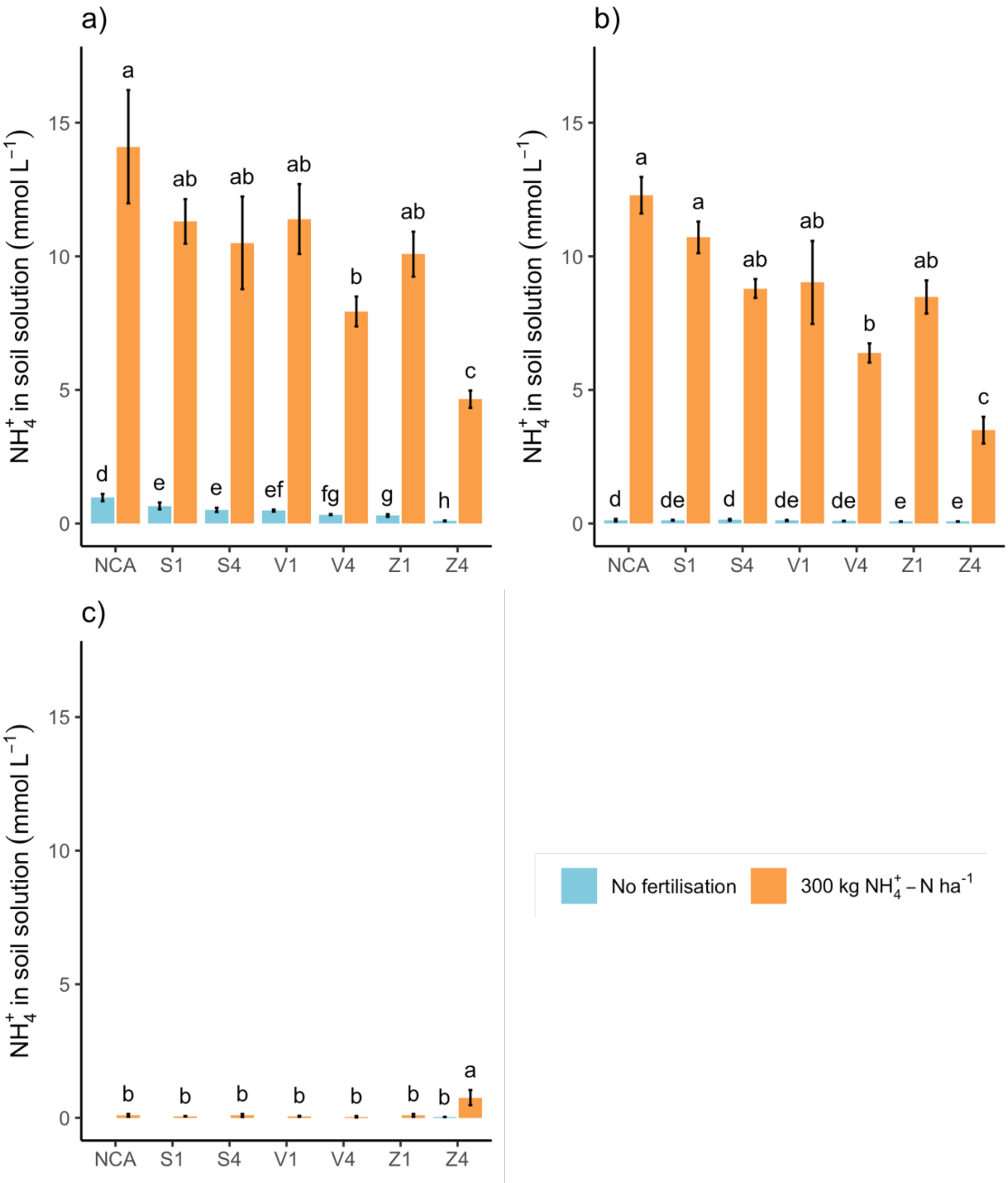

Figure 22: *Solution NH_4^+ concentrations (mNH_4^+) of Miyakonojo with and without clay amendments. The x-axis letters represent the different variants with S= smectite, V = vermiculite, Z = zeolite and NCA = no clay amendment (control). The digit denotes the application amount with 1 = 10 t ha^{-1} and 4 = 40 t ha^{-1}, respectively. Different letters above the bars indicate a significant difference after Tukey´s HSD test on a level of α = 0.05 and on each respective day, which are indicated by a) = 1st day, b) = 8th day and c) = 22nd day. Error bars indicate the standard - deviation and the bar height the arithmetic mean. Note, that the statistical analysis was conducted after $_{10}$log transformation while original data is represented in the figure.*

Table 8: *Different N - pools of Miyakonojo with and without clay amendments after the fertilisation treatment. The abbreviations in the clay amendment column correspond to: NCA = No clay amendment (control), S = smectite, V = vermiculite and Z = zeolite, while the digits indicate the application amount with 1 = 10 t ha^{-1} and 4 = 40 t ha^{-1}.*

Clay amendment	**Day**	**2 M KCl - extracted NH_4^+ - N**[a] (mmol kg^{-1} OD soil)	**Solution NH_4^+ - N at 60% WHC**[a,b] (mmol kg^{-1} OD soil)	**Solution NH_4^+ - N/ 2 M KCl extracted NH_4^+ - N** (in %)	**2 M KCl extracted NO_2^- - & NO_3^- - N**[a] (mmol kg^{-1} OD soil)	**2 M KCl extracted NH_4^+ -, NO_2^- - & NO_3^- - N** (mmol kg^{-1} OD soil)	**N - recovery rate**[c] (in %)
NCA	1	12.2 ± 0.71	5.92 ± 0.89	48	1.02 ± 0.06	13.24	82
	8	7.5 ± 0.7	5.16 ± 0.29	69	2.1 ± 0.07	9.6	59
	22	0.17 ± 0.01	0.04 ± 0.02	24	4.76 ± 0.18	4.93	30
	36	-*	-	-	5 ± 0.35	5	31
S1	1	12 ± 0.32	4.75 ± 0.1	40	0.88 ± 0.08	12.88	79
	8	7.84 ± 0.49	4.5 ± 0.07	57	1.93 ± 0.25	9.77	60
	22	0.23 ± 0.01	0.03 ± 0.001	13	4.6 ± 0.31	4.83	30
	36	0.11	-	-	4.73 ± 0.22	4.84	30
S4	1	13.07 ± 0.93	4.41 ± 0.21	34	0.86 ± 0.07	13.93	86
	8	7.67 ± 0.43	3.69 ± 0.04	48	1.92 ± 0.22	9.59	59
	22	0.22 ± 0.02	0.03 ± 0.01	14	4.34 ± 0.13	4.56	28
	36	-	-	-	4.88 ± 0.3	4.88	30
V1	1	5.86 ± 0.39	4.79 ± 0.16	82	0.99 ± 0.08	6.86	42
	8	4.88 ± 0.3	3.79 ± 0.19	78	2.05 ± 0.11	6.93	43
	22	-	0.02 ± 0.002	-	4.82 ± 0.65	4.82	30
	36	-	-	-	4.91 ± 0.1	4.91	30
V4	1	3.78 ± 0.19	3.33 ± 0.07	88	0.9 ± 0.01	4.68	29
	8	2.65 ± 0.37	2.68 ± 0.04	101	1.85 ± 0.23	4.5	28
	22	0.24	0.02 ± 0.003	8	3.63 ± 0.19	3.63	22
	36	-	-	-	4.05 ± 0.2	4.05	25
Z1	1	13 ± 1.65	4.23 ± 0.1	33	0.8 ± 0.07	13.78	86
	8	8.33 ± 0.45	3.56 ± 0.08	43	1.46 ± 0.11	9.79	60
	22	0.41 ± 0.05	0.04 ± 0.01	10	4.74 ± 0.17	5.15	32
	36	0.14 ± 0.005	-	-	4.8 ± 0.21	4.94	30
Z4	1	14.8 ± 1.39	1.95 ± 0.04	13	0.61 ± 0.05	15.45	95
	8	9.78 ± 0.9	1.47 ± 0.06	15	0.92 ± 0.1	10.7	60
	22	2.69 ± 0.44	0.32 ± 0.03	12	3.36 ± 0.08	6.05	32
	36	0.38 ± 0.03	0.002 ± 0.0001	0.5	4.73 ± 0.22	5.11	30

[a] *Values in those columns show the arithmetic means of triplicates and ± indicates the standard - deviation.*

[b] *Solution NH_4^+ - N kg^{-1} OD soil was obtained by multiplication of the solution concentration with the added water per kg OD soil.*

[c] *N - recovery was calculated by dividing the extracted NH_4^+ -, NO_2^- - and NO_3^- - N by the applied fertiliser amount.*

* *The hyphen (-) denotes NH_4^+ concentrations that were below the detection level of 0.01 mM L^{-1}.*

The results generally reflect the high CEC of smectite, that affected the overall CEC of Miyakonojo if sufficient application rates (40 t ha^{-1}) are chosen (Estevez et al., 2014; Jiang et al., 2011; Murray, 1991). Cavalli et al. (2015) found the ex. - NH_4^+ fraction to be dominating in a smectitic soil over an incubation period of 5 days, even though NH_4^+ applications were two orders of magnitude higher and nitrification and microbial immobilization was inhibited by additional DMPP application in their experiment. Furthermore, the NO_2^- and NO_3^- - N fraction of S1 and S4 was slightly below that of the control, which might be an indicator for reduced nitrification processes when NH_4^+ is retained on an exchange site of the amendment (Hommes et al., 1998; Smith, 1964).

However, on the 22nd day, absolute ex. - NH_4^+ was almost identical for S1, S4 and the control, meaning approximately 30% reduction of the N - recovery for all variants. This loss was primarily attributable to the ex. - NH_4^+ fraction in all variants. As elaborated in *4.2.5*, a nitrification caused *p*H decrease and successively decreasing mNH_4^+ might have induced a release from the ex. - NH_4^+ fraction into the soil solution. The *p*H of S1 and S4 stayed relatively stable between the 1st and the 8th day, indicating *p*H buffering by H^+ adsorption, in these ranges most likely on the broken edges of the mineral (Figure 24). This is also reflected by the smallest R^2 in the S4 variant when predicting the *p*H with NO_2^- and NO_3^- (Figure 25). However, this is accompanied by a CEC decrease (Alshameri et al., 2018; Jeon & Nam, 2019). An abrupt *p*H decrease for S1 and S4 from the 8th to the 22nd day suggests that the *p*H buffering capacity of the amendments was exhausted and CEC further lowered. Ultimately, all investigated N pools hardly differ on the 22nd and 36th day, pointing towards similar processes in all variants and an established equilibrium by that time. As preliminary experiments revealed that the applied smectite does not possess fixation capacities, it is likely that N fixation in the smectite amended Miyakonojo was caused by similar processes as in the control. Conclusively, smectite applications may be helpful for retaining NH_4^+ shortly after fertilisation while their effectiveness is vanishing with time, particularly if H^+ is produced after NH_4^+ application.

4.4.2 NH_4^+ - dynamics Vermiculite amendments

As expected, the vermiculite treatment showed the lowest N - recovery rate (Table 8, Figure 23). V1 approximately halved the recovery rate of the control on the 1st day, while V4 exceeded that reduction with a total loss of 8.5 mmol kg^{-1} OD soil, corresponding to 53%. For both treatments, the solution NH_4^+ - share was extremely high on both the 1st and 8th day. The solution NH_4^+ - N share of V4 on the 8th day was 101%, which hints towards methodological difficulties when aiming to determine the exchangeable fraction of a monovalent ion with low hydration energy. As explained for Yoshiki in *4.2.3*, using K^+ as exchanger for NH_4^+ on vermiculite poses the risk of significantly underestimating the ex. - NH_4^+ fraction due to an interlayer collapse and subsequent NH_4^+ entrapment (Scott & Smith, 1966). In addition, the KCl extract was conducted with air - dried soil, which has been reported to further increase fixation processes (Matsuoka & Moritsuka, 2011; Thompson & Blackmer, 1993). This phenomenon was however not observed for V1 and might indicate that at lower vermiculite application rates NH_4^+ is still retained by pre - existing exchange sites of the soil. The NO_2^- and NO_3^- - N fraction of V1 was nearly identical to the control on all sampling days, while V4 showed a slight reduction of those fractions on the 1st and 8th day and clear reductions on the 22nd and 36th day. On the one hand, this reflects the comparatively slow release when NH_4^+ is fixed in the interlayers of 2:1 clay minerals (Kowalenko, 1978; Kowalenko & Ross, 1980). On the other hand, the NO_2^- and NO_3^- - N fraction still increased over time, suggesting a diffusion - driven successive release of the fixed NH_4^+. It might hence be assumed that this fraction should rather be considered as "weakly" or "recently" fixed and releases NH_4^+ more readily than natively fixed NH_4^+ which might rather be found in less weathered clays as illite (Kowalenko & Ross, 1980; Matsuoka & Moritsuka, 2011; Steffens & Sparks, 1997, 1999). In contrast to the smectite amendments, a *p*H buffer capacity was not apparent for the vermiculite amendments, which is in good agreement with the literature (Figure 24 & 25) (Abollino et al., 2008). Summarizing, vermiculite removes large shares of the fertilised NH_4^+ from the soil solution by fixing it in the mineral´s interlayers from where it is released if the exchangeable and solution NH_4^+ pool are exhausted. However, practical application is excluded due to the cost - intensive production of the clay mineral.

4.4.3 NH_4^+ - dynamics Zeolite amendments

In contrast to the control, the solution NH_4^+ - N share was clearly decreased by both Z1 and Z4 on the 1st, 8th and 22nd day (Table 8, Figure 23). The Z4 treatment showed the highest total extracted NH_4^+ - N values on all sampling days while Z1 resembled the values of S4. The comparatively smaller extractable NH_4^+ - N share of Z1 might generally be explained by enhanced NH_4^+ fixation in the naturally occurring 2:1 clay minerals. However, the higher fertiliser to clay amendment ratio in the Z1 treatment might also have influenced these results. Palanivell et al. (2021) reported increasing NH_4^+ - desorption (2 M KCl) rates with increasing zeolite applications when NH_4^+ fertilisation was unchanged. Furthermore, batch experiments performed with zeolite showed that higher concentrated equilibrating NH_4^+ solutions resulted in slower desorption with 2 M KCl solution, while heterogenous diffusion processes in the desorption process were suggested to be responsible therefore (Aharoni & Sparks, 1991; Kithome et al., 1999). It has frequently been reported that increased solution

NH_4^+ concentrations build a solute concentration gradient and a diffusive force that causes NH_4^+ to migrate deeper into the microporous structures of zeoilte (Cyrus & Reddy, 2011; Du et al., 2005; Li et al., 2020; Vaičiukynienė et al., 2020; Widiastuti et al., 2011). It might hence be hypothesized that Z1 adsorbed NH_4^+ to a greater extent internally than Z4, which resulted in smaller extraction yields when applying the same extraction method. Moreover, the high N - recovery and strong mNH_4^+ reduction of Z4 on the first day are most likely attributable to the high CEC and NH_4^+ selectivity of zeolite in combination with a predominant external adsorption (Huang et al., 2021; Kavoosi, 2007).

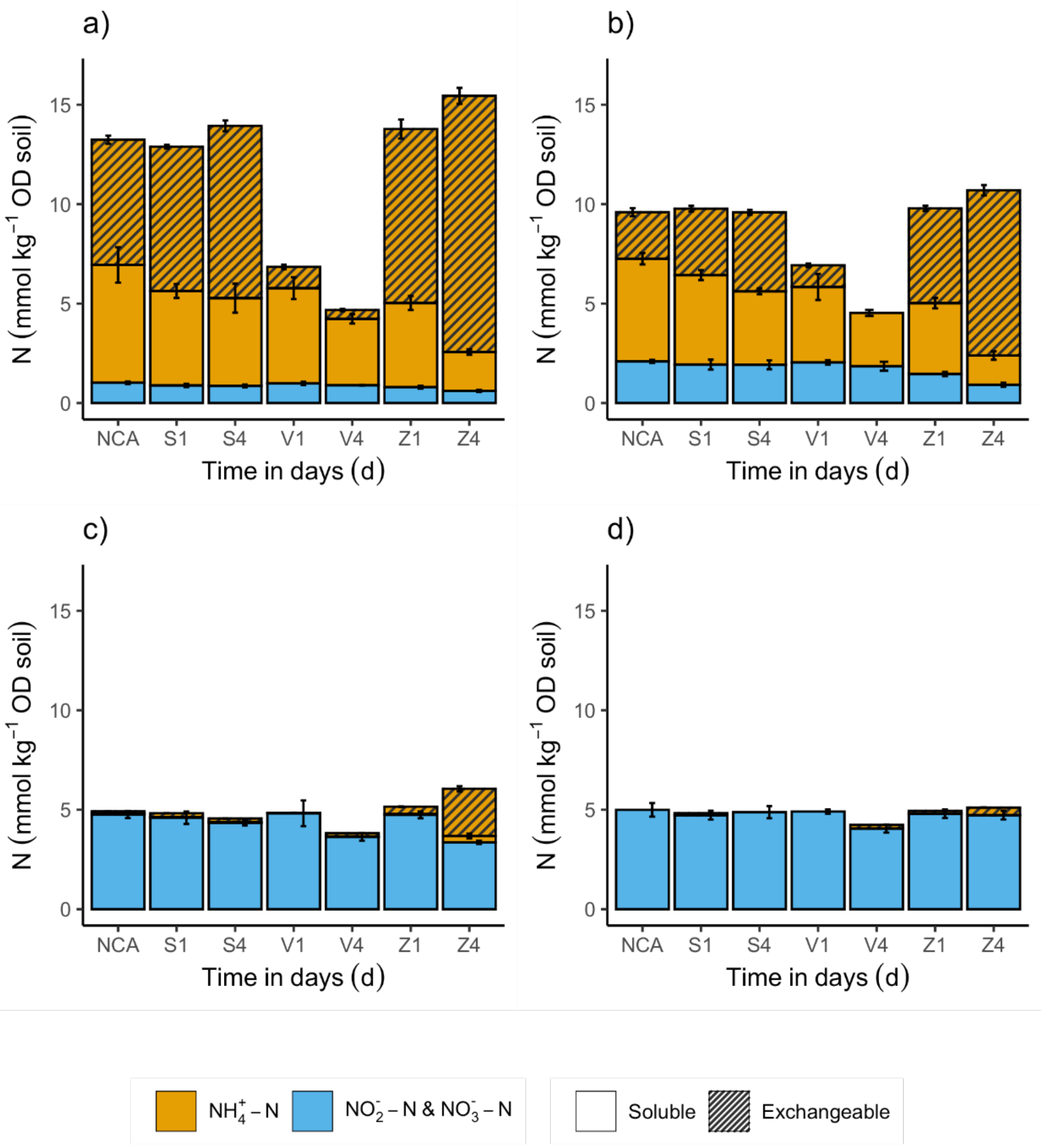

Figure 23: *N - fractions of amended Miyakonojo after the fertilisation treatment. The graph´s captions correspond to: a) = 1st day, b) = 8th day, c) = 22nd day and d) = 36th day. The x-axis letters represent the different variants with S = smectite, V = vermiculite, Z = zeolite and NCA = no clay amendment (control). The digit denotes the application amount with 1 = 10 t ha^{-1} and 4 = 40 t ha^{-1}, respectively. Error bars indicate the standard - deviation and the bar height the arithmetic mean. Note, that NO_2^- and NO_3^- were determined in the 2 M KCl extract but are assumed to be equivalent to the respective solution concentrations.*

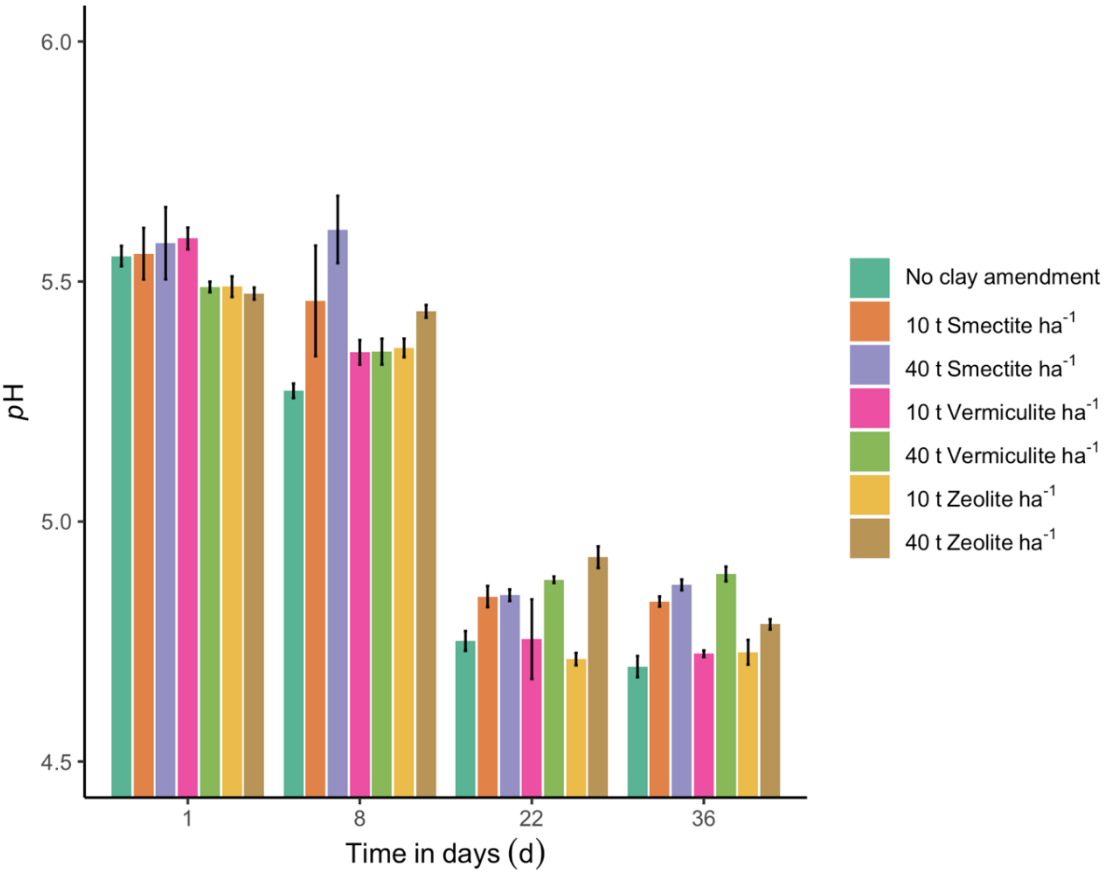

Figure 24: *Time - depended pH changes of Miyakonojo with and without clay amendments after the fertilisation treatment.*

The NO_2^- and NO_3^- - N pool was approximately halved on the 1st and 8th day, indicating less access to nitrifiers of adsorbed NH_4^+ (Aghaalikhani et al., 2012; Flores-Macías et al., 2007; Huang & Petrovic, 1994; Sepaskhah et al., 2007). However, high mNH_4^+ on the 22nd and 36th day reflects that NH_4^+ is abundantly released from the mineral. This is coinciding with the highest relative increase of the NO_2^- and NO_3^- - N pool from the 8th to the 22nd and the 22nd to the 36th day for this treatment, even though the absolute value on the 22nd day was still below all other variants. The discussed results corroborate the common usage of zeolite in agricultural contexts as a slow - release reservoir for NH_4^+ fertilisers, while not only nutrient but also water retention, aeration, infiltration and percolation of a soil are enhanced by its application (Park & Komarneni, 1997). Moreover, the Z4 treatment showed the highest *p*H among all investigated variants on the 22nd day (Figure 24). Again, this is assumed to be due to comparatively low nitrification by then, indicated by the smallest NO_2^- and NO_3^- - N fraction (Table 8, Figure 23 & 25). However, the NO_2^- and NO_3^- - N fraction resembled that of the S4 variant on the 36th day which resulted in a *p*H that was below that of S4, indicating less *p*H buffer capacity of zeolite in comparison to smectite. This is in good agreement with the low H^+ selectivity that has been reported for zeolites, particularly those with wide Si/Al ratios as clinoptilolite (Munthali et al., 2014). Overall, the responses of zeolite amendments towards

NH_4^+ fertilisation are strongly depended on the application rate. Lower application rates seem to lack the capacity of efficiently lower mNH_4^+ at an initial phase (first day). In contrast, 40 t ha^{-1} application rates clearly reduce mNH_4^+ initially but then release the adsorbed NH_4^+ successively, which might eventually favour N - uptake of crops.

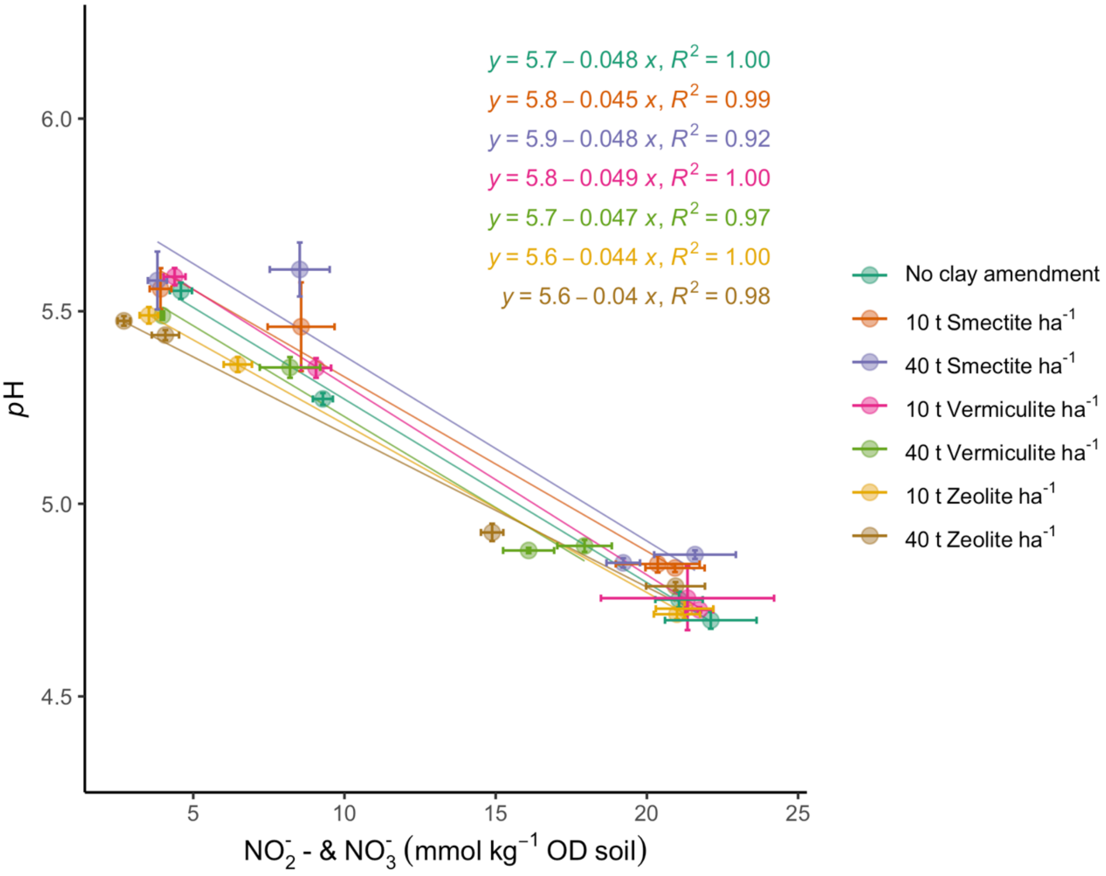

Figure 25: *Relationship between 2 M KCl extracted NO_2^- & NO_3^- and the pH of Miyakonojo with and without clay amendments after the fertilisation treatment.*

4.5 Caesium dynamics of the clay - amended soil

On the 1st day of the experiment, mCs^+ was significantly ($p < 0.05$) reduced by all clay amendments after the fertilisation treatment (Figure 26). The significant difference to the control disappeared for S1 on the 8th day and for S1 and S4 on the 22nd day, respectively. Contrastingly, S1 and S4 exhibited significantly higher mCs^+ than the other clay amendments on the 22nd day, while on the 36th day mCs^+ was even significantly above the control. This phenomenon might be explained by the sharp increase of mMg^{2+} and mCa^{2+} from the 22nd day on, as those ions possess strong competitivity on the interlayer sites of smectites (Appendix D) (Fukushi et al., 2014). It should, however, be noted that the absolute mCs^+ differences were small despite statistical significance. Generally, mCs^+ decreased towards the end of the experiment in all variants. A slight mCs^+ increase was observed for the control, S1 and S4 between the 1st and the 8th day. This may be attributed to a mNH_4^+ share increase in the 2 M KCl extractable NH_4^+ fraction between those days resulting in stronger diffusive forces that caused further desorption of Cs^+. Moreover, the nitrification induced H^+ generation and the assumed CEC drop might also have contributed to the phenomenon. However, it disappeared on the 22nd day with simultaneously decreasing mNH_4^+. The unfertilised variants exhibited similar mCs^+ patterns as the fertilised variants on the 1st and 8th day but ranged on a clearly lower level. On the 22nd and 36th day, the patterns were still similar while the Cs^+ concentration levels of the fertilised and unfertilised variants were resembling. When no fertiliser was applicated, the smectite amendments hardly showed the desired effect of reducing mCs^+ in comparison to the control, although the $^{133}Cs^+$ concentrations in this experiment (> 100 nmol) were clearly above environmental relevant RC pollutions, which were reported to be 30.1 pmol $^{137}Cs\ L^{-1}$ in northern Greece soils after the Chernobyl nuclear catastrophe while 23.7 pmol $^{137}Cs\ kg^{-1}$ OD soil would already signify a limitation of brown rice cultivation in Japan (Rai et al., 2017; Sikalidis et al., 1988). Further, the solution Cs^+ concentrations were strongly correlating with solution NH_4^+ concentrations, indicated by high R^2 for all variants. Apparently, an increase from 10 to 40 t ha^{-1} clay mineral application rate resulted in less steeper slopes for all clay amendments (Figure 27). A linear effect of increasing doses was already described by Valcke et al. (1997b) for zeolite soil amendments. The slopes decreased in the order smectite > zeolite > vermiculite, which is corresponding to the Cs^+ selectivity of those minerals (Belousov et al., 2019; Ferreira et al., 2021; Ohnuki & Kozai, 2013; Sikalidis et al., 1988).

4.5.1 Cs^+ - dynamics Smectite amendments

As elaborated in *1.5*, clay mineral soil amendments are executed to reduce mCs^+ and ultimately the RC TF for crops. Several studies have been conducted in order to evaluate their effectivity in a certain agricultural - environmental context. In this study, the smectite amendments showed the smallest effectivity in reducing mCs^+ among the investigated clay amendments (Figure 26). Smectite amendments were seldomly addressed in the literature and the effect on the RC TF is debatable. For instance, Jones et al. (2004) found no consistent effects of smectite amendments on the RC TF in unfertilised grassland after applying 0.5 and 1.5 t ha^{-1}, respectively, which was explained by the mineral´s low Cs^+ selectivity. In contrast, Vandenhove et al. (2003) reported K^+ - bentonite to increase the RIP of a podzol approximately 1000-fold per added wt%, which ultimately caused a clear RC TF reduction. The authors proved that previously saturating bentonite with K^+ caused an illitization that was accompanied by the development of FES. Further investigations revealed that high layer charge, wetting - drying as well as freezing - thawing cycles are further favouring an RIP increase of K^+ saturated bentonites (Degryse et al., 2004; Onodera et al., 1998). However, none of these aspects apply to the conditions of this experiment. Significant NH_4^+ fixation in the amendment is unlikely to have happened, as was indicated in preliminary experiments with the saturated clay mineral and finds reflection in similar N - recovery on the 22nd and 36th day for S1, S4 and the control (Table 8). Consequently, Cs^+ fixation and adsorption onto FES of significant magnitude can be neglected. The significant effects on the 1st and 8th day for S1 and S4 might be explained by the combination of increased availability of RES rather than FES in combination with decreased mNH_4^+ that reduced Cs^+ desorption.

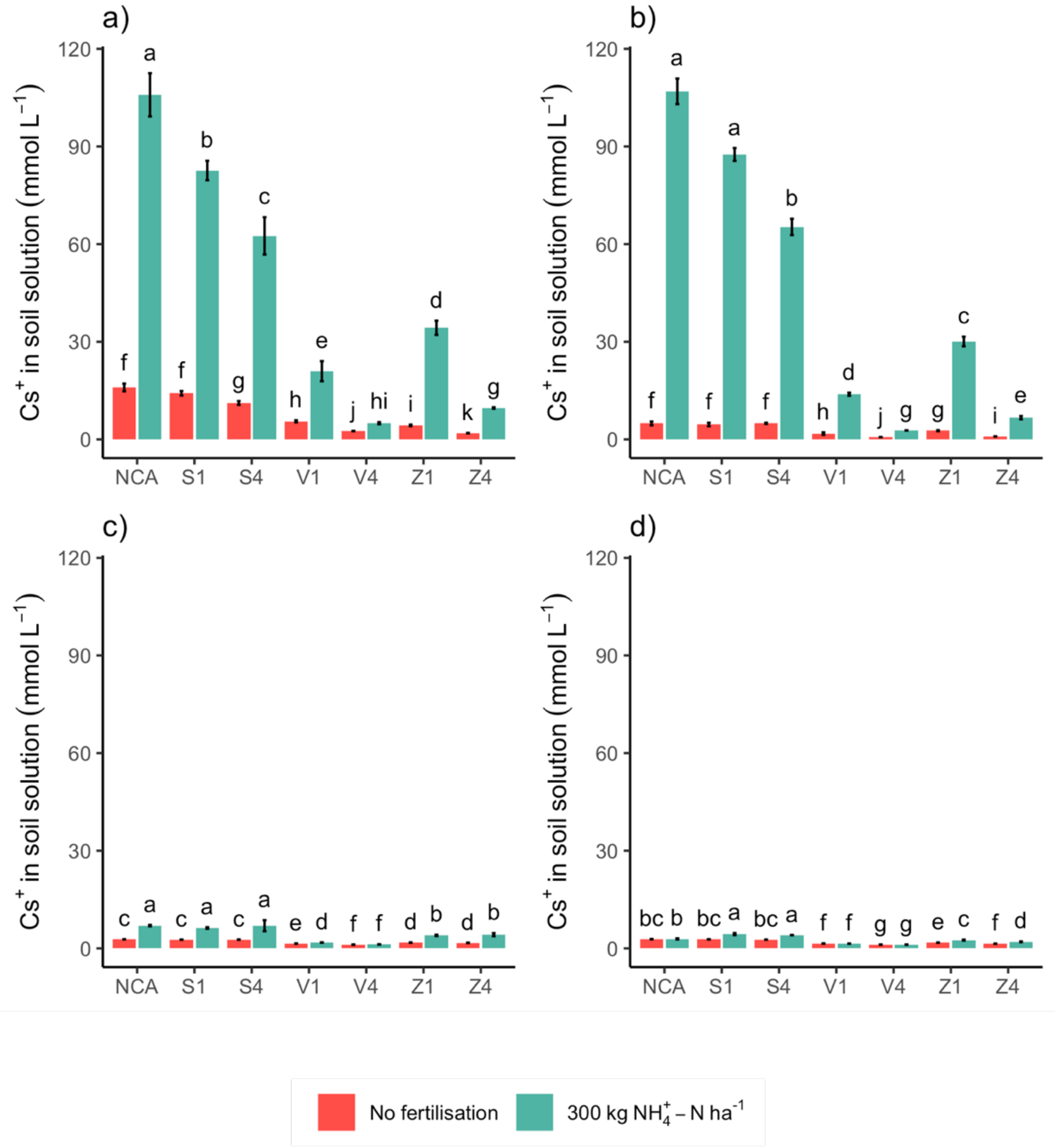

Figure 26: *Solution Cs^+ concentrations (mCs^+) of Miyakonojo with and without clay amendments. The x-axis letters represent the different variants with S= smectite, V = vermiculite, Z = zeolite and NCA = no clay amendment (control). The digit denotes the application amount with 1 = 10 t ha^{-1} and 4 = 40 t ha^{-1}, respectively. Different letters above the bars indicate a significant difference after Tukey´s HSD test on a level of α = 0.05 and on each respective day, which are indicated by a) = 1st day, b) = 8th day and c) = 22nd day. Error bars indicate the standard - deviation and the bar height the arithmetic mean. Note, that the statistical analysis was conducted after $_{10}$log transformation while original data is represented in the figure.*

The subordinated role of highly selective sites in the amendment is once more pronounced in the significantly higher mCs^+ for both S1 and S4 on the 36th day after the fertilisation treatment in comparison to the control (Durrant et al., 2018). Furthermore, the prior K^+ depletion caused that the ex. - K^+ level of the soil was not markedly changed (Table 9). However, mK^+ was predominantly reduced by both S1 and S4 on every day, even though the decrease was not significant (Figure 28). If the CEC is increased by the addition of clay minerals while no additional K^+ is supplied, the RC CF may increase, as it is responding highly sensitive towards mK^+ changes at low mK^+ ranges, as will be discussed in the next section (*4.6*).

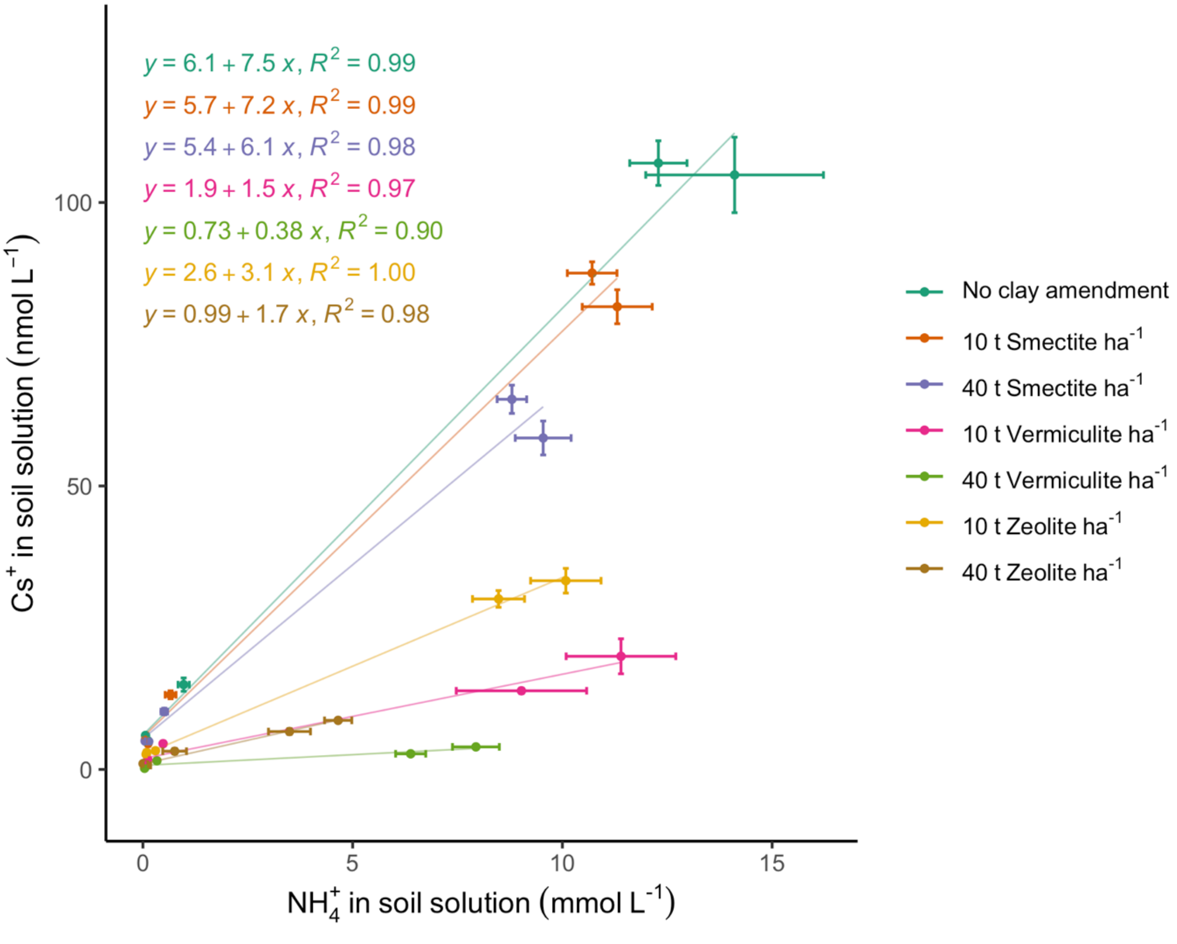

***Figure 27:** Relationship between solution NH_4^+ concentration (mNH_4^+) and solution Cs^+ concentration (mCs^+) of Miyakonojo with and without clay amendments. Data - points include both fertilised and unfertilised variants, respectively. Error bars indicate the standard - deviation.*

This insight is of particular concern as the recommendations for the area affected by the FDNPP accident are based on ex. - K^+ levels (Dengra I Grau et al., 2021). However, it is unlikely that K^+ - depleted minerals will be applied for remediation of RC polluted soils. In contrast, a prior K^+ saturation might yield the demanded combined effect of increased mK^+ and reduced mCs^+. The mCs^+ reduction might even be amplified by a possible K^+ induced illitization that signifies an RIP increase. Abiotic factors as wetting - drying and freezing - thawing might additionally increase the effectiveness of smectite applications.

4.5.2 Cs^+ - dynamics Vermiculite amendments

The vermiculite applications caused the strongest mCs^+ reduction after the fertilisation treatment among all treatments on all days (Figure 26). Particularly the V4 variant yielded the desired effect of decreasing mCs^+, as also indicated by the marginal slope when plotting mNH_4^+ against mCs^+ (Figure 27). Moreover, the relative preference of Cs^+ over NH_4^+ is evident and in good agreement with the literature (Ferreira et al., 2021; Shinzato et al., 2020). Likewise, a significant ex. - Cs^+ (1 M NH_4OAc) reduction was found for an Andosol with low RIP after 1 wt% vermiculite was applied and one wetting - drying cycle conducted (Yamaguchi et al., 2019). However, the treatment resembled the control when aging was conducted for 30 days, while both variants experienced significant ex. - Cs^+ reductions over that time span. Park et al. (2019) suggested that aging (wetting - drying cycles) would cause Cs^+ to migrate from RES to FES. As the ex. - Cs^+ fraction was not investigated in this study, a conclusion about the exact exchange site cannot be drawn. However, extracting NH_4^+ with 2 M KCl yielded the lowest fertiliser recovery rates among the clay treatments on the 1st and 8th day already, indicating the high fixation capacity of vermiculite (Table 6). Furthermore, the $K_{c(Cs\text{-}NH4)}$ of vermiculite strongly increases as the ratio to solution NH_4^+ decreases (Dzene et al., 2015; Sikalidis et al., 1988). On the 1st and 8th day, mNH_4^+ of the fertilised vermiculite amendments exceeded mCs^+ by five to seven orders of magnitude, implying that highly selective adsorption onto FES or interlayer sites took place primarily. Again, it should be noted that the considerable NH_4^+ fixation reduced mNH_4^+, resulting in reduced Cs^+ desorption and increased Cs^+ entrapment due to NH_4^+ - induced interlayer collapse. Furthermore, studies about the effectiveness of vermiculitic soil amendments to reduce the RC TF reveal ambiguous results. For instance, Fujimura et al. (2013) reported that the application of 10 and 50 t ha^{-1} vermiculite reduced the RC TF on a sandy Gleysol collected from the Fukushima prefecture. Contrastingly, Kato et al. (2015) showed that vermiculite applications did merely reduce the RC TF through its release of K^+ on soils in proximity to the FDNPP. It should be noted that the vermiculite used in the studies of Kato et al. (2015) and Fujimura et al. (2013) but also in the aforementioned study of Yamaguchi et al. (2019) was regularly interstratified vermiculite/mica (hydrobiotite or hydrophlogopite) that shows lower selectivity towards cations in the vermiculitic layer due to the orientation of the OH^+ group in the octahedral layer. In contrast, the vermiculite used in this study was preliminary K^+ depleted and therefore possessed higher CEC and selectivity towards cations as NH_4^+, Cs^+

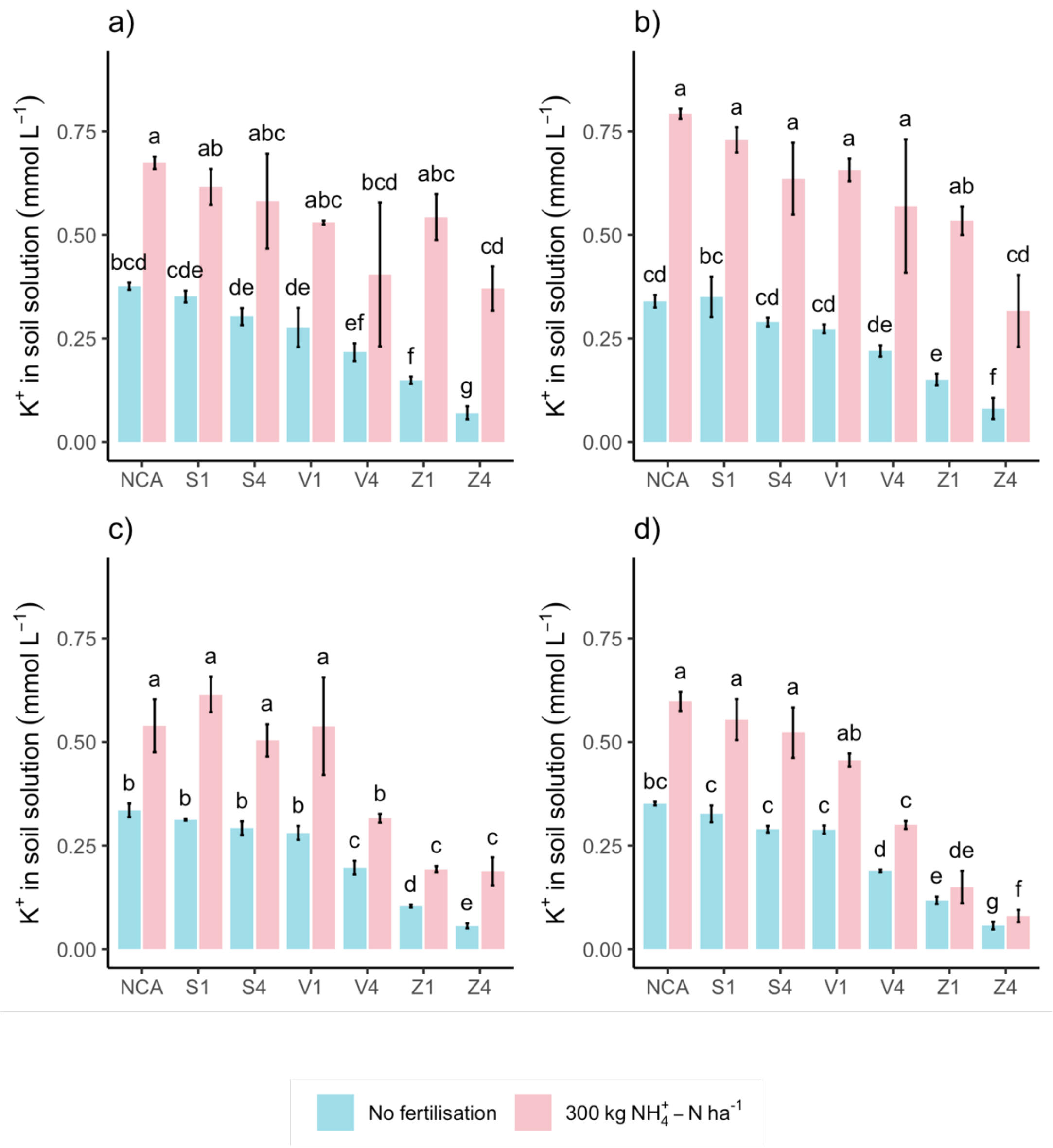

Figure 28: *Solution K^+ concentrations (mK^+) of Miyakonojo with and without clay amendments. The x-axis letters represent the different variants with S= smectite, V = vermiculite, Z = zeolite and NCA = no clay amendment (control). The digit denotes the application amount with 1 = 10 t ha^{-1} and 4 = 40 t ha^{-1}, respectively. Different letters above the bars indicate a significant difference after Tukey´s HSD test on a level of α = 0.05 and on each respective day, which are indicated by a) = 1st day, b) = 8th day and c) = 22nd day. Error bars indicate the standard - deviation and the bar height the arithmetic mean. Note, that the statistical analysis was conducted after $_{10}$log transformation while original data is represented in the figure.*

and K^+. This was in good agreement with a stronger mK^+ reduction of V1 and V4 in comparison to S1 and S4, irrespective of the fertilisation treatment (Figure 28). Eguchi et al. (2015) conducted the same vermiculite pre - treatment and showed that its application on a soil cultivated with brown rice initially adsorbed solution K^+ (rooting stage) but released it at later stages (heading and ripening). It might hence be inferred that the adsorbed K^+ would have been released at later stages when the solution pool was exhausted by crop growth.

Table 9: *1 M NH_4OAc extractable K^+ of clay amended Miyakonojo. The abbreviations in the clay amendment column correspond to: NCA = No clay amendment (control), S = smectite, V = vermiculite and Z = zeolite, while the digits indicate the application amount with 1 = 10 t ha^{-1} and 4 = 40 t ha^{-1}.*

Clay amendment	**Fertilisation** (kg NH_4^+ - N ha^{-1})	**1 M NH_4OAc Ex. - K^+** (mmol kg^{-1} OD soil)[a]
NCA	0	1.42 ± 0.26
	300	1.4 ± 0.28
S1	0	1.22 ± 0.03
	300	1.45 ± 0.24
S4	0	1.28 ± 0.01
	300	1.38 ± 0.06
V1	0	1.26 ± 0.21
	300	1.32 ± 0.2
V4	0	1.05 ± 0.23
	300	1.13 ± 0.06
Z1	0	1.79 ± 0.02
	300	1.94 ± 0.08
Z4	0	3.26 ± 0.36
	300	3.78 ± 0.18

[a] *Values in this column show the arithmetic means of triplicates and ± the standard deviation.*

However, the data at hand excludes the possibility of an RC TF reduction caused by K^+ release. Allover, the vermiculite applications might significantly have raised the RIP of Miyakonojo. Similarly, Delvaux et al. (2000) found the vermiculitic content of a soil to be significantly correlated with its RIP, which in turn was significantly correlated with the RC TF. Vermiculite applications would theoretically represent an appropriate measure to reduce mCs^+ on Andosols with low RIP, particularly in the context of NH_4^+ - fertilisation. However, K^+ depletion prior to the mineral application is economically not feasible. Consequently, the depicted results are of pure scientific interest.

4.5.3 Cs^+ - dynamics Zeolite amendments

Furthermore, mCs^+ of Z1 and Z4 were always significantly below S1 and S4 and significantly above V1 and V4 in the fertilised variants, respectively (Figure 26). The Z4 variant showed significantly lower mNH_4^+ than the V4 variant on the 1st day and 8th day, suggesting zeolite to have a higher NH_4^+ but lower Cs^+ selectivity than vermiculite (Figure 22 & 26) (Ferreira et al., 2021). Investigations of Dengra I Grau et al. (2021) revealed that the RIP of Miyakonojo was increased by increasing zeolite applications (10 and 40 t ha^{-1}) but kept unchanged by progressing K^+ fertiliser loads, which was in straight contrast to Yoshiki, a soil containing considerable amounts of vermiculite. The RIP of zeolites does indicate the presence of highly Cs^+ selective sites but is independent of FES, that may merely be present on micaceous minerals and are formed through interlayer collapses induced by the application of alkali metals such as K^+ (Fan et al., 2014b; Seaman et al., 2001; Yamaguchi et al., 2019). Valcke et al. (1997b) reported the effectiveness of zeolite amendments to be enhanced when the amended soil shows low RIP, as is the case for Miyakonojo. However, the high selectivity of zeolite towards Cs^+ is decoupled from Cs^+ fixation that may take place on 2:1 clay minerals. Likewise, Yamaguchi et al. (2019) reported zeolite to have a high RIP while significant amounts of Cs^+ were still 1 M NH_4OAc extractable. The authors even suggested that zeolite applications could hinder Cs^+ ions to reach FES of 2:1 clay minerals and hence retard Cs^+ fixation, which should find consideration when planning zeolite amendments on soils containing 2:1 clay minerals. Zeolitic soil amendments have severally been investigated in the context of the RC TF. As elaborated in the literature review, the effectiveness of these soil amendments is debatable, with studies indicating both its effectiveness and ineffectiveness (Kato et al., 2015; Kubo et al., 2015; Parajuli et al., 2016; Valcke et al., 1997; Yamaguchi et al., 2019). Analogous to vermiculite amendments, it has frequently been assumed that the effectivity of zeolite amendments in reducing the RC TF is rather based on its ability to release K^+ from its surfaces (Fujimura et al., 2013; Paasikallio, 1999; Shenber & Johanson, 1992; Yamaguchi et al., 2019). Dengra I Grau et al. (2021) concluded that zeolite amendments proved to successfully reduce the RC TF at low mK^+ levels on Miyakonojo. However, this tendency inversed when increasing K^+ fertiliser loads were applied, as zeolite did not anymore function as a source but as a sink for solution K^+. In this study, the control showed significantly higher mK^+ than Z1 and Z4 on every day, irrespective of the fertiliser treatment, which contradicts the results of Dengra I Grau et al. (2021) and excludes the contribution of mK^+ to reduce the RC TF (Figure 28). Opposed to this experiment, Dengra I Grau et al. (2021) depleted soil ex. - K^+ which resulted in reduced mK^+ in the control and would ultimately have caused K^+ release from the applied zeolite. Furthermore, ex. - K^+ was clearly increased by the zeolite amendments in this study, which was also confirmed in the findings of Dengra I Grau et al. (2021) (Table 8). This indicates that the pre - treatment with Na^+, Mg^{2+} and Ca^{2+} did not exchange K^+ to the extent of NH_4^+. As this phenomenon was combined with clearly reduced mK^+, the risk of using ex. - K^+ as a recommendation on zeolite amended soils is even stronger pronounced than in case of smectite amendments and finds reflection in the investigations of Dengra I Grau et al. (2021), who suggested mK^+ to be the more appropriate proxy for modelling the RC TF on zeolite amended soils. It might be concluded that the application of zeolite on an allophanic Andosol as Miyakonojo seems to be an adequate measure to reduce mCs^+ but needs to be coupled to sufficient mK^+, as has been stated before by Yamaguchi et al. (2019).

4.6 Implications for the Caesium plant uptake

The afore elaborated effect of an NH_4^+ fertilisation (*4.2* & *4.4*) has implications not only for mCs^+ but also for mK^+ and consequently the RC CF. As can be inferred from Equation (28), decreasing mK^+ is coupled to an increasing RC CF, particularly at low mK^+ ranges. Simultaneously, the calculated Cs^+ plant uptake is referring to Equation (27) and is therefore depended on mCs^+. The following section is dealing with the implications of the NH_4^+ fertilisation induced mK^+ and mCs^+ changes that are used to predict the actual Cs^+ plant (ryegrass) uptake under the investigated circumstances. As presented in Table 10 & 11, the NH_4^+ - fertilisation treatment caused a decreased Cs^+ uptake for the predominant share of the investigated soils, irrespective of the clay mineral addition. This finding is contradicting several earlier studies, in which NH_4^+ fertilisation did either show no or adverse effects on the RC plant uptake (Dushenkov, 2003; Fuhrmann et al., 2003; Ioannides et al., 2003; Lasat et al., 1998, 1997; Paasikallio & Sormunen-Cristian, 2002; Shaw et al., 1992; Sugiura et al., 2016; Sun et al., 2019). The smectite and zeolite amendments were even amplifying the calculated Cs^+ uptake and thereby reversed the desired effect. However, an effectiveness relative to the control was observed for the vermiculite amended soils.

The calculated CF and Cs^+ uptake of the unamended soils showed distinct responses to the NH_4^+ - fertiliser treatment, which were clearly related to their K^+ - status and selectivity and to a lesser extent to mCs^+ (Table 10) (Smolders et al., 1997; Zhu & Smolders, 2000). The calculated Cs^+ uptake of Groß - Enzersdorf was despite significantly higher mCs^+ clearly below the control on the 8th day after the fertilisation treatment, which reflects the fertiliser induced mK^+ rise that strongly determines the CF. Even though there was no statistical difference between mCs^+ of the 22nd and the 36th day, Cs^+ uptake was still decreased by the fertiliser treatment on those days (Figure 20). In contrast, the calculated CFs of Deshchenka were extremely low, which corresponds to the soil´s high mK^+ level in combination with low K^+ - selectivity, indicated by a low K_D^K (Table 7, Figure 19). This phenomenon is elucidated by the high sand content and the predominance of kaolinite in the clay fraction of Deshchenka, a typical phenomenon of soils with glacial origin in eastern Europe (Table 5, Figure 13) (Fotynma et al., 2013). However, the K^+ - fertilisation management prior to soil sampling must have artificially increased the K^+ status. Although mK^+ was approximately two- to threefold increased by the NH_4^+ fertilisation treatment, the CFs did differ only marginally, indicating the insignificant response of Equation (28) towards higher mK^+ levels. Consequently, the calculated Cs^+ plant uptake was hardly affected by the NH_4^+ - fertilisation. The considerable vermiculitic share in the clay fraction of Yoshiki caused a comparatively high K^+ fixation capacity of the soil, implying that mK^+ was on a level where small differences had drastic influences on the CF (Dengra I Grau et al., 2021; Kubo et al., 2018). As the fertiliser treatment increased mK^+ on every day, the resulting CF was clearly decreased (Figure 19). For instance, the calculated Cs^+ plant - tissue concentration decreased by one order of magnitude when $\min(mK^+)$ was increased by 0.08 mmol after the fertilisation treatment on the first day. In comparison, the calculated Cs^+ uptake of Ogata was reduced by the fertiliser treatment on the 1st and 8th day but increased on the 22nd and 36th day, respectively. Again, the Cs^+ uptake decreased although mCs^+ was significantly above the control after the fertilisation treatment, making increased mK^+ responsible for the decreased Cs^+ uptake. As mK^+ hardly differed between the fertiliser treatment and the control on the 22nd and 36th day, the increased Cs^+ uptake was attributable to slightly increased mCs^+ in the fertilised variants on those days, even though the effect was not significant on the 36th day (Figure 20). The similar mK^+ levels between the unfertilised and the fertilised variant on the 22nd and 36th day are unique for Ogata while elucidation of this phenomenon remains unsolved. However, it might implicate an increased risk of time - delayed RC uptake after an NH_4^+ fertilisation and needs to find consideration in future research on heavy textured smectitic soils as Ogata. The calculated Cs^+ uptake of Miyakonojo was only slightly increased by the fertiliser treatment on the 1st and the 8th day, even though the largest absolute mCs^+ gap among all investigated soils was observed for those variants. This indicated the soil´s low Cs^+ selectivity, a typical phenomenon for allophanic Andosols (Figure 20) (Vandebroek et al., 2012). The simultaneous significant mK^+ increase nevertheless mitigated the effect of the strong mCs^+ increase (Figure 19). Moreover, the Cs^+ uptake was slightly decreased on the 22nd and 36th in the fertilised variants, as mK^+ was still significantly above the control, while Cs^+ was re - adsorbed by that time and mCs^+ did not differ significantly on those days (Figure 19 & 20). The exact mechanisms that caused the contradictive results in comparison to the earlier cited cultivation experiments remains unclear for now. However, a possible explanation might be that the NH_4^+ fertilisation induced K^+ desorption and consequently supplied luxury K^+ to the plant in the early growth stages. This would have implied a stronger K^+ exhaustion in later stages which might imply drastic increases of the RC CF and consequently the RC TF, even if mRC was not increased at that time. This study furthermore showed that merely vermiculite applications would predominantly reduce the Cs^+ uptake relative to the control, while the opposite was observed for the zeolite and smectite amendments (Table 11). With exception of fertilised S1 on the 22nd day, smectite applications caused the relative Cs^+ uptake to increase. The effect was particularly pronounced on the 36th day, where the S1 and the S4 variant caused a three- and fourfold increased Cs^+ uptake relative to the control. Accordingly, mCs^+ of both variants was significantly above the control, which reflected the facile Cs^+ desorption from smectite even at trace concentrations, as were present in this study (Figure 26) (Iijima et al., 2010).

Table 10 (1): *Calculated CF and Cs^+ plant tissue concentration of the unamended soils.*

Soil	**Day**	**Fertilisation** (kg NH_4^+ - N ha^{-1})	**Concentration Factor** (CF)	**Cs^+ in plant - tissue** (nmol kg^{-1})
Groß - Enzersdorf	1	0	-*	-
		300	-	-
	8	0	1,310.03	78.60
		300	12.48	2.75
	22	0	125.17	7.51
		300	75.71	28.77
	36	0	619.77	86.77
		300	300.26	15.01
Deshchenka	1	0	0.05	0.011
		300	0.003	0.013
	8	0	0.04	0.010
		300	0.003	0.010
	22	0	0.1	0.017
		300	0.01	0.003
	36	0	0.07	0.016
		300	0.01	0.003
Yoshiki	1	0	3,133.5	470.02
		300	389.69	77.94
	8	0	4,415.89	485.75
		300	3343.01	501.45
	22	0	4253.92	765.71
		300	1294.9	220.13
	36	0	227.48	25.02
		300	121.92	18.29
Ogata	1	0	2169.7	1540.49
		300	506.79	628.42
	8	0	282.63	203.49
		300	89.64	121.01
	22	0	713.17	228.21
		300	362.14	304.2
	36	0	663.56	378.23
		300	628.52	402.25

Table 10 (2): *Calculated CF and Cs^+ plant tissue concentration of the unamended soils.*

Soil	**Day**	**Fertilisation** (kg NH_4^+ - N ha^{-1})	**Concentration Factor** (CF)	**Cs^+ in plant - tissue** (nmol kg^{-1})
Miyakonojo	1	0	28.16	420.71
		300	4.07	426.78
	8	0	43.12	211.72
		300	2.26	241.71
	22	0	45.16	80.38
		300	11.95	52.46
	36	0	34.73	63.56
		300	6.17	11.78

The relative Cs^+ uptake increase in comparison to the control was amplified by the higher application amount (40 t ha^{-1}), even though this variant showed a stronger mCs^+ reduction.This implicates that the calculated Cs^+ uptake was stronger influenced by mK^+ than by mCs^+ at those K^+ concentration levels. The response to the fertiliser treatment did not show any striking differences in comparison to the control. While the fertiliser treatment caused an increased Cs^+ uptake on the 1st and 8th day for S1, this held true only on the 8th day for S4. Conclusively, smectite amendments seem to be limitedly suited for remediation of RC polluted, although prior K^+ saturation of higher charged smectites may be accompanied by both an RIP and mK^+ increase and may therefore contradict the findings of this study. In contrast to the smectite amended soils, vermiculite applications predominantly caused a relative reduction of the calculated Cs^+ uptake, even though mK^+ suffered a stronger decrease through these amendments. This result is consequently clearly attributable to the strong mCs^+ reduction, that reflects the high selectivity of vermiculite towards Cs^+, particularly at low concentration ranges (Figure 26) (Dzene et al., 2015; Ferreira et al., 2021; Sikalidis et al., 1988). Moreover, the NH_4^+ fertiliser induced K^+ desorption caused a decreased calculated Cs^+ uptake in all cases with exception of the V4 variant on the 1st day. These results consequently suggest that an NH_4^+ fertilisation in combination with vermiculite applications would most effectively reduce the Cs^+ uptake of ryegrass on an allophanic Andosol. However, the conducted vermiculite pre - treatment is extremely cost - intensive and this insight therefore not applicable for remediation of RC polluted soils. Additionally, a K^+ - fertilisation would most likely be preferred over an NH_4^+ fertilisation if an mK^+ increase is aimed. The calculated Cs^+ uptake of the zeolite applications exceeded that of the control on every day and independently of the fertiliser treatment, with exception of fertilised Z1 on the 1st day. As mCs^+ was significantly reduced on all days compared to the control, this

Table 11 (1): *Calculated CF and Cs$^+$ plant tissue concentration Miyakonojo with and without clay amendments.*

Clay amendment	**Day**	**Fertilisation** (kg NH_4^+ - N ha^{-1})	**Concentration factor** (CF)	**Cs$^+$ in plant - tissue** (nmol kg^{-1})	**Relative amendment effect**
NCA	1	0	28.16	420.71	1
		300	4.07	426.78	1
	8	0	43.12	211.72	1
		300	2.26	241.71	1
	22	0	45.16	80.38	1
		300	11.95	52.46	1
	36	0	34.73	63.56	1
		300	6.17	11.78	1
S1	1	0	37.88	500.02	1.19
		300	6.75	550.80	1.29
	8	0	53.38	245.01	1.16
		300	3.27	286.45	1.19
	22	0	51.65	86.77	1.08
		300	6.67	35.08	0.67
	36	0	54.11	96.32	1.52
		300	10.51	35.63	3.02
S4	1	0	67.83	691.87	1.64
		300	9.69	595.93	1.40
	8	0	71.83	354.84	1.68
		300	8.11	529.58	2.19
	22	0	77.53	131.80	1.64
		300	12.44	74.39	1.42
	36	0	70.69	119.47	1.88
		300	14.3	44.04	3.74
V1	1	0	133.64	608.06	1.45
		300	8.72	174.4	0.41
	8	0	89.05	158.51	0.75
		300	4.84	67.28	0.28
	22	0	89.4	42.91	0.53
		300	15.39	8	0.15
	36	0	73.53	36.76	0.58
		300	15.83	6.97	0.59

Table 11 (2): *Calculated CF and Cs*$^+$ *plant tissue concentration Miyakonojo with and without clay amendments.*

Clay amendment	**Day**	**Fertilisation** (kg NH_4^+ - N ha^{-1})	**Concentration factor** (CF)	**Cs^+ in plant - tissue** (nmol kg^{-1})	**Relative amendment effect**
V4	1	0	230.46	357.21	0.85
		300	159.59	635.17	1.49
	8	0	207.28	143.02	0.68
		300	13.57	37.45	0.15
	22	0	321.5	48.23	0.6
		300	55.35	11.62	0.22
	36	0	288.98	43.35	0.68
		300	64.38	9.66	0.82
Z1	1	0	764.85	2,531.65	6.02
		300	9.92	330.34	0.77
	8	0	840.51	2,252.57	10.64
		300	10.69	321.77	1.33
	22	0	2323.07	1,765.53	21.96
		300	298.02	891.08	16.99
	36	0	1670.09	1,252.57	19.71
		300	1851.7	2851.62	242.07
Z4	1	0	12,296.49	11,558.7	27.47
		300	1851.70	16,035.72	37.57
	8	0	12,056.03	11,212.11	52.96
		300	118.14	791.54	3.27
	22	0	21,720.43	15,204.3	189.16
		300	474.8	1,528.86	29.14
	36	0	22,693.83	9,531.41	149.96
		300	7652.41	7,881.98	669.10

phenomenon was apparently attributable to the strong mK^+ decreases, that reflect the high K^+ selectivity of zeolite (Figure 26 & 28) (Jaskunas et al., 2015). This effect was even intensified in the Z4 variant towards the end of the experiment, when NH_4^+ was successively exchanged by K^+ and lost to nitrification or fixation in 2:1 clay mineral structures. This was also indicated by the highest relative Cs^+ uptake increase on the 36th day for both Z1 and Z4 after the fertilisation treatment, whereby the Z4 variant showed a nearly 700 - fold increased uptake in comparison to the control. As stated earlier, the effectiveness of zeolite amendments was suggested to be caused by its K^+ release, which cannot be confirmed for this study (Fujimura et al., 2013; Kato et al., 2015). However, it has also been reported that zeolite soil amendments would lower mK^+ and therefore decrease the RC TF not in the scope as mRC was reduced (Valcke et al., 1997c). In this study, sharp mK^+ decreases caused the calculated CF and consequently the Cs^+ uptake to drastically increase. These results surprisingly suggest that zeolite applications on an allophanic Andosol cause the RC TF to increase and therefore counteract their purpose. Earlier studies were primarily focusing on the effect of K^+ fertilisation, clay mineral amendments or their combined effect. This study introduced NH_4^+ as a classical N - fertiliser into this interplay. Due to its strong competitivity with both Cs^+ and K^+ on natural and artificial exchange sites in soils, dynamics become more complex and less foreseeable. Pursuing this approach may contribute to an optimized application of measures (fertiliser and/or amendment) in the context of RC polluted soils.

5. Conclusions

This study aimed to elucidate the effect of NH_4^+ - fertiliser application on the solution RC dynamics by means of five different soil - types (Chernozem, Podzol, Cambisol, Gleysol and Andosol) with distinct clay mineralogy, such as illite, vermiculite, smectite and allophane. The incubation experiment was conducted over a period of five weeks' time, as NH_4^+ is prone to nitrification processes. It was expected that the fertiliser treatment would cause significant RC desorption into the soil solution, which bears the risk of subsequent plant root absorption. Since 2:1 phyllosilicates possess highly selective binding sites for RC, the magnitude of RC desorption was assumed to be controlled by their presence. An allophanic Andosol, low in 2:1 clay minerals was therefore amended with 10 and 40 t ha^{-1} zeolite, vermiculite and smectite, respectively. It was further assumed that the solution RC would be re - adsorbed when mNH_4^+ and ex. - NH_4^+ decreases due to nitrification or fixation in 2:1 clay minerals. The results of this study showed that NH_4^+ has strong RC desorption capacities, despite the presence of 2:1 clay minerals. With exception of a vermiculitic Cambisol (Yoshiki), mNH_4^+ would operate as a good predictor for mCs^+. As mNH_4^+ showed a falling trend over time for all (amended) soils, this held true for mCs^+. The mCs^+ desorption was particularly found to be reduced by the presence of vermiculite and weathered mica, while allophane and kaolinite showed the opposite effect. The clay minerals that were associated with reduced RC desorption would also cause stronger NH_4^+ fixation by an interlayer collapse, as was indicated by large N - losses (applied fertiliser - N minus the sum of 2 M KCl extractable NH_4^+ - N, NO_2^- - N and NO_3^- - N). However, successively increasing NO_2^- and NO_3^- fractions pointed towards "weak" initial NH_4^+ fixation followed by slow subsequent release and nitrification. Further, all clay amendments induced a decrease of the solution mCs^+ level, while this effect was apparently intensified in the respective 40 t ha^{-1} variants. The mCs^+ solution decrease was irrespective of the fertiliser treatment and followed the order vermiculite > zeolite > smectite > control. However, calculating the RC CF with empirical mK^+ and finally the RC uptake (of ryegrass) with empirical mCs^+ as suggested by Smolders et al. (1997) revealed that the NH_4^+ induced K^+ desorption caused the predicted Cs^+ plant uptake to predominantly decrease among all (clay amended) soils, meaning that the effect of increased mCs^+ was exceeded by the increase of mK^+. This depicts the most striking result of this study and contradicts several earlier findings and assumptions regarding the effect of NH_4^+ fertilisation on RC crop uptake. Additionally, only vermiculite applications caused the predicted Cs^+ uptake to decrease relative to the control. In that case, the effect of strong mCs^+ reduction exceeded that of the mK^+ reduction. While the relative increase of the calculated Cs^+ crop uptake was moderate on the smectite amended soils, the zeolite amended soils increased the modelled Cs^+ uptake up to 670 - fold, which corresponded to sharp significant mK^+ reductions due to zeolite´s high K^+ selectivity. Hence, earlier assumptions that zeolite and vermiculite amendments show the desired effect of lowering the RC TF due to K^+ release could in neither case be confirmed. However, these results have to be interpreted carefully, as all clay minerals were K^+ depleted prior to their application and a subsequent mK^+ reduction was to be expected. Furthermore, K^+ depletion of vermiculite is too cost intensive for practical application and therefore a purely scientific insight. Finally, this study primarily aimed to elucidate the effect of an NH_4^+ - fertilisation on mCs^+ dynamics over time. As mK^+ is a crucial variable that determines the RC plant uptake, future research should focus on the better understanding of the NH_4^+ - K^+ - Cs^+ interplay in soils. The provided insights might be another contribution to the comprehension of the complex factors and their interactions that determine the RC plant uptake in agriculturally used soils.

6. Bibliography

Abdel-Kader, F.H., Jackson, M.L., & Lee, G.B. (1978). Soil Kaolinite, Vermiculite, and Chlorite Identification by an Improved Lithium DMSO X-ray Diffraction Test. Soil Sci. Soc. Am. J. 42, 163–167. https://doi.org/10.2136/sssaj1978.03615995004200010036x

Abollino, O., Giacomino, A., Malandrino, M., & Mentasti, E. (2008). Interaction of metal ions with montmorillonite and vermiculite. Appl. Clay Sci. 38, 227–236. https://doi.org/10.1016/j.clay.2007.04.002

Absalom, J.P., Young, S.D., & Crout, N.M.J. (1995). Radio-caesium fixation dynamics: measurement in six Cumbrian soils. Eur. J. Soil Sci. 46, 461–469. https://doi.org/10.1111/j.1365-2389.1995.tb01342.x

Absalom, J.P., Young, S.D., Crout, N.M.J., Nisbet, A.F., Woodman, R.F.M., Smolders, E., & Gillett, A.G. (1999). Predicting Soil to Plant Transfer of Radiocaesium Using Soil Characteristics. Environ. Sci. Technol. 33, 1218–1223. https://doi.org/10.1021/es9808853

Absalom, J.P., Young, S.D., Crout, N.M.J., Sanchez, A., Wright, S.M., Smolders, E., Nisbet, A.F., & Gillett, A.G. (2001). Predicting the transfer of radiocaesium from organic soils to plants using soil characteristics. J. Environ. Radioact. 52, 31–43. https://doi.org/10.1016/S0265-931X(00)00098-9

Adams, E., Miyazaki, T., & Shin, R. (2019). Contribution of KUPs to potassium and caesium accumulation appears complementary in Arabidopsis. Plant Signal. Behav. 14. https://doi.org/10.1080/15592324.2018.1554468

Agency for Toxic Substances and Disease Registry (2004). Toxicological profile for Caesium (Atlanta, GA: U.S. Department of Health and Human Services, Public Health Service.)

Aghaalikhani, M., Gholamhoseini, M., Dolatabadian, A., Khodaei-Joghan, A., & Sadat Asilan, K. (2012). Zeolite influences on nitrate leaching, nitrogen-use efficiency, yield and yield components of canola in sandy soil. Arch. Agron. Soil Sci. 58, 1149–1169. https://doi.org/10.1080/03650340.2011.572876

Aharoni, C., & Sparks, D.L. (1991). Kinetics of Soil Chemical Reactions—A Theoretical Treatment. In: Rates of Soil Chemical Processes, (John Wiley & Sons, Ltd), 1–18.

Ajazi, A., Miho, L., Bani, A., & Maci, A. (2013). Effect of potassium on fixation of ammonium by clay minerals in different soil layers. Albania J. Acricultural Sci. 12, 675–681.

Alexakhin, R., Anspaugh, L., Balonov, M., Batandjieva, B., Besnus, F., Biesold, H., Bogdevich, I., Byron, D., Carr, Z., Deville-Cavelin, G., et al. (2006). Environmental consequences of the Chernobyl accident and their remediation: Twenty years of experience. Report of the Chernobyl Forum Expert group “Environment” (Vienna: International Atomic Energy Agency)

Aliyu, A.S., Evangeliou, N., Mousseau, T.A., Wu, J., & Ramli, A.T. (2015). An overview of current knowledge concerning the health and environmental consequences of the Fukushima Daiichi Nuclear Power Plant (FDNPP) accident. Environ. Int. 85, 213–228. https://doi.org/10.1016/j.envint.2015.09.020

Allison, F.E. (1973). Chapter 11 - Nonbiological Immobilization of Nitrogen. In: Developments in Soil Science, (Elsevier), 206–229.

Allison, F.E., & Roller, E.M. (1955). Fixation and release of ammonium ions by clay minerals. Soil Sci. 80, 431–442.

Allison, F.E., Doetsch, J.H., & Roller, E.M. (1953a). Availability of fixed ammonium in soils containing different clay minerals. Soil Sci. 75, 361–382.

Allison, F.E., Roller, E.M., & Doetsch, J.H. (1953b). Ammonium Fixation and availability in vermiculite. Soil Sci. 75, 173–180.

Allred, A.L. (1961). Electronegativity values from thermochemical data. J. Inorg. Nucl. Chem. 17, 215–221. https://doi.org/10.1016/0022-1902(61)80142-5

Almgren, S., & Isaksson, M. (2006). Vertical migration studies of ^{137}Cs from nuclear weapons fallout and the Chernobyl accident. J. Environ. Radioact. 91, 90–102. https://doi.org/10.1016/j.jenvrad.2006.08.008

Alshameri, A., He, H., Zhu, J., Xi, Y., Zhu, R., Ma, L., & Tao, Q. (2018). Adsorption of ammonium by different natural clay minerals: Characterization, kinetics and adsorption isotherms. Appl. Clay Sci. 159, 83–93. https://doi.org/10.1016/j.clay.2017.11.007

Amacher, M.C., & Brown, R.W. (2000). Chapter 13 - Mine waste characterization. In: Techniques and Instrumentation in Analytical Chemistry, D. Barceló, ed. (Elsevier), 585–622.

Ames, L.L. (1960). The Cation Sieve Properties of Clinoptilolite. Am. Mineral. 45, 689–700.

Amonette, J., Ismail, F.T., & Scott, A.D. (1985). Oxidation of Iron in Biotite by Different Oxidizing Solutions at Room Temperature. Soil Sci. Soc. Am. J. 49, 772–777. https://doi.org/10.2136/sssaj1985.03615995004900030048x

Andersen, P.K., Ghassemi, A., & Ghassemi, M. (2004). Nuclear Waste. In: Encyclopedia of Energy, C.J. Cleveland, ed. (New York: Elsevier), 449–463.

Anderson, S.P., Blum, J., Brantley, S.L., Chadwick, O., Chorover, J., Derry, L.A., Drever, J.I., Hering, J.G., Kirchner, J.W., Kump, L.R., et al. (2004). Proposed initiative would study earth’s weathering engine. Eos 85, 265–269. https://doi.org/10.1029/2004EO280001

Arai, Y., Sparks, D.L., & Davis, J.A. (2005). Arsenate Adsorption Mechanisms at the Allophane−Water Interface. Environ. Sci. Technol. 39, 2537–2544. https://doi.org/10.1021/es0486770

Avery, S.V. (1995). Caesium accumulation by microorganisms: uptake mechanisms, cation competition, compartmentalization and toxicity. J. Ind. Microbiol. 14, 76–84. https://doi.org/10.1007/BF01569888

Baba, M. (2013). Fukushima accident: What happened? Radiat. Meas. 55, 17–21. https://doi.org/10.1016/j.radmeas.2013.01.013

Bain, D.C., Mellor, A., & Wilson, M.J. (1990). Nature and origin of an aluminous vermiculitic weathering product in acid soils from upland catchments in Scotland. Clay Miner. 25, 467–475. https://doi.org/10.1180/claymin.1990.025.4.05

Bajwa, M.I. (1987). Comparative Ammonium and Potassium Fixation by some Wetland Rice Soil Clays as Affected by Mineralogical Composition and Treatment Sequence. J. Agron. Crop Sci. 158, 65–68. https://doi.org/10.1111/j.1439-037X.1987.tb00613.x

Baker, A.J.M., McGrath, S.P., Sidoli, C.M.D., & Reeves, R.D. (1994). The possibility of in situ heavy metal decontamination of polluted soils using crops of metal-accumulating plants. Resour. Conserv. Recycl. 11, 41–49. https://doi.org/10.1016/0921-3449(94)90077-9

Ballabio, C., Panagos, P., & Monatanarella, L. (2016). Mapping topsoil physical properties at European scale using the LUCAS database. Geoderma 261, 110–123. https://doi.org/10.1016/j.geoderma.2015.07.006

Bange, G.G.J., & Overstreet, R. (1960). Some Observations on Absorption of Caesium by Excised Barley Roots. Plant Physiol. 35, 605–608. https://doi.org/10.1104/pp.35.5.605

Barrett, J.E., & Burke, I.C. (2000). Potential nitrogen immobilization in grassland soils across a soil organic matter gradient. Soil Biol. Biochem. 32, 1707–1716. https://doi.org/10.1016/S0038-0717(00)00089-4

Barshad, I. (1954). Cation exchange in micaceous minerals: II. Replaceability of ammonium and potassium from vermiculite, biotite, and montmorillonite. Soil Sci. 78, 57–76. https://doi.org/10.1097/00010694-195407000-00007

Beauchamp, E.G. (1982). Fixed ammonium and potassium release from two soils. Commun. Soil Sci. Plant Anal. 13, 927–943. https://doi.org/10.1080/00103628209367322

Beauchamp, E., & Drury, C. (1991). Ammonium Fixation, Release, Nitrification, and Immobilization in High and Low-Fixing Soils. Soil Sci. Soc. Am. J. - SSSAJ 55. https://doi.org/10.2136/sssaj1991.03615995005500010022x

Beckmann, C., & Faas, C. (1992). Radioactive contamination of soils in Lower Saxony, Germany, after the Chernobyl accident. Analyst 117, 525–527. https://doi.org/10.1039/AN9921700525

Belli, M., Sansone, U., Ardiani, R., Feoli, E., Scimone, M., Menegon, S., & Parente, G. (1995). The effect of fertilizer applications on ^{137}Cs uptake by different plant species and vegetation types. J. Environ. Radioact. 27, 75–89. https://doi.org/10.1016/0265-931X(94)00038-X

Belousov, P., Semenkova, A., Egorova, T., Romanchuk, A., Zakusin, S., Dorzhieva, O., Tyupina, E., Izosimova, Y., Tolpeshta, I., Chernov, M., et al. (2019). Caesium Sorption and Desorption on Glauconite, Bentonite, Zeolite, and Diatomite. Minerals 9, 625. https://doi.org/10.3390/min9100625

Benedicto, A., Missana, T., & Fernández, A.M. (2014). Interlayer Collapse Affects on Caesium Adsorption Onto Illite. Environ. Sci. Technol. 48, 4909–4915. https://doi.org/10.1021/es5003346

Bergaoui, L., Lambert, J.F., & Prost, R. (2005). Caesium adsorption on soil clay: macroscopic and spectroscopic measurements. Appl. Clay Sci. 1, 23–29. https://doi.org/10.1016/j.clay.2004.09.002

Berthelsen, A. (1992). Mobile Europe. In: A Continent Revealed: The European Geotraverse, Structure and Dynamic Evolution, D.J. Blundell, R. Freeman, and S. Mueller, eds. (Cambridge: Cambridge University Press), 11–32.

Bhattacharyya, L., & Rohrer, J. (2012). Applications of ion chromatography for pharmaceutical and biological products.

Bisdom, E.B.A., Stoops, G., Delvigne, J., Curmi, P., & Altemüller, H.J. (1982). Micromorphology of weathering biotite and its secondary products. Pedologie 32.

Bohn, H., McNeal, B., & O'Connor, G. (1980). Soil Chemistry. Soil Sci. 129.

Bonneville, S.C., Bray, A., & Benning, L. (2016). Structural Fe(II) Oxidation in Biotite by an Ectomycorrhizal Fungi Drives Mechanical Forcing. Environ. Sci. Technol. 50. https://doi.org/10.1021/acs.est.5b06178

Bossemeyer, D., Schlösser, A., & Bakker, E.P. (1989). Specific caesium transport via the Escherichia coli Kup (TrkD) K^+ uptake system. J. Bacteriol. 171, 2219–2221. https://doi.org/10.1128/jb.171.4.2219-2221.1989

Bower, C.A. (1951). Availability of Ammonium Fixed in Difficultly Exchangeable Form by Soils of Semiarid Regions. Soil Sci. Soc. Am. J. 15, 119–122. https://doi.org/10.2136/sssaj1951.036159950015000C0024x

Bradbury, M.H., & Baeyens, B. (2000). A generalised sorption model for the concentration dependent uptake of caesium by argillaceous rocks. J. Contam. Hydrol. 42, 141–163. https://doi.org/10.1016/S0169-7722(99)00094-7

Breck, D.W. (1973). Zeolite Molecular Sieves: Structure, Chemistry, and Use (Wiley)

Bremner, J. m., & Mulvaney, C. s. (1983). Nitrogen—Total. In: Methods of Soil Analysis, (John Wiley & Sons, Ltd), 595–624.

Brevik, E.C., & Burgess, L.C. (2012). Soils and Human Health (CRC Press)

Brigatti, M.F., Galán, E., & Theng, B.K.G. (2013). Chapter 2 - Structure and Mineralogy of Clay Minerals. In: Developments in Clay Science, F. Bergaya, and G. Lagaly, eds. (Elsevier), 21–81.

Britto, D.T., Siddiqi, M.Y., Glass, A.D., & Kronzucker, H.J. (2001). Futile transmembrane NH_4^+ cycling: a cellular hypothesis to explain ammonium toxicity in plants. Proc. Natl. Acad. Sci. U. S. A. 98, 4255–4258. https://doi.org/10.1073/pnas.061034698

Britzke, D., da Silva, L.S., Moterle, D.F., dos Santos Rheinheimer, D., & Bortoluzzi, E.C. (2012). A study of potassium dynamics and mineralogy in soils from subtropical Brazilian lowlands. J. Soils Sediments 12, 185–197. https://doi.org/10.1007/s11368-011-0431-7

Brouwer, E., Baeyens, B., Maes, A., & Cremers, A. (1983). Caesium and rubidium ion equilibria in illite clay. J Phys Chem 87.

Brown, K.R., & Rzucidlo, E. (2011). Acute and chronic radiation injury. J. Vasc. Surg. 53, 15–21. https://doi.org/10.1016/j.jvs.2010.06.175

Browne, E., & Tuli, J.K. (2007). Nuclear Data Sheets 108, 2173 (NNDC)

Bruckman, V.J., & Wriessnig, K. (2013). Improved soil carbonate determination by FT-IR and X-ray analysis. Environ. Chem. Lett. 11, 65–70. https://doi.org/10.1007/s10311-012-0380-4

Bruneel, Y., Van Laer, L., Brassinnes, S., & Smolders, E. (2021). Characterisation of the highly selective caesium sorption on glauconite rich sands of contrasting geological formations. Appl. Geochem. 128, 104926-. https://doi.org/10.1016/j.apgeochem.2021.104926

Bunaciu, A.A., Udriştioiu, E.G., & Aboul-Enein, H.Y. (2015). X-ray diffraction: instrumentation and applications. Crit. Rev. Anal. Chem. 45, 289–299. https://doi.org/10.1080/10408347.2014.949616

Calvo, B., Canoira, L., Morante, F., Martínez-Bedia, J.M., Vinagre, C., García-González, J.-E., Elsen, J., & Alcantara, R. (2009). Continuous elimination of Pb^{2+}, Cu^{2+}, Zn^{2+}, H^+ and NH_4^+ from acidic waters by ionic exchange on natural zeolites. J. Hazard. Mater. 166, 619–627. https://doi.org/10.1016/j.jhazmat.2008.11.087

Carrier, B., Vandamme, M., Pellenq, R., Bornert, M., Van Damme, H., Robin, V., Sardini, P., Regnault, O., Descostes, M., Zanolli, C., et al. (2016). Experimental evidence of the contrasting reactivity of external vs. interlayer adsorption sites on swelling clay minerals: The case of Sr^{2+}- for - Ca^{2+} exchange in vermiculite.

Casella, G. (2008). Completely Randomized Designs. In: Statistical Design, (New York, NY: Springer), 43–90.

Cavalli, D., Consolati, G., Marino, P., & Bechini, L. (2015). Measurement and simulation of soluble, exchangeable, and non-exchangeable ammonium in three soils. Geoderma 259–260, 116–125. https://doi.org/10.1016/j.geoderma.2015.05.011

Chen, C.-C., Turner, F.T., & Dixon, J.B. (1989). Ammonium Fixation by High-Charge Smectite in Selected Texas Gulf Coast Soils. Soil Sci. Soc. Am. J. 53, 1035–1040. https://doi.org/10.2136/sssaj1989.03615995005300040008x

Chiang, P.N., Wang, M.K., Huang, P.M., & Wang, J.J. (2008). Kinetics of radiocaesium released from contaminated soil by fertilizer solutions. J. Environ. Radioact. 99, 159–166. https://doi.org/10.1016/j.jenvrad.2007.07.009

Choi, T.A., Costes, S.V., & Abergel, R.J. (2015). Understanding the Health Impacts and Risks of Exposure to Radiation. In: Reflections on the Fukushima Daiichi Nuclear Accident: Toward Social-Scientific Literacy and Engineering Resilience, J. Ahn, C. Carson, M. Jensen, K. Juraku, S. Nagasaki, and S. Tanaka, eds. (Cham: Springer International Publishing), 259–281.

Choppin, G.R. (2003). Actinide speciation in the environment. Radiochim. Acta 91, 645–650. https://doi.org/10.1524/ract.91.11.645.23469

Claverie, M., Garcia, J., Prevost, T., Brendlé, J., & Limousy, L. (2019). Inorganic and Hybrid (Organic–Inorganic) Lamellar Materials for Heavy Metals and Radionuclides Capture in Energy Wastes Management—A Review. Materials 12, 1399. https://doi.org/10.3390/ma12091399

Clements, B.W., & Casani, J.A.P. (2016). 15 - Nuclear and Radiological Disasters. In: Disasters and Public Health (Second Edition), B.W. Clements, and J.A.P. Casani, eds. (Butterworth-Heinemann), 357–383.

CNR (2006). Health Risks from Exposure to Low Levels of Ionizing Radiation: BEIR VII Phase 2 (Washington, DC: The National Academies Press)

Colella, C., & Wise, W.S. (2014). The IZA Handbook of Natural Zeolites: A tool of knowledge on the most important family of porous minerals. Microporous Mesoporous Mater. 189, 4–10. https://doi.org/10.1016/j.micromeso.2013.08.028

Comans, R., Haller, M., & De Preter, P. (1991). Sorption of caesium on illite: Non-equilibrium behaviour and reversibility. Geochim. Cosmochim. Acta 55, 433–440. https://doi.org/10.1016/0016-7037(91)90002-M

Cornell, R.M. (1993). Adsorption of caesium on minerals: A review. J. Radioanal. Nucl. Chem. 171, 483–500. https://doi.org/10.1007/BF02219872

Cremers, A., Elsen, A., Preter, P.D., & Maes, A. (1988). Quantitative analysis of radiocaesium retention in soils. Nature https://doi.org/10.1038/335247A0

Cubadda, F. (2007). Chapter 19 - Inductively coupled plasma mass spectrometry. In: Food Toxicants Analysis, Y. Picó, ed. (Amsterdam: Elsevier), 697–751.

Cvetkovic, V., Prelević, D., & Schmid, S. (2015). Geology of South-Eastern Europe. In: Environmental Earth Sciences, 1–29.

Cyrus, J.S., & Reddy, G.B. (2011). Sorption and desorption of ammonium by zeolite: Batch and column studies. J. Environ. Sci. Health Part A Tox. Hazard. Subst. Environ. Eng. 46, 408–414. https://doi.org/10.1080/02773813.2010.542398

Dahlgren, R.A., Saigusa, M., & Ugolini, F.C. (2004). The Nature, Properties and Management of Volcanic Soils. Adv. Agron. 82, 113–182. https://doi.org/10.1016/S0065-2113(03)82003-5

Dahlgren, R.A., Macías, F., Arbestain, M.C., Chesworth, W., Robarge, W.P., Macías, F., Bache, B.W., Emerson, W.W., Hartmann, R., Kostic, N., et al. (2008). Andosols. In: Encyclopedia of Soil Science, W. Chesworth, ed. (Dordrecht: Springer Netherlands), 39–46.

Dancer, W.S., Peterson, L.A., & Chesters, G. (1973). Ammonification and Nitrification of N as Influenced by Soil pH and Previous N Treatments. Soil Sci. Soc. Am. J. 37, 67–69. https://doi.org/10.2136/sssaj1973.03615995003700010024x

Dasgupta, P.K., & Dong, S. (1986). Solubility of ammonia in liquid water and generation of trace levels of standard gaseous ammonia. Atmospheric Environ. 1967 20, 565–570. https://doi.org/10.1016/0004-6981(86)90099-5

Davis, S., & Mirick, D.K. (2006). Soil ingestion in children and adults in the same family. J. Expo. Sci. Environ. Epidemiol. 16, 63–75. https://doi.org/10.1038/sj.jea.7500438

Deblonde, G.J.-P., Kersting, A.B., & Zavarin, M. (2020). Open questions on the environmental chemistry of radionuclides. Commun. Chem. 3, 1–5. https://doi.org/10.1038/s42004-020-00418-6

Degryse, F., Smolders, E., & Cremers, A. (2004). Enhanced sorption and fixation of radiocaesium in soils amended with K-bentonites, submitted to wetting–drying cycles. Eur. J. Soil Sci. 55, 513–522. https://doi.org/10.1111/j.1365-2389.2004.00619.x

Delacre, M., Lakens, D., & Leys, C. (2017). Why Psychologists Should by Default Use Welch's t-test Instead of Student's t-test. Int. Rev. Soc. Psychol. 30, 92. https://doi.org/10.5334/irsp.82

Delvaux, B., Kruyts, N., & Cremers, A. (2000). Rhizospheric Mobilization of Radiocaesium in Soils. Environ. Sci. Technol. 34, 1489–1493. https://doi.org/10.1021/es990658g

Dengra I Grau, F.X., Eguchi, T., Toloza, A., Smolders, E., Tarjan, S., Shinano, T., Gerzabek, M.H., Hansen, H.C.B., & Dercon, G. (2021). Evaluation of the radiocaesium behaviour in agricultural Japanese soils based on potassium fertilisation, zeolite amendment and clay mineralogy (Copernicus Meetings)

Deshpande, S., Durdagi, S., & Noskov, S.Yu. (2013). Potassium in Biological Systems. In: Encyclopedia of Metalloproteins, R.H. Kretsinger, V.N. Uversky, and E.A. Permyakov, eds. (New York, NY: Springer), 1799–1804.

Dolcater, D.L., Jackson, M.L., & Syers, S.K. (1972). Cation exchange selectivity in mica and vermiculite. Am. Mineral. 57, 1–9.

Doram, D.R., & Evans, L.J. (1983). Native fixed ammonium and fixation of added ammonium in relation to clay mineralogy in some ontario soils. Can. J. Soil Sci. 63, 631–639. https://doi.org/10.4141/cjss83-063

Dorland, S., & Beauchamp, E.G. (1991). Denitrification and ammonification at low soil temperatures. Can. J. Soil Sci. 71, 293–303. https://doi.org/10.4141/cjss91-029

Dörr, W., & Schmidt, M. (2014). 7.05 - Normal Tissue Radiobiology. In: Comprehensive Biomedical Physics, A. Brahme, ed. (Oxford: Elsevier), 75–95.

Du, Q., Liu, S., Cao, Z., & Wang, Y. (2005). Ammonia removal from aqueous solution using natural Chinese clinoptilolite. Sep. Purif. Technol. 44, 229–234. https://doi.org/10.1016/j.seppur.2004.04.011

Durn, G., Ottner, F., & Slovenec, D. (1999). Mineralogical and geochemical indicators of the polygenetic nature of terra rossa in Istria, Croatia. Geoderma 91, 125–150. https://doi.org/10.1016/S0016-7061(98)00130-X

Durrant, C.B., Begg, J.D., Kersting, A.B., & Zavarin, M. (2018). Caesium sorption reversibility and kinetics on illite, montmorillonite, and kaolinite. Sci. Total Environ. 610–611, 511–520. https://doi.org/10.1016/j.scitotenv.2017.08.122

Dushenkov, V. (2003). Trends in phytoremediation of radionuclides. Plant Soil 249, 167–175. https://doi.org/10.1023/A:1022527207359

Dushenkov, S., Mikheev, A., Prokhnevsky, A., Ruchko, M., & Sorochinsky, B. (1999). Phytoremediation of Radiocaesium-Contaminated Soil in the Vicinity of Chernobyl, Ukraine. Environ. Sci. Technol. 33, 469–475. https://doi.org/10.1021/es980788+

Dutov, A.I., Zuev, N.P., Tkachev, A.V., Breslavets, A.P., & Zueva, E.E. (2021). Features of the main elements of organic farming in agro-landscapes contaminated with ^{137}Cs (on the example of the Chernobyl accident). BIO Web Conf. 39, 01009. https://doi.org/10.1051/bioconf/20213901009

Dzene, L., Tertre, E., Hubert, F., & Ferrage, E. (2015). Nature of the sites involved in the process of caesium desorption from vermiculite. J. Colloid Interface Sci. 226. https://doi.org/10.1016/j.jcis.2015.05.053

Echols, K.R., Meadows, J.C., & Orazio, C.E. (2009). Pollution of Aquatic Ecosystems II: Hydrocarbons, Synthetic Organics, Radionuclides, Heavy Metals, Acids, and Thermal Pollution. In: Encyclopedia of Inland Waters, G.E. Likens, ed. (Oxford: Academic Press), 120–128.

Eckert, D., & Sims, J. (1995). Recommended Soil pH and Lime Requirement Test. Coop. Bull. 493.

Egendorf, S.P., Gailey, A.D., Schachter, A.E., & Mielke, H.W. (2020). Soil toxicants that potentially affect children's health. Curr. Probl. Pediatr. Adolesc. Health Care 50, 100741. https://doi.org/10.1016/j.cppeds.2019.100741

Egli, M., Mirabella, A., & Fitze, P. (2001). Clay mineral transformations in soils affected by fluorine and depletion of organic matter within a time span of 24 years. Geoderma 103, 307–334. https://doi.org/10.1016/S0016-7061(01)00046-5

Eguchi, T., Tanaka, R., Maejima, Y., & Tamura, K. (2012). The influence of aeolian dust in non-allophanic Andosols on Yakushima Island. Soil Sci. Plant Nutr. 58, 191–199. https://doi.org/10.1080/00380768.2012.672926

Eguchi, T., Ohta, T., Ishikawa, T., Matsunami, H., Takahashi, Y., Kubo, K., Yamaguchi, N., Kihou, N., & Shinano, T. (2015). Influence of the nonexchangeable potassium of mica on radiocaesium uptake by paddy rice. J. Environ. Radioact. 147, 33–42. https://doi.org/10.1016/j.jenvrad.2015.05.002

Elprince, A.M., Rich, C.I., & Martens, D.C. (1977). Effect of Temperature and Hydroxy Aluminum Interlayers on the Adsorption of Trace Radioactive Caesium by Sediments Near Water-Cooled Nuclear Reactors. Water Resour. Res. 13, 375–380. https://doi.org/10.1029/WR013i002p00375

Epov, V.N., Lariviere, D., Reiber, K.M., Evans, R.D., & Cornett, R.J. (2004). Extraction and determination of Cs in natural waters by ICP-MS after ion exchange separation. J. Anal. At. Spectrom. 19, 1225–1229. https://doi.org/10.1039/B403013C

Epp, J. (2016). 4 - X-ray diffraction (XRD) techniques for materials characterization. In: Materials Characterization Using Nondestructive Evaluation (NDE) Methods, G. Hübschen, I. Altpeter, R. Tschuncky, and H.-G. Herrmann, eds. (Woodhead Publishing), 81–124.

Estevez, M.M., Linjordet, R., Horn, S.J., & Morken, J. (2014). Improving nutrient fixation and dry matter content of an ammonium-rich anaerobic digestion effluent by struvite formation and clay adsorption. Water Sci. Technol. J. Int. Assoc. Water Pollut. Res. 70, 337–344. https://doi.org/10.2166/wst.2014.236

Fan, Q.H., Tanaka, M., Tanaka, K., Sakaguchi, A., & Takahashi, Y. (2014a). An EXAFS study on the effects of natural organic matter and the expandability of clay minerals on caesium adsorption and mobility. Geochim. Cosmochim. Acta 135, 49–65. https://doi.org/10.1016/j.gca.2014.02.049

Fan, Q.H., Yamaguchi, N., Tanaka, M., Tsukada, H., & Takahashi, Y. (2014b). Relationship between the adsorption species of caesium and radiocaesium interception potential in soils and minerals: an EXAFS study. J. Environ. Radioact. 138, 92–100. https://doi.org/10.1016/j.jenvrad.2014.08.009

Fernandez, G. (1992). Residual Analysis and Data Transformations: Important Tools in Statistical Analysis. HortScience 27, 297–300. https://doi.org/10.21273/HORTSCI.27.4.297

Ferrage, E., Lanson, B., Sakharov, B., & Drits, V. (2005). Investigation of smectite hydration properties by modeling experimental X-ray diffraction patterns: Part I. Montmorillonite hydration properties. Am. Mineral. 90, 1358–1374. https://doi.org/10.2138/am.2005.1776

Ferreira, D.R., Phillips, G.D., & Baruah, B. (2021). A comparison of the adsorption of caesium on zeolite minerals vs. vermiculite. Clays Clay Miner. 69, 663–671. https://doi.org/10.1007/s42860-021-00150-9

Fesenko, S.V., Alexakhin, R.M., Balonov, M.I., Bogdevitch, I.M., Howard, B.J., Kashparov, V.A., Sanzharova, N.I., Panov, A.V., Voigt, G., & Zhuchenka, Y.M. (2007). An extended critical review of twenty years of countermeasures used in agriculture after the Chernobyl accident. Sci. Total Environ. 383, 1–24. https://doi.org/10.1016/j.scitotenv.2007.05.011

Fliedner, T.M., Dörr, H.D., & Meineke, V. (2005). Multi-organ involvement as a pathogenetic principle of the radiation syndromes: a study involving 110 case histories documented in SEARCH and classified as the bases of haematopoietic indicators of effect. Br. J. Radiol. 78, 1–8. https://doi.org/10.1259/bjr/77700378

Flores-Macías, A., Galvis, A., Mendoza, T., González, F.L., & Zelaya, F. (2007). Effect of zeolite (clinoptilolite and mordenite) amended andosols on soil chemical environment and growth of oat. Interciencia 32, 692–696.

Fotyma, M., Ochal, P., & Łabętowicz, J. (2013). Potassium in Soils of Glacial Origin (IntechOpen)

Fritz, J., & Gjerde, D. (2009). Ion Chromatography (Fourth Completely Revised and Enlarged Edition) (Weinhein: Wiley-VCH Verlag GmbH & KGoA Weinhein)

Fuhrmann, M., Lasat, M., Ebbs, S., Cornish, J., & Kochian, L. (2003). Uptake and release of Caesium-137 by five plant species as influenced by soil amendments in field experiments. J. Environ. Qual. 32, 2272–2279. https://doi.org/10.2134/jeq2003.2272

Fujimura, S., Yoshioka, K., Saito, T., Sato, M., Sato, M., Sakuma, Y., & Muramatsu, Y. (2013). Effects of Applying Potassium, Zeolite and Vermiculite on the Radiocaesium Uptake by Rice Plants Grown in Paddy FieldSoils Collected from Fukushima Prefecture. Plant Prod. Sci. 16, 166–170. https://doi.org/10.1626/pps.16.166

Fukushi, K., Sakai, H., Itono, T., Tamura, A., & Arai, S. (2014). Desorption of Intrinsic Caesium from Smectite: Inhibitive Effects of Clay Particle Organization on Caesium Desorption. Environ. Sci. Technol. 48, 10743–10749. https://doi.org/10.1021/es502758s

Fuller, A.J., Shaw, S., Ward, M.B., Haigh, S.J., Mosselmans, J.F.W., Peacock, C.L., Stackhouse, S., Dent, A.J., Trivedi, D., & Burke, I.T. (2015). Caesium incorporation and retention in illite interlayers. Appl. Clay Sci. 108, 128–134. https://doi.org/10.1016/j.clay.2015.02.008

Gaschak, S.P., Makliuk, Y.A., Maksimenko, A.M., Bondarkov, M.D., Chizhevsky, I., Caldwell, E.F., Jannik, G.T., & Farfán, E.B. (2011). Frequence distributions of ^{90}Sr and ^{137}Cs concentrations in an ecosystem of the “red forest” area in the chernobyl exclusion zone. Health Phys. 101, 409–415. https://doi.org/10.1097/HP.0b013e31821d0b81

Gastwirth, J., Gel, Y., & Miao, W. (2010). The Impact of Levene’s Test of Equality of Variances on Statistical Theory and Practice. Stat. Sci. 24. https://doi.org/10.1214/09-STS301

Georgiadis, A., Dietel, J., Dohrmann, R., & Rennert, T. (2020). Review Article. What are the nature and formation conditions of hydroxy-interlayered minerals (HIMs) in soil? J. Plant Nutr. Soil Sci. 183, 12–26. https://doi.org/10.1002/jpln.201900283

Gerzabek, M.H., Strebl, F., & Temmel, B. (1998). Plant uptake of radionuclides in lysimeter experiments. Environ. Pollut. 99, 93–103. https://doi.org/10.1016/S0269-7491(97)00167-X

Ghosh, A., Sharma, A., & Talukder, G. (1993). Effects of caesium on cellular systems. Biol. Trace Elem. Res. 38, 165–203. https://doi.org/10.1007/BF02784052

Gottschalk, U. (2011). 3.57 - Overview of Downstream Processing in the Biomanufacturing Industry. In: Comprehensive Biotechnology (Third Edition), M. Moo-Young, ed. (Oxford: Pergamon), 698–711.

Gould, W.D., Hagedorn, C., & McCready, R.G.L. (1986). Urea Transformations and Fertilizer Efficiency in Soil. In: Advances in Agronomy, N.C. Brady, ed. (Academic Press), 209–238.

Griffin, R.A., Shimp, N.F., Steele, J.D., Ruch, R.R., White, W.A., & Hughes, G.M. (1976). Attenuation of pollutants in municipal landfill leachate by passage through clay. Environ. Sci. Technol. 10, 1262–1268. https://doi.org/10.1021/es60123a006

Gus'kova, A.K., Baranov, A.E., Barabanova, A.V., Gruzdev, G.P., & Piatkin, E.K. (1987). [Acute radiation effects in victims of the accident at the Chernobyl nuclear power station]. Med. Radiol. (Mosk.) 32, 3–18.

Haase, D., Fink, J., Haase, G., Ruske, R., Pécsi, M., Richter, H., Altermann, M., & Jäger, K.-D. (2007). Loess in Europe—its spatial distribution based on a European Loess Map, scale 1:2,500,000. Quat. Sci. Rev. 26, 1301–1312. https://doi.org/10.1016/j.quascirev.2007.02.003

Hamada, N., Ogino, H., & Fujimichi, Y. (2012). Safety regulations of food and water implemented in the first year following the Fukushima nuclear accident. J. Radiat. Res. (Tokyo) 53, 641–671. https://doi.org/10.1093/jrr/rrs032

Handley, R., & Overstreet, R. (1961). Effect of Various Cations upon Absorption of Carrier-Free Caesium. Plant Physiol. 36, 66–69.

Hanway, J.J., Scott, A.D., & Stanford, G. (1957). Replaceability of Ammonium Fixed in Clay Minerals as Influenced by Ammonium or Potassium in the Extracting Solution. Soil Sci. Soc. Am. J. 21, 29–34. https://doi.org/10.2136/sssaj1957.03615995002100010008x

Hara, T., & Tamai, M. (1968). Some factors affecting behaviour of boron in soil. Soil Sci. Plant Nutr. 14, 215–224. https://doi.org/10.1080/00380768.1968.10432768

Harris, W., & Norman White, G. (2008). X-ray Diffraction Techniques for Soil Mineral Identification. In: Methods of Soil Analysis Part 5—Mineralogical Methods, (John Wiley & Sons, Ltd), 81–115.

Harsh, J., Chorover, J., & Nizeyimana, E. (2002). Allophane and Imogolite. In: Soil Mineralogy with Environmental Applications, (John Wiley & Sons, Ltd), 291–322.

Hatano, R., Shinjo, H., & Takata, Y. (2021). Overview. In: The Soils of Japan, R. Hatano, H. Shinjo, and Y. Takata, eds. (Singapore: Springer), 3–9.

Hayashi, K., Hayakawa, A., Akiyama, H., & Yagi, K. (2009). Measurement of ammonia volatilization loss using a dynamic chamber technique: A case study of surface-incorporated manure and ammonium sulfate in an upland field of light-colored Andosol. Soil Sci. Plant Nutr. 55, 571–581. https://doi.org/10.1111/j.1747-0765.2009.00392.x

Haynes, W. (2013). Tukey's Test. In: Encyclopedia of Systems Biology, W. Dubitzky, O. Wolkenhauer, K.-H. Cho, and H. Yokota, eds. (New York, NY: Springer), 2303–2304.

He, Z.L., Alva, A.K., Calvert, D.V., Li, Y.C., & Banks, D.J. (1999). Effects of nitrogen fertilization of grapefruit trees on soil acidification and nutrient availability in a Riviera fine sand. Plant Soil 206, 11–19. https://doi.org/10.1023/A:1004364805789

Hemati Matin, N., & Jalali, M. (2017). The effect of waterlogging on electrochemical properties and soluble nutrients in paddy soils. Paddy Water Environ. 15, 443–455. https://doi.org/10.1007/s10333-016-0562-y

Henderson, J.H., Doner, H.E., Weaver, R.M., Syers, J.K., & Jackson, M.L. (1976). Cation and Silica Relationships of Mica Weathering to Vermiculite in Calcareous Harps Soil. Clays Clay Miner. 24, 93–100. https://doi.org/10.1346/CCMN.1976.0240208

Henrichs, H., Paretzke, H.G., Voigt, G., & Berg, D. (1989). Measurements of Cs absorption and retention in man. Health Phys. 57, 571–578. https://doi.org/10.1097/00004032-198910000-00008

Herrmann, L. (2018). Bodenkunde Xpress (Stuttgart: Eugen Ulmer)

Hill, S.J., & Fisher, A.S. (2017). Atomic Absorption, Methods and Instrumentation. In: Encyclopedia of Spectroscopy and Spectrometry (Third Edition), J.C. Lindon, G.E. Tranter, and D.W. Koppenaal, eds. (Oxford: Academic Press), 37–43.

Hölzer, A. (2018). Simultane Quantifizierung von ^{127}I- und ^{129}I-Spezies in Umweltproben mittels IC-ICP-MS und AMS. Dissertation. Hannover : Gottfried Wilhelm Leibniz Universität Hannover

Hommes, N.G., Russell, S.A., Bottomley, P.J., & Arp, D.J. (1998). Effects of Soil on Ammonia, Ethylene, Chloroethane, and 1,1,1-Trichloroethane Oxidation by Nitrosomonas europaea. Appl. Environ. Microbiol. 64, 1372–1378. https://doi.org/10.1128/AEM.64.4.1372-1378.1998

Hood-Nowotny, R., Umana, N.H.-N., Inselbacher, E., Oswald- Lachouani, P., & Wanek, W. (2010). Alternative Methods for Measuring Inorganic, Organic, and Total Dissolved Nitrogen in Soil. Soil Sci. Soc. Am. J. 74, 1018–1027. https://doi.org/10.2136/sssaj2009.0389

Hu, Q.-H., Weng, J.-Q., & Wang, J.-S. (2010). Sources of anthropogenic radionuclides in the environment: a review. J. Environ. Radioact. 101, 426–437. https://doi.org/10.1016/j.jenvrad.2008.08.004

Huang, Z.T., & Petrovic, A.M. (1994). Clinoptilolite Zeolite Influence on Nitrate Leaching and Nitrogen Use Efficiency in Simulated Sand Based Golf Greens. J. Environ. Qual. 23, 1190–1194. https://doi.org/10.2134/jeq1994.00472425002300060009x

Huang, S., Feng, J., Yu, J., Wang, Y., Liu, J., Chi, R., & Hou, H. (2021). Adsorption and desorption performances of ammonium on the weathered crust elution-deposited rare earth ore. Colloids Surf. Physicochem. Eng. Asp. 613, 126139. https://doi.org/10.1016/j.colsurfa.2021.126139

Hussain, C.M., & Keçili, R. (2020). Chapter 6 - Spectroscopic techniques for environmental analysis. In: Modern Environmental Analysis Techniques for Pollutants, C.M. Hussain, and R. Keçili, eds. (Elsevier), 133–161.

Iijima, K., Tomura, T., & Shoji, Y. (2010). Reversibility and modeling of adsorption behavior of caesium ions on colloidal montmorillonite particles. Appl. Clay Sci. 49, 262–268. https://doi.org/10.1016/j.clay.2010.05.016

Inselsbacher, E., Hinko-Najera Umana, N., Stange, F.C., Gorfer, M., Schüller, E., Ripka, K., Zechmeister-Boltenstern, S., Hood-Novotny, R., Strauss, J., & Wanek, W. (2010). Short-term competition between crop plants and soil microbes for inorganic N fertilizer. Soil Biol. Biochem. 42, 360–372. https://doi.org/10.1016/j.soilbio.2009.11.019

International Atomic Energy Agency (2013). INES: The International Nuclear and Radiological Event Scale User's Manual (Vienna: International Atomic Energy Agency)

International Atomic Energy Agency (2015). The Fukushima Daiichi accident (Vienna, Austria: International Atomic Energy Agency)

International Atomic Energy Agency (2019). Remediation of Radioactive Contaminated Agricultural Land. Project Code: D15019 (IAEA)

International Comission on Radiological Protection (2007). The 2007 Recommendations of the International Commission on Radiological Protection. ICRP publication 103. Ann. ICRP 37, 1–332. https://doi.org/10.1016/j.icrp.2007.10.003

Ioannides, K.G., Papachristodoulou, C.A., Mertzimekis, T.J., & Tzialla, C.E. (2003). Effect of soil amendments on radiocaesium transfer to alfalfa. Health Phys. 84, 637–641. https://doi.org/10.1097/00004032-200305000-00010

Ishikawa, N., Tagami, K., & Uchida, S. (2014). Estimation of 137Cs Plant Root Uptake Using Naturally Existing ^{133}Cs. J. Nucl. Sci. Technol. 45, 146–151. https://doi.org/10.1080/00223131.2008.10875997

Issar, A.S. (2003). Climate Changes during the Holocene and their Impact on Hydrological Systems (Cambridge: Cambridge University Press)

Ito, A., & Wagai, R. (2017). Global distribution of clay-size minerals on land surface for biogeochemical and climatological studies. Sci. Data 4, 170103. https://doi.org/10.1038/sdata.2017.103

Jackson, M.L., Hseung, Y., Corey, R.B., Evans, E.J., & Heuvel, R.C.V. (1952). Weathering Sequence of Clay-size Minerals in Soils and Sediments. Soil Sci. Soc. Am. J. 16, 3–6. https://doi.org/10.2136/sssaj1952.03615995001600010002x

Jagetiya, B., Sharma, A., Soni, A., & Khatik, U.K. (2014). Phytoremediation of Radionuclides: A Report on the State of the Art. In: Radionuclide Contamination and Remediation Through Plants, D.K. Gupta, and C. Walther, eds. (Cham: Springer International Publishing), 1–31.

Jarrell, K.F., Sprott, G.D., & Matheson, A.T. (1984). Intracellular potassium concentration and relative acidity of the ribosomal proteins of methanogenic bacteria. Can. J. Microbiol. 30, 663–668. https://doi.org/10.1139/m84-099

Jaskunas, A., Subačius, B., & Slinksiene, R. (2015). Adsorption of potassium ions on natural zeolite: Kinetic and equilibrium studies. Chemija 26, 69–78.

Jenny, H. (1994). Factors of Soil Formation: A System of Quantitative Pedology (Dover)

Jeon, I., & Nam, K. (2019). Change in the site density and surface acidity of clay minerals by acid or alkali spills and its effect on pH buffering capacity. Sci. Rep. 9, 9878. https://doi.org/10.1038/s41598-019-46175-y

Jiang, X., Ma, Y., Yuan, J., Wright, A., & Li, H. (2011). Soil particle surface electrochemical property effects on abundance of ammonia-oxidizing bacteria and ammonia-oxidizing archaea, NH_4^+ activity, and net nitrification in an acid soil. Soil Biol. Biochem. 43, 2215–2221. https://doi.org/10.1016/j.soilbio.2011.07.014

Jones, E., Michael, S., & Sittampalam, G.S. (2004). Basics of Assay Equipment and Instrumentation for High Throughput Screening. In: Assay Guidance Manual, S. Markossian, A. Grossman, K. Brimacombe, M. Arkin, D. Auld, C.P. Austin, J. Baell, T.D.Y. Chung, N.P. Coussens, J.L. Dahlin, et al., eds. (Bethesda (MD): Eli Lilly & Company and the National Center for Advancing Translational Sciences),

Jordanova, N. (2017). Chapter 2 - Magnetism of soils with a pronounced accumulation of organic matter in the mineral topsoil: Chernozems and Phaeozems. In: Soil Magnetism, N. Jordanova, ed. (Academic Press), 29–64.

Joussein, E., Petit, S., Claire, F., Philippe, V., & Righi, D. (2006). Differences in the dehydration-rehydration behavior of halloysites: New evidence and interpretations. Clays Clay Miner. 54, 473–484. https://doi.org/10.1346/CCMN.2006.0540408

Jungk, A., & Claassen, N. (1997). Ion Diffusion in the Soil–Root System. In: Advances in Agronomy, D.L. Sparks, ed. (Academic Press), 53–110.

Kamoshita, Y. (1959). Soils in Japan. Soil Sci. Plant Nutr. 5, 84–94. https://doi.org/10.1080/00380768.1959.10430899

Kanda, T., Takata, Y., Kohyama, K., Ohkura, T., Maejima, Y., Wakabayashi, S., & Obara, H. (2018). New Soil Maps of Japan based on the Comprehensive Soil Classification System of Japan – First Approximation and its Application to the World Reference Base for Soil Resources 2006. Jpn. Agric. Res. Q. JARQ 52, 285–292. https://doi.org/10.6090/jarq.52.285

Karlen, D.L., & Rice, C.W. (2015). Soil Degradation: Will Humankind Ever Learn? Sustainability 7, 12490–12501. https://doi.org/10.3390/su70912490

Kato, N., Kihou, N., Fujimura, S., Ikeba, M., Miyazaki, N., Saito, Y., Eguchi, T., & Itoh, S. (2015). Potassium fertilizer and other materials as countermeasures to reduce radiocaesium levels in rice: Results of urgent experiments in 2011 responding to the Fukushima Daiichi Nuclear Power Plant accident. Soil Sci. Plant Nutr. 61, 179–190. https://doi.org/10.1080/00380768.2014.995584

Kavoosi, M. (2007). Effects of Zeolite Application on Rice Yield, Nitrogen Recovery, and Nitrogen Use Efficiency. Commun. Soil Sci. Plant Anal. 38, 69–76. https://doi.org/10.1080/00103620601093652

Kawai, K. (1969). Changes in cation exchange capacity of some Andosols with dithionite-citrate treatment. Soil Sci. Plant Nutr. 15, 97–103. https://doi.org/10.1080/00380768.1969.10432787

Keerthisinghe, G., De Datta, S.K., & Mengel, K. (1985). Importance of exchangeable and nonexchangeable soil NH_4^+ in nitrogen nutrition of lowland rice. Soil Sci. USA

Keith, S., Doyle, J.R., Harper, C., Mumtaz, M., Tarrago, O., Wohlers, D.W., Diamond, G.L., Citra, M., & Barber, L.E. (2012). Overview of basic radiation physics, chemistry, and biology (Agency for Toxic Substances and Disease Registry (US))

Kennedy, J.J. (1938). The Alkali Metal Caesium and Some of its Salts. Chem. Rev. 23, 157–163. https://doi.org/10.1021/cr60074a008

Kimpe, C. (1970). Chemical, physical and mineralogical properties of a Podzol soil with fragipan from glacial till in the province of Quebec. Can. J. Soil Sci. 50, 317–330. https://doi.org/10.4141/cjss70-042

Kimura, K., Shirai, O., Kitazumi, Y., & Kano, K. (2016). Transport of caesium and potassium ions across bilayer lipid membranes — Caesium accumulation in biological cells according to the membrane potential. J. Electroanal. Chem. 779, 131–136. https://doi.org/10.1016/j.jelechem.2016.04.007

Kitagawa, Y. (2005). Characteristics of Clay Minerals in Podzols and Podzolic Soils. Soil Sci. Plant Nutr. 51, 151–158. https://doi.org/10.1111/j.1747-0765.2005.tb00020.x

Kitayama, R., Yanai, J., & Nakao, A. (2020). Ability of micaceous minerals to adsorb and desorb caesium ions: Effects of mineral type and degree of weathering. Eur. J. Soil Sci. 71, 641–653. https://doi.org/10.1111/ejss.12913

Kithome, M., Paul, J.W., Lavkulich, L.M., & Bomke, A.A. (1999). Effect of pH on ammonium adsorption by natural Zeolite clinoptilolite. Commun. Soil Sci. Plant Anal. 30, 1417–1430. https://doi.org/10.1080/00103629909370296

Kiuchi, T., Chiba, S., & Sato, T. (1961). Researches on the Hachiro-gata bottom soil I. On the characteristics of the lagoon bottom soil and its changes during drying. Soil Sci. Plant Nutr. 7, 18–23. https://doi.org/10.1080/00380768.1961.10430952

Koch, A., McBratney, A., Adams, M., Field, D., Hill, R., Crawford, J., Minasny, B., Lal, R., Abbott, L., O'Donnell, A., et al. (2013). Soil Security: Solving the Global Soil Crisis. Glob. Policy 4, 434–441. https://doi.org/10.1111/1758-5899.12096

Kögel-Knabner, I., & Amelung, W. (2014). 12.7 - Dynamics, Chemistry, and Preservation of Organic Matter in Soils. In: Treatise on Geochemistry (Second Edition), H.D. Holland, and K.K. Turekian, eds. (Oxford: Elsevier), 157–215.

Komissarova, O., & Paramonova, T. (2019). Land use in agricultural landscapes with Chernozems contaminated after Chernobyl accident: Can we be confident in radioecological safety of plant foodstuff? Int. Soil Water Conserv. Res. 7. https://doi.org/10.1016/j.iswcr.2019.03.001

de Koning, A., & Comans, R.N.J. (2004). Reversibility of radiocaesium sorption on illite2 2Associate editor: D. L. Sparks. Geochim. Cosmochim. Acta 68, 2815–2823. https://doi.org/10.1016/j.gca.2003.12.025

Koshikawa, M.K., Watanabe, M., Tamaoki, M., Ito, S., Takamatsu, T., Murata, T., Saito, T., & Hayashi, S. (2019). Comparison of 0.1 M Stable CsCl and 1 M NH_4NO_3 as an Extraction Reagent to Evaluate Cs-137 Mobility in Soils. Anal. Sci. Int. J. Jpn. Soc. Anal. Chem. 35, 153–158. https://doi.org/10.2116/analsci.18P325

Kowalenko, C.G. (1978). Nitrogen transformations and transport over 17 months in field fallow microplots using ^{15}N. Can. J. Soil Sci. 58, 69–76. https://doi.org/10.4141/cjss78-007

Kowalenko, C.G., & Ross, G.J. (1980). Studies on the dynamics of "recently" clay-fixed NH_4^+ using ^{15}N. Can. J. Soil Sci. 60, 61–70. https://doi.org/10.4141/cjss80-007

Kowalenko, C.G., & Yu, S. (1996). Solution, exchangeable and clay-fixed ammonium in south coast British Columbia soils. Can. J. Soil Sci. 76, 473–483. https://doi.org/10.4141/cjss96-059

Kowalska, J.B., Vögtli, M., Kierczak, J., Egli, M., & Waroszewski, J. (2022). Clay mineralogy fingerprinting of loess-mantled soils on different underlying substrates in the south-western Poland. Catena 210, 105874. https://doi.org/10.1016/j.catena.2021.105874

Kralova, M., Masscheleyn, P.H., & Patrick, W.H. (1992). Redox potential as an indicator of electron availability for microbial activity and nitrogen transformations in aerobic soil. Zentralblatt Für Mikrobiol. 147, 388–399. https://doi.org/10.1016/S0232-4393(11)80348-3

Krettek, A., & Rennert, T. (2021). Mobilisation of Al, Fe, and DOM from topsoil during simulated early Podzol development and subsequent DOM adsorption on model minerals. Sci. Rep. 11, 19741. https://doi.org/10.1038/s41598-021-99365-y

Kubo, K., Nemoto, K., Kobayashi, H., Kuriyama, Y., Harada, H., Matsunami, H., Eguchi, T., Kihou, N., Ota, T., Keitoku, S., et al. (2015). Analyses and countermeasures for decreasing radioactive caesium in buckwheat in areas affected by the nuclear accident in 2011. Field Crops Res. 170, 40–46. https://doi.org/10.1016/j.fcr.2014.10.001

Kubo, K., Hirayama, T., Fujimura, S., Eguchi, T., Nihei, N., Hamamoto, S., Takeuchi, M., Saito, T., Ota, T., & Shinano, T. (2018). Potassium behavior and clay mineral composition in the soil with low effectiveness of potassium application. Soil Sci. Plant Nutr. 64, 265–271. https://doi.org/10.1080/00380768.2017.1419830

Kumari, N., & Mohan, C. (2021). Basics of Clay Minerals and Their Characteristic Properties (IntechOpen)

Kurokawa, K., Nakao, A., Wakabayashi, S., Fujimura, S., Eguchi, T., Matsunami, H., & Yanai, J. (2020). Advanced approach for screening soil with a low radiocaesium transfer to brown rice in Fukushima based on exchangeable and nonexchangeable potassium. Sci. Total Environ. 743, 140458. https://doi.org/10.1016/j.scitotenv.2020.140458

Kurt, M., Güler, C., Alpaslan, M., & Akbulut, C. (2012). Determination of nitrate and nitrite origins in the soils and ground waters of the area between Mersin-Tarsus (Turkey) using geographic information systems. Carpathian J. Earth Environ. Sci. 7, 181–188.

Laeter, J.R. de, Böhlke, J.K., Bièvre, P.D., Hidaka, H., Peiser, H.S., Rosman, K.J.R., & Taylor, P.D.P. (2003). Atomic weights of the elements. Review 2000 (IUPAC Technical Report). Pure Appl. Chem. 75, 683–800. https://doi.org/10.1351/pac200375060683

Lasat, M., Fuhrmann, M., Ebbs, S., Cornish, J., & Kochian, L. (1998). Phytoremediation of a Radiocaesium-Contaminated Soil: Evaluation of Caesium-137 Bioaccumulation in the Shoots of Three Plant Species. J. Environ. Qual. 27, 165–169. https://doi.org/10.2134/jeq1998.00472425002700010023x

Lasat, M.M., Norvell, W.A., & Kochian, L.V. (1997). Potential for phytoextraction of ^{137}Cs from a contaminated soil. Plant Soil 195, 99–106.

Le Pevelen, D.D. (2010). Small Molecule X-Ray Crystallography, Theory and Workflow. In: Encyclopedia of Spectroscopy and Spectrometry (Second Edition), J.C. Lindon, ed. (Oxford: Academic Press), 2559–2576.

Lee, J., Park, S.-M., Jeon, E.-K., & Baek, K. (2017). Selective and irreversible adsorption mechanism of caesium on illite. Appl. Geochem. 85, 188–193. https://doi.org/10.1016/j.apgeochem.2017.05.019

Leggett, G.E., & Moodie, C.D. (1963). The Release of Fixed Ammonium from Soils by Sodium as Affected by Small Amounts of Potassium or Ammonium. Soil Sci. Soc. Am. J. 27, 645–648. https://doi.org/10.2136/sssaj1963.03615995002700060023x

Leggett, R.W., Williams, L.R., Melo, D.R., & Lipsztein, J.L. (2003). A physiologically based biokinetic model for caesium in the human body. Sci. Total Environ. 317, 235–255. https://doi.org/10.1016/S0048-9697(03)00333-4

Li, C., Yu, Y., Zhang, Q., Zhong, H., & Wang, S. (2020). Removal of Ammonium from Aqueous Solutions Using Zeolite Synthesized from Electrolytic Manganese Residue. Int. J. Chem. Eng. 2020. https://doi.org/10.1155/2020/8818455

Li, Z., Zhang, Y., & Li, Y. (2013). Zeolite as Slow Release Fertilizer on Spinach Yields and Quality in a Greenhouse Test. J. Plant Nutr. 36, 1496–1505. https://doi.org/10.1080/01904167.2013.790429

Liang, B.C., & MacKenzie, A.F. (1994). Fertilization rates and clay fixed ammonium in two Quebec soils. Plant Soil 163, 103–109. https://doi.org/10.1007/BF00033946

Linet, M.S., Freedman, D.M., Mohan, A.K., Doody, M.M., Ron, E., Mabuchi, K., Alexander, B.H., Sigurdson, A., & Hauptmann, M. (2005). Incidence of haematopoietic malignancies in US radiologic technologists. Occup. Environ. Med. 62, 861–867. https://doi.org/10.1136/oem.2005.020826

Loft, S., Tipping, E.W., Sanchez, A.L., & Dodd, B.A. (2002). Modelling the role of humic acid in radiocaesium distribution in a British upland peat soil. J. Environ. Radioact. 61, 133–147. https://doi.org/10.1016/s0265-931x(01)00118-7

Maathuis, F.J., & Sanders, D. (1997). Regulation of K^+ absorption in plant root cells by external K^+: interplay of different plasma membrane K^+ transporters. J. Exp. Bot. 48 Spec No, 451–458. https://doi.org/10.1093/jxb/48.Special_Issue.451

Maathuis, F.J.M., & Sanders, D. (1995). Contrasting roles in ion transport of two K^+-channel types in root cells of Arabidopsis thaliana. Planta 197, 456–464. https://doi.org/10.1007/BF00196667

Mahal, N.K., Osterholz, W.R., Miguez, F.E., Poffenbarger, H.J., Sawyer, J.E., Olk, D.C., Archontoulis, S.V., & Castellano, M.J. (2019). Nitrogen Fertilizer Suppresses Mineralization of Soil Organic Matter in Maize Agroecosystems. Front. Ecol. Evol. 7.

Malla, P.B. (1978). Vermiculite. In: Sedimentology, (Berlin, Heidelberg: Springer), 1265–1269.

Mamo, M., Taylor, R.W., & Shuford, J.W. (1993). Ammonium fixation by soil and pure clay minerals. Commun. Soil Sci. Plant Anal. 24, 1115–1126. https://doi.org/10.1080/00103629309368864

Manisalidis, I., Stavropoulou, E., Stavropoulos, A., & Bezirtzoglou, E. (2020). Environmental and Health Impacts of Air Pollution: A Review. Front. Public Health 8, 14. https://doi.org/10.3389/fpubh.2020.00014

Maracchi, G., Sirotenko, O., & Bindi, M. (2005). Impacts of Present and Future Climate Variability on Agriculture and Forestry in the Temperate Regions: Europe. In: Climatic Change, 117–135.

Marschner, H., Häussling, M., & George, E. (1991). Ammonium and nitrate uptake rates and rhizosphere pH in non-mycorrhizal roots of Norway spruce [Picea abies (L.) Karst.]. Trees 5, 14–21. https://doi.org/10.1007/BF00225330

Mather, A. (2009). Tectonic Setting and Landscape Development. In: The Physical Geography of the Mediterranean, J. Woodward, ed. (Oxford University Press), 0.

Mathieu, A., Kajino, M., Korsakissok, I., Périllat, R., Quélo, D., Quérel, A., Saunier, O., Sekiyama, T.T., Igarashi, Y., & Didier, D. (2018). Fukushima Daiichi–derived radionuclides in the atmosphere, transport and deposition in Japan: A review. Appl. Geochem. 91, 122–139. https://doi.org/10.1016/j.apgeochem.2018.01.002

Matsuoka, K., & Moritsuka, N. (2011). Dynamics of clay-fixed ammonium as a sink or source of exchangeable ammonium in a paddy soil. Soil Sci. Plant Nutr. 57, 751–758. https://doi.org/10.1080/00380768.2011.628271

Matus, F., Rumpel, C., Neculman, R., Panichini, M., & Mora, M.L. (2014). Soil carbon storage and stabilisation in andic soils: A review. Catena 120, 102–110. https://doi.org/10.1016/j.catena.2014.04.008

Mazloomi, F., & Jalali, M. (2017). Adsorption of ammonium from simulated wastewater by montmorillonite nanoclay and natural vermiculite: experimental study and simulation. Environ. Monit. Assess. 189, 415. https://doi.org/10.1007/s10661-017-6080-6

Mazloomi, F., & Jalali, M. (2019). Effects of vermiculite, nanoclay and zeolite on ammonium transport through saturated sandy loam soil: Column experiments and modeling approaches. Catena 176, 170–180. https://doi.org/10.1016/j.catena.2019.01.014

McDonough, W., Sun, S., Ringwood, A.E., Jagoutz, E., & Hofmann, A. (1992). Potassium, rubidium, and caesium in the Earth and Moon and the evolution of the mantle of the Earth. Geochim. Cosmochim. Acta 56, 1001–1012. https://doi.org/10.1016/0016-7037(92)90043-I

McTaggart, I.P., & Tsuruta, H. (2003). The influence of controlled release fertilisers and the form of applied fertiliser nitrogen on nitrous oxide emissions from an andosol. Nutr. Cycl. Agroecosystems 67, 47–54. https://doi.org/10.1023/A:1025108911676

Melnikov, P., & Zanoni, L.Z. (2010). Clinical Effects of Caesium Intake. Biol. Trace Elem. Res. 135, 1–9. https://doi.org/10.1007/s12011-009-8486-7

Mengel, K., Kirkby, E.A., Kosegarten, H., & Appel, T. (2001). The Soil as a Plant Nutrient Medium. In: Principles of Plant Nutrition, K. Mengel, E.A. Kirkby, H. Kosegarten, and T. Appel, eds. (Dordrecht: Springer Netherlands), 15–110.

Mettler, F.A.J., Gus'kova, A.K., & Gusev, I. (2007). Health effects in those with acute radiation sickness from the chernobyl accident. Health Phys. 93, 462–469. https://doi.org/10.1097/01.HP.0000278843.27969.74

Michel, H., Levent, D., Barci, V., Barci-Funel, G., & Hurel, C. (2008). Soil and sediment sample analysis for the sequential determination of natural and anthropogenic radionuclides. Talanta 74, 1527–1533. https://doi.org/10.1016/j.talanta.2007.09.030

Mihok, F., Macko, J., Oriňak, A., Oriňaková, R., Kovaľ, K., Sisáková, K., Petruš, O., & Kostecká, Z. (2020). Controlled nitrogen release fertilizer based on zeolite clinoptilolite: Study of preparation process and release properties using molecular dynamics. Curr. Res. Green Sustain. Chem. 3, 100030. https://doi.org/10.1016/j.crgsc.2020.100030

Mile, M., & Mitkova, T. (2012). Soil Moisture Retention Changes in Terms of Mineralogical Composition of Clays Phase.

Miller, A.J., & Cramer, M.D. (2005). Root Nitrogen Acquisition and Assimilation. Plant Soil 274, 1–36. https://doi.org/10.1007/s11104-004-0965-1

Ming, D.W., & Mumpton, F.A. (1989). Zeolites in Soils. In: Minerals in Soil Environments, (John Wiley & Sons, Ltd), 873–911.

Miranda, K.M., Espey, M.G., & Wink, D.A. (2001). A Rapid, Simple Spectrophotometric Method for Simultaneous Detection of Nitrate and Nitrite. Nitric Oxide 5, 62–71. https://doi.org/10.1006/niox.2000.0319

Mirsal, I.A. (2004). Major types of soil pollutants. In: Soil Pollution: Origin, Monitoring & Remediation, I.A. Mirsal, ed. (Berlin, Heidelberg: Springer), 61–71.

Missana, T., García-Gutiérrez, M., & Alonso, Ú. (2004). Kinetics and irreversibility of caesium and uranium sorption onto bentonite colloids in a deep granitic environment. Appl. Clay Sci. 26, 137–150. https://doi.org/10.1016/j.clay.2003.09.008

Missana, T., García-Gutiérrez, M., Benedicto, A., Ayora, C., & De-Pourcq, K. (2014). Modelling of Cs sorption in natural mixed-clays and the effects of ion competition. Appl. Geochem. 49, 95–102. https://doi.org/10.1016/j.apgeochem.2014.06.011

Mizota, C., & Matsuhisa, Y. (1985). Eolian Additions to Soils and Sediments of Japan. Soil Sci. Plant Nutr. 31, 369–382. https://doi.org/10.1080/00380768.1985.10557444

Mizota, C., Kusakabe, M., & Noto, M. (1990). Oxygen isotope composition of quartz in soils developed on late Quaternary volcanic ashes in Japan. Geoderma 46, 319–327. https://doi.org/10.1016/0016-7061(90)90022-2

Mohd Razali, N., & Yap, B. (2011). Power Comparisons of Shapiro-Wilk, Kolmogorov-Smirnov, Lilliefors and Anderson-Darling Tests. J. Stat. Model. Anal. 2, 21–33.

Mondal, M., Biswas, B., Garai, S., Sarkar, S., Hossain, A., Banerjee, H., Brahmachari, K., BANDYOPADHYAY, P., Maitra, S., Brestic, M., et al. (2021). Zeolites Enhance Soil Health, Crop Productivity and Environmental Safety. Agronomy 11. https://doi.org/10.3390/agronomy11030448

Montanarella, L., Pennock, D.J., McKenzie, N., Badraoui, M., Chude, V., Baptista, I., Mamo, T., Yemefack, M., Singh Aulakh, M., Yagi, K., et al. (2016a). World's soils are under threat. SOIL 2, 79–82. https://doi.org/10.5194/soil-2-79-2016

Montanarella, L., Pennock, D.J., McKenzie, N., Badraoui, M., Chude, V., Baptista, I., Mamo, T., Yemefack, M., Singh Aulakh, M., Yagi, K., et al. (2016b). World's soils are under threat. Soil 2, 79–82. https://doi.org/10.5194/soil-2-79-2016

Mori, Y., Yoshida, M., & Wada, S.-I. (2012). Effect of Soil Characteristics and Potassium Application Rate on the Plant-Absorbable Potassium Forms and Transport Mechanisms in Soil. J. Fac. Agric. Kyushu Univ. 57, 485–488.

Mukai, H., Hirose, A., Motai, S., Kikuchi, R., Tanoi, K., Nakanishi, T.M., Yaita, T., & Kogure, T. (2016a). Caesium adsorption/desorption behavior of clay minerals considering actual contamination conditions in Fukushima. Sci. Rep. 6, 21543. https://doi.org/10.1038/srep21543

Mukai, H., Motai, S., Yaita, T., & Kogure, T. (2016b). Identification of the actual caesium-adsorbing materials in the contaminated Fukushima soil. Appl. Clay Sci. 121–122, 188–193. https://doi.org/10.1016/j.clay.2015.12.030

Murota, K., Tanoi, K., Ochiai, A., Utsunomiya, S., & Saito, T. (2020). Desorption mechanisms of caesium from illite and vermiculite. Appl. Geochem. 123, 104768. https://doi.org/10.1016/j.apgeochem.2020.104768

Murray, H.H. (1991). Overview — clay mineral applications. Appl. Clay Sci. 5, 379–395. https://doi.org/10.1016/0169-1317(91)90014-Z

Nakamaru, Y., Ishikawa, N., Tagami, K., & Uchida, S. (2006). Role of soil organic matter in the mobility of radiocaesium in agricultural soils common in Japan. Colloids Surf. Physicochem. Eng. Asp. 306, 111–117. https://doi.org/10.1016/j.colsurfa.2007.01.014

Nakao, A., Thiry, Y., Funakawa, S., & Kosaki, T. (2008a). Characterization of the frayed edge site of micaceous minerals in soil clays influenced by different pedogenetic conditions in Japan and northern Thailand. Soil Sci. Plant Nutr. 54, 479–489. https://doi.org/10.1111/j.1747-0765.2008.00262.x

Nakao, A., Thiry, Y., Funakawa, S., & Kosaki, T. (2008b). Characterization of the frayed edge site of micaceous minerals in soil clays influenced by different pedogenetic conditions in Japan and northern Thailand. Soil Sci. Plant Nutr. 54, 479–489. https://doi.org/10.1111/j.1747-0765.2008.00262.x

Nakao, A., Funakawa, S., & Kosaki, T. (2009). Hydroxy-Al polymers block the frayed edge sites of illitic minerals in acid soils: Studies in southwestern Japan at various weathering stages. Eur. J. Soil Sci. 60, 127–138. https://doi.org/10.1111/j.1365-2389.2008.01097.x

Nakao, A., Takeda, A., Ogasawara, S., Yanai, J., Sano, O., & Ito, T. (2015). Relationships between Paddy Soil Radiocaesium Interception Potentials and Physicochemical Properties in Fukushima, Japan. J. Environ. Qual. 44, 780–788. https://doi.org/10.2134/jeq2014.10.0423

Nanzyo, M. (2010). Chemical properties of volcanic ash soils - Chemical models for their colloidal constituents and elemental concentrations, and plant availability of nutrient elements (JSSPN Awards). Jpn. J. Soil Sci. Plant Nutr. 81, 451–453. https://doi.org/10.20710/dojo.81.5_451

Nanzyo, M., & Kanno, H. (2018). Role of Inorganic Soil Constituents in Selected Topics. In: Inorganic Constituents in Soil: Basics and Visuals, M. Nanzyo, and H. Kanno, eds. (Singapore: Springer), 133–176.

National Research Council. (2014). Lessons Learned from the Fukushima Nuclear Accident for Improving Safety of U.S. Nuclear Plants (Washington, DC: The National Academies Press)

Ndayiragije, S., & Delvaux, B. (2004). Selective sorption of potassium in a weathering sequence of volcanic ash soils from Guadeloupe, French West Indies. Catena 56, 185–198. https://doi.org/10.1016/j.catena.2003.10.010

Neugschwandtner, R.W., Száková, J., Pachtrog, V., Tlustoš, P., Černý, J., Kulhánek, M., Kaul, H.-P., Euteneuer, P., Moitzi, G., & Wagentristl, H. (2020). Basic soil chemical properties after 15 years in a long-term tillage and crop rotation experiment. Int. Agrophysics 34, 133–140. https://doi.org/10.31545/intagr/114880

Nisbet, A.F., & Woodman, R.F. (2000). Soil-to-plant transfer factors for radiocaesium and radiostrontium in agricultural systems. Health Phys. 78, 279–288. https://doi.org/10.1097/00004032-200003000-00005

Nishida, M., & Sato, Y. (2016). Areal variation in the relationship between natural ^{15}N abundances of rice (Oryza sativa L.) and soil. Soil Sci. Plant Nutr. 62, 48–51. https://doi.org/10.1080/00380768.2015.1124024

Noble, A.D., Gillman, G.P., Nath, S., & Srivastava, R.J. (2001). Changes in the surface charge characteristics of degraded soils in the wet tropics through the addition of beneficiated bentonite. Soil Res. 39, 991–1001. https://doi.org/10.1071/sr00063

Nömmik, H. (1957). Fixation and Defixation of Ammonium in Soils. Acta Agric. Scand. 7, 395–436. https://doi.org/10.1080/00015125709434240

Nommik, H., & Vahtras, K. (1982). Retention and Fixation of Ammonium and Ammonia in Soils. In: Nitrogen in Agricultural Soils, (John Wiley & Sons, Ltd), 123–171.

Ogasawara, S., Nakao, A., & Yanai, J. (2013). Radiocaesium interception potential (RIP) of smectite and kaolin reference minerals containing illite (micaceous mineral) as impurity. Soil Sci. Plant Nutr. 59, 852–857. https://doi.org/10.1080/00380768.2013.862158

Ogasawara, S., Nakao, A., & Yanai, J. (2017). A stepwise change of frayed edge site content in biotite in response to the gradual release of potassium from the interlayers. Soil Sci. Plant Nutr. 63, 529–535. https://doi.org/10.1080/00380768.2017.1402660

Ogasawara, S., Eguchi, T., Nakao, A., Fujimura, S., Takahashi, Y., Matsunami, H., Tsukada, H., Yanai, J., & Shinano, T. (2019). Phytoavailability of 137Cs and stable Cs in soils from different parent materials in Fukushima, Japan. J. Environ. Radioact. 198, 117–125. https://doi.org/10.1016/j.jenvrad.2018.12.028

Ogasawara, S., Nakao, A., Eguchi, T., Ota, T., Matsunami, H., Yanai, J., & Shinano, T. (2020). The extractability of potassium and radiocaesium in soils developed from granite and sedimentary rock in Fukushima, Japan. J. Radioanal. Nucl. Chem. 323, 633–640. https://doi.org/10.1007/s10967-019-06971-2

Ohashi, F., Wada, S.-I., Suzuki, M., Maeda, M., & Tomura, S. (2002). Synthetic allophane from highconcentration solutions: nanoengineering of the porous solid. Clay Miner. 37, 451–456. https://doi.org/10.1180/0009855023730052

Ohnuki, T., & Kozai, N. (2013). Adsorption behavior of radioactive caesium by non-mica minerals. J. Nucl. Sci. Technol. 50, 369–375. https://doi.org/10.1080/00223131.2013.773164

Ohtsubo, M., Egashira, K., Tanaka, H., & Mishima, O. (2002). Clay Minerals and Geotechnical Index Properties of Marine Clays in East Asia. Mar. Georesources Geotechnol. 20, 223–235. https://doi.org/10.1080/03608860290051921

Okumura, M., Nakamura, H., & Machida, M. (2013). Mechanism of Strong Affinity of Clay Minerals to Radioactive Caesium: First-Principles Calculation Study for Adsorption of Caesium at Frayed Edge Sites in Muscovite. J. Phys. Soc. Jpn. 82, 033802. https://doi.org/10.7566/JPSJ.82.033802

Oldeman, L.R., Hakkeling, R.T.A., & Sombroek, W.G. (1991). World map of the status of human-induced soil degradation : an explanatory note, 2nd. rev. ed. (Wageningen: ISRIC)

Onodera, Y., Iwasaki, T., Ebina, T., Hayashi, H., Torii, K., Chatterjee, A., & Mimura, H. (1998). Effect of layer charge on fixation of caesium ions in smectites. J. Contam. Hydrol. 35, 131–140. https://doi.org/10.1016/S0169-7722(98)00121-1

Osborne, G.J. (1976). The significance of intercalary ammonium in representative surface and subsoils from southern New South Wales. Soil Res. 14, 381–388. https://doi.org/10.1071/sr9760381

Ott, I. (2013). Biodistribution of Metals and Metallodrugs. Compr. Inorg. Chem. II Second Ed. Elem. Appl. 3, 933–949. https://doi.org/10.1016/B978-0-08-097774-4.00337-5

Paasikallio, A. (1999). Effect of biotite, zeolite, heavy clay, bentonite and apatite on the uptake of radiocaesium by grass from peat soil. Plant Soil 206, 213–222. https://doi.org/10.1023/A:1004412512557

Paasikallio, A., & Sormunen-Cristian, R. (2002). Harvesting strategy and N fertilization influence ^{134}Cs uptake by forage plants (MTT Agrifood Research Finland)

Palanivell, P., Ahmed, O.H., Omar, L., & Abdul Majid, N.M. (2021). Nitrogen, Phosphorus, and Potassium Adsorption and Desorption Improvement and Soil Buffering Capacity Using Clinoptilolite Zeolite. Agronomy 11, 379. https://doi.org/10.3390/agronomy11020379

Parajuli, D., Suzuki, Y., Sato, M., Takahashi, A., Tanaka, H., & Kawamoto, T. (2016). Assessment of the measures for the extraction or fixation of radiocaesium in soil. Geoderma 267, 169–173. https://doi.org/10.1016/j.geoderma.2016.01.001

Pareek, N. (2017). Climate change impact on soils: adaptation and mitigation. MOJ Ecol. Environ. Sci. 2. https://doi.org/10.15406/mojes.2017.02.00026

Park, M., Choi, C.L., Kim, J.S., Lee, D.H., Kim, K.S., Heo, N.H., & Choi, J. (2003). Occlusion potential of zeolites for mixed and non-nitrate salts. Microporous Mesoporous Mater. 62, 1–7. https://doi.org/10.1016/S1387-1811(03)00333-0

Park, M., Kim, J.S., Choi, C.L., Kim, J.-E., Heo, N.H., Komarneni, S., & Choi, J. (2005). Characteristics of nitrogen release from synthetic zeolite Na-P1 occluding NH_4NO_3. J. Control. Release Off. J. Control. Release Soc. 106, 44–50. https://doi.org/10.1016/j.jconrel.2005.02.029

Park, S.-M., Alessi, D.S., & Baek, K. (2019a). Selective adsorption and irreversible fixation behavior of caesium onto 2:1 layered clay mineral: A mini review. J. Hazard. Mater. 369, 569–576. https://doi.org/10.1016/j.jhazmat.2019.02.061

Park, S.-M., Yang, J.-S., Tsang, D.C.W., Alessi, D.S., & Baek, K. (2019b). Enhanced irreversible fixation of caesium by wetting and drying cycles in soil. Environ. Geochem. Health 41, 149–157. https://doi.org/10.1007/s10653-018-0174-0

Passaglia, E., & Sheppard, R. (2001). The Crystal Chemistry of Zeolites. Rev. Mineral. Geochem. 45, 69–116. https://doi.org/10.2138/rmg.2001.45.2

Peel, M., Finlayson, B., & Mcmahon, T. (2007). Updated World Map of the Koppen-Geiger Climate Classification. Hydrol. Earth Syst. Sci. Discuss. 4. https://doi.org/10.5194/hess-11-1633-2007

Plant, J., Whittaker, A., Demetriades, A., De Vivo, B., & Lexa, J. (2005). The geological and tectonic framework of Europe. FOREGS Geochem. Atlas Eur. Part 1 Backgr. Inf. Methodol. Maps

Pöschl, M., & Nollet, L.M.L. (2006). Radionuclide Concentrations in Food and the Environment (Boca Raton: CRC Press)

Poudel, D.D., & West, L.T. (1999). Soil Development and Fertility Characteristics of a Volcanic Slope in Mindanao, the Philippines. Soil Sci. Soc. Am. J. 63, 1258–1273. https://doi.org/10.2136/sssaj1999.6351258x

Preston, D.L., Ron, E., Tokuoka, S., Funamoto, S., Nishi, N., Soda, M., Mabuchi, K., & Kodama, K. (2007). Solid Cancer Incidence in Atomic Bomb Survivors: 1958–1998. Radiat. Res. 168, 1–64. https://doi.org/10.1667/RR0763.1

de Preter, P. (1990). Radiocaesium retention in the aquatic, terrestrial and urban environment: a quantitative and unifying analysis. Dissertation. Katholieke Universiteit te Leuven

Qi, Z., Hampton, C.R., Shin, R., Barkla, B.J., White, P.J., & Schachtman, D.P. (2008). The high affinity K^+ transporter AtHAK5 plays a physiological role in planta at very low K^+ concentrations and provides a caesium uptake pathway in Arabidopsis. J. Exp. Bot. 59, 595–607. https://doi.org/10.1093/jxb/erm330

R Core Team (2021). R: A Language and Environment for Statistical Computing (Vienna, Austria: R Foundation for Statistical Computing)

Rääf, C.L., Falk, R., Lauridsen, B., Rahola, T., & Soogard-Hansen, J. (2006). Human metabolism of caesium (NKS-120) (Denmark)

Rai, H., & Kawabata, M. (2020). The Dynamics of Radio-Caesium in Soils and Mechanism of Caesium Uptake Into Higher Plants: Newly Elucidated Mechanism of Caesium Uptake Into Rice Plants. Front. Plant Sci. 11, 528. https://doi.org/10.3389/fpls.2020.00528

Rai, H., Yokoyama, S., Satoh-Nagasawa, N., Furukawa, J., Nomi, T., Ito, Y., Fujimura, S., Takahashi, H., Suzuki, R., Yousra, Elm., et al. (2017). Caesium Uptake by Rice Roots Largely Depends Upon a Single Gene, HAK1, Which Encodes a Potassium Transporter. Plant Cell Physiol. 58, 1486–1493. https://doi.org/10.1093/pcp/pcx094

Ranjbar, F., & Jalali, M. (2014). Empirical and mechanistic evaluation of NH_4^+ release kinetic in calcareous soils. Arch. Environ. Contam. Toxicol. 66, 606–615. https://doi.org/10.1007/s00244-014-9996-7

Rao, D.L.N., & Batra, L. (1983). Ammonia volatilization from applied nitrogen in alkali soils. Plant Soil 70, 219–228. https://doi.org/10.1007/BF02374782

Reed, G.F., Lynn, F., & Meade, B.D. (2002). Use of Coefficient of Variation in Assessing Variability of Quantitative Assays. Clin. Diagn. Lab. Immunol. 9, 1235–1239. https://doi.org/10.1128/CDLI.9.6.1235-1239.2002

Rich, C.I. (1968). Hydroxy Interlayers in Expansible Layer Silicates. Clays Clay Miner. 16, 15–30. https://doi.org/10.1346/CCMN.1968.0160104

Roberge, M.R. (1972). Some Factors Affecting the Soluble Ammonium-Nitrogen Content of a Black Spruce Humus. Soil Sci. Soc. Am. J. 36, 350–353. https://doi.org/10.2136/sssaj1972.03615995003600020039x

Robinson, D.A., Seaton, F., Sharps, K., Thomas, A., Parry Roberts, F., van der Ploeg, M., Jones, L., Stolte, J., Puig de la Bellacasa, M., Harrison, P., et al. (2017). Soil Resources, the Delivery of Ecosystem Services and Value. In: Oxford Research Encyclopedia of Environmental Science, (Oxford University Press),

Rodríguez-Eugenio, N., McLaughlin, M., & Pennock, D. (2018). Soil pollution: a hidden reality (FAO)

Roig, M., Vidal, M., Rauret, G., & Rigol, A. (2007). Prediction of Radionuclide Aging in Soils from the Chernobyl and Mediterranean Areas. J. Environ. Qual. 36, 943–952. https://doi.org/10.2134/jeq2006.0402

Rosoff, B., Cohn, S.H., & Spencer, H. (1963). I. Caesium-137 metabolism in men. Radiat. Res. 19, 643–654.

Ross, G.J., Phillips, P.A., & Culley, J.L.R. (1985). Transformation of vermiculite to pedogenic mica by fixation of potassium and ammonium in a six-year field manure application experiment. Can. J. Soil Sci. 65, 599–603. https://doi.org/10.4141/cjss85-064

Rouff, A.A., Phillips, B.L., Cochiara, S.G., & Nagy, K.L. (2012). The Effect of Dissolved Humic Acids on Aluminosilicate Formation and Associated Carbon Sequestration. Appl. Environ. Soil Sci. 2012, e430354. https://doi.org/10.1155/2012/430354

Sadhu, B., Sundararajan, M., & Bandyopadhyay, T. (2015). Water-Mediated Differential Binding of Strontium and Caesium Cations in Fulvic Acid. J. Phys. Chem. B 119, 10989–10997. https://doi.org/10.1021/acs.jpcb.5b01659

Saha, U.K., Taniguchi, S., & Sakurai, K. (2001). K^+/Ca^{2+} and NH_4^+ $/Ca^{2+}$ selectivity of hydroxyaluminum-interlayered vermiculite and montmorillonite: Contribution from regular and frayed edge exchange sites. Soil Sci. Plant Nutr. 47, 455–466. https://doi.org/10.1080/00380768.2001.10408410

Saisuga, M., & Matsuyama, N. (1998). Distribution of Allophanic Andosols and Non-allophanic Andosols in Japan. Tohoku J. Agric. Res. 48.

Saito, K., Tanihata, I., Fujiwara, M., Saito, T., Shimoura, S., Otsuka, T., Onda, Y., Hoshi, M., Ikeuchi, Y., Takahashi, F., et al. (2015). Detailed deposition density maps constructed by large-scale soil sampling for gamma-ray emitting radioactive nuclides from the Fukushima Dai-ichi Nuclear Power Plant accident. J. Environ. Radioact. 139, 308–319. https://doi.org/10.1016/j.jenvrad.2014.02.014

Salt, D.E., Blaylock, M., Kumar, N.P.B.A., Dushenkov, V., Ensley, B.D., Chet, I., & Raskin, I. (1995). Phytoremediation: A Novel Strategy for the Removal of Toxic Metals from the Environment Using Plants. Bio/Technology 13, 468–474. https://doi.org/10.1038/nbt0595-468

Salters, V.J.M. (1998). Elements: High field strength. In: Geochemistry, (Dordrecht: Springer Netherlands), 209–210.

Sanchez, A.L., Wright, S.M., Smolders, E., Naylor, C., Stevens, P.A., Kennedy, V.H., Dodd, B.A., Singleton, D.L., & Barnett, C.L. (1999). High Plant Uptake of Radiocaesium from Organic Soils Due to Cs Mobility and Low Soil K Content. Environ. Sci. Technol. 33, 2752–2757. https://doi.org/10.1021/es990058h

Sawhney, B.L. (1964). Sorption and Fixation of Microquantities of Caesium by Clay Minerals: Effect of Saturating Cations. Soil Sci. Soc. Am. J. 28, 183–186. https://doi.org/10.2136/sssaj1964.03615995002800020017x

Sawhney, B.L. (1972). Selective Sorption and Fixation of Cations by Clay Minerals: A Review. Clays Clay Miner. 20, 93–100. https://doi.org/10.1346/CCMN.1972.0200208

Sawilowsky, S. (2009). New Effect Size Rules of Thumb. J. Mod. Appl. Stat. Methods 8, 597–599. https://doi.org/10.22237/jmasm/1257035100

Schaetzl, R.J., & Anderson, S. (2005). Soils: Genesis and Geomorphology (Cambridge University Press)

Scherer, H.W. (1982). Fixed NH4-N in relation to EUF-extractable K. Plant Soil 64, 67–71. https://doi.org/10.1007/BF02375160

Scherer, H.W. (1984). Beziehung zwischen dem Stickstoff-Entzug der Pflanzen und der Abnahme von spezifisch gebundenem NH4-N im Boden. Z. Für Pflanzenernähr. Bodenkd. 147, 29–36. https://doi.org/10.1002/jpln.19841470105

Scherer, H.W. (1987). Einfluß von Bewuchs auf die Mobilisierung von spezifisch gebundenem NH_4^+ im Boden. J. Agron. Crop Sci. 158, 114–120. https://doi.org/10.1111/j.1439-037X.1987.tb01154.x

Scherer, H.W. (1993). Dynamics and availability of the non-exchangeable NH_4^+-N — a review. Eur. J. Agron. 2, 149–160. https://doi.org/10.1016/S1161-0301(14)80124-X

Schmidt, C.S., Richardson, D.J., & Baggs, E.M. (2011). Constraining the conditions conducive to dissimilatory nitrate reduction to ammonium in temperate arable soils. Soil Biol. Biochem. 43, 1607–1611. https://doi.org/10.1016/j.soilbio.2011.02.015

Schnetger, B., & Lehners, C. (2014). Determination of nitrate plus nitrite in small volume marine water samples using vanadium(III)chloride as a reduction agent. Mar. Chem. 160. https://doi.org/10.1016/j.marchem.2014.01.010

Schroth, G., J, L., & Barrios, E. (2003). Chapter 5 - Soil nutrient availability and acidity. In: Trees, Crops and Soil Fertility: Concepts and Research Methods, G. Schroth, and F.L. Sinclair, eds. (CABI),

Schulze, D.G. (2005). Clay minerals. In: Encyclopedia of Soils in the Environment, D. Hillel, ed. (Oxford: Elsevier), 246–254.

Scott, A.D., & Smith, S.J. (1966). Susceptibility of Interlayer Potassium in Micas to Exchange with Sodium. Clays Clay Miner. 14, 69–81. https://doi.org/10.1346/CCMN.1966.0140106

Scott, A.D., Edwards, A.P., & Bremner, J.M. (1960). Removal of Fixed Ammonium from Clay Minerals by Cation Exchange Resins. Nature 185, 792–792. https://doi.org/10.1038/185792a0

Seaman, J.C., Meehan, T., & Bertsch, P.M. (2001). Immobilization of caesium-137 and uranium in contaminated sediments using soil amendments. J. Environ. Qual. 30, 1206–1213. https://doi.org/10.2134/jeq2001.3041206x

Sepaskhah, A.R., Yousefi, F., Sepaskhah, A.R., & Yousefi, F. (2007). Effects of zeolite application on nitrate and ammonium retention of a loamy soil under saturated conditions. Soil Res. 45, 368–373. https://doi.org/10.1071/SR06069

Sethi, S., & Gupta, P. (2020). Soil Contamination: A Menace to Life. In: Soil Contamination, M.L. Larramendy, and S. Soloneski, eds. (Rijeka: IntechOpen), Ch. 15.

Shakhtarin, V.V., Tsyb, A.F., Stepanenko, V.F., Orlov, M.Y., Kopecky, K.J., & Davis, S. (2003). Iodine deficiency, radiation dose, and the risk of thyroid cancer among children and adolescents in the Bryansk region of Russia following the Chernobyl power station accident. Int. J. Epidemiol. 32, 584–591. https://doi.org/10.1093/ije/dyg205

Shaw, G., Hewamanna, R., Lillywhite, J., & Bell, J.N.B. (1992). Radiocaesium uptake and translocation in wheat with reference to the transfer factor concept and ion competition effects. J. Environ. Radioact. 16, 167–180. https://doi.org/10.1016/0265-931X(92)90014-K

Shenber, M.A., & Johanson, K.J. (1992). Influence of zeolite on the availability of radiocaesium in soil to plants. Sci. Total Environ. https://doi.org/10.1016/0048-9697(92)90007-f

Shibata, K., & Adachi, M. (1974). RbSr whole-rock ages of Precambrian metamorphic rocks in the Kamiaso conglomerate from central Japan. Earth Planet. Sci. Lett. 21, 277–287. https://doi.org/10.1016/0012-821X(74)90162-9

Shinzato, M.C., Wu, L.F., Mariano, T.O., Freitas, J.G., & Martins, T.S. (2020). Mineral sorbents for ammonium recycling from industry to agriculture. Environ. Sci. Pollut. Res. Int. 27, 13599–13616. https://doi.org/10.1007/s11356-020-07873-7

Shirai, O., Ohnuki, T., Kitazumi, Y., & Kano, K. (2013). Transport of Caesium Ion Across a Bilayer Lipid Membrane and Its Facilitation in the Presence of Iodide Ion. Electroanalysis 25, 1823–1826. https://doi.org/10.1002/elan.201300148

Shoji, S., & Takahashi, T. (2002). Environmental and agricultural significance of volcanic ash soils. Glob. Environ. Res. 6.

Shoji, S., Nanzyo, M., & Dahlgren, R. (1993). Chapter 8 - Productivity and Utilization of Volcanic Ash Soils. In: Developments in Soil Science, S. Shoji, M. Nanzyo, and R. Dahlgren, eds. (Elsevier), 209–251.

Sikalidis, C.A., Misaelides, P., & Alexiades, C.A. (1988). Caesium selectivity and fixation of vermiculite in the presence of competing cations. Environ. Pollut. 52, 67–79. https://doi.org/10.1016/0269-7491(88)90108-X

Silva, J.A., & Bremner, J.M. (1966). Determination and Isotope-Ratio Analysis of Different Forms of Nitrogen in Soils: 5. Fixed Ammonium. Soil Sci. Soc. Am. J. 30, 587–594. https://doi.org/10.2136/sssaj1966.03615995003000050017x

Singh, J.S., Singh, S.P., & Gupta, S.R. (2014). Ecology, Environmental Science & Conservation (S. Chand Publishing)

Skiba, M. (2007). Clay mineral formation during podzolization in an alpine environment of the Tatra Mountains, Poland. Clays Clay Miner. 55, 618–634. https://doi.org/10.1346/CCMN.2007.0550609

Smith, J.H. (1964). Relationships Between Soil Cation-Exchange Capacity and the Toxicity of Ammonia to the Nitrification Process. Soil Sci. Soc. Am. J. 28, 640–644. https://doi.org/10.2136/sssaj1964.03615995002800050019x

Smolders, E., Van den Brande, K., & Merckx, R. (1997). Concentrations of ^{137}Cs and K in Soil Solution Predict the Plant Availability of ^{137}Cs in Soils. Environ. Sci. Technol. 31, 3432–3438. https://doi.org/10.1021/es970113r

Sokolova, T.A., Zaidel'man, F.R., & Ginzburg, T.M. (2010). Clay minerals in Chernozem-like soils of mesodepressions in the northern forest-steppe of European Russia. Eurasian Soil Sci. 43, 76–84. https://doi.org/10.1134/S1064229310010102

Sonzogni, A.A. (2004). Nuclear Data sheets 103, 1 (NNDC)

Spaargaren, O.C., & Deckers, J. (1998). The World Reference Base for Soil Resources. In: Soils of Tropical Forest Ecosystems, A. Schulte, and D. Ruhiyat, eds. (Berlin, Heidelberg: Springer), 21–28.

Sparks, D.L. (2003). 6 - Ion Exchange Processes. In: Environmental Soil Chemistry (Second Edition), D.L. Sparks, ed. (Burlington: Academic Press), 187–205.

Stautz, J., Hellmich, Y., Fuss, M.F., Silberberg, J.M., Devlin, J.R., Stockbridge, R.B., & Hänelt, I. (2021). Molecular Mechanisms for Bacterial Potassium Homeostasis. J. Mol. Biol. 433, 166968. https://doi.org/10.1016/j.jmb.2021.166968

Steffens, D., & Sparks, D.L. (1997). Kinetics of Nonexchangeable Ammonium Release from Soils. Soil Sci. Soc. Am. J. 61, 455–462. https://doi.org/10.2136/sssaj1997.03615995006100020012x

Steffens, D., & Sparks, D.L. (1999). Effect of residence time on the kinetics of nonexchangeable ammonium release from illite and vermiculite. J. Plant Nutr. Soil Sci. 162, 599–605. https://doi.org/10.1002/(SICI)1522-2624(199912)162:6<599::AID-JPLN599>3.0.CO;2-Y

Stein, L.Y., & Klotz, M.G. (2016). The nitrogen cycle. Curr. Biol. 26, 94–98. https://doi.org/10.1016/j.cub.2015.12.021

Steinhauser, G., Brandl, A., & Johnson, T.E. (2014). Comparison of the Chernobyl and Fukushima nuclear accidents: A review of the environmental impacts. Sci. Total Environ. 470–471, 800–817. https://doi.org/10.1016/j.scitotenv.2013.10.029

Subba Rao, A., Jha, P., Meena, B.P., Biswas, A.K., Lakaria, B.L., & Patra, A.K. (2017). 5 - Nitrogen Processes in Agroecosystems of India. In: The Indian Nitrogen Assessment, Y.P. Abrol, T.K. Adhya, V.P. Aneja, N. Raghuram, H. Pathak, U. Kulshrestha, C. Sharma, and B. Singh, eds. (Elsevier), 59–76.

Sugimori, H., Iwatsuki, T., & Murakami, T. (2008). Chlorite and biotite weathering, Fe^{2+}-rich corrensite formation, and Fe behavior under low PO_2 conditions and their implication for Precambrian weathering. Am. Mineral. - AMER Miner. 93, 1080–1089. https://doi.org/10.2138/am.2008.2663

Sugiura, Y., Ozawa, H., Umemura, M., & Takenaka, C. (2016). Soil amendments effects on radiocaesium translocation in forest soils. J. Environ. Radioact. 165, 286–295. https://doi.org/10.1016/j.jenvrad.2016.10.012

Sun, X., Kobayashi, S., Tokue, A., Itabashi, H., & Mori, M. (2019). Enhanced radiocaesium uptake by rice with fermented bark and ammonium salt amendments. J. Environ. Radioact. 202, 59–65. https://doi.org/10.1016/j.jenvrad.2019.02.008

Suryanarayana, C., & Norton, M.G. (1998). X-Rays and Diffraction. In: X-Ray Diffraction: A Practical Approach, C. Suryanarayana, and M.G. Norton, eds. (Boston, MA: Springer US), 3–19.

Synolakis, C., & Kânoğlu, U. (2015). The Fukushima accident was preventable. Philos. Trans. R. Soc. Math. Phys. Eng. Sci. 373, 20140379. https://doi.org/10.1098/rsta.2014.0379

Taberlet, P., Bonin, A., Zinger, L., & Coissac, E. (2018). Environmental DNA: For Biodiversity Research and Monitoring (Oxford University Press)

Tagiri, M., Dunkley, D.J., Adachi, T., Hiroi, Y., & Fanning, C.M. (2011). SHRIMP dating of magmatism in the Hitachi metamorphic terrane, Abukuma Belt, Japan: Evidence for a Cambrian volcanic arc. Isl. Arc 20, 259–279. https://doi.org/10.1111/j.1440-1738.2011.00764.x

Takahashi, T., Nakano, K., Nira, R., Kumagai, E., Nishida, M., & Namikawa, M. (2020). Conversion of soil particle size distribution and texture classification from ISSS system to FAO/USDA system in Japanese paddy soils. Soil Sci. Plant Nutr. 66, 407–414. https://doi.org/10.1080/00380768.2020.1763143

Takeda, A., Tsukada, H., Nakao, A., Takaku, Y., & Hisamatsu, S. (2013). Time-dependent changes of phytoavailability of Cs added to allophanic Andosols in laboratory cultivations and extraction tests. J. Environ. Radioact. 122, 29–36. https://doi.org/10.1016/j.jenvrad.2013.02.005

Takeda, A., Tsukada, H., Yamaguchi, N., Takeuchi, M., Sato, M., Nakao, A., & Hisamatsu, S. (2014). Relationship between the radiocaesium interception potential and the transfer of radiocaesium from soil to soybean cultivated in 2011 in Fukushima Prefecture, Japan. J. Environ. Radioact. 137, 119–124. https://doi.org/10.1016/j.jenvrad.2014.06.022

Tamura, K., Miura, H., Kaneko, S., Sano, T., & Kubotera, H. (2021). Soil-Forming Factors. In: The Soils of Japan, R. Hatano, H. Shinjo, and Y. Takata, eds. (Singapore: Springer), 13–51.

Tanaka, H. (2007). Geotechnical properties of Hachirogata Clay. Characterisation Eng. Prop. Nat. Soils 3, 1831–1852. https://doi.org/10.1201/NOE0415426916.ch6

Tarsitano, D., Young, S., & Crout, N. (2011). Evaluating and reducing a model of radiocaesium soil-plant uptake. J. Environ. Radioact. 102, 262–269. https://doi.org/10.1016/j.jenvrad.2010.11.017

Thompson, T.L., & Blackmer, A.M. (1993). Fixation and release of ^{15}N-labeled ammonium during soil drying. Commun. Soil Sci. Plant Anal. 24, 613–622. https://doi.org/10.1080/00103629309368827

Thornton, S.F., Lerner, D.N., & Tellam, J.H. (2001). Attenuation of landfill leachate by clay liner materials in laboratory columns: 2. Behaviour of inorganic contaminants. Waste Manag. Res. J. Int. Solid Wastes Public Clean. Assoc. ISWA 19, 70–88. https://doi.org/10.1177/0734242X0101900108

Tong, Y.-A., Emteryd, O., Grip, H., & Lu, D.-Q. (2004). Soil NH_4^+ fixation and fertilizer N recovery as affected by soil moisture and fertilizer application methods. Pedosphere 14, 247–252.

Tóth, G., Montanarella, L., Stolbovoy, V., Mate, F., Bodis, K., Jones, A., Panagos, P., & Van Liedekerke, M. (2008). Soils of the European Union. (LU: OPOCE)

Trnka, M., Kersebaum, K., Eitzinger, J., Hayes, M., Hlavinka, P., Svoboda, M., Dubrovský, M., Semeradova, D., Wardlow, B., Pokorný, E., et al. (2013). Consequences of climate change for the soil climate in Central Europe and the central plains of the United States. Clim. Change 120. https://doi.org/10.1007/s10584-013-0786-4

Tsukada, H., Hasegawa, H., Hisamatsu, S., & Yamasaki, S. (2002). Transfer of ^{137}Cs and stable Cs from paddy soil to polished rice in Aomori, Japan. J. Environ. Radioact. 59, 351–363. https://doi.org/10.1016/S0265-931X(01)00083-2

Tsukada, H., Takeda, A., Hisamatsu, S., & Inaba, J. (2008). Concentration and specific activity of fallout ^{137}Cs in extracted and particle-size fractions of cultivated soils. J. Environ. Radioact. 99, 875–881. https://doi.org/10.1016/j.jenvrad.2007.11.014

Tsuru, T., Park, J.-O., Takahashi, N., Kodaira, S., Kido, Y., Kaneda, Y., & Kono, Y. (2000). Tectonic features of the Japan Trench convergent margin off Sanriku, northeastern Japan, revealed by multichannel seismic reflection data. J. Geophys. Res. Solid Earth 105, 16403–16413. https://doi.org/10.1029/2000JB900132

Uematsu, S., Smolders, E., Sweeck, L., Wannijn, J., Van Hees, M., & Vandenhove, H. (2015). Predicting radiocaesium sorption characteristics with soil chemical properties for Japanese soils. Sci. Total Environ. 524–525, 148–156. https://doi.org/10.1016/j.scitotenv.2015.04.028

Uematsu, S., Vandenhove, H., Sweeck, L., Van Hees, M., Wannijn, J., & Smolders, E. (2016). Variability of the soil-to-plant radiocaesium transfer factor for Japanese soils predicted with soil and plant properties. J. Environ. Radioact. 153, 51–60. https://doi.org/10.1016/j.jenvrad.2015.12.012

United Nations Scientific Committee on the Effects of Atomic Radiation (2011). Sources and Effects of Ionizing Radiation, UNSCEAR 2008 Report. (United Nations Publication)

United Nations Scientific Committee on the Effects of Atomic Radiation (2014). Sources, Effects and Risks of Ionizing Radiation, Unscear 2013 Report Levels and Effects of Radiation Exposure Due to the Nuclear Accident After the 2011 Great East-japan Earthquake (United Nations Publication)

Urakawa, R., Ohte, N., Shibata, H., Isobe, K., Tateno, R., Oda, T., Hishi, T., Fukushima, K., Inagaki, Y., Hirai, K., et al. (2016). Factors contributing to soil nitrogen mineralization and nitrification rates of forest soils in the Japanese archipelago. For. Ecol. Manag. 361, 382–396. https://doi.org/10.1016/j.foreco.2015.11.033

Vaičiukynienė, D., Mikelionienė, A., Baltušnikas, A., Kantautas, A., & Radzevičius, A. (2020). Removal of ammonium ion from aqueous solutions by using unmodified and H_2O_2-modified zeolitic waste. Sci. Rep. 10, 352. https://doi.org/10.1038/s41598-019-55906-0

Valcke, E., Engels, B., & Cremers, A. (1997a). The use of zeolites as amendments in radiocaesium- and radiostrontium-contaminated soils: A soil-chemical approach. Part I: Cs-K exchange in clinoptilolite and mordenite. Zeolites 18, 205–211. https://doi.org/10.1016/S0144-2449(96)00146-7

Valcke, E., Vidal, M., Cremers, A., Ivanov, J., & Perepelyatnikov, G. (1997b). The use of zeolites as amendments in radiocaesium- and radiostrontium-contaminated soils: A soil-chemical approach. Part III: A soil-chemical test to predict the potential effectiveness of zeolite amendments. Zeolites 18, 218–224. https://doi.org/10.1016/S0144-2449(96)00148-0

Valcke, E., Elsen, A., & Cremers, A. (1997c). The use of zeolites as amendments in radiocaesium- and radiostrontium-contaminated soils: A soil-chemical approach. Part IV: A potted soil experiment to verify laboratory-based predictions. Zeolites 18, 225–231. https://doi.org/10.1016/S0144-2449(96)00149-2

Valentin, J. (2003). Relative biological effectiveness (RBE), quality factor (Q), and radiation weighting factor (wR): ICRP Publication 92. Ann. ICRP 33, 1–121. https://doi.org/10.1016/S0146-6453(03)00024-1

Vandebroek, L., Van Hees, M., Delvaux, B., Spaargaren, O., & Thiry, Y. (2012). Relevance of Radiocaesium Interception Potential (RIP) on a worldwide scale to assess soil vulnerability to ^{137}Cs contamination. J. Environ. Radioact. 104, 87–93. https://doi.org/10.1016/j.jenvrad.2011.09.002

Vandenhove, H., Smolders, E., & Cremers, A. (2003). Potassium bentonites reduce radiocaesium availability to plants. Eur. J. Soil Sci. 54, 91–102. https://doi.org/10.1046/j.1365-2389.2003.00509.x

Vargas, R. (2017). Threats to soils: Global trends and perspectives: A Contribution from the Intergovernmental Technical Panel on Soils , Global Soil Partnership Food and Agriculture Organization of the United Nations

Velde, B., & Barré, P. (2009). Introduction: Objectives and Background. In: Soils, Plants and Clay Minerals (Berlin, Heidelberg: Springer)

Vermeulen, K., Van Bockstaele, D.R., & Berneman, Z.N. (2003). The cell cycle: a review of regulation, deregulation and therapeutic targets in cancer. Cell Prolif. 36, 131–149. https://doi.org/10.1046/j.1365-2184.2003.00266.x

Wada, K. (1958). Adsorption of alkali chloride and ammonium halide on halloysite. Soil Sci. Plant Nutr. 4, 137–144. https://doi.org/10.1080/00380768.1958.10430876

Wada, K. (1959). Oriented penetration of ionic compounds between the silicate layers of halloysite. Am. Mineral. 44, 153–165.

Wada, K. (1985). The Distinctive Properties of Andosols. In: Advances in Soil Science, B.A. Stewart, ed. (New York, NY: Springer), 173–229.

Wada, K., & Ataka, H. (1958). The ion uptake mechanism of allophane. Soil Sci. Plant Nutr. 4, 12–18. https://doi.org/10.1080/00380768.1958.10431933

Wada, K., & Okamura, Y. (1980). Electric Charge Characteristics of Ando a, and Buried a, Horizon Soils. J. Soil Sci. 31, 307–314. https://doi.org/10.1111/j.1365-2389.1980.tb02083.x

Waegeneers, N., Smolders, E., & Merckx, R. (1999). A Statistical Approach for Estimating the Radiocaesium Interception Potential of Soils. J. Environ. Qual. 28, 1005–1011. https://doi.org/10.2134/jeq1999.00472425002800030034x

Wakabayashi, S., Itoh, S., & Takahashi, S. (2017). Influence of flooding on exchangeability and release of stable and radioactive caesium in contaminated paddy soil. Soil Sci. Plant Nutr. 63, 110–118. https://doi.org/10.1080/00380768.2017.1294466

Wakeford, R. (2009). Radiation in the workplace-a review of studies of the risks of occupational exposure to ionising radiation. J. Radiol. Prot. Off. J. Soc. Radiol. Prot. 29, A61-79. https://doi.org/10.1088/0952-4746/29/2A/S05

Wakeford, R. (2018). UN Scientific Committee launches a new evaluation of thyroid cancer data in regions affected by the Chernobyl accident. J. Radiol. Prot. 38, 876–877. https://doi.org/10.1088/1361-6498/aac2fa

Wakita, K. (2013). Geology and tectonics of Japanese islands: A review – The key to understanding the geology of Asia. J. Asian Earth Sci. 72, 75–87. https://doi.org/10.1016/j.jseaes.2012.04.014

Wauters, J., Sweeck, L., Valcke, E., Elsen, A., & Cremers, A. (1994). Availability of radiocaesium in soils: a new methodology. Sci. Total Environ. 157, 239–248. https://doi.org/10.1016/0048-9697(94)90585-1

Wauters, J., Elsen, A., Cremers, A., Konoplev, A.V., Bulgakov, A.A., & Comans, R.N.J. (1996a). Prediction of solid/liquid distribution coefficients of radiocaesium in soils and sediments. Part one: a simplified procedure for the solid phase characterisation. Appl. Geochem. 11, 589–594. https://doi.org/10.1016/0883-2927(96)00027-3

Wauters, J., Vidal, M., Elsen, A., & Cremers, A. (1996c). Prediction of solid/liquid distribution coefficients of radiocaesium in soils and sediments. Part two: a new procedure for solid phase speciation of radiocaesium. Appl. Geochem. 11, 595–599. https://doi.org/10.1016/0883-2927(96)00028-5

Wegner, L.H., & Raschke, K. (1994). Ion Channels in the Xylem Parenchyma of Barley Roots (A Procedure to Isolate Protoplasts from This Tissue and a Patch-Clamp Exploration of Salt Passageways into Xylem Vessels. Plant Physiol. 105, 799–813. https://doi.org/10.1104/pp.105.3.799

Wen, Y., Mao, Y., Kang, Z., & Luo, Q. (2019). Application of an ammonium ion-selective electrode for the real-time measurement of ammonia nitrogen based on pH and temperature compensation. Measurement 137, 98–101. https://doi.org/10.1016/j.measurement.2019.01.031

White, P.J., & Broadley, M.R. (2000). Mechanisms of caesium uptake by plants. New Phytol. 147, 241–256. https://doi.org/10.1046/j.1469-8137.2000.00704.x

White, P.J., & Tester, M.A. (1992). Potassium channels from the plasma membrane of rye roots characterized following incorporation into planar lipid bilayers. Planta 186, 188–202. https://doi.org/10.1007/BF00196248

Widiastuti, N., Wu, H., Ang, H.M., & Zhang, D. (2011). Removal of ammonium from greywater using natural zeolite. Desalination 277, 15–23. https://doi.org/10.1016/j.desal.2011.03.030

Wild, A. (1993). Soils and the Environment (Cambridge: Cambridge University Press)

Wilschefski, S.C., & Baxter, M.R. (2019). Inductively Coupled Plasma Mass Spectrometry: Introduction to Analytical Aspects. Clin. Biochem. Rev. 40, 115. https://doi.org/10.33176/AACB-19-00024

de Winter, J. (2013). Using the Student’s t-test with extremely small sample sizes. Pract. Assess. Res. Eval. 18.

Wolt, J.D. (1994). Soil solution chemistry: applications to environmental science and agriculture (Wiley)

Worden, R. (2005). Analytical Methods | Geochemical Analysis (Including X-ray). In: Encyclopedia of Geology, 54–76.

World Refernce Book (2006). World reference base for soil resources 2006 : a framework for international classification, correlation and communication (Rome: FAO)

World Refernce Book (2014). WRB World Reference Base for Soil Resources 2014: International Soil Classification for Naming Soils and Creating Legends for Soil Maps (Rome: FAO)

Wu, H., Hu, J., Shaaban, M., Xu, P., Zhao, J., & Hu, R. (2021). The effect of dolomite amendment on soil organic carbon mineralization is determined by the dolomite size. Ecol. Process. 10, 8. https://doi.org/10.1186/s13717-020-00278-x

Yamaguchi, N., Hikono, A., & Saito, T. (2019). Effects of zeolite and vermiculite addition on exchangeable radiocaesium in soil with accelerated ageing. J. Environ. Radioact. 203, 18–24. https://doi.org/10.1016/j.jenvrad.2019.02.011

Yanyan, S. (2008). Testing the assumptions of analysis of variance. In: Best Practices in Quantitative Methods, J.W. Osborne, ed. (Thousand Oaks, Calif: Sage Publications), 324–340.

Yin, K., Hanlie, H., Churchman, J., Li, Z., Han, W., & Wang, C. (2014). Characterisation of the hydroxy-interlayered vermiculite from the weathering of illite in Jiujiang red earth sediments. Soil Res. 52, 554. https://doi.org/10.1071/SR14014

Yoshida, M. (1992). Effects of dry grinding on P retention properties of andosols. Soil Sci. Plant Nutr. 38, 637–645. https://doi.org/10.1080/00380768.1992.10416693

Yoshida, S., Muramatsu, Y., Dvornik, A.M., & Zhuchenko, T.A. (2004). Equilibrium of radiocaesium with stable caesium within the biological cycle of contaminated forest ecosystems. J. Environ. Radioact. 75, 301–313. https://doi.org/10.1016/j.jenvrad.2003.12.008

Zhang, A., Pan, L., Zhang, H., Liu, S., Ye, Y., Xia, M.-S., & Chen, X.-G. (2012). Effects of acid treatment on the physic-chemical and pore characteristics of halloysite. Colloids Surf. -Physicochem. Eng. Asp. 396, 182–188. https://doi.org/10.1016/j.colsurfa.2011.12.067

Zhang, X., Bai, W., Gilliam, F.S., Wang, Q., Han, X., & Li, L. (2011). Effects of in situ freezing on soil net nitrogen mineralization and net nitrification in fertilised grassland of northern China. Grass Forage Sci. 66, 391–401. https://doi.org/10.1111/j.1365-2494.2011.00789.x

Zhao, D., Cleare, K., Oliver, C., Ingram, C., Cook, D., Szostak, R., & Kevan, L. (1998). Characteristics of the synthetic heulandite-clinoptilolite family of zeolites. Microporous Mesoporous Mater. 21, 371–379. https://doi.org/10.1016/S1387-1811(98)00131-0

Zhu, Y., & Smolders, E. (2000). Plant uptake of radiocaesium: a review of mechanisms, regulation and application. J. Exp. Bot. 51, 1635–1645. https://doi.org/10.1093/jexbot/51.351.1635

Zhu, Y.-G., Shaw, G., Nisbet, A.F., & Wilkins, B.T. (1999). Effects of External Potassium Supply on Compartmentation and Flux Characteristics of Radiocaesium in Intact Spring Wheat Roots. Ann. Bot. 84, 639–644. https://doi.org/10.1006/anbo.1999.0962

Zielinski, J.M., Shilnikova, N.S., & Krewski, D. (2008). Canadian National Dose Registry of radiation workers: overview of research from 1951 through 2007. Int. J. Occup. Med. Environ. Health 21, 269–275. https://doi.org/10.2478/v10001-008-0037-5

7. Appendices

Appendix A

```
##Uploading dataset

library(readxl)
tTest_Data <- read_excel(“Documents/~tTest_Data.xlsx)
str(tTest_Data)
tibble [118 × 7] (S3: tbl_df/tbl/data.frame)
 $ Day          : chr [1:118] "1" "1" "1" "1" ...
 $ Fertilisation: chr [1:118] "0" "0" "0" "1" ...
 $ Cesium       : num [1:118] 0.308 0.135 0.301 0.556 0.586 ...
 $ Ammonium     : num [1:118] 0 0 0 2.52 2.99 ...
 $ Potassium     : num [1:118] 0 0 0 0 0 ...
 $ Replicate    : chr [1:118] "-1" "-1" "-1" "+1" ...
 $ Soil         : chr [1:118] "Chernozem" "Chernozem" "Chernozem" "Chernozem" ...

## Performance of t-tests for solution NH4+ concentration of the unamended soils

##Testing for Normality example

library(tidyverse)

shapiro.test(tTest_Data %>% filter(Day == 1, Soil == "Allophanic Andosol",
Fertilisation == "No") %>% pull(Ammonium))

Shapiro-Wilk normality test

W = 0.94372, p-value = 0.5426

##Testing for effect size if data was not normally distributed example

library(rstatix)

CohensDData <- tTest_Data %>% filter(Day == 22, Soil == "Vermiculitic Cambisol")

cohens_d(CohensDData, Ammonium ~ Fertilisation, paired = FALSE)

  .y.      group1 group2 effsize    n1    n2 magnitude
* <chr>    <chr>  <chr>    <dbl> <int> <int> <ord>
1 Ammonium 300kg  No        56.7     3     3 large

## t-tests
## Deshchenka

subset(tTest_Data, Soil == "Anthrosol") %>%
  group_by(Day) %>%
  t_test(Ammonium~Fertilisation) %>%
  adjust_pvalue(method = "none") %>%
  add_significance("p.adj") %>%
  mutate(Day=fct_relevel(Day, c("1","8","22","36"))) %>% arrange(Day) %>%
  slice(-c(3,4))


  Day   .y.      group1 group2    n1    n2 statistic     df          p       p.adj
p.adj.signif
* <chr> <chr>    <chr>  <chr>  <int> <int>     <dbl>  <dbl>      <dbl>       <dbl> <chr>
1 1     Ammonium 300kg  No         3     3      15.2   2.00  0.00428     0.00428   "**"
2 8     Ammonium 300kg  No         3     3     215.    2.04  0.0000178   0.0000178 "****"

## Yoshiki

subset(tTest_Data, Soil == "Vermiculitic Cambisol") %>%
  group_by(Day) %>%
  t_test(Ammonium~Fertilisation) %>%
  adjust_pvalue(method = "none") %>%
  add_significance("p.adj") %>%
```

```
  mutate(Day=fct_relevel(Day, c("1","8","22","36"))) %>% arrange(Day) %>%
  slice(-c(4))

  Day   .y.      group1 group2    n1    n2 statistic    df         p     p.adj p.adj.signif
  <fct> <chr>    <chr>  <chr>  <int> <int>     <dbl> <dbl>     <dbl>     <dbl> <chr>
1 1     Ammonium 300kg  No         3     3      68.4  2.30 0.0000749 0.0000749 ****
2 8     Ammonium 300kg  No         3     3      24.1  2.29 0.000838  0.000838  ***
3 22    Ammonium 300kg  No         3     3      69.5  3.54 0.0000011 0.0000011 ****

## Ogata

subset(tTest_Data, Soil == "Smectitic Gleysol") %>%
  group_by(Day) %>%
  t_test(Ammonium~Fertilisation) %>%
  adjust_pvalue(method = "none") %>%
  add_significance("p.adj") %>%
  mutate(Day=fct_relevel(Day, c("1","8","22","36"))) %>% arrange(Day) %>%
  slice(-c(4))

  Day   .y.      group1 group2    n1    n2 statistic    df         p     p.adj p.adj.signif
  <fct> <chr>    <chr>  <chr>  <int> <int>     <dbl> <dbl>     <dbl>     <dbl> <chr>
1 1     Ammonium 300kg  No         3     2      20.5  2.05 0.00212   0.00212   **
2 8     Ammonium 300kg  No         3     3      18.7  2.04 0.00259   0.00259   **
3 22    Ammonium 300kg  No         3     3      90.9  2.23 0.0000502 0.0000502 ****

## Miyakonojo

subset(tTest_Data, Soil == "Allophanic Andosol") %>%
  group_by(Day) %>%
  t_test(Ammonium~Fertilisation) %>%
  adjust_pvalue(method = "none") %>%
  add_significance("p.adj") %>%
  mutate(Day=fct_relevel(Day, c("1","8","22","36"))) %>% arrange(Day) %>%
  slice(-c(3,4))

  Day   .y.      group1 group2    n1    n2 statistic    df        p    p.adj p.adj.signif
  <fct> <chr>    <chr>  <chr>  <int> <int>     <dbl> <dbl>    <dbl>    <dbl> <chr>
1 1     Ammonium 300kg  No         3     3      10.7  2.02 0.00836  0.00836  **
2 8     Ammonium 300kg  No         3     3      30.8  2.02 0.000999 0.000999 ***

## Performance of t-tests for solution Cs+ concentrations

## Groß – Enzersdorf

subset(tTest_Data, Soil == "Chernozem") %>% slice(-c(16)) %>%
  group_by(Day) %>%
  t_test(Cesium~Fertilisation) %>%
  adjust_pvalue(method = "none") %>%
  add_significance("p.adj") %>%
  mutate(Day=fct_relevel(Day, c("1","8","22","36"))) %>% arrange(Day)

  Day   .y.    group1 group2    n1    n2 statistic    df      p  p.adj p.adj.signif
  <fct> <chr>  <chr>  <chr>  <int> <int>     <dbl> <dbl>  <dbl>  <dbl> <chr>
1 1     Cesium 300kg  No         2     3     5.54   2.27 0.0233 0.0233 *
2 8     Cesium 300kg  No         3     3     9.65   2.09 0.0091 0.0091 **
3 22    Cesium 300kg  No         2     3     0.559  1.55 0.646  0.646  ns
4 36    Cesium 300kg  No         3     3    -1.76   2.34 0.202  0.202  ns


## Deshchenka

subset(tTest_Data, Soil == "Anthrosol") %>%
  group_by(Day) %>%
  t_test(Cesium~Fertilisation) %>%
  adjust_pvalue(method = "none") %>%
  add_significance("p.adj") %>%
  mutate(Day=fct_relevel(Day, c("1","8","22","36"))) %>% arrange(Day)


  Day   .y.    group1 group2    n1    n2 statistic    df         p     p.adj p.adj.signif
  <fct> <chr>  <chr>  <chr>  <int> <int>     <dbl> <dbl>     <dbl>     <dbl> <chr>
1 1     Cesium 300kg  No         3     3     35.0   2.02 0.000778  0.000778  ***
2 8     Cesium 300kg  No         3     3     48.1   2.89 0.000027  0.000027  ****
3 22    Cesium 300kg  No         3     3     18.4   4    0.0000517 0.0000517 ****
4 36    Cesium 300kg  No         3     3      1.26  4.00 0.277     0.277     ns
```

```
## Yoshiki

subset(tTest_Data, Soil == "Vermiculitic Cambisol") %>%
  group_by(Day) %>%
  t_test(Cesium~Fertilisation) %>%
  adjust_pvalue(method = "none") %>%
  add_significance("p.adj") %>%
  mutate(Day=fct_relevel(Day, c("1","8","22","36"))) %>% arrange(Day)

  Day   .y.    group1 group2    n1    n2 statistic   df       p  p.adj p.adj.signif
  <fct> <chr>  <chr>  <chr>  <int> <int>     <dbl> <dbl>  <dbl>  <dbl> <chr>
1 1     Cesium 300kg  No         3     3     1.21   3.90 0.295  0.295  ns
2 8     Cesium 300kg  No         3     3     1.88   3.23 0.15   0.15   ns
3 22    Cesium 300kg  No         3     3    -0.294  2.47 0.792  0.792  ns
4 36    Cesium 300kg  No         3     3     4.65   2.94 0.0196 0.0196 *

## Ogata

subset(tTest_Data, Soil == "Smectitic Gleysol") %>%
  group_by(Day) %>%
  t_test(Cesium~Fertilisation) %>%
  adjust_pvalue(method = "none") %>%
  add_significance("p.adj") %>%
  mutate(Day=fct_relevel(Day, c("1","8","22","36"))) %>% arrange(Day)

  Day   .y.    group1 group2    n1    n2 statistic   df         p    p.adj p.adj.signif
  <fct> <chr>  <chr>  <chr>  <int> <int>     <dbl> <dbl>    <dbl>    <dbl> <chr>
1 1     Cesium 300kg  No         3     2     34.0   2.33 0.000343 0.000343 ***
2 8     Cesium 300kg  No         3     3      6.39  3.29 0.00586  0.00586  **
3 22    Cesium 300kg  No         3     3      9.92  2.65 0.00362  0.00362  **
4 36    Cesium 300kg  No         3     3      1.70  2.72 0.198    0.198    ns

## Miyakonojo

subset(tTest_Data, Soil == "Allophanic Andosol") %>%
  group_by(Day) %>%
  t_test(Cesium~Fertilisation) %>%
  adjust_pvalue(method = "none") %>%
  add_significance("p.adj") %>%
  mutate(Day=fct_relevel(Day, c("1","8","22","36"))) %>% arrange(Day)

  Day   .y.    group1 group2    n1    n2 statistic   df         p    p.adj p.adj.signif
  <fct> <chr>  <chr>  <chr>  <int> <int>     <dbl> <dbl>    <dbl>    <dbl> <chr>
1 1     Cesium 300kg  No         3     3    23.0    2.13 0.00137  0.00137  **
2 8     Cesium 300kg  No         3     3    44.5    2.09 0.000385 0.000385 ***
3 22    Cesium 300kg  No         3     3     1.62   2.00 0.247    0.247    ns
4 36    Cesium 300kg  No         3     3     0.777  2.24 0.511    0.511    ns

## Performance of t-tests for solution K+ concentrations

## Groß – Enzersdorf

subset(tTest_Data, Soil == "Chernozem" & Day == "36")%>%
  t_test(Potassium~Fertilisation) %>%
  adjust_pvalue(method = "none") %>%
  add_significance("p.adj")

  Day   .y.   group1 group2    n1    n2 statistic    df     p p.adj p.adj.signif
* <chr> <chr> <chr>  <chr>  <int> <int>     <dbl> <dbl> <dbl> <dbl> <chr>
1 36    Potassium     0      1          3     3   -0.0165  3.00 0.988 0.988 ns


## Deshchenka

subset(tTest_Data, Soil == "Anthrosol”)%>%
  t_test(Potassium~Fertilisation) %>%
  adjust_pvalue(method = "none") %>%
  add_significance("p.adj") %>%
  mutate(Day=fct_relevel(Day, c("1","8","22","36"))) %>% arrange(Day)

  Day   .y.   group1 group2    n1    n2 statistic    df         p     p.adj p.adj.signif
  <fct> <chr> <chr>  <chr>  <int> <int>     <dbl> <dbl>     <dbl>     <dbl> <chr>
1 1     K     0      1          3     3     -20.4  2.04 0.00216   0.00216   **
```

```
2 8     K     0     1         3     3     -18.9  2.01 0.00274   0.00274   **
3 22    K     0     1         3     3     -22.3  2.71 0.000377  0.000377  ***
4 36    K     0     1         3     3     -25.7  3.77 0.0000228 0.0000228 ****

## Yoshiki

subset(tTest_Data, Soil == "Vermiculitic Cambisol”)%>%
  t_test(Potassium~Fertilisation) %>%
  adjust_pvalue(method = "none") %>%
  add_significance("p.adj") %>%
  mutate(Day=fct_relevel(Day, c("1","8","22","36"))) %>% arrange(Day)

Day   .y.   group1 group2    n1    n2 statistic    df      p  p.adj p.adj.signif
  <fct> <chr> <chr>  <chr>  <int> <int>     <dbl> <dbl>  <dbl>  <dbl> <chr>
1 1     K     0      1          3     3     -4.01  2.57 0.0369 0.0369 *
2 8     K     0      1          3     3     -1.52  2.54 0.241  0.241  ns
3 22    K     0      1          3     3     -4.01  2.80 0.0316 0.0316 *
4 36    K     0      1          3     3     -2.04  2.34 0.159  0.159  ns


## Ogata

subset(tTest_Data, Soil == "Smectitic Gleysol”)%>%
  t_test(Potassium~Fertilisation) %>%
  adjust_pvalue(method = "none") %>%
  add_significance("p.adj") %>%
  mutate(Day=fct_relevel(Day, c("1","8","22","36"))) %>% arrange(Day)


  Day   .y.   group1 group2    n1    n2 statistic    df      p  p.adj p.adj.signif
  <fct> <chr> <chr>  <chr>  <int> <int>     <dbl> <dbl>  <dbl>  <dbl> <chr>
1 1     K     0      1          3     3    -1.48   2.50 0.253  0.253  ns
2 8     K     0      1          3     3    -2.73   3.95 0.0531 0.0531 ns
3 22    K     0      1          3     3    -0.113  3.04 0.917  0.917  ns
4 36    K     0      1          3     3    -0.389  3.89 0.718  0.718  ns

## Miyakonojo

subset(tTest_Data, Soil == "Allophanic Andosol”)%>%
  t_test(Potassium~Fertilisation) %>%
  adjust_pvalue(method = "none") %>%
  add_significance("p.adj") %>%
  mutate(Day=fct_relevel(Day, c("1","8","22","36"))) %>% arrange(Day)


  Day   .y.   group1 group2    n1    n2 statistic    df          p      p.adj p.adj.signif
  <fct> <chr> <chr>  <chr>  <int> <int>     <dbl> <dbl>      <dbl>      <dbl> <chr>
1 1     K     0      1          3     3    -29.9   3.21 0.0000488  0.0000488  ****
2 8     K     0      1          3     3    -40.5   3.80 0.00000373 0.00000373 ****
3 22    K     0      1          3     3     -5.36  2.26 0.0251     0.0251     *
4 36    K     0      1          3     3    -18.1   2.13 0.00225    0.00225    **


###########################################################################################


## Performance of an ANOVA for solution K+ concentrations of the clay amended
## soil

## Uploading dataset

library(readxl)
ANOVA_Data <- read_excel(“Documents/~ANOVA_Data.xlsx)
str(ANOVA_Data)

> str(ANOVA_Data)
tibble [168 × 6] (S3: tbl_df/tbl/data.frame)
 $ Day          : chr [1:168] "1" "1" "1" "1" ...
 $ Fertilisation: chr [1:168] "0" "0" "0" "1" ...
 $ Ammonium     : num [1:168] 0.352 0.284 0.26 10.995 9.908 ...
 $ Potassium    : num [1:168] 0.154 0.155 0.139 0.517 0.607 ...
 $ Claymineral  : chr [1:168] "Z1" "Z1" "Z1" "Z1" ...
 $ Cesium       : num [1:168] 4.53 4.28 4.1 35.51 35.6 ...
```

```
## Creating an ANOVA model with log10 – transformed data
## FirstDay

library(tidyverse)

FirstDayAnova <- ANOVA_Data %>% filter(Day == 1) %>% mutate(Ammonium =
              Ammonium*1000)

FirstDayAnovaModel <- aov(log10(Ammonium) ~ Fertilisation * Claymineral, data =
                            FirstDayAnova)
summary(FirstDayAnovaModel)

                          Df Sum Sq Mean Sq F value   Pr(>F)    
Fertilisation              1 20.063  20.063 6878.61  < 2e-16 ***
Claymineral                6  1.991   0.332  113.74  < 2e-16 ***
Fertilisation:Claymineral  6  0.280   0.047   15.98 6.78e-08 ***
Residuals                 28  0.082   0.003                     
---
Signif. codes:  0 ‘***’ 0.001 ‘**’ 0.01 ‘*’ 0.05 ‘.’ 0.1 ‘ ’ 1

## Testing for Normality example

qqnorm(residuals(FirstDayAnova))

## Testing for homoscedasticity example

levene_test(FirstDayAnova)

    df1   df2 statistic     p
  <int> <int>     <dbl> <dbl>
1    13    28     0.343 0.977

## Performing Tukey HSD test

TukeyFirstDay <- TukeyHSD(FirstDayAnovaModel)
library(multcompView)
FirstLetter <- multcompLetters4(FirstDayAnovaModel, TukeyFirstDay)

FirstLetter

$Fertilisation
  1   0 
"a" "b" 

$Claymineral
NCA  S1  V1  S4  Z1  V4  Z4 
"a" "b" "b" "b" "c" "c" "d" 

$`Fertilisation:Claymineral`
1:NCA  1:V1  1:S1  1:S4  1:Z1  1:V4  1:Z4 0:NCA  0:S1  0:S4  0:V1  0:V4  0:Z1  0:Z4 
  "a"  "ab"  "ab"  "ab"  "ab"   "b"   "c"   "d"   "e"   "e"  "ef"  "fg"   "g"   "h" 

## Eight Day

EightDayAnova <- ANOVA_Data %>% filter(Day == 8) %>% mutate(Ammonium =
              Ammonium*1000)

EightDayAnovaModel <- aov(log10(Ammonium) ~ Fertilisation * Claymineral, data =
                            EightDayAnova)))
summary(EightDayAnovaModel)

                          Df Sum Sq Mean Sq  F value   Pr(>F)    
Fertilisation              1  37.50   37.50 8290.800  < 2e-16 ***
Claymineral                6   0.62    0.10   22.689  1.5e-09 ***
Fertilisation:Claymineral  6   0.16    0.03    5.878 0.000458 ***
Residuals                 28   0.13    0.00                      
---
Signif. codes:  0 ‘***’ 0.001 ‘**’ 0.01 ‘*’ 0.05 ‘.’ 0.1 ‘ ’ 1


## Performing Tukey HSD test

TukeyEightDay <- TukeyHSD(EightDayAnovaModel)
library(multcompView)
EightLetter <- multcompLetters4(EightDayAnovaModel, TukeyEightDay)
```

```
EigthLetter

$Fertilisation
  1   0
"a" "b"

$Claymineral
 NCA   S1   S4   V1   Z1   V4   Z4
 "a"  "a"  "a" "ab"  "b"  "b"  "c"


$`Fertilisation:Claymineral`
1:NCA  1:S1  1:V1  1:S4  1:Z1  1:V4  1:Z4  0:S4  0:S1 0:NCA  0:V1  0:V4  0:Z1  0:Z4
  "a"   "a"  "ab"  "ab"  "ab"   "b"   "c"   "d"   "d"  "de"  "de"  "de"   "e"   "e"

## Twenty-second day

TwenDayAnova <-     ANOVA_Data %>% filter(Day == 22) %>% mutate(Ammonium = Ammonium
                    * 1000) %>% slice(-c(39,41,9)) %>% mutate(Claymineral =
                    as.factor(case_when(Claymineral == 'Z4' & Fertilisation == '1' ~
                    'NZ4', TRUE ~as.character(Claymineral))))

TwenDayAnovaModel <- (aov(log10(Ammonium) ~ Claymineral, data = TwenDayAnova))
TwenDayAnovaModel

            Df Sum Sq Mean Sq F value   Pr(>F)
Claymineral  7  3.609  0.5155   12.66 4.33e-05 ***
Residuals   14  0.570  0.0407
---
Signif. codes:  0 ‘***’ 0.001 ‘**’ 0.01 ‘*’ 0.05 ‘.’ 0.1 ‘ ’ 1

## Performing Tukey HSD test

TukeyTwenDay <- TukeyHSD(TwenDayAnovaModel)
library(multcompView)
TwenLetter <- multcompLetters4(TwenDayAnovaModel, TukeyTwenDay)

TwenLetter

            Df Sum Sq Mean Sq F value   Pr(>F)
Claymineral  7  3.609  0.5155   12.66 4.33e-05 ***
Residuals   14  0.570  0.0407
---
Signif. codes:  0 ‘***’ 0.001 ‘**’ 0.01 ‘*’ 0.05 ‘.’ 0.1 ‘ ’ 1

## Performance of an ANOVA for solution Cs+ concentrations of the clay amended
## soil

## First Day

FirstDayAnovaCs <- ANOVA_Data %>% filter(Day == 1) %>% mutate(Cesium =
                    Cesium*1000)

FirstDayAnovaModelCs <- aov(log10(Cesium) ~ Fertilisation * Claymineral, data =
                           FirstDayAnovaCs)

summary(FirstDayAnovaModelCs)

                          Df Sum Sq Mean Sq F value   Pr(>F)
Fertilisation              1  6.330   6.330 6144.87  < 2e-16 ***
Claymineral                6  8.566   1.428 1385.92  < 2e-16 ***
Fertilisation:Claymineral  6  0.367   0.061   59.44 1.22e-14 ***
Residuals                 28  0.029   0.001
---
Signif. codes:  0 ‘***’ 0.001 ‘**’ 0.01 ‘*’ 0.05 ‘.’ 0.1 ‘ ’ 1

## Performing Tukey HSD test

TukeyFirstDayCs <- TukeyHSD(FirstDayAnovaModelCs)

FirstLetterCs <- multcompLetters4(FirstDayAnovaModelCs, TukeyFirstDayCs)

FirstLetterCs
```

```
$Fertilisation
  1   0 
"a" "b" 

$Claymineral
NCA  S1  S4  Z1  V1  Z4  V4 
"a" "b" "c" "d" "d" "e" "f" 

$`Fertilisation:Claymineral`
1:NCA  1:S1  1:S4  1:Z1  1:V1 0:NCA  0:S1  0:S4  1:Z4  0:V1  1:V4  0:Z1  0:V4  0:Z4 
  "a"   "b"   "c"   "d"   "e"   "f"   "f"   "g"   "g"   "h"  "hi"   "i"   "j"   "k" 
## Eight Day

EightDayAnovaCs <- ANOVA_Data %>% filter(Day == 8) %>% mutate(Cesium = 
                     Cesium*1000)
EightDayAnovaModelCs <- aov(log10(Cesium) ~ Fertilisation * Claymineral, data = 
                            EightDayAnovaCs)

summary(EightDayAnovaModelCs)

                          Df Sum Sq Mean Sq F value Pr(>F)    
Fertilisation              1 10.962  10.962 8930.93 <2e-16 ***
Claymineral                6  8.203   1.367 1113.86 <2e-16 ***
Fertilisation:Claymineral  6  0.598   0.100   81.25 <2e-16 ***
Residuals                 28  0.034   0.001                   
---
Signif. codes:  0 ‘***’ 0.001 ‘**’ 0.01 ‘*’ 0.05 ‘.’ 0.1 ‘ ’ 1

## Performing Tukey HSD test

TukeyEightDayCs <- TukeyHSD(EightDayAnovaModelCs)

EightLetterCs <- multcompLetters4(EightDayAnovaModelCs, TukeyEightDayCs)

EightLetterCs

$Fertilisation
  1   0 
"a" "b" 

$Claymineral
 NCA   S1   S4   Z1   V1   Z4   V4 
 "a" "ab"  "b"  "c"  "d"  "e"  "f" 

$`Fertilisation:Claymineral`
1:NCA  1:S1  1:S4  1:Z1  1:V1  1:Z4  0:S4 0:NCA  0:S1  1:V4  0:Z1  0:V1  0:Z4  0:V4 
  "a"   "a"   "b"   "c"   "d"   "e"   "f"   "f"   "f"   "g"   "g"   "h"   "i"   "j" 

## Twenty-Second Day

TwenDayAnovaCs <- ANOVA_Data %>% filter(Day == 22) %>% mutate(Cesium = 
                     Cesium*1000) %>% slice(-c(6, 18, 24))
TwenDayAnovaModelCs <- aov(log10(Cesium) ~ Fertilisation * Claymineral, data = 
                            TwenDayAnovaCs)

summary(TwenDayAnovaModelCs)

                          Df Sum Sq Mean Sq F value  Pr(>F)    
Fertilisation              1  1.950  1.9501  733.91 < 2e-16 ***
Claymineral                6  7.437  1.2395  466.48 < 2e-16 ***
Fertilisation:Claymineral  6  0.315  0.0526   19.79 2.2e-08 ***
Residuals                 25  0.066  0.0027                    
---
Signif. codes:  0 ‘***’ 0.001 ‘**’ 0.01 ‘*’ 0.05 ‘.’ 0.1 ‘ ’ 1


## Performing Tukey HSD test

TukeyTwenDayCs <- TukeyHSD(TwenDayAnovaModelCs)

TwenLetterCs <- multcompLetters4(TwenDayAnovaModelCs, TukeyTwenDayCs)

TwenLetterCs

$Fertilisation
  1   0 
```

```
"a" "b"

$Claymineral
 S4  S1 NCA  Z4  Z1  V1  V4
"a" "a" "a" "b" "b" "c" "d"

$`Fertilisation:Claymineral`
1:NCA  1:S4  1:S1  1:Z4  1:Z1 0:NCA  0:S4  0:S1  1:V1  0:Z1  0:Z4  0:V1  1:V4  0:V4
  "a"   "a"   "a"   "b"   "b"   "c"   "c"   "c"   "d"   "d"   "d"   "e"   "f"   "f"

## Thirty-sixth Day

ThirtDayAnovaCs <- ANOVA_Data %>% filter(Day == 36) %>% mutate(Cesium =
                    Cesium*1000)
ThirtDayAnovaModelCs <- aov(log10(Cesium) ~ Fertilisation * Claymineral, data =
                          ThirtDayAnovaCs)


summary(ThirtDayAnovaModelCs)

                          Df Sum Sq Mean Sq F value   Pr(>F)
Fertilisation              1  0.307  0.3071  388.79  < 2e-16 ***
Claymineral                6  6.907  1.1512 1457.58  < 2e-16 ***
Fertilisation:Claymineral  6  0.283  0.0471   59.67 1.16e-14 ***
Residuals                 28  0.022  0.0008
---
Signif. codes:  0 ‘***’ 0.001 ‘**’ 0.01 ‘*’ 0.05 ‘.’ 0.1 ‘ ’ 1


## Performing Tukey HSD test

TukeyThirtDayCs <- TukeyHSD(ThirtDayAnovaModelCs)

ThirtLetterCs <- multcompLetters4(ThirtDayAnovaModelCs, TukeyThirtDayCs)

ThirtLetterCs

$Fertilisation
  1   0
"a" "b"

$Claymineral
 S1  S4 NCA  Z1  Z4  V1  V4
"a" "a" "b" "c" "d" "e" "f"

$`Fertilisation:Claymineral`
 1:S1  1:S4 1:NCA 0:NCA  0:S1  0:S4  1:Z1  1:Z4  0:Z1  0:V1  1:V1  0:Z4  1:V4  0:V4
  "a"   "a"   "b"  "bc"  "bc"  "bc"   "c"   "d"   "e"   "f"   "f"   "f"   "g"   "g"

## Performance of an ANOVA for solution K+ concentrations of the clay amended
## soil

## First Day

FirstDayAnovaK <- ANOVA_Data %>% filter(Day == 1)

FirstDayAnovaModelK <- aov(log10(Potassium) ~ Fertilisation * Claymineral, data =
                          FirstDayAnovaK)

summary(FirstDayAnovaModelK)

                   Df Sum Sq Mean Sq F value   Pr(>F)
Soil                6 1.0630  0.1772    32.9 1.96e-11 ***
Fertilisation       1 1.4352  1.4352   266.5 7.72e-16 ***
Soil:Fertilisation  6 0.3359  0.0560    10.4 4.55e-06 ***
Residuals          28 0.1508  0.0054
---
Signif. codes:  0 ‘***’ 0.001 ‘**’ 0.01 ‘*’ 0.05 ‘.’ 0.1 ‘ ’ 1
## Performing Tukey HSD test

TukeyFirstDayK <- TukeyHSD(FirstDayAnovaModelK)

FirstLetterK <- multcompLetters4(FirstDayAnovaModelK, TukeyFirstDayK)
```

```
FirstLetterK

$Claymineral
 NCA   S1   S4   V1   V4   Z1   Z4 
 "a"  "a"  "a" "ab"  "b"  "b"  "c" 

$Fertilisation
  1   0 
"a" "b" 

$`Claymineral:Fertilisation`
NCA:1  S1:1  S4:1  Z1:1  V1:1  V4:1 NCA:0  Z4:1  S1:0  S4:0  V1:0  V4:0  Z1:0  Z4:0 
  "a"  "ab" "abc" "abc" "abc" "bcd" "bcd"  "cd" "cde"  "de"  "de"  "ef"   "f"   "g" 

## Eighth Day

EighthDayAnovaK <- ANOVA_Data %>% filter(Day == 8)

EighthDayAnovaModelK <- aov(log10(Potassium) ~ Fertilisation * Claymineral, data =
                          EighthDayAnovaK)

summary(EighthDayAnovaModelK)

                   Df Sum Sq Mean Sq F value   Pr(>F)    
Soil                6 1.2023  0.2004  49.284 1.33e-13 ***
Fertilisation       1 1.8733  1.8733 460.731  < 2e-16 ***
Soil:Fertilisation  6 0.1024  0.0171   4.199  0.00391 ** 
Residuals          28 0.1138  0.0041                     
---
Signif. codes:  0 ‘***’ 0.001 ‘**’ 0.01 ‘*’ 0.05 ‘.’ 0.1 ‘ ’ 1

## Performing Tukey HSD test

TukeyEigthDayK <- TukeyHSD(EigthDayAnovaModelK)

EigthLetterK <- multcompLetters4(EighthDayAnovaModelK, TukeyEigthDayK)

EigthLetterK

$Claymineral

 NCA   S1   S4   V1   V4   Z1   Z4 
 "a"  "a" "ab" "ab" "bc"  "c"  "d" 

$Fertilisation
  1   0 
"a" "b" 

$`Claymineral:Fertilisation`
NCA:1  S1:1  V1:1  S4:1  V4:1  Z1:1  S1:0 NCA:0  Z4:1  S4:0  V1:0  V4:0  Z1:0  Z4:0 
  "a"   "a"   "a"   "a"   "a"  "ab"  "bc"  "cd"  "cd"  "cd"  "cd"  "de"   "e"   "f" 

## Twenty-second Day

TwenDayAnovaK <- ANOVA_Data %>% filter(Day == 22)

TwenDayAnovaModelK <- aov(log10(Potassium) ~ Fertilisation * Claymineral, data =
                          TwenDayAnovaK)

summary(TwenDayAnovaModelK)

         Df Sum Sq Mean Sq F value   Pr(>F)    
Soil                6 2.3262  0.3877 217.096  < 2e-16 ***
Fertilisation       1 0.8632  0.8632 483.337  < 2e-16 ***
Soil:Fertilisation  6 0.1063  0.0177   9.924 6.93e-06 ***
Residuals          28 0.0500  0.0018                     
---
Signif. codes:  0 ‘***’ 0.001 ‘**’ 0.01 ‘*’ 0.05 ‘.’ 0.1 ‘ ’ 1
```

```
## Performing Tukey HSD test

TukeyTwenDayK <- TukeyHSD(TwenDayAnovaModelK)

TwenLetterK <- multcompLetters4(TwenDayAnovaModelK, TukeyTwenDayK)
TwenLetterK

$Claymineral
 S1 NCA  V1  S4  V4  Z1  Z4 
"a" "a" "a" "a" "b" "c" "d" 

$Fertilisation
  1   0 
"a" "b" 

$`Claymineral:Fertilisation`
 S1:1 NCA:1  V1:1  S4:1 NCA:0  V4:1  S1:0  S4:0  V1:0  V4:0  Z1:1  Z4:1  Z1:0  Z4:0 
  "a"   "a"   "a"   "a"   "b"   "b"   "b"   "b"   "b"   "c"   "c"   "c"   "d"   "e" 

## Thirty-sixth Day

ThirtDayAnovaK <- ANOVA_Data %>% filter(Day == 36)

ThirtDayAnovaModelK <- aov(log10(Potassium) ~ Fertilisation * Claymineral, data =
                          ThirtDayAnovaK)

summary(ThirtDayAnovaModelK)

                   Df Sum Sq Mean Sq F value   Pr(>F)    
Soil                6  3.556  0.5927 255.463  < 2e-16 ***
Fertilisation       1  0.393  0.3935 169.596 2.11e-13 ***
Soil:Fertilisation  6  0.028  0.0046   1.989    0.101    
Residuals          28  0.065  0.0023                     
---
Signif. codes:  0 ‘***’ 0.001 ‘**’ 0.01 ‘*’ 0.05 ‘.’ 0.1 ‘ ’ 1

## Performing Tukey HSD test

TukeyThirtDayK <- TukeyHSD(ThirtDayAnovaModelK)

ThirtLetterK <- multcompLetters4(ThirtDayAnovaModelK, TukeyThirtDayK)

ThirtLetterK


$Claymineral
 NCA   S1   S4   V1   V4   Z1   Z4 
 "a" "ab" "ab"  "b"  "c"  "d"  "e" 

$Fertilisation
  1   0 
"a" "b" 

$`Claymineral:Fertilisation`
NCA:1  S1:1  S4:1  V1:1 NCA:0  S1:0  V4:1  S4:0  V1:0  V4:0  Z1:1  Z1:0  Z4:1  Z4:0 
  "a"   "a"   "a"  "ab"  "bc"   "c"   "c"   "c"   "c"   "d"  "de"   "e"   "f"   "g" 
```

Figure A1: *R - script of the conducted t-tests and ANOVAs.*

Appendix B

Table A1: *Air - dried water content and exchangeable NH_4^+, NO_2^- and NO_3^- of all soils.*

Soil	**Day**	**Fertilisation** (kg NH_4^+ - N ha^{-1})	**Rep.**	**Water content of air - dried soil** (%)	**Ex. - NH_4^+** (mmol kg^{-1} OD soil)	**Ex. - NO_2^- & NO_3^-** (mmol kg^{-1} OD soil)
Groß – Enzersdorf	1	0	1	1.31	-*	1.2014
			2	1.05	-	1.1999
			3	1.23	-	1.3338
		300	1	1.25	4.8704	1.3739
			2	1.4	4.3309	1.107
			3	1.26	3.7931	1.5622
	8	0	1	1.45	-	1.5888
			2	1.38	-	0.9578
			3	1.28	-	1.6452
		300	1	1.26	1.5832	5.5641
			2	1.52	2.0053	5.4711
			3	1.26	1.7469	5.7522
	22	0	1	1.47	-	1.5331
			2	1.4	-	1.1062
			3	1.46	-	1.3350
		300	1	1.34	-	7.0046
			2	1.34	-	6.0279
			3	1.21	0.1409	10.237
	36	0	1	1.27	-	5.0621
			2	1.4	-	1.9987
			3	1.41	-	5.0429
		300	1	1.4	-	10.4354
			2	1.26	-	9.8803
			3	1.4	-	10.5631
Deshchenka	1	0	1	0.73	0.8168	3.1374
			2	0.74	0.7313	2.8365
			3	0.6	0.7594	2.6919
		300	1	0.53	8.1622	2.6954
			2	0.53	7.5196	3.0627
			3	0.6	6.9039	2.5242
	8	0	1	0.66	0.7654	2.5069
			2	0.67	0.7377	2.17
			3	0.86	0.7701	2.5218
		300	1	0.53	4.6298	5.6795
			2	0.67	-	7.7531
			3	0.73	3.5684	6.5311
	22	0	1	0.73	-	3.9226
			2	0.2	-	4.0775
			3	0.8	-	3.2943
		300	1	0.6	-	9.8846
			2	0.46	-	12.8542
			3	0.67	-	11.8694
	36	0	1	0.8	-	6.567
			2	0.73	-	6.0205
			3	0.6	-	7.7674
		300	1	0.44	-	15.9102
			2	0.67	-	14.4838
			3	0.73	-	16.2445
Yoshiki	1	0	1	0.73	0.7475	0.4797
			2	0.74	0.7502	0.6204
			3	0.6	-	0.5758
		300	1	0.53	1.4644	0.5836
			2	0.53	1.3334	0.4673
			3	0.6	1.3138	0.5129
	8	0	1	0.66	0.1484	2.0048
			2	0.67	0.1573	1.7074

			3	0.86	0.1739	1.4898
		300	1	0.53	0.9942	1.9651
			2	0.67	0.95	1.8109
			3	0.73	0.8901	1.9099
	22	0	1	0.73	0.1401	3.2302
			2	0.2	0.1482	2.3085
			3	0.88	0.1788	2.6312
		300	1	0.6	0.6488	5.0160
			2	0.46	0.8026	5.0053
			3	0.67	0.5837	5.0479
	36	0	1	0.8	-	4.2340
			2	0.73	-	4.0017
			3	0.6	-	4.6814
		300	1	0.4	0.4695	5.2998
			2	0.67	0.5439	6.7055
			3	0.73	0.4156	7.9637
Ogata	1	0	1	3.41	1.6318	0.7374
			2	3.37	1.5022	0.7175
			3	-	-	-
		300	1	3.38	7.9399	0.6637
			2	3.34	7.7440	0.8666
			3	3.51	9.4844	0.7188
	8	0	1	3.49	0.9264	1.9436
			2	3.43	0.8705	2.1698
			3	3.42	0.7328	2.3836
		300	1	3.19	5.3438	2.9512
			2	3.19	5.8010	2.8176
			3	3.14	5.0850	5.7999
	22	0	1	3.41	0.3849	3.0025
			2	3.46	0.3636	3.7178
			3	3.53	0.3380	3.2561
		300	1	3.64	2.9241	8.5078
			2	3.4	3.2988	8.5771
			3	3.73	3.4771	8.1951
	36	0	1	3.75	0.2083	3.7350
			2	3.91	0.1845	4.1363
			3	3.88	0.1994	5.1403
		300	1	3.99	1.4100	14.5243
			2	4.47	1.2686	14.6158
			3	3.95	1.6949	14.9966
Miyakonojo	1	0	1	4.99	1.0918	4.2542
			2	4.65	0.8556	4.2733
			3	4.78	0.8462	4.4080
		300	1	5.45	16.6671	4.8500
			2	5.37	15.6013	4.3339
			3	5.5	14.8622	4.3778
	8	0	1	6.38	0.3458	5.4577
			2	6.15	0.3581	5.0466
			3	5.85	0.2855	4.9725
		300	1	5.39	8.9401	8.9344
			2	5.24	9.3270	9.3391
			3	5.25	10.6567	9.5871
	22	0	1	5.39	0.1595	5.6325
			2	5.24	0.1546	7.7754
			3	5.25	0.1635	5.6307
		300	1	5.92	0.2129	20.3501
			2	5.74	0.2121	20.9359
			3	6.03	0.2238	21.9023
	36	0	1	5.58	0.1616	6.6602
			2	6.19	0.1529	6.3490
			3	6.61	0.1489	7.1326
		300	1	5.18	-	22.7563
			2	2.39	-	20.4056
			3	5.86	-	23.3314
Miyakonojo with 10t ha^{-1} smectite	1	0	1	6.55	1.7639	4.2489

			2	6.11	1.5579	4.4093
			3	5.61	1.3972	4.5428
		300	1	5.98	15.9131	4.3306
			2	5.91	15.1571	3.7326
			3	6.07	15.2293	3.6884
	8	0	1	5.7	0.4162	5.6703
			2	5.42	0.4844	5.7853
			3	5.54	0.3443	5.7429
		300	1	6.04	10.5431	7.8020
			2	5.64	10.3274	8.0620
			3	5.92	9,.3562	9.8345
	22	0	1	5.1	-	6.2552
			2	5.65	-	6.4278
			3	4.62	-	6.0147
		300	1	5.91	0.2898	21.6811
			2	6.48	0.2765	20.4781
			3	6.01	0.3065	18,9174
	36	0	1	5.57	0.1933	7.2360
			2	5.73	0.1736	7.2102
			3	5.28	0.1704	7.0978
		300	1	5.73	-	21.9329
			2	5.72	0.1359	19.9771
			3	6.3	-	20.8811
Miyakonojo with 40 t ha^{-1} smectite	1	0	1	5.91	1.2143	4.2006
			2	6.22	1.3036	4.1814
			3	6.49	1.3315	4.0552
		300	1	6.77	17.6759	4.1471
			2	6.66	17.3105	3.7789
			3	6.58	15.4441	3.5212
	8	0	1	5.81	0.4778	5.2399
			2	5.97	0.4062	5.1891
			3	5.58	0.3295	5.5266
		300	1	6.07	10.4782	7.8284
			2	5.13	9.6947	8.0788
			3	5.08	9.3993	9.6567
	22	0	1	5.33	-	6.1578
			2	5.47	-	6.2828
			3	5.77	-	6.4314
		300	1	5.3	0.2715	19.2715
			2	6.65	0.3125	19.7437
			3	6.6	0.2603	18.6393
	36	0	1	5.52	-	6.9096
			2	5.66	-	7.0617
			3	5.47	-	6.7268
		300	1	5.84	-	21.0618
			2	5.39	-	20.5874
			3	5.13	-	23.1265
Miyakonojo with 10 t ha^{-1} vermiculite	1	0	1	4.85	0.4890	3.8739
			2	4.8	0.4983	4.5130
			3	4.99	0.5372	3.9456
		300	1	5.73	7.9416	4.7440
			2	5.4	6.9708	4.3811
			3	5.32	7.6830	4.0253
	8	0	1	5.84	0.2318	5.0218
			2	5.95	0.2448	4.9386
			3	5.86	0.1880	5.4138
		300	1	6.37	6.6191	8.6409
			2	5.87	6.3455	8.9275
			3	5.9	5.8602	9.6104
	22	0	1	5.45	0.2469	6.01
			2	4.98	0.1894	5.9967
			3	5.12	0.2079	6.2623
		300	1	5.74	-	19.7087

			2	6.2	-	24.6496
			3	5.64	-	19.6736
	36	0	1	6.12	-	6.5706
			2	4.78	-	6.5618
			3	5.47	-	6.8511
		300	1	5.18	-	21.7202
			2	2.39	-	21.2864
			3	5.86	-	22.2036
Miyakonojo with 40 t ha^{-1} vermiculite	1	0	1	6.07	0.2672	3.8467
			2	5.14	0.2589	4.0977
			3	5.26	0.2792	3.9196
		300	1	6.23	5.1420	4.0424
			2	5.7	4.7321	3.9261
			3	6.62	4.7141	3.9659
	8	0	1	5.74	0.1287	4.5017
			2	5.83	0.1442	6.0751
			3	5.75	0.132	4.8086
		300	1	4.78	3.9232	7.1316
			2	4.96	3.3220	8.3513
			3	5	2.9935	9.1137
	22	0	1	5.6	0.1392	5.3760
			2	4.76	0.1305	5.5609
			3	5.34	0.1379	6.0064
		300	1	5.86	-	15.1171
			2	6.18	-	16.6075
			3	5.8	0.2418	16.5464
	36	0	1	5.38	-	6.9142
			2	5.58	-	6.8767
			3	5.98	-	6.7524
		300	1	5.58	-	17.0593
			2	4.99	-	17.9017
			3	4.77	-	18.8590
Miyakonojo with 10 t ha^{-1} zeolite	1	0	1	5.9	1.3334	3.8823
			2	5.54	1.4922	3.8104
			3	5.94	1.4573	3.7130
		300	1	5.96	14.2753	3.8864
			2	5.89	18.2335	3.3623
			3	5.84	17.5576	3.3502
	8	0	1	5.32	0.9851	4.6196
			2	5.15	1.0399	4.3749
			3	5.26	0.9217	4.8468
		300	1	5.13	10.2033	6.1391
			2	5.06	11.3441	6.2733
			3	5.06	10.5708	7.0045
	22	0	1	5.36	0.1629	7.1921
			2	5.38	0.1661	6.5215
			3	4.96	0.1548	6.3856
		300	1	5.92	0.5380	21.7716
			2	5.59	0.4685	20.9671
			3	5.9	0.5847	20.2458
	36	0	1	5.47	-	7.1956
			2	5.67	-	7.0542
			3	5.64	-	6.89
		300	1	5.4	0.1801	22.3341
			2	5.28	0.1884	20.8277
			3	5.54	-	20.5767
Miyakonojo with 40 t ha^{-1} zeolite	1	0	1	5.73	1.6910	3.1309
			2	5.25	1.7040	2.7458
			3	5.26	1.6368	3.2424
		300	1	5.8	21.1136	2.8148
			2	5.86	17.8246	2.8386

		3	6.02	18.2838	2.4687
8	0	1	4.68	1.3259	3.6962
		2	5.51	1.3997	3.7272
		3	4.91	1.3311	3.6670
	300	1	5.02	13.1447	3.7236
		2	5.28	13.3307	3.9266
		3	4.9	11.2436	4.5861
22	0	1	5.61	0.7148	5.0563
		2	5.37	0.8520	5.1634
		3	5.29	0.5415	5.1526
	300	1	6.11	3.7211	14.7625
		2	6.24	2.8133	15.2973
		3	6.64	3.8487	14.5897
36	0	1	5.38	-	7.1653
		2	5.37	-	6.7910
		3	5.43	-	7.8357
	300	1	5.02	0.4615	19.8335
		2	5.2	0.5277	21.3840
		3	5.37	0.4588	21.6262

** The hyphen (-) denotes NH_4^+ concentrations that were below the detection level of 0.01 mM L^{-1}.*

Appendix C

Table A2: *Air - dried water content, exchangeable K^+ and CEC of all soils.*

Soil	**Fertilisation** (kg NH_4^+ – N ha^{-1})	**Rep.**	**Water content of air-dried soil** (%)	**Ex. - K^+** (mmol kg^{-1} OD soil)	**CEC** (cmol$_{(+)}$ kg^{-1} OD soil)
Groß – Enzersdorf	0	1	1.3	2.8366	15.1894
		2		2.8311	17.8329
	300	1	1.3	3.2454	15.3994
		2		28324	17.6286
Deshchenka	0	1	0.7	3.0355	4.1559
		2		3.2618	5.1134
	300	1	0.9	3.3774	3.7054
		2		3.3797	4.4791
Yoshiki	0	1	5.8	0.6563	7.6849
		2		0.3519	7.0571
	300	1	5.46	0.3130	6.2215
		2		0.2867	8.3857
Ogata	0	1	4.3	2.3124	26.0848
		2		2.0716	28.8641
	300	1	3.8	2.3362	26.8389
		2		1.9857	28.0583
Miyakonojo	0	1	4.9	1.6051	8.9755
		2		1.2320	9.8715
	300	1	4.9	1.5943	8.4613
		2		1.1963	9.2020
Miyakonojo with 10t ha^{-1} smectite	0	1	5.7	1.2347	10.3307
		2		1.1955	10.3307
	300	1	5.9	1.6257	10.0835
		2		1.2809	10.2156
Miyakonojo with 40t ha^{-1} smectite	0	1	5.7	1.2786	12.3311
		2		1.29	11.6052
	300	1	5.8	1.418	12.3409
		2		1.3395	12.8086
Miyakonojo with 10t ha^{-1} vermiculite	0	1	5.8	1.4075	9.1607
		2		1.1054	11.1994
	300	1	5.5	1.4564	9.5315
		2		1.1755	10.2027
Miyakonojo with 40t ha^{-1} vermiculite	0	1	6	1.2113	10.2565
		2		0.8929	15.3455
	300	1	5.6	1.0928	10.2527
		2		1.1747	11.8691
Miyakonojo with 10t ha^{-1} zeolite	0	1	5.7	1.81	8.5301
		2		1.7795	10.1352
	300	1	6.3	1.9981	8.4804
		2		1.8816	9.9853
Miyakonojo with 40t ha^{-1} zeolite	0	1	5.8	3.5095	8.3090
		2		3.0018	10.3828
	300	1	5.6	3.9086	8.6298
		2		3.6516	10.0124

Appendix D

Table A3: *Soil solution cations and pH of all soils.*

Day	Fertilisation (kg NH_4^+ - N ha^{-1})	Rep.	Na^+ (mmol L^{-1})	K^+ (mmol L^{-1})	Ca^{2+} (mmol L^{-1})	Mg^{2+} (mmol L^{-1})	NH_4^+ (mmol L^{-1})	Cs^+ (nmol L^{-1})	*p*H
Groß - Enzersdorf									
1	0	1	n.d.*	n.d.	n.d.	n.d.	-**	0.3083	8.262
		2	n.d.	n.d.	n.d.	n.d.	-	0.1353	8.447
		3	n.d.	n.d.	n.d.	n.d.	-	0.3008	8.329
	300	1	n.d.	n.d.	n.d.	n.d.	2.5178	0.5564	8.060
		2	n.d.	n.d.	n.d.	n.d.	2.991	0.5865	8.121
		3	n.d.	n.d.	n.d.	n.d.	5.4423	0.7594	8.035
8	0	1	4.5149	0.1187	2.8661	3.4079	-	0.0301	8.242
		2	n.d.	n.d.	n.d.	n.d.	-	0.0752	8.272
		3	n.d.	n.d.	n.d.	n.d.	0.383	0.0827	8.279
	300	1	6.6632	0.4726	28.9394	3.7458	0.4745	0.218	8.036
		2	6.9806	0.6536	37.414	4.8426	0.3349	0.2256	7.941
		3	6.8958	0.5763	36.0816	4.5453	-	0.2256	8.044
22	0	1	n.d.	n.d.	n.d.	n.d.	-	0.0902	8.415
		2	n.d.	n.d.	n.d.	n.d.	-	0.0301	8.197
		3	5.0372	0.2383	7.7199	1.0144	-	0.0526	8.174
	300	1	5.3351	0.2767	40.4129	4.8165	-	0.0451	7.850
		2	5.2179	0.3675	44.4207	5.3849	-	0.9699	8.040
		3	5.5605	0.3309	46.6494	5.3774	-	0.1128	7.990
36	0	1	5.3003	0.2544	8.0668	1.0474	-	0.1805	8.429
		2	5.3744	0.2145	4.514	0.6881	-	0.2105	8.437
		3	5.2797	0.1482	4.4487	0.604	-	0.0376	8.398
	300	1	5.5809	0.1838	42.909	5.0471	-	0.0752	7.925
		2	5.3238	0.2288	45.5511	5.3393	-	0.0376	7.859
		3	n.d.	n.d.	n.d.	n.d.	-	0.0226	7.934
Deshchenka									
1	0	1	1.4913	2.4297	5.7607	1.3286	0.0231	0.2256	6.324
		2	1.5171	2.3998	5.5214	1.2751	0.0242	0.2256	6.325
		3	1.5448	2.4666	5.7036	1.3908	0.022	0.203	6.313
	300	1	2.1191	5.8015	14.8217	3.1893	13.0716	4.1128	6.206
		2	1.9112	6.3131	16.5266	3.5916	15.8496	4.5113	6.079
		3	2.1295	6.3764	17.0548	3.668	16.1779	4.3835	6.080
8	0	1	1.5849	2.5728	6.4856	1.5514	0.0335	0.1955	6.414
		2	1.5773	2.5808	6.4742	1.5772	0.0284	0.2857	6.261
		3	1.5303	2.6005	6.4668	1.5827	0.0201	0.2707	6.315
	300	1	2.0211	6.2388	25.3886	5.3595	8.2554	3.2481	5.815
		2	1.9391	5.7095	23.5909	5.1878	8.1896	3.2857	5.806
		3	2.0909	6.2847	25.5294	5.5062	8.3217	3.4361	5.688
22	0	1	5.7571	2.1908	6.476	1.6446	-	0.1729	6.266
		2	5.4046	2.1699	5.9592	1.4968	-	0.1579	6.302
		3	5.7608	1.9639	5.7658	1.5463	-	0.1654	6.273
	300	1	6.7645	4.4409	41.9077	8.6112	-	0.2857	5.224
		2	7.0599	4.2995	41.1609	8.603	-	0.2782	5.294
		3	n.d.	n.d.	n.d.	n.d.	-	0.2707	5.256
36	0	1	5.6019	2.4615	7.5458	1.9338	-	0.2857	6.256
		2	5.4941	2.3949	7.5605	1.8479	-	0.2256	6.248
		3	5.4984	2.2404	6.6689	1.6775	-	0.188	6.174
	300	1	6.9041	4.5077	41.0348	8.5577	0.0322	0.3383	5.211
		2	6.4031	4.3973	41.2092	8.6123	0.0242	0.2632	5.288
		3	6.6442	4.5712	41.5029	8.946	0.0319	0.2481	5.275
Yoshiki									
1	0	1	16.7258	0.1079	3.0316	0.8149	0.1504	0.1579	6.477
		2	16.9468	0.1445	3.0133	0.8191	0.1374	0.188	6.724
		3	17.6640	0.0916	3.1814	0.8599	0.1403	0.1053	6.841
	300	1	29.3669	0.1863	14.2150	3.4435	1.1495	0.2406	5.946
		2	29.9219	0.1701	14.7654	3.6313	1.1495	0.1429	5.955
		3	30.0413	0.1893	14.9606	3.5354	1.1927	0.203	6.008
8	0	1	18.6781	0.0864	3.8407	1.0365	0.0537	0.1053	6.445
		2	18.8802	0.1094	3.8602	1.0477	0.0516	0.1429	6.556
		3	17.9659	0.0827	3.5277	0.9596	0.0671	0.0752	6.517
	300	1	30.848	0.1306	16.4278	4.0821	0.5104	0.1654	5.751
		2	31.1098	0.1678	16.6981	4.1909	0.4741	0.1579	5.757
		3	30.6077	0.0898	16.6665	4.143	0.5362	0.1278	5.718

22	0	1	20.5466	0.0836	4.9533	1.2919	0.0237	0.2105	6.366
		2	19.9729	0.0944	4.6582	1.2728	0.0208	0.1729	6.184
		3	20.8072	0.0998	5.0108	1.3398	0.0207	0.1654	6.222
	300	1	31.9842	0.1191	18.7275	4.6973	0.1415	0.1504	5.276
		2	32.7229	0.1416	19.8924	4.8545	0.137	0.1128	5.371
		3	32.8627	0.1547	20.6519	4.9686	0.1409	0.2481	5.324
36	0	1	23.4378	0.2332	5.7926	1.5484	-	0.1053	6.207
		2	22.8420	0.1996	4.8454	1.2882	-	0.0902	6.071
		3	23.4404	0.2314	4.8999	1.3684	-	0.1203	6.046
	300	1	35.1913	0.3687	20.6886	4.9913	0.0483	0.1504	5.149
		2	34.9006	0.2930	19.7013	4.9098	0.0452	0.1579	5.128
		3	35.9192	0.2402	21.0495	5.1478	0.0519	0.1429	5.210
Ogata									
1	0	1	14.2069	0.1022	9.3134	3.484	0.1383	0.7191	6.040
		2	14.9132	0.1728	8.2262	3.5508	0.1171	0.7104	6.077
		3	n.d.	n.d.	n.d.	n.d.	n.d.	n.d.	n.d.
	300	1	29.3669	0.1863	14.215	3.4435	2.3556	1.2698	5.734
		2	29.9219	0.1701	14.7654	3.6313	2.1201	1.2413	5.758
		3	30.0413	0.1893	14.9606	3.5354	2.0232	1.2183	5.790
8	0	1	16.7721	0.2663	10.4886	4.3584	0.0965	0.8101	5.789
		2	15.9671	0.1871	9.7882	4.1951	0.0733	0.6337	5.786
		3	15.7760	0.1902	9.4882	4.0234	0.0607	0.7026	5.763
	300	1	21.8977	0.2632	16.6160	7.0849	2.1139	1.2643	5.578
		2	21.1497	0.3556	15.9846	6.6291	1.7719	1.5194	5.499
		3	22.1276	0.3435	16.6380	6.9289	1.9997	1.2647	5.560
22	0	1	16.3357	0.2226	10.7831	4.5613	0.0194	0.3355	5.698
		2	16.9305	0.1852	11.225	4.6905	0.0154	0.2759	5.831
		3	16.5386	0.1422	10.9056	4.6509	0.0202	0.336	5.608
	300	1	23.1516	0.1742	20.5402	8.8123	0.5931	0.8299	5.218
		2	22.7516	0.2109	19.9606	8.5618	0.5955	0.7589	5.182
		3	21.893	0.1738	19.0931	8.2237	0.6129	0.9273	5.180
36	0	1	16.6946	0.1785	11.5201	4.8954	0.3198	0.642	5.618
		2	16.4061	0.1452	11.3862	4.8078	0.0937	0.5321	5.798
		3	20.0155	0.1898	18.2416	7.674	0.1195	0.5483	5.635
	300	1	22.3098	0.1923	23.4748	10.0173	0.1305	0.6576	4.867
		2	19.9079	0.1979	18.0365	7.7444	0.1538	0.6461	4.917
		3	22.9386	0.1476	23.4401	9.8041	0.1224	0.6087	4.903
Miyakonojo									
1	0	1	0.4960	0.3864	1.9016	0.7883	0.9349	16.015	5.524
		2	0.4767	0.3714	1.8021	0.7627	1.1202	15.188	5.513
		3	0.4458	0.3712	1.8169	0.7553	0.8598	13.6842	5.409
	300	1	0.5739	0.6593	1.7187	0.741	13.4675	101.856	5.538
		2	0.4675	0.6749	1.7522	0.7648	12.3777	100.2432	5.568
		3	0.4504	0.6892	1.9703	0.8438	16.4693	112.4917	5.605
8	0	1	0.5161	0.3568	2.8878	1.0899	0.1756	5.3512	5.274
		2	0.4912	0.3271	2.8141	1.1714	0.1071	5.1245	5.311
		3	0.5111	0.3366	2.9558	1.1034	0.086	4.2507	5.412
	300	1	0.6541	0.8067	3.8864	1.6005	12.6846	110.4469	5.255
		2	0.5986	0.785	3.1653	1.3305	11.4997	102.6916	5.279
		3	0.6287	0.7868	3.4975	1.5093	12.6796	107.7098	5.283
22	0	1	0.5507	0.3538	3.4506	1.3714	-	1.8106	5.384
		2	0.5344	0.3226	3.4057	1.3405	-	1.7828	5.394
		3	0.5213	0.3293	3.3511	1.3413	-	1.7574	5.366
	300	1	0.776	0.6059	13.0672	4.4193	0.0542	5.8454	4.738
		2	0.6219	0.4788	10.7052	3.6683	0.0707	6.1597	4.741
		3	1.0221	0.5327	12.7591	4.5394	0.1511	1.1735	4.775
36	0	1	0.5	0.3488	3.5888	1.371	-	1.8605	5.221
		2	0.55	0.3564	3.6093	1.3933	-	1.8437	5.256
		3	0.5568	0.3493	3.7254	1.4717	-	1.7807	5.366
	300	1	0.8266	0.625	13.3850	4.4183	-	2.0323	4.722
		2	0.7993	0.5874	13.3954	4.3416	-	1.9777	4.692
		3	0.7859	0.5826	12.9098	4.3053	-	1.7123	4.679
Miyakonojo with 10t ha^{-1} smectite									
1	0	1	0.5239	0.3399	1.9715	0.8385	0.8061	13.9614	5.401
		2	0.5027	0.3471	1.9203	0.8208	0.6067	12.9367	5.505
		3	0.4374	0.3671	1.8143	0.789	0.5649	12.6236	5.49
	300	1	0.5044	0.5674	1.7368	0.8179	12.0743	84.6261	5.500
		2	0.4836	0.6332	1.5609	0.8212	11.4284	81.597	5.568
		3	0.4426	0.6487	1.7997	0.8336	10.4197	78.6354	5.606
8	0	1	0.5488	0.4032	3.0255	1.278	0.1377	4.6557	5.411

		2	0.506	0.307	2.6686	1.1277	0.1239	5.0919	5.422
		3	0.5426	0.3409	2.7475	1.1728	0.1042	4.032	5.409
	300	1	0.5965	0.7629	3.267	1.5017	11.1528	87.6018	5.453
		2	0.6339	0.7034	3.5331	1.5518	10.0374	85.558	5.348
		3	0.729	0.7231	3.9172	1.5949	10.9353	89.5045	5.578
22	0	1	0.5238	0.31	3.3008	1.3796	-	1.684	5.339
		2	0.5967	0.3145	3.2875	1.4509	-	1.7071	5.25
		3	0.5434	0.3133	3.2413	1.4234	-	1.6349	5.228
	300	1	0.7615	0.5692	13.0066	4.6412	0.0554	5.0433	4.866
		2	0.7833	0.6222	12.5732	4.5424	0.0663	5.4975	4.843
		3	0.7431	0.6541	12.7335	4.6074	0.0572	5.2383	4.822
36	0	1	0.5752	0.3464	3.5081	1.515	-	1.7706	5.265
		2	0.5417	0.3057	3.4278	1.5153	-	1.8169	5.465
		3	0.539	0.3278	3.4928	1.466	-	1.7403	5.461
	300	1	0.8576	0.4974	12.7271	4.5649	-	3.1911	4.823
		2	0.8303	0.5791	13.0591	4.5147	-	3.7698	4.833
		3	0.8063	0.5862	12.9744	4.6879	-	3.2189	4.844
Miyakonojo with 40t ha^{-1} smectite									
1	0	1	0.5379	0.326	1.7788	0.8844	0.5947	10.372	5.280
		2	0.5057	0.2859	1.6138	0.7338	0.4391	9.5649	5.534
		3	0.497	0.297	1.7307	0.8988	0.4959	10.6972	5.535
	300	1	0.5943	0.5095	2.1496	1.0644	10.013	60.5801	5.665
		2	0.5415	0.7141	1.9955	1.0723	9.0711	56.3511	5.551
		3	0.5422	0.5218	2.2298	1.1291	12.4298	67.6966	5.523
8	0	1	0.5323	0.2866	2.5219	1.2004	0.1724	5.1128	5.316
		2	0.5748	0.2811	2.6014	1.2105	0.1152	4.9624	5.282
		3	0.5430	0.3013	2.6704	1.2225	0.1253	4.7368	5.273
	300	1	0.6503	0.5372	3.4562	1.7274	8.3895	62.6108	5.657
		2	0.6618	0.6710	3.6087	1.7582	9.0099	67.5368	5.640
		3	0.7194	0.7	3.9548	1.8853	8.989	65.7285	5.528
22	0	1	0.5437	0.3081	3.0854	1.4709	-	1.7514	5.301
		2	0.5625	0.2748	3.1366	1.4773	-	1.6312	5.296
		3	0.5579	0.2931	3.1492	1.4689	-	1.7156	5.248
	300	1	0.9198	0.4909	12.1607	5.0245	0.0495	4.9733	4.835
		2	0.8625	0.4731	11.6688	4.7774	0.0565	5.0362	4.846
		3	0.9723	0.548	13.2966	5.2943	0.1272	7.9388	4.859
36	0	1	0.619	0.2982	3.4238	1.616	-	1.7236	5.414
		2	0.5866	0.2824	3.3743	1.5421	-	1.6716	5.393
		3	0.5607	0.2878	3.3056	1.5285	-	1.6721	5.517
	300	1	0.9413	0.5696	12.4996	5.0474	-	3.109	4.858
		2	0.9532	0.4539	12.9201	5.2086	-	3.0482	4.880
		3	0.9046	0.5442	12.3718	5.0041	-	3.0839	4.866
Miyakonojo with 10t ha^{-1} vermiculite									
1	0	1	0.5975	0.3274	1.8669	0.8559	0.5229	4.4627	5.463
		2	0.524	0.2337	1.6065	0.6333	0.4484	4.284	5.373
		3	0.5194	0.2696	1.6635	0.7622	0.4716	4.9018	5.370
	300	1	0.6232	0.5351	2.0407	0.8252	10.3303	23.0857	5.599
		2	0.5979	0.5257	1.7815	0.8049	12.8545	16.9197	5.606
		3	0.5969	0.5292	1.8536	0.761	11.0044	19.878	5.564
8	0	1	0.5998	0.2846	2.47	1.088	0.1065	1.62	5.333
		2	0.5896	0.2716	2.6196	1.0855	0.1392	2.2127	5.421
		3	0.5817	0.2637	2.6009	1.1367	0.0939	1.4957	5.321
	300	1	0.7822	0.6264	3.3004	1.5081	7.3764	13.8755	5.379
		2	0.8258	0.6658	3.6063	1.5368	9.2287	13.4099	5.351
		3	0.7375	0.6785	3.6667	1.7147	10.4646	14.349	5.328
22	0	1	0.6178	0.2818	3.1163	1.2825	-	0.5231	5.350
		2	0.6176	0.2967	3.1943	1.3384	-	0.464	5.364
		3	0.6377	0.2634	3.183	1.3335	-	0.4601	5.433
	300	1	1.0583	0.5005	12.6223	4.456	0.0461	0.7889	4.850
		2	0.9643	0.4441	11.9515	4.425	0.0505	0.7585	4.718
		3	0.7438	0.6705	13.2734	4.3695	0.0756	5.64	4.697
36	0	1	0.6668	0.2877	3.4327	1.4593	-	0.5381	5.688
		2	0.6844	0.2988	3.3956	1.4322	-	0.4926	5.684
		3	0.6371	0.2791	3.3022	1.4033	-	0.4781	5.621
	300	1	0.9342	0.4404	12.626	4.6023	-	0.4349	4.717
		2	1.0059	0.4556	13.2915	4.667	-	0.4488	4.728
		3	0.9683	0.4727	13.098	4.6244	-	0.4361	4.729
Miyakonojo with 40t ha^{-1} vermiculite									
1	0	1	0.8102	0.2404	1.7619	0.815	0.3494	1.5646	5.385
		2	0.8273	0.1988	1.7918	0.8087	0.337	1.5114	5.463

		3	0.7748	0.2118	1.7837	0.8833	0.3164	1.5621	5.448
	300	1	0.9469	0.5677	2.2942	1.2267	8.5001	3.6434	5.476
		2	1.0003	0.4245	2.7103	1.1244	7.3839	4.0043	5.496
		3	0.6285	0.2217	1.6042	0.8713	7.9304	4.3014	5.494
8	0	1	0.5998	0.2846	2.4700	1.0880	0.0939	0.6852	5.443
		2	0.5896	0.2716	2.6196	1.0855	0.0849	0.6771	5.471
		3	0.5817	0.2637	2.6009	1.1367	0.1026	0.7176	5.520
	300	1	1.1102	0.461	3.8802	1.8749	6.0224	2.7457	5.376
		2	1.1003	0.4939	4.1444	1.837	6.3874	2.8025	5.362
		3	0.7126	0.7550	3.6728	1.5916	6.7396	2.7398	5.324
22	0	1	0.9301	0.1801	3.0581	1.3582	-	0.171	5.561
		2	0.9115	0.1972	3.0754	1.3763	-	0.1522	5.51
		3	0.9388	0.2132	3.1078	1.3778	-	0.1239	5.491
	300	1	1.3434	0.3037	10.3731	4.2731	0.0183	0.1846	4.877
		2	1.344	0.3206	10.6721	4.3719	0.0317	0.1936	4.873
		3	1.3920	0.3237	11.0146	4.5551	0.0694	0.2619	4.8863
36	0	1	0.9426	0.1859	3.3465	1.452	-	0.1581	5.527
		2	0.951	0.1927	3.3432	1.4993	-	0.1623	5.676
		3	0.9297	0.1882	3.318	1.4572	-	0.1365	5.596
	300	1	1.5001	0.2992	11.0158	4.5590	-	0.1435	4.9
		2	1.4258	0.2904	11.4634	4.8296	-	0.1581	4.873
		3	1.3666	0.3096	11.2987	4.6900	-	0.1574	4.899
Miyakonojo with 10t ha^{-1} zeolite									
1	0	1	1.1532	0.1540	1.5576	0.6851	0.3523	3.5337	5.412
		2	1.0755	0.1549	1.3841	0.598	0.2837	3.2839	5.415
		3	1.0729	0.1392	1.4661	0.6048	0.2597	3.1021	5.426
	300	1	1.659	0.517	1.8478	0.7103	10.9955	34.5058	5.468
		2	1.635	0.6068	1.8871	0.8227	9.9076	34.5957	5.511
		3	1.6634	0.5061	1.8819	0.824	9.3418	30.7748	5.489
8	0	1	1.1416	0.1547	2.1205	0.9274	0.0764	2.4893	5.229
		2	1.1366	0.1626	2.0774	0.877	0.0676	2.8099	5.221
		3	1.1332	0.1354	2.2044	0.8546	0.0826	2.7433	5.188
	300	1	1.8808	0.4949	3.0478	1.3503	9.1769	31.7501	5.384
		2	1.9321	0.5585	2.8458	1.2326	7.9911	29.5634	5.351
		3	1.8856	0.5501	3.0171	1.2105	8.2647	28.9319	5.35
22	0	1	0.9916	0.1001	3.1988	1.2581	-	0.7602	5.119
		2	1.0158	0.1051	3.2032	1.3344	-	0.7882	5.211
		3	1.0122	0.1069	3.2316	1.3183	-	0.7324	5.215
	300	1	1.5899	0.1842	12.4719	4.427	0.0542	3.1399	4.728
		2	1.607	0.1976	12.4707	4.4574	0.0707	2.8495	4.708
		3	1.6359	0.1973	12.2313	4.3737	0.1511	2.9859	4.704
36	0	1	1.0489	0.1278	3.4224	1.4002	-	0.7704	5.606
		2	1.0574	0.1104	3.4376	1.4195	-	0.7434	5.663
		3	1.0293	0.1152	3.3553	1.3717	-	0.7342	5.524
	300	1	1.5426	0.1835	12.6997	4.4362	-	1.4379	4.698
		2	1.5424	0.1587	13.3517	4.5807	-	1.7024	4.741
		3	1.4567	0.1071	12.9462	4.4584	-	1.4737	4.744
Miyakonojo with 40t ha^{-1} zeolite									
1	0	1	1.5104	0.0610	1.2870	0.5626	0.1141	0.9594	5.391
		2	1.532	0.0889	1.2345	0.5522	0.094	0.9907	5.298
		3	1.3952	0.0613	1.1275	0.5221	0.0839	0.87	5.309
	300	1	3.7427	0.3109	2.2209	0.8739	5.0208	8.7467	5.461
		2	3.9828	0.412	2.3454	0.9396	4.4048	8.8174	5.479
		3	3.8533	0.3899	2.2199	0.9638	4.5362	8.4146	5.485
8	0	1	1.5407	0.0713	1.5786	0.6526	0.0764	0.9236	5.282
		2	1.5644	0.0614	1.5943	0.6632	0.0676	0.9078	5.298
		3	1.5815	0.1107	1.6266	0.7409	0.0826	0.944	5.291
	300	1	3.6388	0.2425	2.3556	1.0214	3.329	6.508	5.448
		2	3.85	0.2953	2.6261	1.2316	3.0967	6.3115	5.443
		3	3.9828	0.412	2.3454	0.9396	4.0552	7.2674	5.423
22	0	1	1.5316	0.0515	2.5496	1.0677	0.0287	0.7264	5.230
		2	1.534	0.0539	2.4741	1.0801	0.0309	0.729	5.229
		3	1.4950	0.0634	2.5208	1.0885	0.2	0.6463	5.218
	300	1	3.4063	0.2256	8.5688	3.3496	0.926	3.577	4.945
		2	2.9678	0.1604	8.6357	3.3853	0.4296	2.6786	4.901
		3	3.4157	0.1774	8.8935	3.3817	0.9143	3.4079	4.931
36	0	1	1.5193	0.0509	3.3401	1.4009	-	0.4337	5.475
		2	1.5022	0.0521	3.269	1.4039	-	0.4214	5.698
		3	1.4809	0.0675	3.2197	1.3784	-	0.4143	5.466
	300	1	2.2672	0.0969	12.0196	4.5631	0.004	1.0355	4.774

2	2.2862	0.0726	12.0293	4.5837	0.005	1.143	4.790
3	2.2181	0.0703	11.5206	4.3975	0.0033	0.8982	4.794

** n.d. indicates that soil solution sampling was hindered.*

*** The hyphen (-) denotes NH_4^+ concentrations that were below the detection level of 0.01 mM L^{-1}.*

Appendix E

Table A4: *Total mineral distribution indicated as semiquantitative mass (in %) of the unamended soils.*

Layer - silicates	Amphibole	Quartz	K^+ feldspar	Plagioclase	Calcite	Dolomite	Pyroxen	amorphous
Groß - Enzsersdorf								
39	1	30	-[a]	7	9	14	-	-
Deshchenka								
4	3	78	9	7	-	-	-	-
Yoshiki								
21	2	30	17	30	-	-	-	-
Ogata								
50	-	24	7	17	-	-	2	
Miyakonojo								
*	-	*[b]	-	*	-	-	*	***[c]

[a] *denotes the absence of the respective mineral.*
[b] *denotes the presence of traces of the respective mineral.*
[c] *denotes the abundant prensence of the respective mineral.*